

**Water Resources Institute
Annual Technical Report
FY 2012**

Introduction

The University of Wisconsin WRI serves as the gateway to federal WRI grants for all Wisconsin colleges and universities. While the WRI's federal base funding from the U.S. Geological Survey totals less than \$100,000 per year, every federal dollar is matched with at least two nonfederal dollars. All WRI grants are awarded on a competitive, peer-reviewed basis. WRI funds are leveraged with additional funding from the UW System Groundwater Research Program, part of Wisconsin's Groundwater Research and Monitoring Program. Faculty members and research staff who have achieved PI status from any UW System campus are eligible to apply for this funding. Guided by the Wisconsin Groundwater Coordinating Council, this program is the mechanism whereby the UW System and the state departments of Natural Resources, Safety & Professional Services, and Agriculture, Trade & Consumer Protection pool limited state and federal resources to support a coordinated, comprehensive and multidisciplinary response to the state's critical water resource issues. Together, these programs have helped establish the University of Wisconsin as a national leader in groundwater research.

The Wisconsin WRI funds an average of 15 short-term research projects of either a fundamental or applied nature that typically involve about 50 faculty, staff and students at a half-dozen campuses around the state each year. By supporting short-term projects, the institute is able to quickly respond to issues as they emerge. WRI annually provides about 30 graduate and undergraduate students in the UW System with opportunities for training and financial support while they work toward their degrees. During the current reporting period a total of 45 students/trainees (16 undergraduates, 16 master's degree students, 10 Ph.D. students and five post-doctoral students) received WRI support from both Federal and non-Federal sources.

WRI research and other water-related information are readily accessible via a Web site (www.wri.wisc.edu) and the Water Resources Library (WRL), a nationally unique collection of documents covering every major water resource topic. The library's catalog is available online and searchable via the Internet, making the WRL a national and global resource. The WRL became the first academic library in the state to make its collection available online to the public when it launched "Wisconsin's Water Library" (www.aqua.wisc.edu/waterlibrary) in 2003. The portal permits Wisconsin residents to check out WRL books and other documents free of charge via their local libraries. WRI also helps organize and cosponsor state and regional conferences on water issues.

The WRI is housed in the Aquatic Sciences Center which also houses the UW Sea Grant Institute, part of another federal-state partnership of 30 university programs that promote research, education, and outreach on Great Lakes and ocean resources. This unique administrative union of Wisconsin's federal Water Resources Research Institute and Sea Grant programs enables the UW Aquatic Sciences Center to address the full range of water-related issues in Wisconsin, from surface water to groundwater, from the Mississippi River to the shores of Lakes Michigan and Superior.

Research Program Introduction

As established by Wisconsin's Groundwater Law of 1984, the state provides \$250,000 to \$300,000 annually to the UW System to support groundwater research and monitoring. In 1989, the WRI became the UW System's lead institution for coordinating the calls for proposals and peer reviews for distribution of the funds. To avoid duplication and better target groundwater research funding, several other state agencies (the departments of Safety & Professional Services, Natural Resources, and Agriculture, Trade and Consumer Protection) agreed to partner with the WRI to establish an annual Joint Solicitation for Groundwater Research and Monitoring. This annual solicitation has funded more than 400 groundwater research and monitoring projects since its inception and has helped establish Wisconsin as a leader in groundwater research. The results of the Wisconsin Groundwater Research and Monitoring Program (WGRMP) are recognized internationally, and WRI plays an important role in coordinating project reporting and making all technical reports available through our institute's library and website.

Our priorities for groundwater research are established annually by the Wisconsin Groundwater Research Advisory Council (GRAC) and are included as part of the Joint Solicitation. The GRAC is our institute's advisory council and also convenes to make project funding decisions. All proposals submitted to the Joint Solicitation receive rigorous external peer review (coordinated by the WRI) and relevancy review by the Research Subcommittee of the state's Groundwater Coordinating Council.

Beginning in 2010, the annual 104(B) allocation was used to expand the scope of the joint solicitation to include research on the effects of climate change on Wisconsin's water resources. Priorities for climate change research were established through a partnership between the WRI and the Wisconsin Initiative on Climate Change Impacts (WICCI). Established in 2007, WICCI is a university-state partnership created to: (a) assess and anticipate the effects of climate change on specific Wisconsin natural resources, ecosystems and regions; (b) evaluate potential effects on industry, agriculture, tourism and other human activities; and (c) develop and recommend adaptation strategies that can be implemented by businesses, farmers, public health officials, municipalities, resource managers and other stakeholders.

We believe these partnerships with other state agencies provides WRI with the ability to fund highly relevant research and allows our limited funds for 104(B) to be leveraged to the fullest extent.

Award No. 08HQGR0148 The Transport, Fate and Cycling of Mercury in Watersheds and Air Sheds

Basic Information

Title:	Award No. 08HQGR0148 The Transport, Fate and Cycling of Mercury in Watersheds and Air Sheds
Project Number:	2008WI244S
Start Date:	9/15/2008
End Date:	9/14/2013
Funding Source:	Supplemental
Congressional District:	2nd
Research Category:	Water Quality
Focus Category:	Toxic Substances, Wetlands, Water Quality
Descriptors:	mercury, catchment processes
Principal Investigators:	Jim Hurley, David P. Krabbenhoft

Publications

1. Kolker, A., Olson, M., Krabbenhoft, D.P., Tate, M.T., and Engle, M.A., 2010, Patterns of mercury dispersion from local and regional emission sources, rural Central Wisconsin, USA, *Atmos. Chem. Phys.*, 10, 1–10, 2010.
2. Engle, M.A., Tate, M.T., Krabbenhoft, D.P., Schauer, J.J., Kolker, A., Shanley, J.B., Bothner, M.H. 2010, Comparison of Atmospheric Mercury Speciation and Deposition at Nine Sites across Central and Eastern North America, *Geophysical Research* (in press).
3. Engle, MA, MT Tate, DP Krabbenhoft, A Kolker, ML Olson, ES Edgerton, JF DeWild, and AK McPherson. 2008. Characterization and cycling of atmospheric mercury along the central US Gulf of Mexico coast. *Applied Geochemistry* 23, 419-437
4. Geboy N, DP Krabbenhoft, MA Engle, and T Sabin. 2011. The Solubility of Mercury-Containing Aerosols in Fresh and Sea Water. In the Proceedings of the 10th International Conference on Mercury as a Global Pollutant, Halifax, Nova Scotia. 1 page.
5. Engle, M.A., Tate, M.T., Krabbenhoft, D.P., Schauer, J.J., Kolker, A., Shanley, J.B., Bothner, M.H. 2010, Comparison of Atmospheric Mercury Speciation and Deposition at Nine Sites across Central and Eastern North America, *J. Geophys. Res.*, 115, D18306, doi:10.1029/2010JD014064

Annual Progress Report

Selected Reporting Period: 3/1/2010 - 2/28/2011

Submitted By: David Krabbenhoft
Submitted: 5/27/2011

Project Title

WR08R005: The Transport, Fate and Cycling of Mercury in Watersheds and Air Sheds

Project Investigators

James Hurley, University of Wisconsin

Progress Statement

This project looks at two mercury related questions: (1) mercury in watersheds; and, (2) mercury cycling and transport in the atmosphere. During reporting period the project completed its second year of "recovery" (i.e., no longer loading mercury to the study watershed) on the Mercury Experiment to Assess Atmospheric Loadings in Canada and the US (METAALICUS) project. Our portion of the project is to monitor the watershed-scale response of the artificial load of mercury that was administered from 2001 through 2007 using three different stable isotopes (198Hg, 201Hg, 202Hg) to the study wetland, uplands and lake, respectively. During this phase of the project, we will quantify the response of the watershed to a mercury "load reduction" through continuous monitoring of the isotope concentrations and water flux from the terrestrial flows into the study lake. On the atmospheric studies, the project performed one assessment study of mercury deposition spanning time and space domain near a emission stack in central Wisconsin; and significantly enhanced our field monitoring system by securing the extra instrumentation needed to make "gradient" measurements (Eddy Correlation method) of mercury concentrations in the atmosphere above our study sites.

Principal Findings and Significance

Principal Findings and Significance

- Description** Our results show that in coastal settings, the intersection of terrestrially based mercury emission sources interacting with chemical oxidants formed in the marine boundary layer result in exacerbated mercury deposition in the near coastal environments. These finds have direct implications for water-resource rich ecosystems along the East Coast of the US, and people who fish in those waters. Also, the application of the mercury deposition model developed by this project to these field settings provides a scientifically based explanation for why coastal areas in the southeastern US are among the highest mercury deposition zones.
- Description** Results from the past year of data collection revealed that despite the cessation of loading the watershed on the METAALICUS project, concentrations in runoff continued to increase. This phenomenon reveals the inherent time lags that are part of the natural response to changes in loading watersheds. On the atmospheric studies portion of the project the assessment revealed the importance of the marine boundary layer for facilitating atmospheric mercury reactions and deposition.
- Description** The expanded ability to measure mercury concentration in the atmosphere using the Eddy Correlation method will significantly improve our ability to understand the bi-directional nature of mercury fluxes between the atmosphere and the land/water surface.

Journal Articles & Other Publications

Publication Type Journal Article/Book Chapter (Peer-Reviewed)
Title Characterization and cycling of atmospheric mercury along the central U.S. Gulf of Mexico Coast
Author(s) Engle, M.A., Tate, M.T., Krabbenhoft, D.P., Kolker, A., Olson, M.L., Edgerton, E.S., DeWild, J.F., and McPherson, A.K.
Publication/Publisher Applied Geochemistry 23 (2008), pp. 419–437.
Year Published 2008
Volume & Number 23
Number of Pages 19
Description
Any Additional Citation Information

.....

Publication Type Journal Article/Book Chapter (Peer-Reviewed)
Title Patterns of mercury dispersion from local and regional emission sources, rural Central Wisconsin, USA
Author(s) Kolker, A., Olson, M., Krabbenhoft, D.P., Tate, M.T., and Engle, M.A.,
Publication/Publisher Atmos. Chem. Phys.,
Year Published 2010
Volume & Number 10, 1–10
Number of Pages 10
Description Abstract. Simultaneous real-time changes in mercury (Hg) speciation- reactive gaseous Hg (RGM), elemental Hg (Hg⁰), and fine particulate Hg (Hg-PM2.5), were determined from June to November, 2007, in ambient air at three locations in rural Central Wisconsin. Known Hg emission sources within the airshed of the monitoring sites include: 1) a 1114 megawatt (MW) coal-fired electric utility generating station; 2) a Hg-bed chlor-alkali plant; and 3) a smaller (465 MW) coal-burning electric utility. Monitoring sites, showing sporadic elevation of Hg⁰, Hg-PM2.5, and RGM were positioned at distances of 25, 50 and 100 km northward of the larger electric utility. Median concentrations of Hg⁰, Hg-PM2.5, and RGM were 1.3–1.4 ng m⁻³, 2.6–5.0 pg m⁻³, and 0.6–0.8 pg m⁻³, respectively. A series of RGM events were recorded at each site. The largest, on 23 September, occurred under prevailing southerly winds, with a maximum RGM value (56.8 pg m⁻³) measured at the 100 km site, and corresponding elevated SO₂ (10.4 ppbv; measured at 50 km site). The finding that RGM, Hg⁰, and Hg-PM2.5 are not always highest at the 25 km site, closest to the large generating station, contradicts the idea that RGM decreases with distance from a large point source. This may be explained if: 1) the 100 km site was influenced by emissions from the chlor-alkali facility or by RGM from regional urban sources; 2) the emission stack height of the larger power plant promoted plume transport at an elevation where the Hg is carried over the closest site; or 3) RGM was being generated in the plume through oxidation of Hg⁰. Operational changes at each emitter since 2007 should reduce their Hg output, potentially allowing quantification of the environmental benefit in future studies.
Any Additional Citation Information

.....

Publication Type Journal Article/Book Chapter (Peer-Reviewed)
Title Comparison of Atmospheric Mercury Speciation and Deposition at Nine Sites across Central and Eastern North America
Author(s) Engle, M.A., Tate, M.T., Krabbenhoft, D.P., Schauer, J.J., Kolker, A., Shanley, J.B., Bothner, M.H.
Publication/Publisher Geophysical Research
Year Published In Press
Volume & Number
Number of Pages
Description
Any Additional Citation Information

Publication Type Proceedings/Symposium (Not Peer-Reviewed)
Title The Solubility of Mercury-Containing Aerosols in Fresh and Sea Water
Author(s) Geboy, N., Krabbenhoft, D., Engle, M., and Sabin, T.
Publication/Publisher Proceeding of the 10th International Conference on Mercury as a Global Pollutant
Year Published 2010
Volume & Number 1
Number of Pages 1
Description Abstract presented at this international meeting
Any Additional Citation Information

Students & Post-Docs Supported

Student Name Nicholas Ostrowski
Campus University of Wisconsin-Madison

Advisor Name Kenneth Bradbury
Advisor Campus University of Wisconsin-Madison

Degree Masters
Graduation Month August
Graduation Year 2012
Department IES
Program Letters and Science
Thesis Title
Thesis Abstract

Grant No. G09AP00068 Influence of Coupling Erosion and Hydrology on the Long-Term Performance of Engineered Surface Barriers

Basic Information

Title:	Grant No. G09AP00068 Influence of Coupling Erosion and Hydrology on the Long-Term Performance of Engineered Surface Barriers
Project Number:	2009WI245S
Start Date:	5/15/2009
End Date:	8/31/2012
Funding Source:	Supplemental
Congressional District:	WI-2
Research Category:	Engineering
Focus Category:	Management and Planning, Models, Hydrology
Descriptors:	
Principal Investigators:	Anders W. Andren, Craig H Benson

Publications

There are no publications.

Annual Progress Report

Selected Reporting Period: 3/1/2011 - 2/29/2012

Submitted By: Craig Benson

Submitted: 5/25/2012

Project Title

WR09R007: Influence of Coupling Erosion and Hydrology on the Long-Term Performance of Engineered Surface Barriers

Project Investigators

Craig Benson, University of Wisconsin-Madison

Progress Statement

The overall objective of this research project is to assess the performance of erosion controls for low-level radioactive waste disposal systems, and the coupling of erosion control strategies and hydrological performance of the cover. The specific objectives of this work are:

- (1) Prepare an extensive literature review regarding erosion control strategies being employed for waste containment facilities in both humid and arid regions.
- (2) Select a combination of models that can predict erosion and hydrological performance of covers in humid and arid regions and compare/validate the models with field data.
- (3) Perform model simulations to identify strategies likely to be effective in managing erosion and hydrology of covers.

We conducted a literature review on models for simulating erosion processes and evaluated a collection of models used to simulate variably saturated flow for cover systems. We selected the SIBERIA model for simulating erosion and the SVFLUX model for simulating variably saturated flow.

SIBERIA was selected for several reasons. First, the model is mechanistic and thus properly represents the physics of erosion processes. Second, the model simulates landform evolution and therefore will be useful in evaluating long-term impacts of erosion. Third, the model has been applied to long-term erosion and landform evolution modeling at mine closure sites in Australia and Canada. These sites have many similarities to LLRW disposal facilities in North America.

We selected SVFLUX for three reasons. First, the code is well documented and can be used in 1, 2, or 3D modes. Second, SVFLUX has a reliable algorithm that simulates infiltration and runoff mechanistically with a high degree of realism, regardless of antecedent conditions or precipitation intensity. Third, SVFLUX includes algorithms for simulating soil-plant-atmosphere interactions, which are key to predicting the hydrology of final covers.

We are using two UMTRA mill tailings disposal facilities as base cases for our simulations: Grand Junction, CO and Canonsburg, PA. The US Department of Energy's Division of Legacy Management has provided topographic information and cover profiles of these sites.

FINDINGS TO DATE

- In semi-arid and humid climates, comparable erosion control can be achieved with riprap surfaces and gravel-amended surfaces, although maximum erosion is slightly lower with a riprap surface (see next slide).
- In semi-arid and humid climates, erosion on gravel-amended surfaces is less sensitive to the geometry of the slope (angle, length, grade change) than for a riprap surface.
- In semi-arid and humid climates, terracing reduces erosion relative to that on concave slopes. The shorter length of the steeper sections combined with step grade changes in a terrace reduces head cutting and erosion.

- In semi-arid climates, deep concave side slopes have reduced maximum erosion and less average elevation change than uniform side slopes. Sediment trapping at the base of the concave slope diminishes erosion.
- Maximum erosion is not systematically related to type of climate. The magnitude of episodic events and antecedent conditions prior to episodic events have a greater influence than "wetness" of climate.
- Average erosion is consistently greater in the semi-arid climate than in the humid climate. Erosion occurred in a more widespread and distributed manner in a semi-arid climate and more as gullies in a humid climate.
- Covers with gravel-amended surface layers consistently transmitted less percolation than covers with a riprap surface (see next slide).
- A riprap surface funnels water into the underlying soils, and then traps the water in the underlying soils via a capillary break. More water is stored in the cover, and more percolation occurs (water "harvesting").
- A gravel-amended surface limits infiltration due to its lower saturated hydraulic conductivity, and permits a capillary conduit for water removal via evapotranspiration. Less water enters and is stored in the cover, and less percolation occurs.
- A cover with a gravel-amended surface layer undergoes comparable erosion, but transmits less percolation, than a riprap cover.

PROJECT STATUS

- Calibration with field information from literature is complete.
- Modeling is 90% complete. Some re-runs are being conducted to address uncertainty about mechanisms as sections of report are being prepared.
- Final report has been drafted and is 70% complete. Expect submission in late summer 2012

Principal Findings and Significance

Principal Findings and Significance

Description This project will result in design methodologies for more sustainable and effective cover systems. New cover system profiles will be developed as an outcome of this study. These profiles will be more resistant to erosion and more effective in limiting percolation into underlying waste. As a result, they will require less maintenance and be more effective in protecting groundwater.

Awards, Honors & Recognition

Title Diplomat Geotechnical Engineer
Event Year 2009
Recipient Craig H Benson
Presented By Academy of Geoprofessionals
Description Inducted as a diplomate



Title Academy of Distinguished Alumni
Event Year 2009
Recipient Craig H Benson
Presented By University of Texas at Austin
Description Inducted into academy of distinguished alumni in Civil & Environmental Engineering.

.....

Title Award of Merit
Event Year 2011
Recipient Craig H. Benson
Presented By ASTM
Description

.....

Title National Academy of Engineering
Event Year 2012
Recipient Craig H. Benson
Presented By National Academies
Description PI was elected to NAE in January 2012, with a citation to his work related to long-term containment of low-level radioactive wastes.

Partners

Name/Organization
Affiliation US Department of Energy/CRESP
Affiliation Type Federal
Email
Description

.....

Name/Organization
Affiliation US Department of Energy/Legacy Management
Affiliation Type Federal
Email
Description

Students & Post-Docs Supported

Student Name Chris Bareither
Campus University of Wisconsin-Madison

Advisor Name Craig Benson
Advisor Campus University of Wisconsin-Madison

Degree Post Doc
Graduation Month
Graduation Year
Department Geological Engineering
Program
Thesis Title
Thesis Abstract

.....

Student Name Crystal Smith
Campus University of Wisconsin-Madison

Advisor Name Craig Benson
Advisor Campus University of Wisconsin-Madison

Degree Masters
Graduation Month August
Graduation Year 2012
Department Geological Engineering
Program Geological Engineering
Thesis Title NA
Thesis Abstract NA

Implications of Climate Change and Biofuel Development for Great Lakes Regional Water Quality and Quantity

Basic Information

Title:	Implications of Climate Change and Biofuel Development for Great Lakes Regional Water Quality and Quantity
Project Number:	2010WI253G
Start Date:	9/1/2010
End Date:	8/31/2013
Funding Source:	104G
Congressional District:	WI-002
Research Category:	Climate and Hydrologic Processes
Focus Category:	Models, Water Quality, Water Quantity
Descriptors:	None
Principal Investigators:	Anita Thompson, Bruno Basso, Mike Fienen, David Hyndman, Randall Jackson, K. G. Karthikeyan, Anthony Kendall, Brian J Lepore

Publication

1. Stenjem, Ryan S. 2013. Subsurface water and nutrient dynamics of cellulosic biofuel cropping systems. M.S. Thesis, Biological Systems Engineering, University of Wisconsin, Madison, WI. 134p.

Annual Progress Report

Selected Reporting Period: 3/1/2012 - 2/28/2013

Submitted By: Anita Thompson

Submitted: 5/28/2013

Project Title

WR10R008: Implications of Climate Change and Biofuel Development for Great Lakes Regional Water Quality and Quantity

Project Investigators

Anita Thompson, University of Wisconsin-Madison

Progress Statement

Objective 1 - Data Collection and Compilation

Plot-scale Field Data Collection: Leachate samples were collected from the 11 lysimeters approximately weekly during wet periods and biweekly during dry periods. Samples (over 120) were analyzed for volume, TN, TP, DRP, NO₃, and DOC. Hourly soil temperature and moisture data were collected and analyzed. Soil samples were collected within continuous corn and switchgrass plots and analyzed for water extractable NO₃. In-situ calibration of water content reflectometers was performed. Maintenance on the lysimeter systems included: (i) excavation, repair and reinstallation of one damaged lysimeter, (ii) replacement of valves, pumps and wiring in the control boxes as needed, and (iii) repair and reinstallation of two control boxes.

Surface runoff was collected from small-scale (1m X 1m) runoff plots in Miscanthus, continuous corn, and switchgrass (3 replicates in each system). Fourteen natural rainfall events were sampled (over 100 samples) and analyzed for TS, TN, TP, TDP and organic matter (OM). Surface soil moisture was measured prior to rainfall/runoff events. A rainfall simulation (75mm/hr for 1hr) was conducted in November 2012. Samples were analyzed for TS, TN, TP, TDP, OM, and particle size. Rainfall data (5-min interval) were collected for each event. Leaf Area Index (LAI) was measured for continuous corn, switchgrass, Miscanthus and Hybrid Poplar.

GIS Data Collection: We are assembling GIS databases in preparation for building ILHM simulations for the Trout River, Black Earth Creek, and Muskegon River watersheds. These include surficial hydrology, subsurface sediment characteristics, basic basemap layers, digital elevation models, SSURGO soil textures, remotely sensed LAI. We have also collected some climate data to drive the models, including NEXRAD hourly precipitation estimates, climate change forecasts (see below), and historical climate reanalyses (also see below).

Objective 2 - Model Coupling and Development

SALUS Model Development: Simulation runs of Arlington-specific SALUS models have been completed. The results for the water balance were successfully validated while some improvements in the soil biochemistry and crop development will be completed in summer 2013 (Brena et al., in preparation).

ILHM Model Development: Prior to the start of this project, the research team had an ILHM simulation of the Muskegon River Watershed. We have continued to improve this during the last year, and have incorporated enhancements including: substantial improvement of SSURGO soil hydraulic properties mapping, improved precipitation data inputs, and improved wetlands simulations. These improvements are incorporated in Kendall and Hyndman (in preparation). Simulations of the Middle Rock and Flambeau watersheds will be constructed starting summer of 2013.

Climate Projection Development: During the past year we improved our methods of developing climate forecasts. Improvements include creating continuous daily climate scenarios from 1870-2100 using the 20th Century Version 2 Reanalysis and the 24 models within the CMIP-3 database used by the IPCC AR4. Along with creating continuous scenarios, this gives us the capability to rapidly assess the bias of individual CMIP-3 models relative to the 20thCv2 reanalysis.

Biofuels Land Use Scenario Development: Work completed on a related project is yielding insights into a range of adaptive management strategies that

may be employed by biofuels agricultural production systems in response to climate changes during the 21st century. These findings will be used along with the originally envisioned regional biofuels production scenarios later in this project.

Objective 3 - Model Validation

Stream Discharge Monitoring: In July 2011, 3 pressure and temperature transducers were installed in streams in the Yahara River. These are being monitored and downloaded regularly, with stream discharge measurements collected at regular intervals to construct a stage-discharge relationship for each stream gauge station. This has yielded over 2 years of detailed stream flow estimates for this watershed. During the low flows season of 2012 (Oct.), stream flow samples were collected and analyzed for NO₃, NH₃, total N, t P, DRP, pH, EC, and stream discharge. Above activities will be repeated in June (high flows) and Oct. 2013.

Groundwater Level Monitoring: In July 2011, 5 pressure and temperature transducers were installed in wells nearby the Arlington site. Water levels are monitored quarterly.

Objective 4 - Model Intercomparison

Comparison of SALUS-ILHM and GSFLOW models for the three watersheds is anticipated to begin in Winter of 2013.

Principal Findings and Significance

Principal Findings and Significance

Description

Plot-scale analysis:

Field data collected by our project team at the Arlington Experimental site provided valuable information about the temporal variability of recharge and runoff processes among different biofuel cropping systems. The Arlington site, as did much of the US Midwest, experienced significant climate variability over the past two years. The extreme dry summer observed in 2012 and the abrupt drop in precipitation had significant impacts on the seasonal water balance, especially between the summers in 2011 (precipitation=345 mm) and 2012 (precipitation=82 mm).

At the plot scale, total subsurface drainage over the first 18 months of the study was greatest for Switchgrass followed by continuous corn and then Hybrid Poplar; most drainage occurred in the spring and early growing season. More drainage occurred from Switchgrass than continuous corn in spring and winter seasons and this trend was reversed during summer and fall. Seasonal drainage from Hybrid Poplar was always lower than Switchgrass and continuous corn. Miscanthus generated 25% less recharge than the Switchgrass despite having similar vegetation cover values (LAI). Total subsurface NO₃ loading during the first 18 months followed the patterns (temporal and between cropping systems) observed for subsurface drainage. Seasonal NO₃ concentrations and loads were higher for continuous corn than Switchgrass throughout the year. No samples from Hybrid Poplar during the study had detectable NO₃ concentrations.

Three types of mechanisms that generated recharge were identified at the Arlington experimental plots: snowmelt-based, rainfall-based and combined. The results also suggested that recharge is a highly variable process between seasons and strongly differed among plantations despite similar climate and physical soil characteristics.

Runoff generation was highly dynamic and subjected to climate variability. Among the three plots with runoff collectors, continuous corn generated 369 mm of water, followed by Miscanthus and Switchgrass, which respectively had approximately only 33% (125 mm) and 10% (36 mm) of the observed runoff for continuous corn. For all three plots, most runoff was generated during the summer season (May-September), which accounted for 87 to 95% of the annual runoff in 2011-2012 and 73 to 90% in 2012-2013. Even during the dry summer of 2012 (precipitation = 82mm) runoff values were higher than those observed during the winter of 2012 (precipitation = 242mm).

Most of the runoff during the first two years of the study was generated during June and July of 2011. Despite mild drought conditions during the summer of 2011, the total runoff was significant with respect to measured recharge for Miscanthus and Continuous Corn, whereas Switchgrass showed almost no runoff and recharge was the dominant flux. In 2012, despite a few rainfall-runoff events in June-July the dominant flux at the three sites was recharge. Overall, recharge was the dominant water balance component for Miscanthus (290 mm vs 125 mm of runoff) and Switchgrass (393 mm vs 36 mm of runoff) during the first 18 months of the study. Continuous Corn showed a similar proportion of runoff and recharge (327-410 mm of recharge vs 369 mm of runoff). The sum of both fluxes yielded a mean annual value of 280, 286 and 464 mm/year for Miscanthus, Switchgrass and Continuous Corn, respectively. Given the same climate conditions and similar soil texture properties (silty clay loam) among the three sites, the observed low values of combined recharge and runoff for the grass plots implies higher evapotranspiration rates.

Because of the wet 2012-2013 winter, Hybrid Poplar showed a substantial rise in recharge (12 to 52 mm in 2012 vs. 269 mm in 2013) while *Miscanthus* presented an opposite response (122 mm in 2011-2012 and only 42 mm in 2013). During summer, *Miscanthus* unexpectedly displayed low recharge values (38 mm in 2011) and high values in extreme dry conditions (135 mm in 2012). In contrast, recharge rates in summer for Hybrid Poplar remained close to zero for both years. During summer, the expected high transpiration rates of Hybrid Poplar are likely to diminish recharge and, hence, nutrient leaching into the aquifer. However, the high frequency of moderate rainfall events and the mild temperatures during the winter of 2012-2013 (precipitation = 315 mm, recharge = 269 mm) compensated for the low recharge values during summer (precipitation = 82 mm, recharge = 9 mm).

With the exception of Continuous Corn, the mild winter of 2011-2012 followed by the drought during summer did not reduce summer recharge rates. Even when summer recharge was not observed after the end of June, the amount of recharge generated around the snowmelt period compensated for the low rates reached with the onset of the drought. The magnitude of recharge during the spring season is significant. The average observed recharge Switchgrass, Continuous Corn and Hybrid Poplar was 78, 46 and 93% of the total rainfall during the same period. The mechanisms that generated recharge also differed. For instance, the drainage system of Hybrid Poplar mainly responded during snowmelt conditions (temperatures above zero degrees C but no rainfall) while most of the recharge for Continuous Corn was observed during rainfall events in April (snowpack had already melted and temperatures far above the freezing point). The combination of both snowmelt conditions and earlier rainfall events in February was the foremost mechanism of recharge for Switchgrass (positive temperatures during the day and intense rainfall storms).

Watershed-scale analysis:

Stream discharge and nutrient samples were collected from 26 sites during the low flows season in October 2012 by the MSU Hydrogeology lab. The sites were located in the Middle Rock (13 sites) and Flambeau (13 sites) watersheds. Sites include USGS discharge gauge locations, project stream gauges, and non-gauge locations. Differences in the intrinsic physical properties and land cover of the study sites imply different discharge and nutrient concentration patterns within the watersheds. For instance, the Northern Wisconsin sites in the Flambeau watershed with a dominant forest cover had approximately an order of magnitude lower concentrations of Total Nitrogen (TN) and Nitrogen Oxides (NO_x) compared to the Middle Rock watershed to the south, which is dominated by urban and agricultural land cover. Ammonia (NH₃), TP and Soluble Reactive Phosphorus (SRP) concentrations were also lower in the forested sites but did not have the level of difference as seen with TN and NO_x. Despite low flow conditions, concentrations at the Middle Rock sites tended to be inverse to discharge. Two USGS groundwater wells are also used to show water levels near the two watersheds over the past decade; significant low water levels were observed in both wells, including a record low during the summer of 2012 for the well near the Middle Rock watershed.

At the watershed scale, our findings revealed fairly uniform leached concentrations in watersheds dominated by a forest land cover (Flambeau basin) and an indirect proportional relationship between concentrations and streamflow in agricultural watersheds (Middle Rock basin). Such patterns were observed during the late summer when streamflow is mainly generated by groundwater outflow through the riparian areas and streambeds.

Groundwater levels reached minima 10-year values at the Middle Rock watershed whereas the wells near the Flambeau sites did not show a significant decline. Overall, despite large soil moisture deficits and plant water stress, runoff at the plot scale was more affected than recharge during 2012. A reduction of 75% in summer precipitation from 2011 to 2012 did not cause a similar percentage drop in recharge. Unlike the summer of 2011, recharge during the summer of 2012 was overall higher than precipitation. This could imply that even during extreme drought conditions water storage in the unsaturated zone continues to generate recharge within the top 1-meter soil layer. Model simulations also showed that the decline in transpiration and soil evaporation because of higher water stress in the growing season of 2012 was moderate.

Model Analysis:

Recharge and evapotranspiration fluxes were simulated using the System Approach to Land Use Sustainability (SALUS) model. The SALUS model is a process based model that integrates crop productivity with water, carbon, and nutrient fluxes in a spatially explicit manner. The approach of SALUS involves management practices, water balance, soil OM, N and P dynamics, heat balance, plant growth and plant development. The water balance considers multiple processes such as surface runoff, infiltration, surface evaporation, saturated and unsaturated soil water flow, drainage, root water uptake, soil evaporation and transpiration. The soil OM and nutrient model simulates organic matter decomposition, N mineralization and formation of ammonium and nitrate, N immobilization, gaseous N losses and three pools of phosphorous. The development and growth of plants requires the environmental conditions (particularly temperature and light) to calculate the potential rates of growth for the plant. This growth is then reduced based on water and nitrogen limitations.

The main water balance components simulated at the Arlington site were transpiration, soil evaporation and recharge in three sites. The dominant flux for Corn and Switchgrass was Recharge, followed by Soil Evaporation (E) and Transpiration (T). Estimates of recharge for Hybrid Poplar were not only substantial lower with respect to E and T but also when compared to the other two sites. The year of 2012 had a negative impact on recharge at the 3 sites and E and T for Continuous Corn. Simulations of E and T for Switchgrass and Hybrid Poplar showed slight impacts from the previous year. Overall, the implications for groundwater were higher for Hybrid Poplar with average recharge values approximately 60% below the estimated recharge at the two other biofuel crops.

For comparison purposes during similar periods, modeled evapotranspiration (ET) and recharge in the growing season of 2011 and 2012 revealed that transpiration was the dominant flux in both years followed by soil evaporation and recharge. The values of ET and recharge in 2012 did not seem to be affected by the drought with the exception of recharge at the Hybrid Poplar site. Moreover, among the three modeled sites, Hybrid Poplar experienced the highest and lowest ET and recharge rates, respectively. The high ratio of ET to percolation suggests the strong controls of woody species on groundwater recharge during summer.

Total groundwater recharge from April 2011 to April 2013 was validated for Corn, Switchgrass and Hybrid Poplar. Currently, a model for the Miscanthus crop is being developed and tested. The results for the Corn and Poplar experimental plots fit within an acceptable error range whereas the Switchgrass site was slightly underestimated (a difference of ~100 mm). Model calibration at the three sites was not required. In general, the model confirmed the marked differences in recharge between Hybrid Poplar and Corn and Switchgrass under normal and extreme dry climate conditions.

Journal Articles & Other Publications

Publication Type Journal Article/Book Chapter (Peer-Reviewed)
Title Simulating Spatial and Temporal Variability of Regional Evapotranspiration and Groundwater Recharge: Influences of Land Use, Soils, and Lake-Effect Climate
Author(s) Kendall and Hyndman
Publication/Publisher Advances in Water Resources
Year Published
Volume & Number
Number of Pages
Description In Preparation
Any Additional Citation Information

.....

Publication Type Journal Article/Book Chapter (Peer-Reviewed)
Title Water and nutrient fluxes in an experimental multi-species biofuel crop plantation
Author(s) Brena, A., Kendall, A. Basso, B., and Hyndman, D
Publication/Publisher
Year Published
Volume & Number
Number of Pages
Description In Preparation
Any Additional Citation Information

.....

Publication Type Thesis/Dissertation
Title Subsurface water and nutrient dynamics of cellulosic biofuel cropping systems
Author(s) Stenjem, R.
Publication/Publisher University of Wisconsin - Madison

Year Published
Volume & Number
Number of Pages
Description M.S. Thesis
Any Additional Citation Information

Other Project Support

Source USDA-NIFA Hatch
Dollar Value \$270,983
Description Linking Cropping System Diversity with Nutrient Loss Dynamics in Alternative Biofuel Production Systems
Start Date 10/1/2009
End Date 9/30/2013

.....

Source Wisconsin Groundwater Coordinating Council/UW Water Resources Institute
Dollar Value \$104,695
Description Groundwater Recharge Characteristics and Subsurface Nutrient Dynamics Under Alternate Biofuel Cropping Systems in Wisconsin
Start Date 7/1/2010
End Date 6/30/2012

Presentations & Public Appearances

Title Water and nutrient fluxes under biofuel cropping systems
Presenter(s) Stenjem, R., A.M. Thompson, B.J. Lepore
Presentation Type Poster session
Event Name Annual Meeting of the American Water Resources Associate WI Section
Event Location Lake Delton, WI
Event Date 3/1/2012
Target Audience Scientific audience
Audience Size 50
Description

.....

Title Surface and subsurface water and nutrient dynamics for biofuel feedstock cropping systems
Presenter(s) Stenjem, R., A.M. Thompson, K.G. Karthikeyan, M. Polich and B.J. Lepore
Presentation Type Professional meeting
Event Name Annual International Meeting of the American Society of Agricultural and Biological Engineers
Event Location Dallas, TX
Event Date 7/29/2012
Target Audience Scientific audience
Audience Size 25
Description

.....

Title Runoff Water and Nutrient Fluxes from Biofuel Cropping Systems
Presenter(s) Polich, M., A.M. Thompson, and K.G. Karthikeyan
Presentation Type Poster session
Event Name Annual Meeting of the American Water Resources Associate WI Section
Event Location Lake Delton, WI
Event Date 3/1/2012
Target Audience Scientific audience
Audience Size 50
Description

Students & Post-Docs Supported

Student Name Augustin Brena
Campus Other

Advisor Name David Hyndman
Advisor Campus Other

Degree Post Doc
Graduation Month
Graduation Year
Department Geological Sciences
Program
Thesis Title
Thesis Abstract



Student Name Anthony Kendall
Campus Other

Advisor Name David Hyndman
Advisor Campus Other

Degree Post Doc
Graduation Month
Graduation Year
Department Geological Sciences
Program
Thesis Title
Thesis Abstract



Student Name Damodhar Mailapalli
Campus University of Wisconsin-Madison

Advisor Name Anita Thompson
Advisor Campus University of Wisconsin-Madison

Degree Post Doc
Graduation Month
Graduation Year
Department Biological Systems Engineering
Program

Thesis Title
Thesis Abstract

.....

Student Name Austin Parish
Campus Other

Advisor Name David Hyndman
Advisor Campus Other

Degree Masters
Graduation Month
Graduation Year
Department Geological Sciences
Program
Thesis Title
Thesis Abstract

.....

Student Name Michael Polich
Campus University of Wisconsin-Madison

Advisor Name Anita Thompson
Advisor Campus University of Wisconsin-Madison

Degree Expected Masters
Graduation Month
Graduation Year
Department Biological Systems Engineering
Program
Thesis Title
Thesis Abstract

.....

Student Name Ryan Stenjem
Campus University of Wisconsin-Madison

Advisor Name Anita Thompson
Advisor Campus University of Wisconsin-Madison

Degree Expected Masters
Graduation Month
Graduation Year
Department Biological Systems Engineering
Program Biological Systems Engineering
Thesis Title
Thesis Abstract

Undergraduate Students Supported

New Students: 0
Continuing Students: 2

Groundwater Research Characteristics and Subsurface Nutrient Dynamics Under Alternate Biofuel Cropping Systems in Wisconsin

Basic Information

Title:	Groundwater Research Characteristics and Subsurface Nutrient Dynamics Under Alternate Biofuel Cropping Systems in Wisconsin
Project Number:	2010WI2820
Start Date:	7/1/2010
End Date:	6/30/2012
Funding Source:	Other
Congressional District:	WI 2nd
Research Category:	Ground-water Flow and Transport
Focus Category:	Nutrients, Agriculture, Groundwater
Descriptors:	
Principal Investigators:	Anita Thompson, Randall Jackson, K. G. Karthikeyan

Publication

1. Stenjem, Ryan S. 2013. Subsurface water and nutrient dynamics of cellulosic biofuel cropping systems. M.S. Thesis, Biological Systems Engineering, University of Wisconsin, Madison, WI 134p.

Groundwater Recharge Characteristics and Subsurface Nutrient Dynamics Under Alternate Biofuel
Cropping Systems in Wisconsin

WRI Project Number WR10R003

Final Report

Submitted to the
University of Wisconsin
Water Resources Institute

January 2013

By

Anita Thompson
K.G. Karthikeyan
Randall Jackson

TABLE OF CONTENTS

List of Figures and Tables	ii
Project Summary	1
Introduction.....	3
Procedures and Methods.....	4
Results and Discussion	6
Conclusions and Recommendations.....	12
References.....	13
Appendix A: Publications and Presentations	15
Appendix B: Additional Material.....	16

LIST OF FIGURES AND TABLES

- Figure 1. Daily average soil profile water storage for SG, CC, and HP (cm of water per cm of soil). Water content measurements taken at 20 and 65 cm.
- Figure 2. Cumulative drainage for Period I in SG and CC. Error bars indicate cumulative standard error.
- Figure 3. Cumulative drainage for Period II from SG, CC, and HP. Error bars indicate cumulative standard error.
- Figure 4. Cumulative NO₃-N loading in SG and CC for Period I. Error bars indicate cumulative standard error.
- Figure B1. Locations of Arlington, WI; AARS; and the Biofuel Research Plots at AARS (Stenjem, 2013).
- Figure B2. Map of Great Lakes Bioenergy Research Center Biofuel Plots located at AARS (Courtesy of Gregg Sanford, GLBRC).
- Figure B3. (a) Lysimeter and spring plate inside soil cavity with screw jacks for installation beneath. Tensiometer wires shown to the left of lysimeter. (b) Lysimeter and spring plate installed. Woodenblocks under spring plate to maintain spring force and lysimeter contact with cavity ceiling.
- Figure B4. (a) Wooden weather treated support frames installed beneath angle irons to provide support to soil profile above cavity. (b) Weather treated plywood covering to prevent cavity from damage during backfilling. PVC tubes contain sensor wires and lysimeter tubing extends to the control box on soil surface.
- Figure B5. Volumetric water content at 20 cm (top) and 65 cm (bottom) in SG, CC, and HP from 5 Mar 2011 to 31 Aug 2012. At 20 cm time periods where soil was frozen have been excluded.
- Figure B6. Time series of drainage depths and Leaf Area Index for continuous corn during study.
- Figure B7. Time series of drainage depths and Leaf Area Index for switchgrass during study.
- Table 1. Seasonal time periods used to compare the cropping systems.
- Table 2. Cumulative drainage and standard errors for SG, CC, and HP during the study period. Means within a time period with different letters are statistically different ($p < 0.10$).
- Table 3. Average seasonal drainage depths, NO₃-N loads, DRP loads, and DOC loads for SG, CC, and HP. Values in parentheses are standard errors. Means with different letters are significantly different ($p < 0.10$).
- Table 4. Summer 2011 and 2012 water balances for CC and SG.
- Table 5. Average seasonal NO₃-N, DRP and DOC concentrations for SG, CC, and HP. Values in parentheses are standard errors. Means with different letters are significantly different ($p < 0.10$).
- Table B1. Planting and harvest dates, for the cellulosic biofuel cropping systems.
- Table B2. 2011 cellulosic biofuel cropping system yields at AARS.
- Table B3. 2011 growing season GLBRC fertilizer application dates, rates, and cumulative nutrient application rates for cellulosic biofuel cropping systems at AARS. Fertilizer guaranteed analysis (%N-%P₂O₅-%K₂O) provided.
- Table B4. Instrumentation installation depths in experimental field plots at AARS including GLBRC installed instrumentation.
- Table B5. AETL installation periods, data collection, water sampling, and nutrient analysis starting dates.
- Table B6. Precipitation (cm liquid water equivalent) depths for Arlington, WI during 2011 and 2012 (NOAA).
- Table B7. Monthly and 30 year average air temperatures (°C) during 2011 and 2012 at Arlington, WI (NOAA).
- Table B8. Soil NO₃-N analysis for CC and SG plots performed in August 2012.

PROJECT SUMMARY

Title: Groundwater Recharge Characteristics and Subsurface Nutrient Dynamics Under Alternate Biofuel Cropping Systems in Wisconsin

Project I.D.: WR10R003

Investigators: Anita Thompson, K.G. Karthikeyan, Randall Jackson

Period of Contract: July 1, 2010 – June 30, 2012

Background/Need: High yielding cropping systems such as perennial switchgrass and hybrid poplar trees have been proposed to supply feedstock to the latent cellulosic ethanol industry. Maintaining or expanding acreage in perennial crops and some pastures (or even idle Conservation Reserve Program (CRP) lands) will reduce acreage devoted to corn. While these systems are well known for producing large quantities of aboveground biomass, an important consideration is their relative sustainability in a variety of agroecological settings. The potential for widespread introduction of non-traditional agronomic cropping systems and management for cellulosic biofuel production has generated concerns about associated unintended environmental consequences. Knowledge gaps exist with regard to water and nutrient dynamics when alternative cropping systems are used in the context of meeting the needs for biofuel production. Few studies have investigated subsurface drainage from cellulosic biofuel crops under continued biofuel cropping management within the same environmental conditions.

Objectives: The major goal of this project was to further understanding of water and nutrient dynamics associated with biofuel cropping systems. The specific objective was to measure subsurface (below the root zone) drainage and nutrient (N, P, C) fluxes for continuous corn (CC), monoculture switchgrass (SG) and hybrid poplar (HP) cropping systems.

Methods: The study was conducted at the University of Wisconsin (UW) Arlington Agricultural Research Station (AARS) Arlington, Wisconsin. Experimental plots were established in a randomized complete block design near the southwest corner of the research station in the spring of 2008 by the DOE Great Lakes Bioenergy Research Center (GLBRC). Automated Equilibrium Tension Lysimeters, soil moisture and temperature sensors, and tensiometers were installed within eight plots (representing five different cropping treatments): two CC, two rotational corn (RC), two monoculture SG, one monoculture Miscanthus (MIS), and one HP cropping treatments. Sub-surface (below the root zone) drainage samples were collected weekly during wet periods (e.g. spring, early summer) and bi-weekly during dry periods (e.g. late summer, fall, winter). Samples were analyzed in our laboratory for dissolved reactive phosphorus (DRP), nitrite (NO_2), nitrate plus nitrite ($\text{NO}_3 + \text{NO}_2$), ammonium (NH_4^+), total nitrogen (TN), total phosphorus (TP), dissolved organic carbon (DOC), pH, and EC. The focus of this report is on the SC, CC, and HP cropping systems. Results for MIS and RC are not included because: (i) the MIS crop over the AETL was not well established during the study period, (ii) the crop rotation for one of the RC plots was changed after AETL installation, and (iii) only one replicate was available for each cropping system.

Results and Discussion:

Freeze/thaw dates for SG, CC, and HP varied by only a few days and only slight differences in temperature ($<2^\circ\text{C}$) were observed throughout the soil profiles during most of the study period. The largest differences occurred mainly during the early growing season when temperatures were warm and canopy among cropping systems was most different. Soil water depletion during the growing season was greater for CC than SG in 2011, but the opposite trend was observed in 2012; changes were more pronounced at shallow depths. We observed the perennial crops (SG and HP) to have higher soil water holding capacity throughout most of the study period. Differences in soil water are attributable to physiological differences between the crops including canopy cover and root structure.

Total drainage throughout the study period followed the order SG > CC >> HP and most drainage occurred in the spring and early growing season. More drainage occurred from SG than CC in spring and winter seasons and this trend was reversed during summer and fall. Seasonal drainage from HP was always lower than SG and CC.

Total nitrate (NO₃-N) loading during the study period followed the order CC >> SG > HP and the greatest loads occurred in the spring and early growing season. Average seasonal NO₃-N concentrations were higher for CC than SG throughout the year and exceeded 90 mg/L in most seasons. No samples from HP during the study had detectable NO₃-N concentrations. Greater NO₃-N loads were calculated for CC than SG throughout the study period; NO₃-N load from HP could not be determined. Almost all of the N losses occurred in the NO₃-N form. Differences between cropping systems could be due in part to excessive fertilizer applied to the CC plots.

Similar to the drainage trends, DRP loadings were greater for SG than for CC during spring and winter with the opposite trend occurring during summer and fall. All seasonal loads were below 0.30 kg/ha; the highest and lowest export was observed for SG and HP, respectively. Similar to our observations for N, most of the P losses occurred in the dissolved form.

No significant differences in DOC concentration were observed among cropping treatments within seasons. The overall average DOC concentration of all samples was 5.0 ± 0.3 mg/L. Seasonal differences in DOC loading followed drainage trends. DOC loading in CC was significantly higher than SG in summer and fall; conversely, in winter and spring, DOC loading from SG was significantly higher than both CC and HP. The ability of SG to store more carbon in the soil profile may have contributed to the greater DOC loadings in winter and spring.

Conclusions/Implications/Recommendations: As cellulosic biofuel production expands, cropping systems will need to be matched to climate, soils, and environmental concerns in a region, due to differential impacts of each cropping system on water and nutrient dynamics. Results from this study suggest that high yielding perennial cropping systems, such as switchgrass and hybrid poplar, could reduce NO₃-N losses compared to systems involving corn (as the latter also requires additional N inputs). However, switchgrass systems could be vulnerable to leak more nutrients during seasons when ET demand is low (spring, winter) leading to high drainage volumes. Limited data (only for 1 season) indicate that both drainage rates and nutrient losses could be lower under hybrid poplar throughout the year. Selection of appropriate cropping systems for a region should consider potential differences in leachate dynamics and nutrient concentrations to minimize environmental impacts of biofuel production systems.

Research on subsurface drainage quantity and quality should be extended to additional cropping systems with continued biomass removal on different soil types and physiographic conditions. These cropping systems could include native species, such as, prairie plantings or other biodiverse combinations (e.g., annual + perennial crops). Future studies should also encompass long-term monitoring (over several growing seasons), which will facilitate the development and rigorous validation of models that can be applied at various spatial scales. With the cellulosic biofuel demand expected to grow rapidly in the next decade, research needs to keep up with implementation and relay information to producers to ensure that reducing fossil fuel imports does not come at the cost of degraded environmental resources.

Related Publications: Stenjem, R.S. 2013. Subsurface water and nutrient dynamics of cellulosic biofuel cropping systems. M.S. Thesis, University of Wisconsin – Madison.

Key Words: Nitrogen, Phosphorus, Carbon, Leachate, Corn, Switchgrass, Hybrid Poplar

Funding: University of Wisconsin – Madison Water Resources Institute

I. INTRODUCTION

Corn grain is currently the primary feedstock for biofuel ethanol production in the United States (U.S.), which spurred farmers to plant the most U.S. corn acres since WWII (93.5 million ac.) in 2007, and the last three years had the 4th, 3rd and 2nd most U.S. acres of corn planted, respectively, since WWII (NASS, 2010). Biofuel production from grain-based crop production systems, by promoting increases in corn acreage, can have significant water quality implications. Use of corn grain for ethanol potentially diverts food grain; in 2011, an estimated 5 billion bushels of corn grain (40% of total production) was dedicated to ethanol production (USDA, 2012). Additionally, corn is a high input crop requiring fertilizers, herbicides, and pesticides to maximize yields (Sims et al., 2010). Cellulosic ethanol production, where the vegetative part of plants is converted to fuel, promises to relieve our reliance on fossil fuels to a greater degree than grain-based ethanol (Sims et al., 2006; Escobar et al., 2009). To maximize fuel yields, fast growing, high biomass-yielding crops are the most favorable alternatives (Solomon et al., 2007). However, the infrastructure to generate ethanol from potential sources such as perennial grasses and fast growing woody species is not well developed as those existing for grain-based sources.

High yielding cropping systems (e.g., perennial switchgrass, hybrid poplar trees) have been proposed to supply feedstock to the latent cellulosic ethanol industry. Maintaining or expanding acreage in perennial crops and some pastures (or even idle Conservation Reserve Program (CRP) lands) will reduce acreage devoted to corn. While these systems are well known for producing large quantities of aboveground biomass, an important consideration is their relative sustainability in a variety of agroecological settings (Jordan et al., 2007). While alternative cropping systems are better suited to provide and sustain beneficial ecosystem services, their effects on water and nutrient dynamics when used in the context of meeting the needs for biofuel production are unknown. Current estimates for cellulosic fuel yields range widely because of variations in climate, soils, topography, and conversion technologies. Based on fuel yield estimates for corn stover and switchgrass in climates similar to the Midwestern U.S. (Schmer et al., 2012; Sindelar et al., 2012), roughly 16-35 million ha of suitable land would be needed to achieve the U.S. goal (Energy Independence and Security Act of 2007) of 60.6 billion L yr⁻¹ of cellulosic biofuels by 2022.

The potential widespread introduction of non-traditional agronomic cropping systems and management for cellulosic biofuel production has generated environmental concerns. If cellulosic biofuels gain acceptance, modern agriculture is expected to produce enough crops to meet the food, fiber, and energy demands of an ever growing population (Uhlenbrook, 2007; Escobar et al., 2009). From an environmental sustainability standpoint, competition for and contamination of irrigation or drinking water supplies needs to be considered, as well as all potential impacts on the hydrologic balance (Uhlenbrook, 2007). Feedstock crops will need to be selected based on land types due to spatial variations in water availability, soils, topography, etc. (Carroll and Somerville, 2009) and to minimize environmental impacts.

Field plots comprising cropping systems that are well known for their biomass production potential and favored in the Great Lakes Region for cellulosic ethanol production were established in 2008 through the DOE Great Lakes Bioenergy Research Center (GLBRC) at the Arlington Agricultural Research Station (AARS), Arlington WI. Two of these systems represent Type I feedstock crops (U.S. DOE, 2006), continuous corn and corn-soybean rotation, i.e., being historically used for food production they have undergone extensive selection for grain production traits. Switchgrass is a C4 perennial grass that is native to North America (Sanderson et al., 2006) and has been identified for its biofuel feedstock potential because it: (i) is perennial, tolerates repeated defoliation, (ii) is adapted to a wide range of environmental conditions (Sanderson and Wolf, 1995; Casler et al., 2004), (iii) has high tolerance to drought, nutrient deficiencies, and high temperatures (Sage and Zhu, 2011), (iv) sequesters large amounts of C in soils, and (v) provides good wildlife habitat. In addition, switchgrass has been sown on millions of acres of CRP land throughout the Midwest. Hybrid poplar has been identified as a key feedstock for biofuel production throughout much of the U.S., including the Great Lakes Region (U.S. DOE, 2006). The trees produce large quantities of aboveground biomass in 5-yr cycles. Poplar provides several advantages relative to

traditional row crops: it requires less fertilizer, can be grown on marginally productive soils, and provides structural and biological diversity within a landscape.

Understanding water and nutrient dynamics associated with biofuel crop production will be critical to protecting water resources. Few studies have investigated subsurface drainage from cellulosic biofuel crops under continued biofuel cropping management within the same environmental conditions. This report summarizes findings from a study investigating subsurface (below the root zone) drainage and nutrient loads from continuous corn, monoculture switchgrass, and hybrid poplar.

II. PROCEDURES AND METHODS

Study Site: The study was conducted at the University of Wisconsin (UW) AARS, Arlington, WI (43° 17' N, 89° 22' W; Fig. B1, Appendix B). Experimental plots were established in a randomized complete block design (60 plots divided into five, 12-plot blocks; Fig. B2, Appendix B) near the southwest corner of the research station in the spring of 2008 by GLBRC. Eight plots (representing five different cropping treatments) were selected to investigate subsurface drainage and nutrient dynamics: two continuous corn (CC), two rotational corn (RC), two monoculture switchgrass (SG), one monoculture Miscanthus (MIS), and one hybrid poplar (HP) cropping treatments. Each plot measured 27.4 m W by 42.7 m L and was subdivided into a main plot section and two edge effect sections. All drainage and soil monitoring equipment was installed within or immediately adjacent to the main plot area and disturbance associated with installation was limited to the edge areas. Crops were managed (by GLBRC personnel) according to UW-Extension recommendations for planting, harvesting, and rates of pesticide, herbicide, and fertilizer application. Planting and harvest dates, 2011 yields, fertilizer rates and application dates are provided in Tables B1-B3 of Appendix B (data provided by Dr. Sanford, Assistant Scientist, GLBRC).

Soils and Climate: The primarily prairie soils and continental humid climate of Arlington, WI, are typical for the upper Midwestern U.S. The soils within the study plots are primarily well drained Plano Silt Loam soils with 0-6% slopes. Average profiles for these soils are: silt loam 0-0.3m, clay loam 0.3-1.1m, and sandy loam 1.1-1.5m (NRCS Web Soil Survey). Average annual precipitation at Arlington is 83.7 cm, with nearly half (40.1 cm) falling from Jun. through Sep. Average monthly maximum temperatures range from -5°C (Jan.) to 27.2°C (Jul.) and minimum temperatures from -13.3°C (Jan.) to 15.6°C (Jul.).

Equipment: Automated Equilibrium Tension Lysimeters (AETLs) were installed to measure subsurface (below the root zone) drainage from each cropping system. The AETLs utilized suction to sample water draining through the soil profile directly above the lysimeter. The suction was automatically adjusted based on measured soil-water tension in the surrounding soil, thereby minimizing convergent/divergent flows to/around the lysimeter. Each AETL included a lysimeter, soil monitoring instrumentation, control box, and control program.

Lysimeters measured 25cm W x 75cm L x 15 cm H (constructed by Dick's Superior Metal Sales, Madison, WI.) and were constructed of 1.6 mm thick stainless steel, with a 1 mm thick porous stainless steel top with 0.2 µm diameter pores (Mott Metallurgical Corporation, Farmington, CT) that allowed water to flow from the soil into the lysimeter. Two sheets of filter paper (1.0 µm over 0.5 µm; Pargreen Process Technologies, Addison, IL) were placed on the top of the porous plate and wetted with DI water. The filter paper maintained moisture near the porous plate during dry periods. Two stainless steel tubes (6.4 mm O.D.) at the base of the lysimeter functioned as vacuum and sample tubes. Electric tensiometers (heat dissipation sensors; model 229, Campbell Scientific, Logan, UT) were used to measure soil-water tension and set appropriate lysimeter suction. Each tensiometer was calibrated using a pressure plate extractor system (Product Number 1600; Soil Moisture Equipment Corporation, Goleta, CA). Water content reflectometers (CS616; Campbell Scientific, Logan, UT) were used to monitor changes in soil water storage and a site specific calibration was conducted. Type-T (copper-Constantine) thermocouples were used to monitor temperature throughout the soil profile. Each AETL was operated by a control box that consisted of a datalogger (10X, 23X, CR1000; Campbell Scientific, Logan, UT) to run the control program and measure soil sensors, an excitation module to heat the tensiometers, pneumatic valves

(operated by a 12V relay driver) for controlling pumping and bleeding, and a pump to pull air from the lysimeter. Dataloggers were programmed to: (i) measure matric potential, moisture content and temperature, (ii) monitor and set appropriate suction in the lysimeter, and (iii) store hourly averages of all data. Instrumentation depths are provided in Table B4 of Appendix B.

Installation: Eleven lysimeters were installed within the eight plots: for CC and SG (3; within and between plot replication); RC¹ (2; between plot replication); HP (2; within plot replication) and MIS (1; no replication). Lysimeters were installed beneath undisturbed soil profiles by excavating into the wall of large soil pits as close to the main plot as possible. Lysimeters within SG and MIS plots were installed just inside the main plot. Lysimeters within RC and CC plots were installed one corn row just east of the main plot and spanned two corn rows. Lysimeters within the HP plot were installed within the edge section. Lysimeters were positioned such that the top was just above the interface of the clay-loam B and sandy C horizons. Any water leaving the B horizon was considered representative of potential ground water recharge. Due to spatial variation in soil horizons, the lysimeter depths varied among plots (0.6 – 1.45m). Two or four water content reflectometers and two or four thermocouples were installed in the soil pit wall near the lysimeter. Tensiometers were installed above the porous plate of the lysimeter and in the bulk soil (in the B-Horizon 10-15 cm from the back edge and at the depth of the top of the lysimeter); differences measured indicated convergent/divergent flow or tensiometer failure.

Lysimeters were positioned in contact with the ceiling of the soil cavity and supported by a spring plate and wood blocks (Fig. B3, Appendix B). Stainless steel tubing was connected to the sample and vacuum tubes and extended outside the cavity where rubber tubing was attached and extended to the soil surface. Wooden support frames supported the soil above the cavity and plywood covered the soil cavity and protected the lysimeter during backfilling (Fig. B4, Appendix B). All wires/tubes were bundled inside PVC pipe and connected to a control box outside of the plot. Additional details on the equipment, calibration procedures, instrumentation levels and depths of sensors are provided in Stenjem (2013).

Sampling: Subsurface (below the root zone) drainage samples were collected weekly during wet periods (e.g. spring, early summer) and bi-weekly during dry periods (e.g. late summer, fall, winter), to ensure sufficient volumes for nutrient analyses. Due to differences in installation dates and troubleshooting periods, data collection start times for each lysimeter varied (Table B5, Appendix B).

Leachate was collected via the lysimeter sampling tube using a ½ HP vacuum pump and 0.75 L vacuum trap, powered by a portable generator. Approximately 750 mL of water from each lysimeter was collected to flush the vacuum trap and sample hoses. Another 750 mL was then collected, split and sub-sampled for nutrient analyses. A 125 mL sub-sample was acid preserved for NO₃, NH₄, TN, TP and DOC analysis. An additional 120 mL was divided into two 60 mL bottles: one was field-filtered (0.45 µm) for NO₃ and DRP analyses and the other unfiltered for pH and EC. Additional water was pumped from the lysimeter and the total volume was recorded. During dry periods, when < 750 mL of water was present in the lysimeter, no nutrient analyses were conducted, due to contamination issues with insufficient flush volume.

Samples were analyzed in our laboratory for dissolved reactive phosphorus (DRP), nitrite (NO₂), nitrate plus nitrite (NO₃ + NO₂), ammonium (NH₄⁺), total nitrogen (TN), total phosphorus (TP), dissolved organic carbon (DOC), pH, and EC. All nutrients (except DOC) were analyzed using an AQ2 Discrete Analyzer (Seal Analytical, Hampshire, U.K.) according to USEPA methods. DOC was analyzed using a DR5000 UV-vis spectrophotometer (Hach Company, Loveland, CO) and pre-assembled test kit (Product # 2815945; Hach Company, Ames IA) following digestion using a Hach DRB200 Digital Reactor Block. Additional details on the analytical methods are provided in Stenjem (2013).

¹ In 2011 plot 406 (Fig. B2, Appendix B) was planted in corn as part of a corn-canola-soybean rotation. Plot 408 utilized the same rotation and was installed in Oct 2011, with corn production expected in 2012. In spring 2012 the cropping rotations were modified by the GLBRC. Plot 406 was then designated as part of a continuous corn with winter cover crop rotation and plot 408 was planted in a corn-soybean rotation, starting with soybeans in 2012.

Data Analysis: Two cumulative time periods (Period I: 14 Apr 2011 to 31 Aug 2012; Period II: 13 Jul 2011 to 31 Aug 2012) were selected for analysis. The start dates correspond to the first sampling date for the SG/CC and HP cropping systems. Additionally, the study period was sub-divided into six seasons (Table 1) for comparison of drainage depth, average nutrient concentrations and loadings among SG, CC, and HP. Results for MIS and RC are not included as: (i) the MIS crop over the AETL was not well established, (ii) the crop rotation for one of the RC plots was changed after AETL installation, and (iii) only one replicate is available for each cropping system; however results are provided in Stenjem (2013).

Table 1 – Seasonal time periods used to compare the cropping systems.

Season	Time Period
Spring 2011	1 Apr 2011 to 15 June 2011
Summer 2011	15 June 2011 to 21 Sept 2011
Fall 2011	21 Sept 2011 to 20 Dec 2011
Winter 2012	20 Dec 2011 to 20 Mar 2012
Spring 2012	20 Mar 2012 to 12 June 2012
Summer 2012	12 June 2012 to 31 Aug 2012

Average drainage depth, nutrient (NO₃-N, NH₄-N, DRP, DOC) concentration and load were calculated for each sampling date and cropping system and summed for each time period. Cumulative standard errors were calculated for seasonal values of drainage depth, nutrient concentration and load. A water balance was calculated for summer 2011 and 2012. Evapotranspiration (ET) was estimated as the residual of measured precipitation (P), runoff (RO), soil water storage (Δ S), and drainage (D). Runoff was directly measured using 1 m² drainage area collectors installed in CC and SG cropping systems. Samples with concentrations below the detectable limit were excluded from the average. If an AETL was not functioning during a sampling interval that replicate was excluded from the treatment average and variance calculations for that interval. Cumulative nutrient loads and standard errors for each time period and cropping system were calculated. Pairwise Welch's t-tests were performed for statistical comparisons among cropping treatments ($\alpha = 0.1$). Welch's t-test has less power than the standard t-test; however, it was selected due to the low level of replication and large variability within/among cropping systems.

III. RESULTS AND DISCUSSION

Climatic Conditions: During the study period (1 Apr 2011 to 31 Aug 2012) there was 114.0 cm of precipitation (rainfall and snow liquid water equivalent). Precipitation from Apr to Dec 2011 and from Jan to Aug 2012 was below the 30-year annual average (1981-2010) for Arlington, WI, by 5.0 and 12.2 cm, respectively. Air temperatures for 10 of the 17 study months were warmer than the 30-year monthly average temperatures (1981-2010) for Arlington, WI. Monthly precipitation and average air temperatures are given in Appendix B (Tables B6 and B7).

Soil Temperature: Differences in soil profile temperatures between SG, CC, and HP were not large; freeze/thaw dates varied by only a few days and only slight differences (1-2°C) were observed throughout the soil profiles during most of the study period. The largest differences occurred mainly during the early growing season when temperatures were warm and canopy among cropping systems was most different.

In 2012, the soil profile in all treatments was thawed (temperature at 20 cm > 0°C) between 5 - 9 Mar, approximately 3 wks earlier than in 2011. The thaw date for HP was later than SG and CC, possibly because leaf litter was not removed from HP. Residue remaining on the soil surface acts as an insulator, resulting in later thaw dates in the spring (Dormaar and Carefoot, 1996).

Slight differences in soil temperature were measured early in the growing season (May-Jun). From 1 Jun 2011 to 1 Jul 2011 the soil temperature at 20 cm in CC was 0.5 to 2 °C warmer than that in SG. The fast growing thick canopy of the SG likely shaded the ground while the CC had much more exposed soil. Later in the growing season, after canopy development in CC, these differences were not observed. The same trend with larger differences was observed in 2012. Soil temperatures for the cropping systems were

generally within 0.5 °C during Mar and Apr. By 25 May 2012, temperature at 20 cm was in the following order: CC (21.5 °C) > SG (19.7 °C) > HP (18.6 °C). The difference between CC and SG fluctuated in June; however, CC was approximately 2 °C higher than SG until after 4 Jul 2012. After 25 May, temperatures for SG and HP were similar (within 1 °C).

Soil Moisture: Average daily volumetric water content (VWC) data for CC, SG, and HP (at 20 and 65 cm) are included in Appendix B (Fig. B5). VWC measurements were used to estimate average daily soil profile water storage (cm water/cm soil) from the soil surface to a depth of 65 cm (Fig. 1). Periods when soil was frozen below 20 cm depth were excluded. The decrease in VWC during the growing season was greater for CC than SG in 2011 but greater for SG than CC in 2012; changes were more pronounced at 20 cm depth. In 2011, both SG and CC maximum and minimum VWC measurements occurred on the same dates (except min. VWC at 20 cm) (Fig. B5, Appendix B). Warm and dry conditions in 2012 resulted in larger differences in soil-water distribution among the cropping systems. Maximum VWC was attained earlier in SG and HP (7-8 May) than in CC plots (25 May); warmer conditions in spring 2012 caused HP and SG to begin transpiring earlier than in 2011 and well before CC was planted. The field capacity, wilting point, and saturation for Plano Silt Loam soil are approximately 30.3, 15.2 and 40% over 0-60cm depth (NRCS Web Soil Survey).

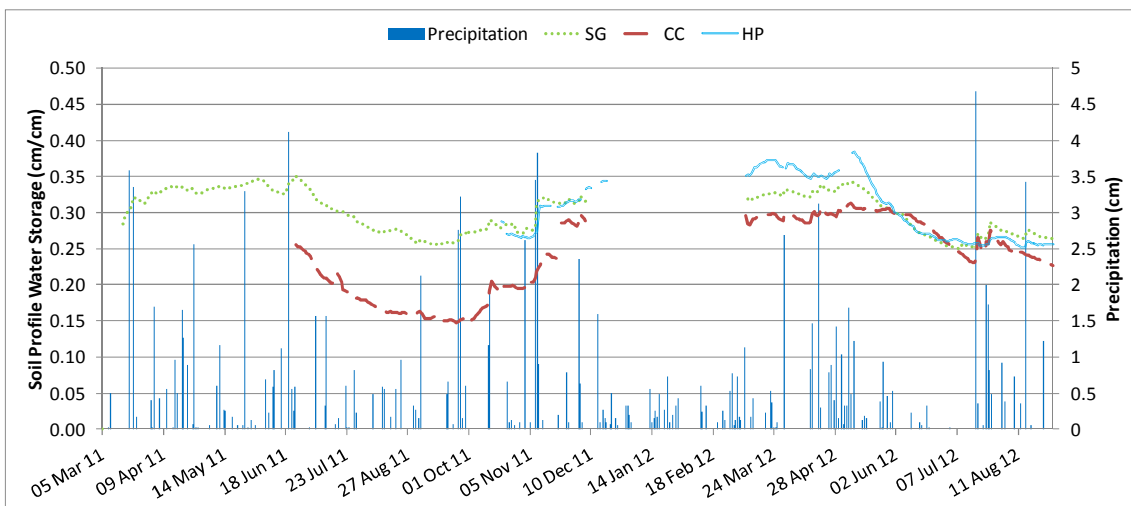


Figure 1. Daily average soil profile water storage for SG, CC, and HP (cm of water per cm of soil). Water content measurements taken at 20 and 65 cm.

We observed the perennial crops to have higher soil water holding capacity through most of the study period. The water stored in the soil profile in SG was higher than CC from the beginning of data collection until 1 Jun 2012 (Fig. 1); in early-Oct 2011 this difference was as large as 0.13 cm/cm. Soil water storage was higher under HP than both CC and SG during spring 2012; however, as the cropping systems began transpiring differences in soil water content became negligible.

The soil-water differences between SG and CC are likely due to physiological differences between the crops. According to McClassac et al. (2010), the dense canopy of switchgrass provides more shade than corn, which reduces evaporation throughout the growing season resulting in higher soil-water content. Furthermore, the root structure of switchgrass is dense and deep and the constant decay of dead roots provides organic matter enrichment (Percival et al., 2000; Blanco-Canqui, 2010) which improves water holding capacity of the soil, preventing the draw down observed in the corn crop (Fageria, 2012).

Drainage Depth: For Period I, cumulative drainage at SG and CC represented 44% and 36% of the total 115.2 cm of precipitation received (30-year average = 127.4 cm); drainage for CC and SG was not significantly different ($p=0.27$; Table 2). For Period II, drainage for SG, CC, and HP represented 45%,

30%, and 5%, respectively, of the total 88.6 cm of precipitation (30-year average = 99.9 cm); drainage in SG and CC were significantly greater than that in HP ($p < 0.05$) and SG was significantly different from CC ($p < 0.05$). All drainage during this time period occurred after 10 Nov 2011. Brye et al. (2000) reported similar drainage-to-precipitation ratios for no-till corn fields at AARS (35% in 1996; 43% in 1997). Most of the drainage from SG and CC occurred during spring and early summer (Fig. 2 and 3), prior to significant aboveground vegetation development (indicated by inverse relationship between Leaf Area Index (LAI) and drainage depth as shown in Appendix B, Figures B6 and B7). No drainage was measured during the mid-growing season, attributable to increased ET, and late fall. Similar season-dependent trends were reported by Brye et al. (2000).

Table 2. Cumulative drainage and standard errors for SG, CC, and HP during the study period. Means within a time period with different letters are statistically different ($p < 0.10$).

	Precipitation (cm)	Drainage (cm)		
		SG	CC	HP
14-Apr-11 to 31-Aug-12	115.2	50.9 ^a ± 4.8	41.4 ^a ± 1.8	-
13-Jul-11 to 31-Aug-12	89.1	39.8 ^a ± 4.0	26.3 ^b ± 1.3	4.8 ^c ± 1.4

Switchgrass has been reported to lower soil bulk density compared to corn rotations (Bharati et al., 2002; Rachman et al., 2004), partly explained by more continuous macropores created by root channels and biological activity (Blanco-Canqui, 2010). Additionally, dense switchgrass canopy cover intercepts raindrops, preventing soil surface sealing, reducing runoff and increasing infiltration (Blanco-Canqui, 2010). These properties may explain the drainage differences between CC and SG.

Interestingly, a single sampling period, from 20 Feb 2012 to 5 Mar 2012, yielded 9.1 cm of drainage from SG, which is 18% of the total drainage from SG for the entire study period. This sampling period coincided with the earlier and faster than normal thaw in 2012 and suggests that increased infiltration facilitated by SG may allow for more drainage during large rainfall or thaw events. Drainage from SG was the greatest overall, with most occurring early in the growing seasons of 2011 and 2012.

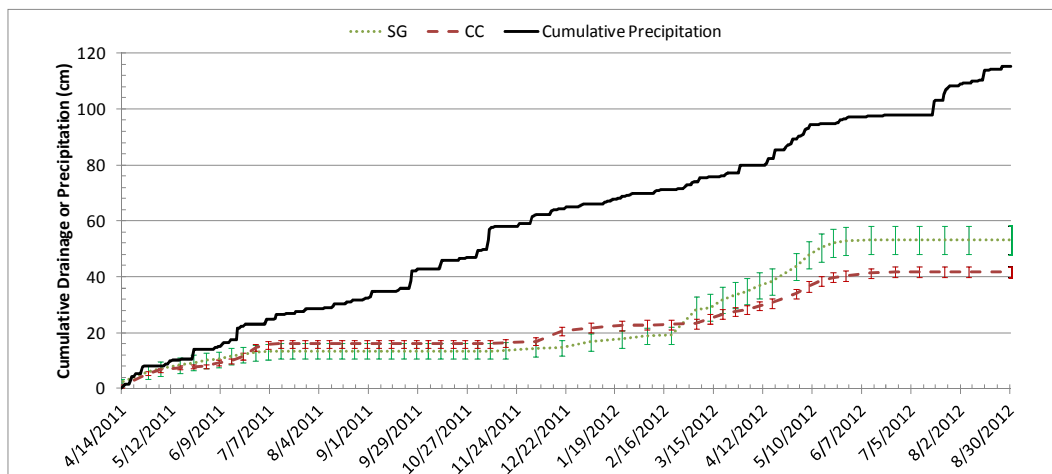


Figure 2. Cumulative drainage for Period I in SG and CC. Error bars indicate cumulative standard error.

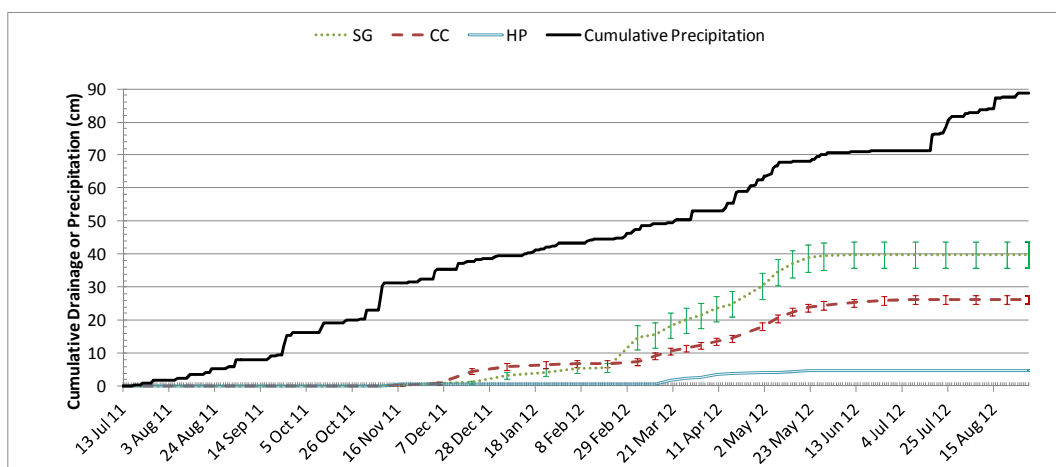


Figure 3. Cumulative drainage for Period II from SG, CC, and HP. Error bars indicate cumulative standard error.

Seasonal differences in drainage were observed among these cropping systems (Table 3). More drainage occurred from SG than CC in spring 2011 (4.6 cm; $p=0.37$), winter 2012 (10.6 cm; $p<0.10$), and spring 2012 (6.5 cm; $p<0.05$). Conversely, more drainage occurred from CC than SG in summer 2011 (4.1 cm; $p<0.05$), fall 2011 (2.5 cm; $p=0.29$), and summer 2012 (0.9 cm; $p<0.05$). Drainage from HP was always lower than in SG and CC. The differences in drainage among cropping systems could be partially attributed to differences in soil surface cover. After harvest and before planting (winter and spring), CC had lower surface residue cover, which results in reduced infiltration (Blanco-Conqui and Lal, 2009). Additionally, macropore development in SG likely enhanced infiltration and drainage during winter and spring. During summer and fall, ET differences between the cropping systems, particularly in the early summer when SG canopy developed earlier than CC, likely impacted drainage.

Table 3. Average seasonal drainage depths, $\text{NO}_3\text{-N}$ loads, DRP loads, and DOC loads for SG, CC, and HP. Values in parentheses are standard errors. Means within seasons with different letters are significantly different ($p<0.10$).

Season	Drainage Depth (cm)			$\text{NO}_3\text{-N}$ load (kg/ha)			DRP load (kg/ha)			DOC load (kg/ha)		
	SG	CC	HP	SG	CC	HP ¹	SG	CC	HP	SG	CC	HP
Spring 11	14.1 ^a (2.8)	9.5 ^a (0.8)	-	12.6 ^a (0.5)	85.2 ^b (1.5)	-	0.06 ^a (0.01)	0.02 ^a (0.002)	-	-	-	-
Summer 11	1.7 ^a (0.6)	5.8 ^b (1.1)	-	2.0 ^a (0.3)	55.3 ^b (3.0)	-	0.02 ^a (0.004)	0.09 ^b (0.011)	-	0.48 ^a (0.25)	1.87 ^b (0.35)	-
Fall 11	3.1 ^a (1.0)	5.6 ^a (1.2)	0.7 ^a (0.8)	0.3 ^a (0.4)	26.2 ^a (7.0)	0.0 (0.0)	0.00 ^a (0.002)	0.04 ^a (0.009)	0.00 ^a (0.0)	0.14 ^a (0.13)	2.1 ^b (0.03)	0.00 ^a (0.0)
Winter 12	16.4 ^a (3.6)	5.8 ^b (0.5)	1.0 ^c (1.1)	6.1 ^a (1.3)	56.5 ^a (15.1)	0.0 (0.0)	0.29 ^a (0.023)	0.03 ^b (0.011)	0.00 ^b (0.0)	8.59 ^a (0.41)	2.36 ^b (0.11)	1.11 ^c (0.13)
Spring 12	20.5 ^a (1.4)	14.0 ^b (0.6)	3.1 ^c (1.0)	9.4 ^a (2.5)	137.5 ^b (11.0)	0.0 (0.0)	0.17 ^a (0.008)	0.06 ^b (0.008)	0.00 ^c (0.001)	7.05 ^a (0.36)	4.30 ^b (0.31)	0.54 ^c (0.04)
Summer 12	0.0 ^a (0.0)	0.9 ^b (0.2)	0.0 ^a (0.0)	0.0 ^a (0.0)	4.7 ^a (3.0)	0.0 (0.0)	0.00 ^a (0.00)	0.00 ^a (0.001)	0.00 ^a (0.0)	0.00 ^a (0.0)	0.26 ^a (0.12)	0.00 ^a (0.0)

Water Balance: A water balance was calculated for summer 2011 and summer 2012. In both summers, more drainage occurred from CC than SG and soil water storage in CC decreased more than SG. Lower water requirements for CC than SG in the early summer (result of different growth stages), likely explain the greater drainage from CC. Evapotranspiration, the residual of the measured water balance components, was the largest component of the water balance for CC and SG in both summers (Table 4). Despite very dry conditions in Jun 2012, more rainfall occurred in summer 2012 than summer 2011. However, the heaviest rainfall occurred after crops were established and virtually no runoff was produced during summer 2012.

Table 4. Summer 2011 and 2012 water balances for CC and SG

Summer 2011			Summer 2012		
	CC	SG		CC	SG
Precip(cm)	13.4	13.4	Precip (cm)	17.7	17.7
ΔS (cm)	-14.0	-12.9	ΔS (cm)	-1.5	-0.1
Runoff (cm)	1.7	0.1	Runoff (cm)	0.0	0.0
Drainage(cm)	5.8	1.7	Drainage (cm)	0.9	0.1
ET (cm)	19.9	24.5	ET (cm)	18.3	17.7

Nitrate: Nitrate loading during Period I was greater in CC than SG (Fig. 4). The total NO₃-N load to the lysimeters during this time was 329.5 ± 15.7 kg/ha in CC, and 28.0 ± 3.4 kg/ha in SG. Both cropping treatments exhibited similar patterns in loading; the highest rates of loading occurred in Mar-Jun, no loading occurred during Jul-Aug, followed by minimal loading between Sep-Feb. Nitrate loading for Period II was greater in CC than SG and no loading was measured in HP. Total NO₃-N loading during this time was 189.3 ± 15.1 kg/ha in CC and 15.3 ± 3.3 kg/ha in SG.

Nitrogen fertilization likely contributed to the different NO₃-N loadings. Both CC and SG received similar levels of N fertilizer in 2011 (65 kg/ha in CC; 55 kg/ha in SG), despite high soil test NO₃-N in the CC plot (#411, Fig. B2) (149 kg NO₃-N/ha). At this soil N level, UW-Extension does not recommend N fertilizer application to corn grown in silt loam soils (Laboski et al., 2006). Trends in water-extractable NO₃-N (Table B8, Appendix B) also point to the presence of higher soil NO₃-N in the CC plots.

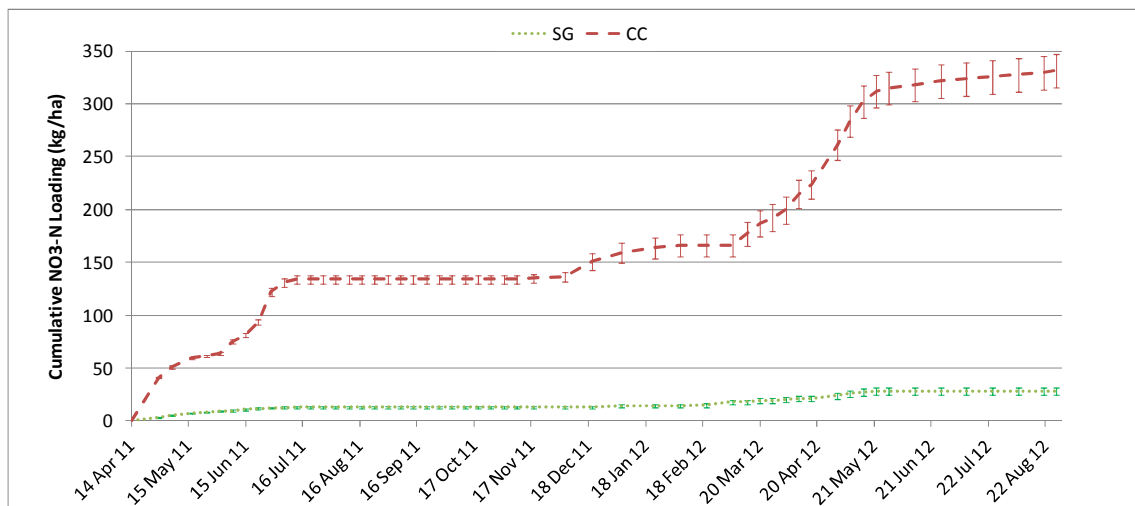


Figure 4. Cumulative NO₃-N loading in SG and CC for Period I. Error bars indicate cumulative standard error.

Average seasonal NO₃-N leachate concentration was higher for CC than SG at all times of the year (Table 5). During spring 2011, summer 2011, winter 2012, and spring 2012, NO₃-N concentrations from CC exceeded 90 mg/L (range of 93.7 to 98.8 mg/L). During all seasons, NO₃-N concentrations from CC were significantly greater than those in drainage from SG plots (p<0.10). It is important to note that average NO₃-N concentrations from SG plots exceeded the EPA drinking water standard of 10 mg/L during the spring (10.7 mg/L) and summer (12.3 mg/L) of 2011. No samples collected during the study from the HP cropping system had detectable concentrations of NO₃-N (0.25 mg /L).

Nitrate concentrations for CC were greater than the range of 15-40 mg/L reported for corn in similar studies in the Midwestern U.S. (Owens, 1990; Andraski et al., 2000; Brye et al., 2003; Rekha et al., 2011). The higher NO₃-N concentrations could be due to excessive fertilizer applied to the CC plots; other studies aimed to apply optimum levels of N fertilizer. The higher NO₃-N concentrations in CC resulted in greater loads than SG throughout the study period which were significantly different (p<0.1) in

spring and summer 2011, and spring 2012 (Table 3). The differences were not significant during fall 2011 ($p=0.17$), winter 2012 ($p=0.19$), and summer 2012 ($p=0.26$).

During our 17-month study period, ~330 kg NO₃-N/ha leached from the CC cropping system while <190 kg N/ha was added in the form of N fertilizers. The soil-test NO₃-N level in one of the CC plots was 149 kg NO₃-N/ha. Brye et al. (2003) attempted to quantify the N balance for corn cropping systems with varying tillage and reported net N leaving the soil profile (as high as 150 kg NO₃-N/ha) in corn cropping systems. However, the authors pointed to the difficulty in quantifying the N cycle in-situ at small (plot) scale levels. Over their 3.5-year study duration, the average annual N balance residual in no-till optimally-fertilized corn ranged between -64 and +115 kg/ha (negative number indicates N outputs > N inputs). Brye et al. (2003) suggested longer periods of time (>5 years) are required to evaluate the N balance of corn as mineralization rates of soil organic matter are driven by climatic conditions and can vary greatly from year to year and spatially depending on soil conditions.

Table 5. Average seasonal NO₃-N, DRP and DOC concentrations for SG, CC, and HP. Values in parentheses are standard errors. Means within seasons with different letters are significantly different ($p<0.10$).

Season	NO ₃ -N concentration (mg/L)			DRP concentration (mg/L)			DOC concentration (mg/L)		
	SG	CC	HP	SG	CC	HP	SG	CC	HP
Spring 11	10.8 ^a (0.76)	98.4 ^b (1.95)	-	0.06 ^a (0.01)	0.02 ^b (0.002)	-	-	-	-
Summer 11	12.3 ^a (0.92)	97.6 ^b (5.7)	-	0.09 ^a (0.02)	0.12 ^a (0.02)	-	3.4 ^a (1.6)	2.6 ^a (0.8)	-
Fall 11	5.9 ^a (2.7)	53.3 ^b (18.2)	0.43 (0.0)	0.04 ^a (0.02)	0.10 ^a (0.03)	0.06 ^a (0.02)	1.7 ^a (1.0)	3.6 ^a (1.6)	1.7 ^a (0.8)
Winter 12	4.6 ^a (1.6)	98.8 ^b (18.3)	0.0 (0.0)	0.11 ^a (0.02)	0.05 ^b (0.01)	0.02 ^c (0.004)	5.9 ^a (1.0)	4.2 ^a (1.4)	7.5 ^a (1.3)
Spring 12	5.7 ^a (1.5)	93.66 ^b (8.2)	0.0 (0.0)	0.08 ^a (0.00)	0.04 ^b (0.01)	0.02 ^c (0.01)	3.1 ^a (0.4)	3.2 ^a (0.4)	3.8 ^a (1.0)
Summer 12	0.0 ^a (0.0)	70.99 ^b (11.2)	0.0 (0.0)	0.00 (0.00)	0.03 (0.00)	0.00 (0.0)	0.00 (0.0)	3.9 (0.3)	0.00 (0.0)

Ammonium: NH₄-N concentrations/loadings were low for all treatments with the majority (81%) of samples containing < 0.02 mg/L. NH₄-N average concentrations (< 0.11mg/L) were not statistically different among cropping systems during any season. Loadings for all treatments were <0.06 kg NH₄-N/ha, except in winter 2012 (<0.12 kg NH₄-N/ha).

Total N: Almost all of the N losses occurred in the NO₃-N form, with the ratio of NO₃-N/TN > 0.95 for almost 90% of the leachate samples.

Dissolved Reactive Phosphorus (DRP): Average DRP concentrations were below 0.12 mg/L throughout the study period (Table 5). There were no significant differences among cropping systems in summer 2011 (SG-CC: $p=0.38$) and fall 2011 (SG-CC: $p=0.16$, SG-HP: $p=0.61$, CC-HP: $p=0.37$); however, concentrations from CC were greater than those measured for the other cropping systems. In winter 2012, average DRP concentration in SG leachate was significantly greater than both CC ($p<0.05$) and HP ($p<0.01$), and DRP concentration in CC was significantly greater than HP ($p<0.05$). Similarly, in spring 2012 average DRP concentration in SG was greater than CC ($p<0.01$), and both were significantly greater than HP ($p<0.01$). Our DRP concentrations (Table 5) are similar to those reported by Brye et al. (2002).

Cumulative DRP loadings measured in all cropping systems during the study were below 0.30 kg/ha, with season-dependent differences among the cropping systems (Table 3). DRP loadings for SG were greater than for CC during spring and winter; conversely, DRP loadings for CC were greater than for SG during summer and fall. The lowest DRP loading was obtained for the HP treatment.

Total phosphorus (TP): Similar to our observations for N, most of the P losses occurred in the dissolved form. All measured TP concentrations were < 0.05 mg P/L. Water entered the lysimeters through 1.0 and 0.5 µm filter paper, which could have removed all particulate P forms.

Carbon: No significant differences in DOC concentration were observed among cropping treatments within seasons (p-values ranged from 0.11 to 1.0); leachate collected after 22 June 2011 was analyzed for DOC. The highest DOC concentrations occurred during winter 2012 in all cropping systems. Agren et al. (2012) attributed higher DOC concentrations in soil-water to a “freeze-out” effect as frost develops in the soil profile, which could potentially lead to higher concentrations in leachate during winter months. The average seasonal DOC concentrations for all treatments are summarized in Table 5. In general the ranges of concentrations within a season were similar among cropping systems, although in summer 2011 and winter 2012, SG concentrations varied more than either CC or HP (Table 5). The overall average DOC concentration of all samples analyzed was 5.0 ± 0.3 mg/L. DOC concentrations fall within ranges reported by other studies. McCarthy and Bremner (1992) reported average DOC concentrations in tile drain effluent of ≤ 3.0 mg/L from agricultural catchments in Indiana. Brye et al. (2000) reported DOC concentrations of 5-20 mg/L for leachate measured with AETLs in prairie and corn at AARS.

Differences in DOC loading among cropping systems varied seasonally (Table 3). During summer and fall 2011, DOC loading in CC was significantly greater ($p < 0.05$ and $p < 0.1$, respectively) than SG. Conversely, in winter of 2012, DOC loading from SG was significantly higher than both CC ($p < 0.01$) and HP ($p < 0.01$). Likewise, in spring 2012, DOC loading in SG was significantly greater than CC ($p < 0.05$) and HP ($p < 0.01$). Higher DOC loading in SG in winter and spring 2012 may be due to the ability of SG to store more C in the soil profile. Organic matter inputs to soil are generally greater in warm season grasses than row crops (Brown et al, 2004; Frank et al., 2004); the additional C in the soil increases the likelihood of higher DOC leachate concentrations. DOC loadings measured in the present study are at the lower end of reported values. Annual exports of soluble C from most agricultural catchments in North America was estimated to be 10-100 kg/ha (Hope et al., 1994). Dalzell (2007) reported DOC losses via tile drains of 15-20 kg/ha for a modeled agricultural and forested watershed. Brye et al. (2000) reported DOC losses of 17-48 kg/ha from prairie and 90-180 kg/ha from no-till corn.

IV. CONCLUSIONS AND RECOMMENDATIONS

Cellulosic biofuels provide renewable alternatives to fossil fuels; however, the potential water resource impacts of wide scale production of cellulosic biofuel crops have not yet been extensively studied. Rapid expansion in the production of biofuels is expected in the next decade across the U.S., with many different cropping systems being investigated to meet the growing demands. Field studies are necessary to assess the environmental impacts of these cropping systems, including changes in the quantity and quality of subsurface drainage.

Seasonal differences in drainage were observed among the three cropping treatments evaluated in this project. Drainage during spring and winter was greater in SG than in CC and HP attributable, in part, to differences in surface residue coverage. In winter and spring, the CC plots had minimal residue coverage allowing the potential for surface crusting to develop, which is known to reduce infiltration by increasing runoff. Additionally, the deep fibrous root structures of SG and HP could have promoted greater infiltration compared to the CC plots. The trend in drainage amount was reversed during summer with CC plots yielding more leachate than the SG and HP plots. In both SG and HP plots, due to ET demands the soil moisture was depleted earlier in the growing season than in the CC plots.

Due to small differences in nutrient concentrations, seasonal nutrient loading among cropping systems followed the trends in drainage depth, except for $\text{NO}_3\text{-N}$. Throughout the study period, $\text{NO}_3\text{-N}$ loading from CC exceeded that of the other cropping systems. Seasonal $\text{NO}_3\text{-N}$ loading for CC varied between 4.7 and 137.5 kg $\text{NO}_3\text{-N/ha}$ while $\text{NO}_3\text{-N}$ loads for SG were between 0 and 12.3 kg $\text{NO}_3\text{-N/ha}$. Leachate samples from HP plots had very low $\text{NO}_3\text{-N}$ concentrations. Despite comparable N fertilizer application rates in CC and SG, substantially more $\text{NO}_3\text{-N}$ leaked out of CC cropping system throughout the year.

As cellulosic biofuel production expands, cropping systems will need to be matched to climate, soils, and environmental concerns in a region, due to differential impacts of each cropping system on water and nutrient dynamics. Results from this study suggest that high yielding perennial cropping systems (e.g. switchgrass, hybrid poplar) could reduce NO₃-N losses compared to systems involving corn (as the latter also requires additional N inputs). However, switchgrass systems could be vulnerable to leak more nutrients during seasons when ET demand is low (spring, winter) and that produce high drainage volumes. Limited data (only for 1 season) indicate that both drainage rates and nutrient losses could be lower under hybrid poplar throughout the year. Selection of appropriate cropping systems for a region should consider potential differences in leachate dynamics and nutrient concentrations to minimize environmental impacts of biofuel production systems.

Research on subsurface drainage quantity and quality should be extended to additional cropping systems with continued biomass removal on different soil types and physiographic conditions. These cropping systems could include native species, such as, prairie plantings or other biodiverse combinations (e.g., annual + perennial crops). Future studies should also encompass long-term monitoring (over several growing seasons), which will facilitate the development and rigorous validation of models that can be applied at various spatial scales. With the cellulosic biofuel demand expected to grow rapidly in the next decade, research needs to keep up with implementation and relay information to producers to ensure that reducing fossil fuel imports does not come at the cost of degraded environmental resources.

V. REFERENCES

- Agren, A. M., M. Haei, P. Blomkvist, M.B. Nilsson and H. Laudon. 2012. Soil frost enhances stream dissolved organic carbon concentrations during episodic spring snow melt from boreal mires. *Global Change Biology*. 18(6):1895-1903.
- Andraski, T. W., L.G. Bundy and K.R. Brye. 2000. Crop management and corn nitrogen rate effects on nitrate leaching. *Journal of Environmental Quality*. 29(4).
- Bharati, L., K.H. Lee, T.M. Isenhart and R.C. Schultz. 2002. Soil-water infiltration under crops, pasture, and established riparian buffer in Midwestern USA. *Agroforestry Systems*. 56(3):249-257.
- Blanco-Canqui, H. 2010. Energy crops and their implications on soil and environment. *Agronomy J*. 102(2):403-419.
- Blanco-Canqui, H. and R. Lal. 2009. Crop residue removal impacts on soil productivity and environmental quality. *Crit. Rev. in Plant Sci*. 28(3):139-163.
- Brown, R. A., N.J. Rosenberg, C.J. Hays, W.E. Easterling and L.O. Mearns. 2000. Potential production and environmental effects of switchgrass and traditional crops under current and greenhouse-altered climate in the central United States: a simulation study. *Agric. Ecosys. & Env*. 78(1):31-47.
- Brye, K. R., T.W. Andraski, W.M. Jarrell, L.G. Bundy and J.M. Norman. 2002. Phosphorus leaching under a restored tallgrass prairie and corn agroecosystems. *J. Environ. Qual*. 31(3):769-781.
- Brye, K. R., J.M. Norman, L.G. Bundy and S.T. Gower. 2000. Water-budget evaluation of prairie and maize ecosystems. *Soil Science Society of America Journal*. 64(2):715-724.
- Brye, K. R., J.M. Norman, S.T. Gower, S. T. and L.G. Bundy. 2003. Methodological limitations and N-budget differences among a restored tallgrass prairie and maize agroecosystems. *Agriculture Ecosystems & Environment*. 97(1-3):181-198.
- Carroll, A. and C. Somerville. 2009. Cellulosic Biofuels. *Ann. Rev. of Plant Biology*. 60:165-182.
- Dalzell, B.J., T.R. Filley, J.M. Harbor. 2007. The role of hydrology in annual organic C loads and organic matter export from a midwestern agricultural watershed. *Geochim. Cosmochim. Acta*. 71:1448-1462.
- Dormaar, J. F. and J.M. Carefoot. 1996. Implications of crop residue management and conservation tillage on soil organic matter. *Canadian Journal of Plant Science*. 76(4): 627-634.
- Escobar, J. C., E.S. Lora, O.J. Venturini, E.E. Yanez, E.F. Castillo and O. Almazan, O. 2009. Biofuels: Environment, technology and food security. *Ren. & Sust. Energy Reviews*. 13(6-7):1275-1287.
- Fageria, N. K. 2012. Role of soil organic matter in maintaining sustainability of cropping systems. *Comm. in Soil Sci. and Plant Anal*. 43(16):2063-2113.

- Frank, A. B., J.D. Berdahl, J. D. Hanson, M.A. Liebig and H.A. Johnson. 2004. Biomass and carbon partitioning in switchgrass. *Crop Science*. 44(4):1391-1396.
- Hope, D., M.F. Billett and M.S. Cresser. 1994. A review of the export of carbon in river water: Fluxes and processes. *Environ. Pollut.* 84:301–324.
- Jordan, N., G. Boody, W. Broussard, J. D. Glover, D. Keeney, B. H. McCown, G. McIsaac, M. Muller, H. Murray, J. Neal, C. Pansing, R. E. Turner, K. Warner, and D. Wyse. 2007. Environment - Sustainable development of the agricultural bio-economy. *Science*. 316:1570-1571.
- Laboski, C.A.M., J.B. Peters and L.G. Bundy. 2006. Nutrient application guidelines for field, vegetable, and fruit crops in Wisconsin. UWEX Publ. A2809. pp 68.
- McCarty, G.W. and J.M. Bremner. 1992. Availability of organic carbon for denitrification of nitrate in subsoils. *Biol. Fertil. Soils*. 14:219–222.
- McIsaac, G. F., M.B. David and C.A. Mitchell. 2010. Miscanthus and switchgrass production in central Illinois: impacts on hydrology and inorganic nitrogen leaching. *J. Env. Quality*. 39(5):1790-1799.
- NASS (National Agriculture Statistical Service). 2010. Corn, Field. National Statistics. [Online] <http://www.nass.usda.gov/QuickStats/index2.jsp>. Verified 4/6/2010.
- Owens, L.B. 1990. Nitrate-nitrogen concentration in percolate from lysimeter planted to a legume–grass mixture. *J. Environ. Qual.* 19:131–135.
- Percival, H. J., R.L. Parfitt and N.A. Scott. 2000. Factors controlling soil carbon levels in New Zealand grasslands: Is clay content important? *Soil Sci. Soc. Am. J.* 64(5):1623-1630.
- Rachman, A., S.H. Anderson, C.J. Gantezer, and E.E. Albert. 2004. Soil hydraulic properties influenced by stiff-stemmed grass hedge systems. *Soil Sci. Soc. Am. J.* 68:1386-1393
- Rekha, P. N., R.S. Kanwar, A.K. Nayak, C.K. Hoang and C.H. Pederson 2011. Nitrate leaching to shallow groundwater systems from agricultural fields with different management practices. *J. Environ. Monit.* 13(9):2550-2558.
- Sage, R. F. and X.G. Zhu. 2011. Exploiting the engine of C(4) photosynthesis. *J. Exp. Botany*. 62(9):2989-3000.
- Sanderson, M. A. and D. D. Wolf. 1995. Morphological Development of Switchgrass in Diverse Environments. *Agronomy J.* 87:908-915.
- Sanderson, M. A., P. R. Adler, A. A. Boateng, M. D. Casler, and G. Sarath. 2006. Switchgrass as a biofuels feedstock in the USA. *Can. J. Plant Sci.* 86:1315-1325.
- Schmer, M. R., K.P. Vogel, R.B. Mitchell, B.S. Dien, M.D. Casler. 2012. Temporal and spatial variation in switchgrass biomass composition and theoretical ethanol yield. *Agronomy J.* 104(1):54-64.
- Sims, R. E. H., A. Hastings, B. Schlamadinger, G. Taylor and P. Smith. 2006. Energy crops: current status and future prospects. *Global Change Biol.* 12:2054-2076.
- Sims, R. E. H., W. Mabee, J.N. Saddler, J. N. and M. Taylor. 2010. An overview of second generation biofuel technologies. *Bioresource Technology*. 101(6):1570-1580.
- Sindelar, A. J., J.A. Lamb, C.C. Sheaffer, H.G. Jung and C.J. Rosen, C. J. 2012. Response of corn grain, cellulosic biomass, and ethanol yields to nitrogen fertilization. *Agronomy J.* 104(2):363-370.
- Solomon, B. D., J.R. Barnes, and K.E. Halvorsen. 2007. Grain and cellulosic ethanol: History, economics, and energy policy. *Biomass & Bioenergy*. 31(6):416-425.
- Stenjem, R. 2013. Subsurface water and nutrient dynamics of cellulosic biofuel cropping systems. M.S. Thesis, University of Wisconsin – Madison.
- Uhlenbrook, S. 2007. Biofuel and water cycle dynamics: what are the related challenges for hydrological processes research? *Hydrological Processes*. 21(26):3647-3650.
- USDA. 2012. *World Agricultural Supply and Demand Estimates*. (June 12, 2012). Retrieved <http://www.usda.gov/oce/commodity/wasde/latest.pdf>.
- U.S. DOE. 2006. Breaking the Biological Barriers to Cellulosic Ethanol: A Joint Research Agenda. DOE/SC-0095. U.S. DOE Office of Science and Office of Energy Efficiency and Renewable Energy.

APPENDIX A Awards/Publications/Reports/Patents/Presentations

Publications:

Stenjem, R.S. 2013. Subsurface water and nutrient dynamics of cellulosic biofuel cropping systems. M.S. Thesis, University of Wisconsin – Madison.

Presentations:

Stenjem, R.S., A.M. Thompson and B.J. Lepore. 2012. Water and nutrient fluxes under biofuel cropping systems. Annual Meeting of the American Water Resources Association Wisconsin Section. Wisconsin Dells, WI, March 1-2, 2012.

Stenjem, R.S., A.M. Thompson, K.G. Karthikeyan, M. Polich and B.J. Lepore. 2012. Surface and subsurface water and nutrient dynamics for biofuel feedstock cropping systems. Annual International Meeting of the American Society of Agricultural and Biological Engineers. Dallas, TX, July 29 – Aug 1, 2012.

APPENDIX B

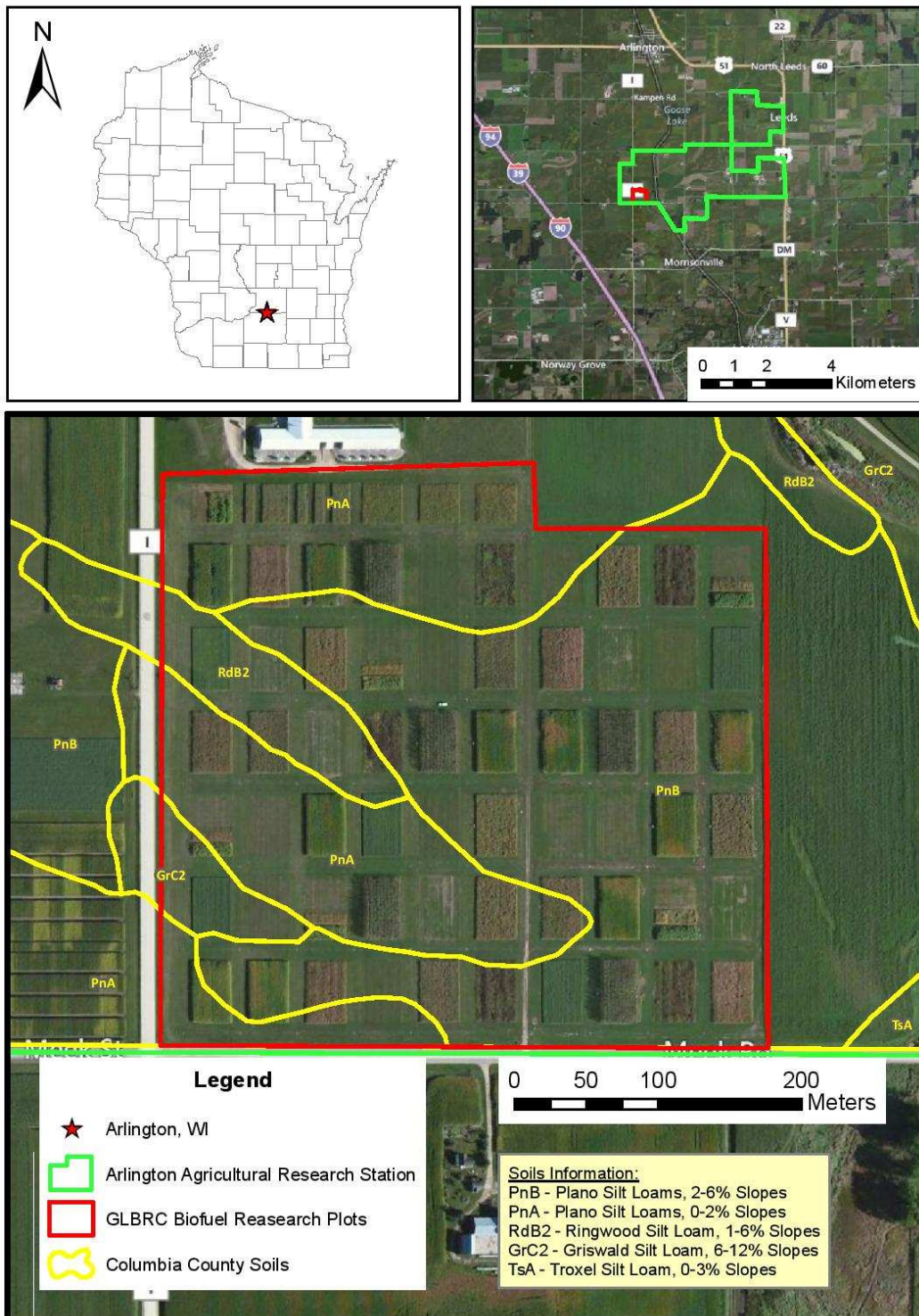


Figure B1. Locations of Arlington, WI; AARS; and the Biofuel Research Plots at AARS (Stenjem, 2013).

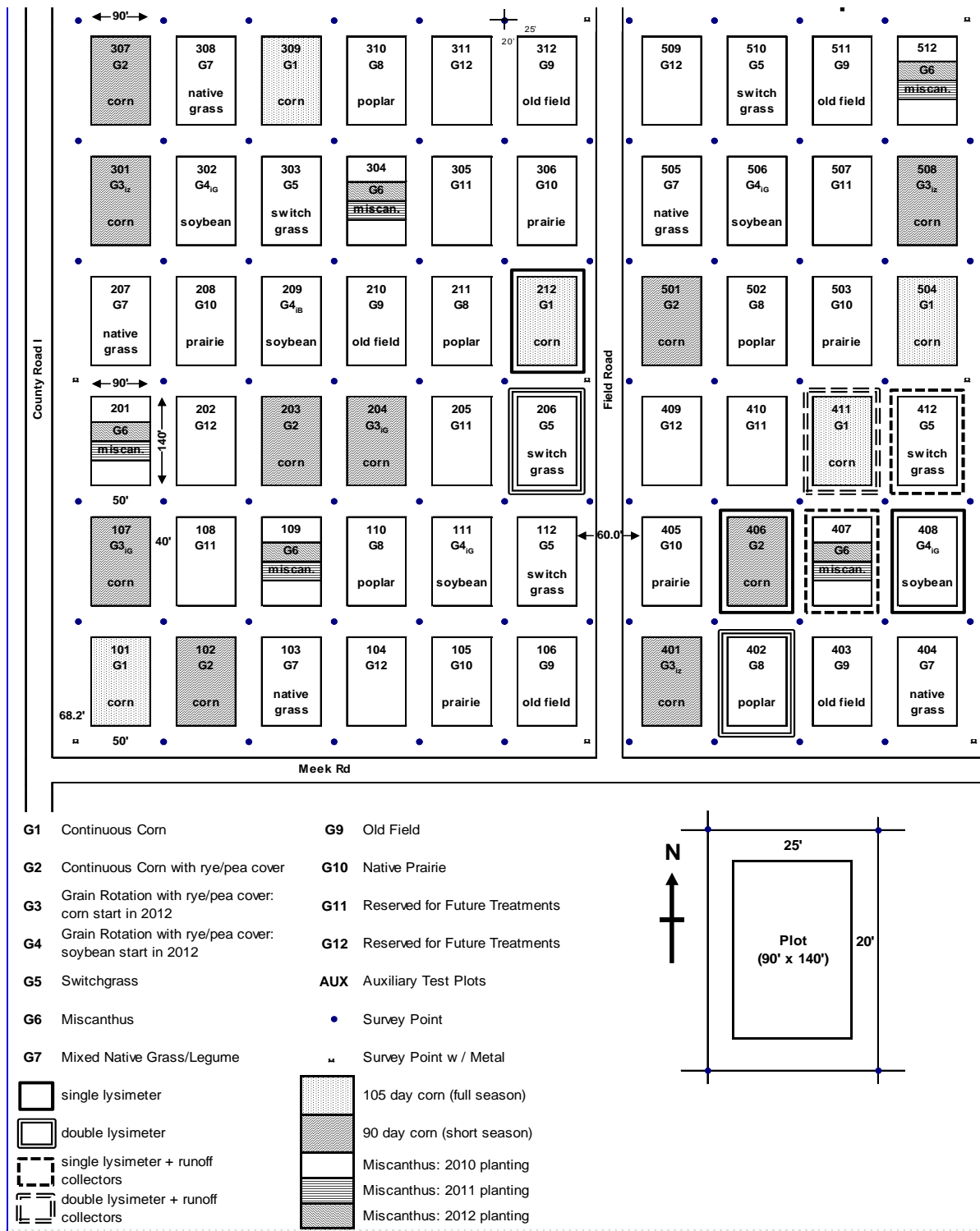


Figure B2. Map of Great Lakes Bioenergy Research Center Biofuel Plots located at AARS (Courtesy of Gregg Sanford, GLBRC).



Figure B3. (a) Lysimeter and spring plate inside soil cavity with screw jacks for installation beneath. Tensiometer wires shown to the left of lysimeter. (b) Lysimeter and spring plate installed. Wooden blocks under spring plate to maintain spring force and lysimeter contact with cavity ceiling.

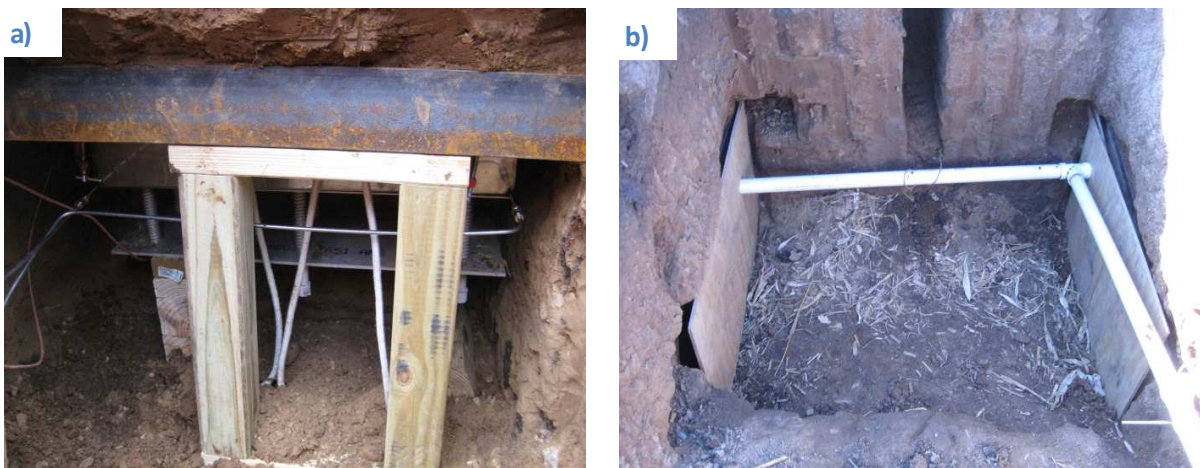


Figure B4. (a) Wooden weather treated support frames installed beneath angle irons to provide support to soil profile above cavity. (b) Weather treated plywood covering to prevent cavity from damage during backfilling. PVC tubes contain sensor wires and lysimeter tubing extends to the control box on soil surface.

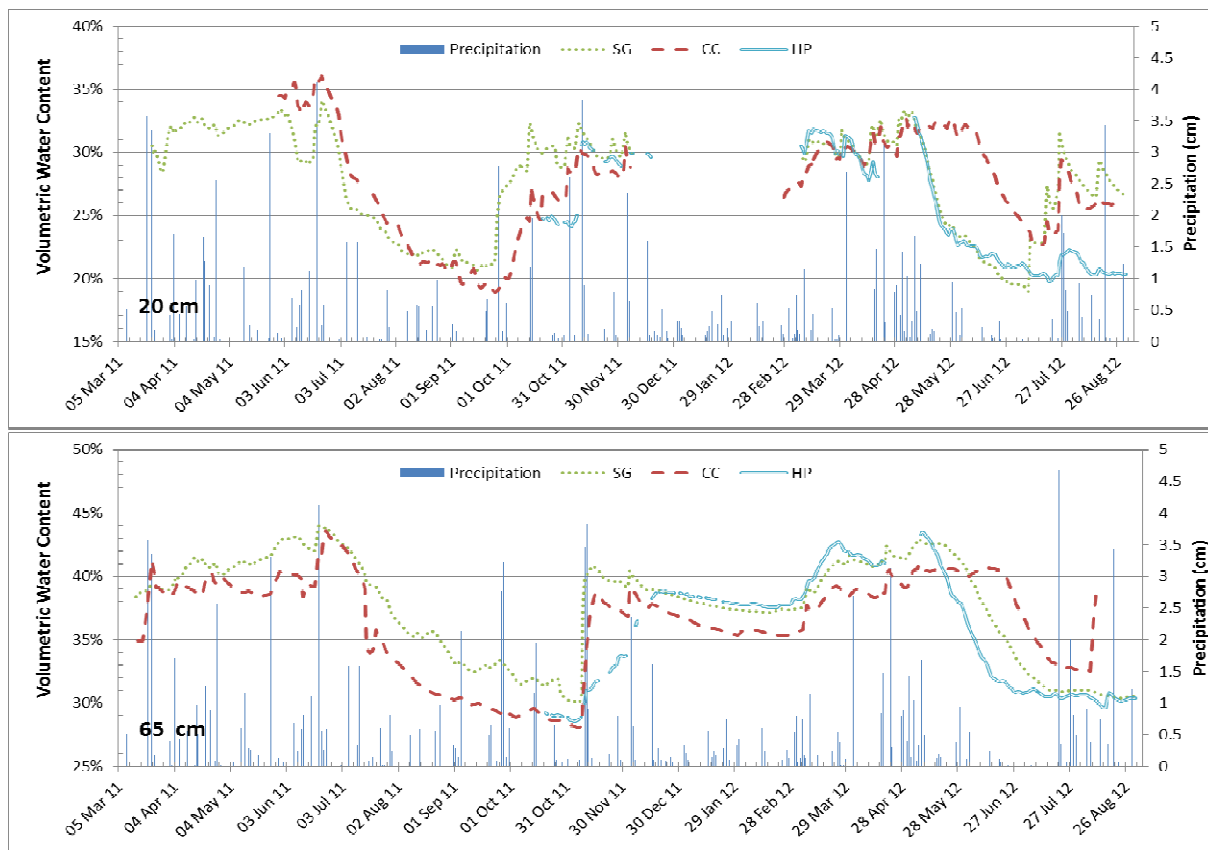


Figure B5. Volumetric water content at 20 cm (top) and 65 cm (bottom) in SG, CC, and HP from 5 Mar 2011 to 31 Aug 2012. At 20 cm time periods where soil was frozen have been excluded.

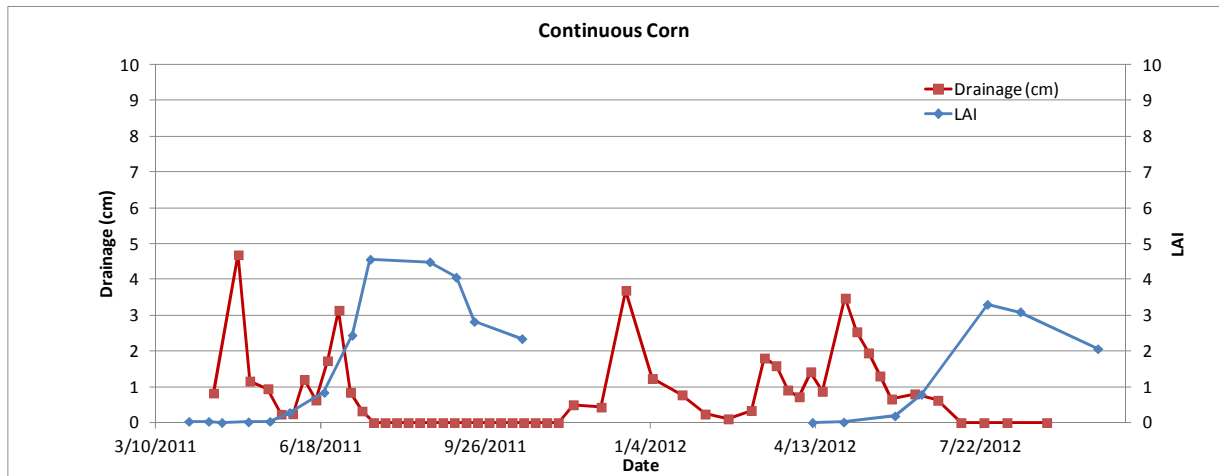


Figure B6. Time series of drainage depths and Leaf Area Index (LAI) for continuous corn during study. LAI data provided by Dr. Oates, Assistant Scientist, GLBRC.

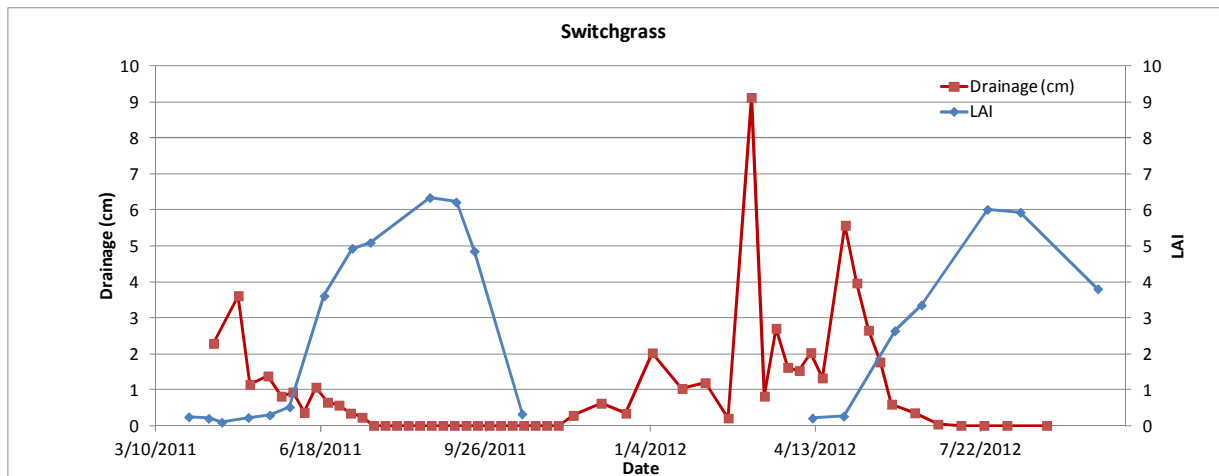


Figure B7. Time series of drainage depths and Leaf Area Index (LAI) for switchgrass during study. LAI data provided by Dr. Oates, Assistant Scientist, GLBRC.

Table B1. Planting and harvest dates, for the cellulosic biofuel cropping systems.

Cropping Treatment	Planting Date		Harvest Date	
	2011	2012	2011	2012*
RC	6 May	10 May	25 Oct	9 Oct
CC	6 May	10 May	25 Oct	9 Oct
SG	May 2008	--	10 Oct	9 Nov
MIS	19 May	--	10 Oct	9 Nov
HP	May 2008	--	--	--

*Data collection ended 31 Aug 2012

Table B2. 2011 cellulosic biofuel cropping system Yields at AARS.

Treatment (Plot #)	Grain		Stover/Biomass	
	m ³ /ha	bu/ac	Mg/ha	ton/ac
RC (406)	18.9	219	5.6	2.5
RC (408)*	-	-	-	-
CC (212)	18.6	215.2	6.3	2.9
CC (411)	17.5	202.3	6.3	2.9
SG (206)	-	-	6.9	3.1
SG (412)	-	-	6.5	3.0
MIS (407)	-	-	18.3	7.5
HP (402)**	-	-	-	-

* Planted in Canola during 2011

**Not harvested in 2011

Table B3. 2011 growing season GLBRC fertilizer application dates, rates, and cumulative nutrient application rates for cellulosic biofuel cropping systems at AARS. Fertilizer guaranteed analysis (%N-%P₂O₅-%K₂O) provided.

	Fertilizer Application Date			Fertilizer Application Guaranteed Analysis (N-P ₂ O ₅ -K ₂ O): Rate (kg/ha)			Total Added (kg/ha)		
	N	P	K	N	P	K	N	P	K
RC	14 May 25 June	14 May	4 May 14 May	5-14-42: 112 28-0-0: 97	5-14-42: 112	0-0-60: 50.4 5-14-42: 112	64.6	6.8	63.9
CC	14 May 35 June	14 May	4 May 14 May	5-14-42: 112 28-0-0: 210.6	5-14-42: 112	0-0-60: 50.4 5-14-42: 112	64.6	6.8	63.9
SG	27 May	-	-	34-0-0: 164.6	-	-	56.0	-	-
MIS	27 May	-	-	34-0-0: 164.6	-	-	56.0	-	-
HP	-	-	-	-	-	-	-	-	-

Table B4. Instrumentation installation depths in experimental field plots at AARS including GLBRC installed instrumentation

Plot	Treatment	Lysimeter* depths (cm)		TDR depths (cm)		Thermocouple depths (cm)	
		This Study	GLBRC	This Study	GLBRC	This Study	GLBRC
206	G5- SG	N-90 S-110	120	20, 65	2, 20, 35, 50, 65, 95, 125	20	2, 10, 20, 35, 50, 65, 95, 125 (two at each depth)
212	G1- CC	90	120	20, 65	2, 20, 35, 50, 65, 95, 125	20	2, 10, 20, 35, 50, 65, 95, 125 (two at each depth)
402	G8- Poplar	N - 80 S - 90	120	20, 65	2, 20, 35, 50, 65, 95, 125		2, 10, 20, 35, 50, 65, 95, 125 (two at each depth)
406	G2- Rotation (Corn in 2011)	120	120	4, 20, 35, 65	-	10, 20, 35, 50, 65	-
407	G6- MIS	185	120	4, 20, 35, 65	-	10, 20, 35, 50, 65	-
408	G4- Rotation (Corn in 2012)	190	120	4, 20, 35, 65	-	10, 20, 35, 50, 65	-
411	G1- CC	N-105 S-100	120	20, 65	2, 20, 35, 50, 65, 95, 125	20	2, 10, 20, 35, 50, 65, 95, 125 (two at each depth)
412	G5- SG	195	120	20(2), 65	2, 20, 35, 50, 65, 95, 125	20	2, 10, 20, 35, 50, 65, 95, 125 (two at each depth)

*GLBRC lysimeters are suction cup type lysimeters, not equilibrium tension lysimeters

Table B5. AETL installation periods, data collection, water sampling, and nutrient analysis starting dates

Plot Number	Installation	Soil Sensor Data Collection	Water Sample Collection	Nutrient Analyses
206	Nov 2010	17 Mar 2011	14 Feb 2011	29 May 2011
212	Oct 2010	21 Nov 2010	6 Apr 2011	29 May 2011
402	July 2011	19 Oct 2011	18 Nov 2011	18 Nov 2011
406	Oct 2010	24 Jan 2011	28 Feb 2011	29 May 2011
407	Oct 2010	13 Apr 2011	17 May 2011	29 May 2011
408	Oct 2011	23 Nov 2011	5 Mar 2012	5 Mar 2012
411	Oct 2010	5 Mar 2011	15 Mar 2011	29 May 2011
412	Nov 2010	2 Mar 2011	6 Mar 2011	29 May 2011

Table B6. Precipitation (cm liquid water equivalent) depths for Arlington, WI during 2011 and 2012 (NOAA)

	Jan	Feb	Mar	Apr	May	Jun	Jul	Aug	Sep	Oct	Nov	Dec	Total
2011	1.75*	2.79*	8.08*	11.12	6.15	8.94	5.44	3.84	10.16	4.06	11.48	6.48	80.28
2012	3.20	1.73	6.35	9.40	7.69	0.74	10.14	7.08	-	-	-	-	-
30 yr Avg	2.69	2.90	5.11	8.20	8.71	10.31	9.80	10.80	9.19	6.20	6.10	3.40	83.41

*Outside of the study period but offer insight into the climate conditions preceding the study.

Table B7. Monthly and 30 year average air temperatures (°C) during 2011 and 2012 at Arlington, WI (NOAA)

	Jan	Feb	Mar	Apr	May	Jun	Jul	Aug	Sep	Oct	Nov	Dec
2011	-9.8*	-6.8*	-0.8*	6.2	12.9	19.2	23.3	19.8	13.6	9.5	2.9	-2.1
2012	-5.2	-2.6	8.5	7.4	16.3	21.5	24.6	19.6	-	-	-	-
30-year Average	-9.0	-6.0	0.5	7.5	14.0	19.0	21.5	20.5	16.0	9.5	1.0	-5.5

*Outside of the study period but offer insight into the climate conditions preceding the study.

Table B8. Soil NO₃-N analysis for CC and SG plots performed in August 2012.

Plot ¹ (Crop)	NO ₃ -N (water extractable – soils from top 95 cm)
206 (SG)	0.8 mg/kg of soil
412 (SG)	0.7 mg/kg of soil
411 (CC)	19.0 mg/kg of soil
212 (CC)	3.2 mg/kg of soil

¹ Plot numbers shown in Fig. B2

Reducing Nitrate in Groundwater with Slow-Release Fertilizer

Basic Information

Title:	Reducing Nitrate in Groundwater with Slow-Release Fertilizer
Project Number:	2010WI283O
Start Date:	7/1/2010
End Date:	6/30/2012
Funding Source:	Other
Congressional District:	WI 2nd
Research Category:	Ground-water Flow and Transport
Focus Category:	Agriculture, Nitrate Contamination, Management and Planning
Descriptors:	
Principal Investigators:	, Birl Lowery

Publication

1. Bero, N.J. 2012. Controlled release fertilizer effect on groundwater nitrogen concentration in sandy soils under potato production. MS Thesis, Department of Soil Science, University of Wisconsin, Madison, WI. 170p.

Reducing nitrate in groundwater with slow-release fertilizer

Authors:

Dr. Matthew Ruark

Dr. Birl Lowery

Mr. Nick Bero

Table of Contents

List of Figures and Tables	2
Project Summary.....	2
Introduction	3
Procedures and Methods.....	4
Results and Discussion	6
Yield and N Uptake.....	6
Groundwater elevation and nitrate concentrations.....	7
Discussion.....	8
Conclusions and Recommendations	12
References	13
Appendix A.....	14
Appendix B	14
Tracer study	15

List of Figures and Tables

Figure 1. Depth to water table from the soil surface. 1 June 2010 through 1 June 2011 (a) and 27 May 2011 through 1 June 2012 (b).

Figure 2. Groundwater NO₃-N concentration from 2010. Gray bar in down center indicates the date at which the center well was raised and the well screen intersected the water table. The conventional fertilizer, RCONV, 280 kg N ha⁻¹ as 93 kg ha⁻¹ ammonium sulfate applied at emergence and 187 kg N ha⁻¹ as ammonium nitrate; recommended controlled-release fertilizer, RPCU, 280 kg N ha⁻¹ as PCU applied at emergence; low rate controlled-release fertilizer, LPCU – 224 kg N ha⁻¹ as PCU applied at emergence. Standard error reported from SAS mixed model with repeated measures.

Figure 3. Groundwater NO₃-N concentration from 2011. The conventional fertilizer, RCONV, 280 kg N ha⁻¹ as 93 kg ha⁻¹ ammonium sulfate applied at emergence and 187 kg N ha⁻¹ as ammonium nitrate; recommended controlled-release fertilizer, RPCU, 280 kg N ha⁻¹ as PCU applied at emergence; low rate controlled-release fertilizer, LPCU – 224 kg N ha⁻¹ as PCU applied at emergence. Standard error reported from SAS mixed model with repeated measures.

Table 1. Marketable and total potato yields for 2010 and 2011

Table 2. Potato nitrogen uptake

Project Summary

Title: Reducing groundwater nitrate with slow-release fertilizer

Project ID: WR10R004

Investigators: Dr. Matthew Ruark, Assistant Professor, Dr. Birl Lowery, Professor, and Mr. Nick Bero, graduate student, Dept. of Soil Science, University of Wisconsin, Madison.

Period contract: July 1, 2010 to June 30, 2012

Objectives: The objective of our study was to investigate fertilizer effect on groundwater NO₃-N concentration, yields, and plant growth parameters in sandy soils under potato production, using the best management practices currently available compared with controlled-release fertilizer technology.

Methods: A 2-yr field experiment was conducted at the Hancock Agricultural Research Station using Russet Burbank potato (*Solanum tuberosum* L.), planted in Plainfield sand. The experimental design was randomized complete block with three replicates which included four nitrogen (N) fertilizer treatments: (1) no nitrogen, (2) 224 kg ha⁻¹ as PCU, (3) 280 kg ha⁻¹ as PCU, and (4) 280 kg ha⁻¹ split applied as ammonium sulfate and ammonium nitrate (AS-AN). The PCU was applied entirely at plant emergence and conventional fertilizer at potato emergence and at tuber initiation. Three groundwater monitoring wells were installed in each plot, were sampled weekly during the growing season, and analyzed for NO₃-N.

Results and Discussion: Controlled-release fertilizer, specifically polymer coated urea (PCU), may reduce the amount of nitrate-nitrogen (NO₃-N) leaching to groundwater; however, few if any field scale studies have been performed in Wisconsin on sandy soils to validate these assertions. Potato growth parameters and yields were maintained between conventional fertilizer and PCU and as a result, N use efficiency was greatly improved at the 224 kg ha⁻¹ over both 280 kg ha⁻¹ treatments. There were no significant treatment effects between any nitrogen treatments, as plot-to-plot variation was much greater than the differences between mean concentrations.

Conclusions: The use of controlled-release PCU fertilizer is a viable alternative to current management practices of AS-AN applications, but its benefits to water quality are not immediately realized. It is clear that measurements of nitrogen use efficiency are the best way to evaluate the short-term impacts to groundwater quality on sandy soils, while groundwater monitoring should be reserved for evaluating effects over the long-term.

Related publications:

Bero, N.J., M.D. Ruark, and B. Lowery. 2013. Controlled-release fertilizer effect on groundwater nitrogen concentration in sandy soil under potato production. *Agronomy Journal* (In review).

Bero, N.J., M.D. Ruark, and B. Lowery. 2012. Controlled-release fertilizer effect on groundwater nitrogen concentration in sandy soils under vegetable production. *Science-based Policy for Wisconsin's Water Resources – 36th Annual Meeting American Water Resources Association – Wisconsin Section*. 1-2 March, Wisconsin Dells, WI.

Bero, N.J., M.D. Ruark, and B. Lowery. 2011. Slow-release fertilizer effect on groundwater nitrogen concentration in sandy soils under potato production. *Wisconsin's Role in Great Lake Restoration – 35th Annual Meeting American Water Resources Assoc. – Wisconsin Section*, 3-4 March 2011, Appleton, WI.

Bero, N.J., M.D. Ruark, and B. Lowery. 2011. Slow-release fertilizer effect on groundwater nitrogen concentration in sandy soils under potato production. *North Central Extension and Industry Soil Fertility Conference Vol. 27*, 16-17 Nov., Des Moines, IA.

Key words: groundwater, nitrate, potato, nitrogen, fertilizer

Funding: Wisconsin Groundwater Coordinating Council

Introduction

Many previous studies have focused on NO₃-N flux through the root zone as measured by porous cup samplers, and NO₃-N leaching on the groundwater has only been inferred from these data (Diez et al., 1994; Errebhi et al., 1998; Arriaga et al., 2009; Cooley et al., 2009; Wilson et al., 2010). Several

researchers have also studied residual soil N from soil cores that have implicated reduced $\text{NO}_3\text{-N}$ leaching from PCU or split application (Cameron et al., 1979; Hill, 1986; Zvomuya and Rosen 2001; Zvomuya et al., 2003). In studies where there has been direct sampling of groundwater, there has not been a comparison of different fertilizer sources effect on groundwater $\text{NO}_3\text{-N}$ concentration (Hubbard et al., 1984; Bergstrom and Brink, 1986; Hill, 1986; Kraft and Stites, 2003). Few, if any, researchers have attempted to directly assess the difference of PCU fertilizer vs. conventional soluble fertilizer effect on groundwater $\text{NO}_3\text{-N}$ concentrations. The main reason might be that there are difficulties in assessing the groundwater directly. A lag time of a few weeks to months exists between the timing of application of fertilizer N and its arrival in the groundwater (Saffigna and Keeney, 1971; Hubbard et al., 1984; Landon et al., 2000; Burkart, 2002). Additionally, Olsen et al. (1970) found that more $\text{NO}_3\text{-N}$ leaching occurred between fall and spring samplings than during the growing season. Therefore, research should be conducted to determine the effect of different rates and forms of fertilizer on groundwater $\text{NO}_3\text{-N}$ concentrations by directly monitoring shallow groundwater. The objective of our study was to investigate fertilizer effect on groundwater $\text{NO}_3\text{-N}$ concentration, yields, and plant growth parameters in sandy soils under potato production, using the best management practices currently available compared with PCU technology.

Procedures and Methods

This study was conducted at the Hancock Agricultural Research Station on a Plainfield loamy sand (mixed, mesic Typic Udipsamments) in 2010 and 2011. The experimental design was a randomized complete block with three replications. Four N management treatments were evaluated: (i) a recommended rate (280 kg N ha^{-1}) of conventional fertilizer (RCONV), (ii) a recommended rate (280 kg N ha^{-1}) of PCU (RPCU), (iii) a lower than recommended rate (220 kg N ha^{-1}) of PCU (LPCU), and (iv) no fertilizer N inputs (0 N). Plot sizes were 14.6 by 15.2 m, encompassing 16 potato rows. Different field locations were used for each year of the study. The 2010 field was located at $44^\circ 07' 1'' \text{N}$, $89^\circ 32' 46'' \text{W}$ at the east midpoint and the 2011 field was located at $44^\circ 06' 52'' \text{N}$, $89^\circ 32' 37'' \text{W}$ at the west midpoint. The full rate of each the LPCU and RPCU treatments was applied at emergence on 17 May 2010 and 20 May 2011. The RCONV treatment included a split application with 93 kg ha^{-1} of N applied as ammonium sulfate at emergence and 187 kg ha^{-1} of N applied as ammonium nitrate at potato tuber initiation on 2 June 2010 and 9 June 2011. All fertilizers were applied by hand to the top of the hill and mechanically incorporated by hilling. The PCU product used in this study was Environmentally Smart Nitrogen® (ESN®) (Agrium, Inc., Calgary, AB).

Russet Burbank potatoes were mechanically planted at 0.9-m row spacing with a seed density of $36,600 \text{ seeds ha}^{-1}$ and planted on 29 Apr. 2010 and on 25 Apr. 2011. Potassium chloride and calcium sulfate were applied prior to planting at rates of 430 kg ha^{-1} and 560 kg ha^{-1} , respectively. Starter fertilizer was applied at planting at a rate of 616 kg ha^{-1} , providing 37 kg ha^{-1} of N, 185 kg ha^{-1} of P_2O_5 , 135 kg ha^{-1} of K_2O , and 25 kg ha^{-1} of S. The starter fertilizer also contained Thiamethoxam, a systemic insecticide. A surfactant consisting of 10% alkoxyated polyols and 7% glucoethers (Irrigaid, Aquatrols, Paulsboro, NJ) was applied at emergence and tuber initiation fertilization in both years. Irrigation was managed by the Hancock Agricultural Research Station staff and insecticide, fungicide, and herbicide applications were applied by the station staff as needed to reduce pest and disease pressures.

In 2010, groundwater monitoring wells were installed between 10 and 17 May to a depth of 9.8 m from the soil surface with 1.5-m screens. Three wells were placed diagonally across each plot at a distance of 4.9, 7.6, and 9.8 m, respectively, from the south edge of each plot. The average depth to groundwater was 6.7 m at the time of well installation in 2010 and as a result wells were installed approximately 3.1 m below the water table, leaving the top of the screen 1.6 m below the water table, which was to account for the anticipated typical seasonal drawdown of the water table. However, this seasonal drawdown did not occur in 2010, and in response, on 14 Oct. 2010, the center well within each plot was raised so that the screened portion of the well intersected the water table. In 2011, wells were

installed between 27 Apr. and 2 May, at a depth of 9.1 m from the soil surface with 2.3-m screens. Depth to groundwater averaged 7.3 m at the time of well installation, and wells screens were within the groundwater surface for all of 2011. Groundwater monitoring wells and screens were constructed from schedule 40 polyvinyl chloride (PVC) pipe with an internal diameter of 3.18 cm. Screens had 0.51-mm slot widths and 3.18 mm between slots. A 7.5-cm long PVC point was attached to the bottom of the screen. Holes for the wells were drilled with a truck-mounted hydraulic probe with drilling capabilities (Giddings Machine Co., Windsor, CO) and 7-cm diam. augers. After well holes were completed, the PVC wells were inserted by hand and the excavated sand from the auger hole was repacked around the well. Sand was replaced to within 30 to 50 cm of the surface, and bentonite clay was used to fill the remaining depth to prevent preferential flow down the side of the wells. Wells were developed by hand bailing to remove as much sediment in the bottom of the well as possible. Wells were cut to 20 cm from the top of the potato hill and then capped with a 3.18 cm schedule 40 cap.

Two observation wells were installed at the north-south midpoint of both fields in both years, outside of the field boundary, to continuously record of depth to water table with an Instrumentation Northwest PS-9805 submersible pressure/temperature transducer (Instrumentation Northwest, Kirkland, WA) placed inside the well at a depth of 1.22 m under the water table. The pressure transducer, along with an Onset RG3 tipping bucket rain gauge (Onset Computer Corp., Bourne, MA) was then connected to a Campbell Scientific 10X data logger (Campbell Scientific, Logan, UT). The rain gauge and pressure transducers were calibrated in the laboratory prior to installation. Measurements were logged with a Campbell Scientific SM192 storage module (Campbell Scientific, Logan, UT) every 15 min. Maximum and minimum daily air temperatures were recorded by a weather station managed by the Hancock Agricultural Research Station. A third observation well that only monitored depth to water table was installed approximately 1000 m south of the observation well from the field in 2010 and 500 m west of the observation well from the field used in 2011 at 44°06'49"N, 89°32'43.15"W. This well was installed 25 Aug. 2011 and with the other two observation wells, provided a large triangle grid for determining groundwater flow direction. Well elevations and positions were determined with a Leica GPS 1200 (Leica Geosystems, Norcross, GA, 30092). A fixed control point, DH5653 managed by the State of Wisconsin cartographer's office, was used to calibrate the surveyed points and determine absolute orthometric height of each well above mean sea level.

Potato yields were obtained by mechanical harvesting of 3.1-m sections of four rows in each plot on 30 Aug. 2010 and 12 Sept. 2011. Harvest rows were determined by observation of rows least disturbed by well drilling. Potatoes were mechanically graded into sizes of B grade (< 85 g), 85 to 113, 114 to 170, 171 to 283, 284 to 368, 369 to 454, and > 454 g. Culled potatoes (knobby, green, or rotted) were removed manually. Yields are reported as total and marketable, which excludes B grade and culled potatoes. Ten potatoes from the size class of 170 to 283 g were subsampled and analyzed for specific gravity and disease. Plant N status was assessed by sampling petioles, tubers, and above-ground biomass. Potatoes emerged on 17 May 2010 and 20 May 2011, and petioles were sampled at 32, 44, 58, and 73 days after emergence (DAE) in 2010 and 27, 40, 54, and 67 DAE in 2011. Twenty petioles were collected from the center two rows from each plot. The fourth petiole from the plant crown was removed by hand, stripped of leaves, and dried and ground. Above-ground biomass (AGB) and tubers were collected at mid-season (DAE 44 in 2010 and DAE 47 in 2011) and at the end of season (AGB – DAE 92 in 2010 and DAE 97 in 2011; tubers – DAE 105 in 2010 and DAE 115 in 2011). Mid-season AGB and tuber samples were taken from five plants per plot. End-of-season AGB samples were from five plants pre-vine kill and tuber samplers were from six potatoes collected from the 170 to 283 g size class at harvest. Petiole NO₃-N, and AGB and tuber total N and total C were assessed at the UW-Madison Soil and Plant Analysis Laboratory using total Kjeldahl N (Ruzicka, 1983; Leco Corp., 1995), EPA nitrate 353.2, and the Leco Corp. procedure for C by dry combustion on a Leco CNS-2000 analyzer (Leco Corp., 2002, 2003), respectively. Total N uptake in AGB was converted to dry matter N uptake per unit area by

multiplying dry matter N concentration by the seeding density and total N uptake in tubers was converted to dry matter N uptake per unit area by multiplying dry matter N concentration by total yield.

Groundwater was sampled weekly between planting and 1 month after harvest (19 May to 14 Oct. 2010 and 6 May to 31 Oct. 2011). Groundwater was sampled monthly while the field was out of production (14 Oct. 2010 through 23 May 2011 and 31 Oct. 2011 through 26 Apr. 2012). Water samples were collected from each well with a 375-mL stainless steel bailer. The first sample extraction was discarded, and subsequent water extractions were placed into 500-mL plastic Nalgene bottles. Upon collection, samples were transported back to the laboratory, filtered within 24 h after collection, and stored at 4°C until analysis could be performed.

Groundwater samples were analyzed for nitrate, ammonium, and total N. Nitrate concentration was determined using the single vanadium chloride reagent method (Doane and Horwath, 2003) and was reported as NO₃-N. Since this method reduces nitrate to nitrite, selected well samples were assessed for only nitrite with the same method, by not adding vanadium chloride to the reagent. All samples analyzed for nitrite (NO₂-N) concentration were below the detection limit and thus all N determined using this method was assumed to be NO₃-N.

Analysis of variance was conducted to determine treatment differences in yield, size grade, petiole NO₃-N, AGB and tuber total N content, AGB and tuber total N uptake using Proc GLM in SAS (SAS Institute Inc., Cary, NC). Tukey's studentized range was used for means comparison at the $\alpha=0.1$ significance level. Analysis of variance was conducted to determine treatment differences in groundwater NO₃-N concentrations across all weeks using Proc Mixed with repeated measures on plot, with an auto regression correlation structure in SAS at the $\alpha=0.1$ level of significance. The adjusted Tukey-Kramer adjusted P-value was used to determine the differences in treatment means. Nitrate, NH₄-N and organic N concentrations were averaged across three wells to provide one concentration value per plot per sample time. Variation in the NO₃-N concentration was then determined by the three replicate blocks, and blocks were considered a random effect in the model. The model used the correlation structure and repeated measures on the plot to relate the adjacent week's NO₃-N concentration to the current week's NO₃-N concentration. The model then is able to account for the actual NO₃-N concentration and change in NO₃-N concentration between weeks among treatments.

Results and Discussion

The 2010 growing season was quite different with respect to rainfall amount and temperature patterns, with 2010 having greater rainfall and greater average temperature than 2011. There was 540 mm of rainfall and 213 mm of irrigation during the 2010 growing season and 217 mm of rainfall and 283 mm of irrigation during the 2011 growing season (Fig. 1). Average air temperature was 19.2°C for the 2010 growing season and 18.2°C for the 2011 growing season. The average growing season rainfall and temperature over the past 30 yr (1982 to 2012) has been 435 mm and 17.5°C, respectively.

Yield and N Uptake

Both growing seasons produced statistically equivalent yields in all plots between all treatments with supplemental fertilizer, which were all significantly greater than the 0 N. The RPCU fertilizer plots had the greatest overall average in both marketable and total yield in 2010 (Table 1), but was not significantly greater than the RCONV or LPCU. The 2010 potato growing season had overall average marketable yields near 40 Mg ha⁻¹ for all plots receiving supplemental fertilizer. The average marketable yields from all fertilized treatments in 2011 were 50 Mg ha⁻¹, which was 10 Mg ha⁻¹ greater than 2010 (Table 1). Total yields in 2010 were 8.8 Mg ha⁻¹ greater than marketable yields, whereas in 2011 total yields were 5.6 Mg ha⁻¹ greater than marketable yields, making the difference between total yield and marketable yield smaller in 2011 compared with 2010. In both years, potato size grades showed similar

trends. Higher yields were in the smaller size grades in lower rates of fertilizer contrasted with greater yields in the larger size grades in the higher fertilizer rates.

The AGB N uptake from in 2010 was similar across fertilizer treatments and sample dates (Table 2). The AGB N uptake at mid-season in 2011 was only significantly greater in the RPCU over the RCONV. However, by harvest in 2011, all fertilizer treatments had statistically similar AGB N uptake. Tuber N uptake was similar across all treatments receiving fertilizer at the end of the season for both years (Table 2). Total N uptake (AGB + tuber) was similar across treatments receiving fertilizer at both sample dates in 2010. Total N uptake in 2011 was greater in the RPCU than the RCONV at mid-season sampling, but by the end of season all fertilizer treatments had equivalent total N uptake. The proportion of total N uptake at mid-season vs. the harvest averaged 91% for the RCONV treatment, 97% for RPCU, 89% for the LPCU, and 108% for the 0 N. In, 2011, N uptake at the middle of the season as a percentage of final N uptake was 67% for RCONV treatment, 84% for the RPCU, 79% for the LPCU, and 70% for the 0 N. Harvest total N uptake from an N budget standpoint (total N uptake ÷ N applied) was less in 2010 than that in 2011. In 2010, total N uptake as a percentage of fertilizer applied averaged 58% in the RCONV, 51% in the RPCU, and 67% in the LPCU. In 2011, total N uptake as a percentage of fertilizer applied averaged 100% in the RCONV, 98% in the RPCU, and 121% in the LPCU.

Groundwater elevation and nitrate concentrations

The water table in the 2010 field rose from about 6.7 m below the soil surface to 5.6 m below the soil surface during the course of the growing season (Fig. 3). Then during the winter of 2010-2011, the water table declined consistently, with a subsequent rise during the spring thaw. The potato field in 2010 was within the cone of depression of the irrigation pumping well, and its effect can be seen in the sharp changes in the water table when pumping occurred (Fig. 3). The 2011 growing season had a continuous and consistent drop of the water table throughout the growing season from 7.3 to 7.9 m below the soil surface, and showed no indication of the effects of pumping (Fig. 3).

Groundwater flow direction was to the southwest at approximately 230° SW. When irrigation wells were pumping, the observation well from the first year of the study in 2010 was within the cone of depression, and apparent groundwater flow direction shifted to the northwest toward the pumping well. However, the observation well from the second year of the study and the third observation well did not show a pumping affect and groundwater flow may have still been to the southwest in this field.

Average NO₃-N concentrations in the 2010 potato field had no significant differences between treatments, including the 0 N (Fig. 4). Average NO₃-N concentrations for the entire growing season ranged from 15.8 to 22.6 mg NO₃-N L⁻¹. Individual well ranges for the growing season were 11.4 to 28.3 mg NO₃-N L⁻¹. After the raising of the center well, overall plot averages expanded to between 14.9 and 26.1 mg NO₃-N L⁻¹ with individual wells range expanding to between 6.9 and 43.5 mg NO₃-N L⁻¹. Separating the NO₃-N concentrations by treatment into plot average was inspected and all treatments and the 0 N had similar ranges of averages from 13.2 to 29.9 mg NO₃-N L⁻¹ (Fig. 5).

With well screens that intersected the water table for the entire growing season, average NO₃-N concentrations in the second year of the study, in a new field, also had no statistical differences between treatments including the 0 N (Fig. 6). The plot averages of NO₃-N concentrations ranged between 7.4 and 19.2 mg NO₃-N L⁻¹. These average concentrations were less than what was measured in the first growing season dropping from the 2010 average range of 15.8 to 22.6 mg NO₃-N L⁻¹. Variability persisted both between and amongst treatments as individual well NO₃-N concentrations ranged from 0.4 to 40.1 mg NO₃-N L⁻¹. Although no statistically significant differences were observed in the second year of the study, the average of the RCONV treatment was greater than both PCU treatments for the entire growing season. No correlation between precipitation or irrigation events was observed. Nitrate concentrations separated by treatments into each plot average had similar ranges of averages between

2.0 and 37.3 mg NO₃-N L⁻¹ across blocks for the three treatments and the 0 N as well (Fig. 7). An increase in NO₃-N concentration was seen in all treatments over the winter of 2012.

There was little to no NH₄-N or organic-N in the groundwater for the duration of the study. The greatest NH₄-N concentrations were seen early in the season in both years; however, NH₄-N contributed very little to groundwater N concentration. In 2010, the plot average NH₄-N concentrations were between the minimum detection of 0.05 to 0.35 mg NH₄-N L⁻¹. The average concentration was 0.08 mg NH₄-N L⁻¹, and the median was 0.06 NH₄-N L⁻¹. There was no statistical difference between treatments. In 2011, the range of plot averages was between 0.05 and 0.20 mg NH₄-N L⁻¹. The average concentration was 0.07 mg NH₄-N L⁻¹, and the median was 0.06 NH₄-N L⁻¹. There was no statistical significance between treatments in either year of the study. Plot average organic N concentrations ranged between 0 and 1.2 mg organic N L⁻¹ in 2010. Treatment averages were 0.58 mg organic N L⁻¹ with the median at 0.46 mg organic N L⁻¹. Plot average organic N concentration in 2011 was between 0 and 0.69 mg organic N L⁻¹. Treatment averages were 0.13 mg organic N L⁻¹ with the median at 0.08 mg organic N L⁻¹. No dates for either 2010 or 2011 had a statistically significant difference in organic N concentration.

Discussion

Both the use of PCU and a reduction in N rate with use of PCU maintains yield while increasing N use efficiency. Both PCU treatments maintained average total and marketable yields as the split applied RCONV treatment. The fact that the LPCU treatment maintained yields of the RPCU and RCONV which had greater rates of N applied is similar to findings of Hopkins et al. (2008), who found that all potato size categories with PCU had greater yields at lesser rates of application, than that of urea at greater rates of application. Thus, it follows that an optimum economic rate of PCU N may be below the recommended conventional rates thereby increasing uptake efficiency. Results from other studies have also demonstrated that potato grown in sandy soils using PCU fertilizers are able to maintain or even increase yield (Liegel and Walsh, 1976; Zvomuya et al., 2003; Pack et al., 2006; Worthington et al., 2007; Hyatt et al., 2010). Data from these studies have shown that PCU fertilizers produce equivalent yields to AN or urea fertilizers even under a variety of leaching environments. It is also interesting to note that several researchers have reported a delay in tuber growth when high amounts of soil N are available early in the season (Cox and Addiscott, 1976; Kleinkopf et al., 1981; Westermann and Kleinkopf, 1985; Errebhi et al., 1998). However, applying all of the PCU fertilizer at emergence did not seem to delay tuber growth or final tuber yield in this study. The PCU application also did not affect final petiole NO₃-N concentrations in potato, although the RCONV treatment had greater petiole NO₃-N concentrations than both PCU treatments in 2010 and the LPCU in 2011 early in the season. These results are similar to the findings presented by Liegel and Walsh (1976). According to Haverkort and van de Waart (1994), high leaf NO₃-N concentrations early in the season were not associated with high yields at the end of the season. The lack of correlation between yield and early and midseason N concentration held true for this study.

The nitrogen budget data reinforces Hopkins et al. (2008) assertion that optimum economic rates of PCU fertilizers can be lesser than RCONV fertilizer. The increase in use efficiency between years can be explained by available system N. Nitrogen is present in the irrigation water, and Bundy and Andraski (2005) found that irrigation could provide 3.9 to 5.2 kg N ha⁻¹ per 25 mm of irrigation applied (Arriaga et al., 2009). This means that in 2010, irrigation supplied between 33 and 44 kg N ha⁻¹ and between 44 and 59 kg N ha⁻¹ in 2011. This N applied by irrigation in 2010 would have been leached by frequent heavy rainfall events; however, in 2011, with few rainfall events, and no large single rain storms, N from irrigation water would have been more available to be utilized by potato plants.

Rainfall and temperature patterns exert tremendous control on yield and N use efficiency. The growing season in 2010 was warmer, had a greater amount of precipitation, and had more intense rainfall events than 2011. As a result, the 2011 potato yields were greater than the 2010 yields (most

likely the result of differences in soil N availability). In 2010, it is possible that the PCU fertilizer had exhausted its supply of N because of increased dissolution of urea from the fertilizer prior to the end of potato uptake, leading to reduced yields. The PCU fertilizer used has a thermoplastic shell, and the porosity of the shell increases with increasing temperature, and with 2010 being wet and warm, N release may have been more rapid than 2011. The drier weather in 2011 not only limited the release of N from the PCU treatments but also limited the leaching from the RCONV treatment which reduced the advantage of PCU, which acts as to buffer against intense rainfall events.

The variation in NO₃-N concentration, both within and among treatments led to an inability to determine a significant difference or treatment effect on groundwater NO₃-N concentration. Similar large variation has been found in several other studies as well (Saffigna et al., 1977; Hubbard et al., 1984; Hill, 1986; Hubbard et al., 1986). Variation provided large standard errors (2.1 in 2010 and 6.9 in 2011), and with average NO₃-N at similar concentrations amongst treatments throughout the year, there was not a significant difference among treatments. This variation may be due in part to whether or not the monitoring wells in a given plot intercepted a preferential flow path. These flow paths can lead to solutes entering the water table in a much smaller cross section than what would be applied to the plot (Kung, 1990a,b). The short time scale of this study was not sufficient to overcome the variation in NO₃-N concentrations in order to determine treatment differences. This is not uncommon as other studies have shown that groundwater quality responses to new agricultural practices can take decades (e.g. Tomer and Burkart, 2003). From an N budget standpoint, the amount of N available for leaching from the application of fertilizer was calculated, i.e., the N removed by plant uptake compared with N applied (CREC). This indicated that there was less N available for leaching in the LPCU ($P \geq 0.007$ in 2010 and $P \geq 0.055$ in 2011). The calculated remaining nitrogen in the field after harvest ($(1 - \text{CREC}) \times \text{N applied}$) in the RCONV, RPCU and LPCU averaged 181, 199, and 137 kg N ha⁻¹, respectively in 2010, and 154, 162, and 107 kg N ha⁻¹, respectively in 2011. This further indicated that variation in the background groundwater NO₃-N concentration masked what would have been expected lower concentrations from less leached N in the LPCU.

The vertical placement of wells is critical when attempting to measure the amount of NO₃-N reaching the surface of the water table from a specific fertilizer treatment. Nitrate concentrations are generally greatest at the top of a shallow water table and decrease with depth because of dilution and mixing (Hill, 1982; Hubbard et al., 1986; Mueller and Helsel, 1996). The large amount of rainfall in 2010 led to a rise in the water table and after installing the well screens 1.6 m below the water table to account for the anticipated seasonal decline, the rise seen in 2010 put the screens, on average 3.0 m below the water table. As changes in NO₃-N typically decrease with depth in the water table as noted by Hubbard et al. (1986), Power and Schepers (1989), Spalding and Exner (1993), and Mueller and Helsel (1996), the water samples from the wells that were 3.0 m below the water table measured the bulk, mixed water rather than from nitrates that reached the surface of the water table that were leached from the N applied plot. Our results are consistent, as when the center well was raised after the growing season, higher average groundwater NO₃-N concentration were measured than when the well were deeper. This also impacted statistical comparisons as with one well intersecting the water table, the average range, and therefore variation, of NO₃-N concentrations increased. Had the 2010 wells intersected the water table during the wet growing season, they may have shown more leaching, as leaching of N occurs mainly during periods of high precipitation (Bergstrom and Brink, 1986). The sharp increase in the NO₃-N concentrations in the raised wells reinforces this conclusion, and the raised wells would give a better indication of the nitrates leached from a specific plot and fertilizer treatment, whereas the deeper well NO₃-N measurements could be that of water carried from off plot by groundwater flow, which has also been pointed out as a difficulty by Hubbard et al. (1984).

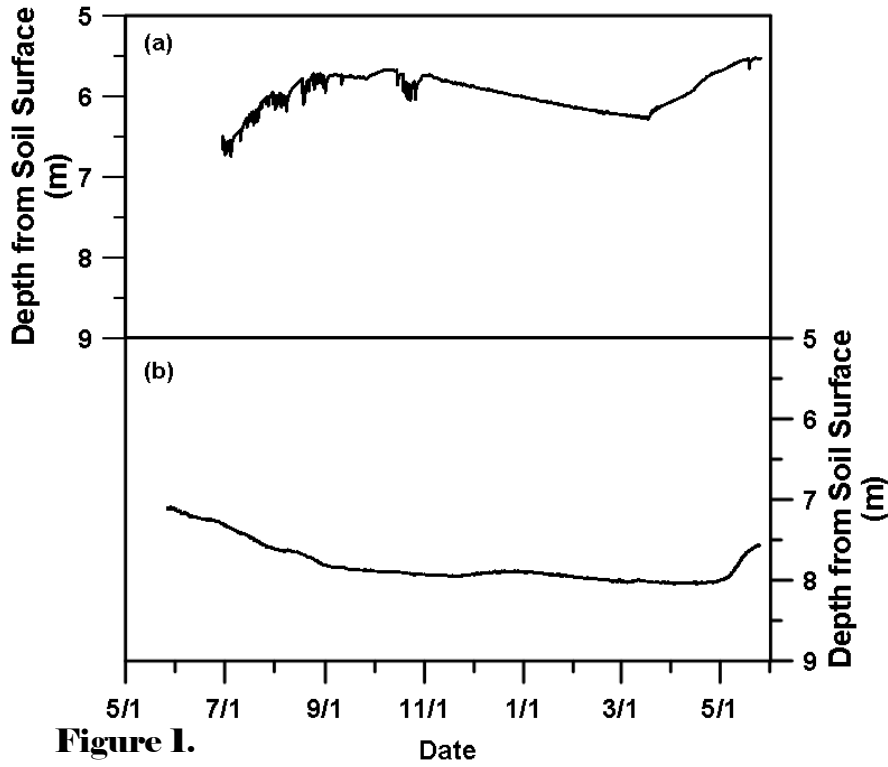


Figure 1.

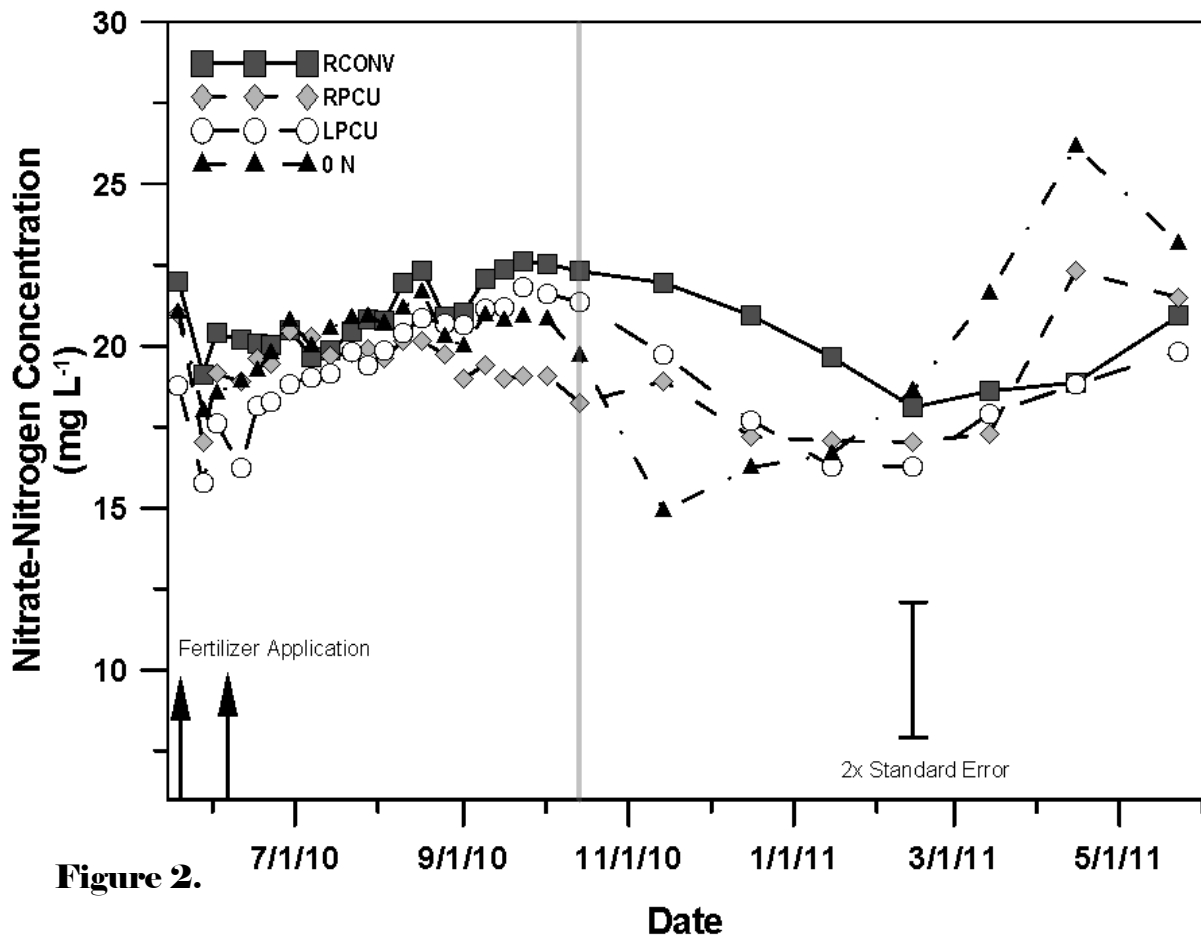


Figure 2.

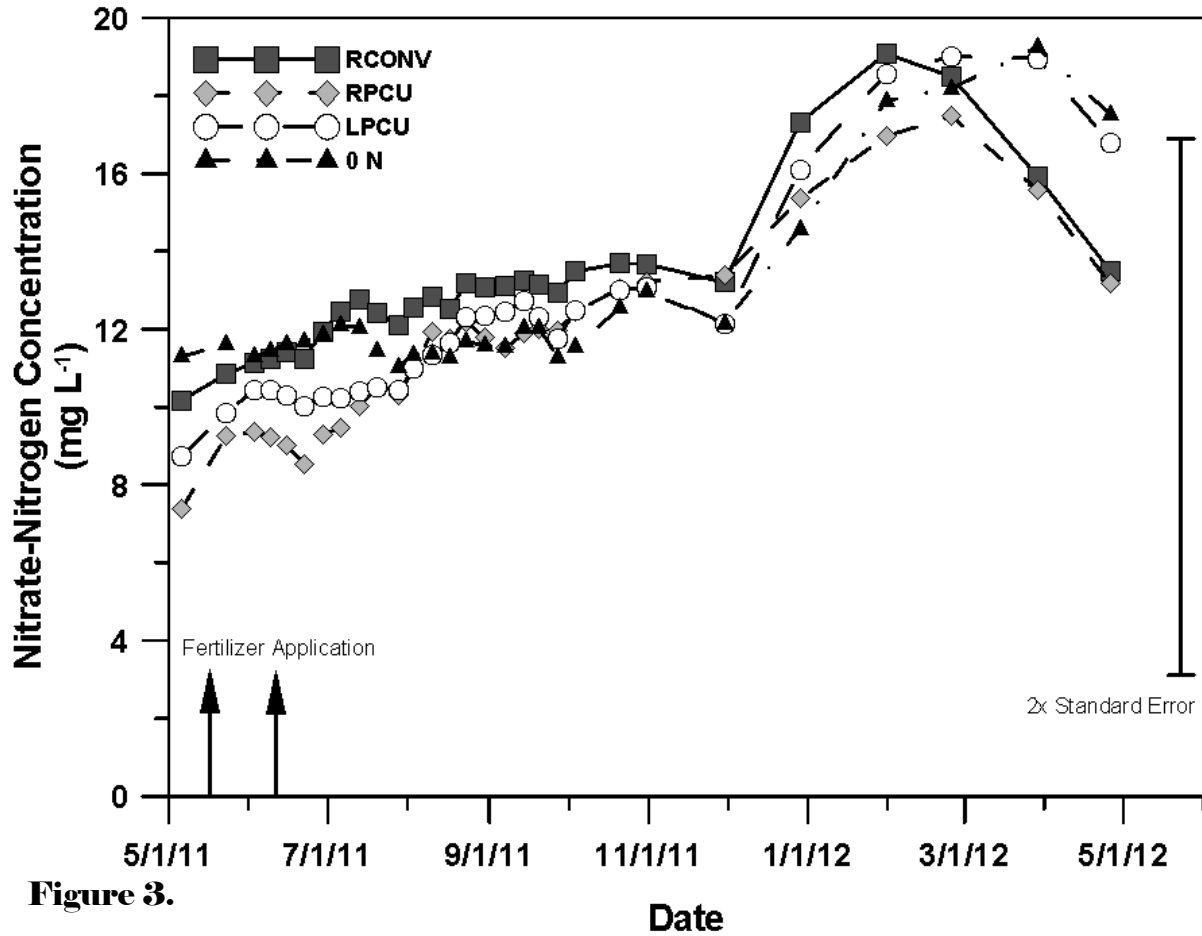


Figure 3.

Table 1. Marketable and total potato yields for 2010 and 2011.

Treatment †	2010		2011	
	Marketable	Total	Marketable	Total
	----- Mg ha ⁻¹ -----			
RCONV	39.9 a ‡	48.8 a	50.0 a	54.7
RPCU	41.8 a	50.2 a	50.9 a	56.5
LPCU	39.3 a	47.8 a	52.1 a	56.5
0 N	21.6 b	30.9 b	41.1 b	48.7
P>F	<0.001	<0.001	0.025	0.138

† The conventional fertilizer, RCONV, 280 kg N ha⁻¹ as 93 kg ha⁻¹ ammonium sulfate applied at emergence and 187 kg N ha⁻¹ as ammonium nitrate; recommended controlled-release fertilizer, RPCU, 280 kg N ha⁻¹ as PCU applied at emergence; low rate controlled-release fertilizer, LPCU – 224 kg N ha⁻¹ as PCU applied at emergence.

‡ Mean values followed by letters indicate statistically significant difference at the $\alpha=0.10$ level. Table 2. Potato N uptake.

Table 2. Potato nitrogen uptake.

Year	Treatment †	AGB ‡		MS	Tubers		Total uptake	
		MS	Harvest		Harvest	MS	Harvest	
----- kg ha ⁻¹ -----								
2010	RCONV	128 a §	49 a	18	113 a	147 a	162 a	
	RPCU	117 a	29 ab	22	115 a	139 a	144 a	
	LPCU	110 a	39 a	24	110 a	134 a	150 a	
	0 N	44 b	10 b	23	53 b	68 b	63 b	
	P>F	<0.001	0.030	0.714	<0.001	0.004	<0.001	
2011	RCONV	170 b	92 a	17 b	189 a	187 b	281 a	
	RPCU	203 a	74 a	25 b	199 a	228 a	273 a	
	LPCU	192 ab	66 a	23 b	206 a	215 ab	272 a	
	0 N	72 c	20 b	37 a	135 b	109 c	155 b	
	P>F	<0.001	0.007	0.015	<0.001	<0.001	<0.001	

† Above-ground biomass (AGB) and tubers at mid-season (MS) samples taken day after emergence (DAE) 44 in 2010 and DAE 47 in 2011. Harvest AGB samples were taken at DAE 92 in 2010 and DAE 97 in 2011 and harvest tubers were taken at DAE 105 in 2010 and DAE 115 in 2011.

‡ The conventional fertilizer, RCONV, 280 kg N ha⁻¹ as 93 kg ha⁻¹ ammonium sulfate applied at emergence and 187 kg N ha⁻¹ as ammonium nitrate; recommended controlled-release fertilizer, RPCU, 280 kg N ha⁻¹ as PCU applied at emergence; low rate controlled-release fertilizer, LPCU – 224 kg N ha⁻¹ as PCU applied at emergence.

§ Mean values followed by letters indicate statistically significant difference at the $\alpha=0.10$ level.

Conclusions and Recommendations

The controlled release PCU maintained plant growth response to applied N compared conventional split applied management practices. When applied at less than recommended rates, PCU led to measured improvements in the PFP and PNB NUE components. The magnitude of increase in these NUE components is still dependent on growing season conditions, but use of PCU should be considered as an alternative fertilizer source for potato. An added benefit of PCU is the one-time application, which would save fuel costs and time in the field possibly preventing crop damage.

Although large plots, 15 by 15 m, were sufficient in size to reduce the impact of plot to plot contamination, variability in NO₃-N concentrations at the surface of the groundwater made it difficult to determine a fertilizer treatment effect on water quality. While a statistical difference was not found between treatments, trends suggest that future research into fertilizer effect on groundwater NO₃-N using PCU treatments might be warranted as conventional split-applied fertilizer management had greater NO₃-N concentrations than the PCU treatments through most of the sample period. In the short term, data collection should continue using the near surface measurements from porous cup samplers and soil tests, which have shown decreases in NO₃-N flux in the root zone using PCU fertilizers. Using N use efficiencies or root zone fluxes may be better at determining the impact of fertilizer on groundwater quality in the short term until more efficient strategies of directly monitoring groundwater can be developed. Future use of wells that directly monitor groundwater could overcome variability in NO₃-N concentrations and groundwater flow with field size plots dedicated to a single treatment, monitored over a very long time, which could allow cumulative fertilizer effects to supersede the difficulties present in direct groundwater monitoring. These large, long-term studies, while costly, may produce statistical differences and allow better conclusions to be made comparing conventional split applied fertilizer to PCU treatments.

References

- Arriaga, F., B. Lowery, and K. Kelling. 2009. Surfactant impact on nitrogen utilization and leaching in potatoes. *Am. J. Potato Res.* 86:383–390.
- Bergström, L., and N. Brink. 1986. Effects of differentiated applications of fertilizer N on leaching losses and distribution of inorganic N in the soil. *Plant Soil* 93(3):333–345.
- Bundy, L.G., and T.W. Andraski. 2005. Recovery of fertilizer nitrogen in crop residues and cover crops on an irrigated sandy soil. *Soil Sci. Soc. Am. J.* 69:640–648.
- Burkart, M.R. 2002. Nitrate in aquifers beneath agricultural systems. In: J.D. Stoner (ed.) *Water science and technology*. p. 19–28.
- Cameron, D.R., C.G. Kowalenko, and C.A. Campbell. 1979. Factors affecting nitrate nitrogen and chloride leaching variability in a field plot. *Soil Sci. Soc. Am. J.* 43:455–460.
- Cooley, E.T., B. Lowery, K.A. Kelling, P.E. Speth, F.W. Madison, W.L. Bland, and A. Tapsieva. 2009. Surfactant use to improve soil water distribution and reduce nitrate leaching in potatoes, *Soil Sci.* 174:321–329.
- Cox, D., and T.M. Addiscott. 1976. Sulphur-coated urea as a fertiliser for potatoes. *J. Sci. Food Agric.* 27:1015–1020.
- Díez, J.A., R. Roman, M.C. Cartagena, A. Vallejo, A. Bustos, and R. Caballero. 1994. Controlling nitrate pollution of aquifers by using different nitrogenous controlled release fertilizers in maize crop. *Agric. Ecosys. Environ.* 48(1):49–56.
- Doane, T.A., and W.R. Horwáth. 2003. Spectrophotometric determination of nitrate with a single reagent. *Anal. Letters* 36(12):2713.
- Errebhi, M., C.J. Rosen, S.C. Gupta, and D.E. Birong. 1998. Potato yield response and nitrate leaching as influenced by nitrogen management. *Agron. J.* 90:10–15.
- Haverkort, A.J., and M. van de Waart. 1994. Yield and leaf nitrate concentration of starch potato on sandy humic soils supplied with varying amounts of starter and supplemental nitrogen fertilizer. *Euro. J. Agron.* 3:29–41.
- Hill, A.R. 1982. Nitrate distribution in the ground water of the Alliston region of Ontario, Canada. *Ground Water* 20:696–702.
- Hill, A.R. 1986. Nitrate and chloride distribution and balance under continuous potato cropping. *Agric. Ecosys. Environ.* 15(4):267–280.
- Hopkins, B.G., C.J. Rosen, A.K. Shiffler, and T.W. Taysom. 2008. Enhanced efficiency fertilizers for improved nutrient management: Potato (*Solanum tuberosum*). In: *Crop management*, p. 16, Online.
- Hubbard, R.K., G.J. Gascho, J.E. Hook, and W.G. Knisel. 1986. Nitrate movement into shallow ground water through a coastal plain sand. *Trans. Am. Soc. Agric. Engr.* 1564–1571.
- Hubbard, R.K., L.E. Asmussen, and H.D. Allison. 1984. Shallow groundwater quality beneath an intensive multiple-cropping system using center pivot irrigation. *J. Environ. Qual.* 13:156–161.
- Hyatt, C.R., R.T. Venterea, C.J. Rosen, M. McNearney, M.L. Wilson, and M.S. Dolan. 2010. Polymer-coated urea maintains potato yields and reduces nitrous oxide emissions in a Minnesota loamy sand. *Soil Sci. Soc. Am. J.* 74:419–428.
- Kleinkopf, G.E., D.T. Westermann, and R.B. Dwelle. 1981. Dry matter production and nitrogen utilization by six potato cultivars. *Agron. J.* 73:799–802.
- Kraft, G.J., and W. Stites. 2003. Nitrate impacts on groundwater from irrigated-vegetable systems in a humid north-central U.S. sand plain. *Agric. Ecosys. Environ.* 100(1):63–74.
- Kung, K.J.S. 1990a. Preferential flow in a sandy vadose zone: 1. Field observation. *Geoderma* 46:51–58.
- Kung, K.J.S. 1990b. Preferential flow in a sandy vadose zone: 2. Mechanism and implications. *Geoderma* 46:59–71.

- Landon, M.K., G.N. Delin, S.C. Komor, and C.P. Regan. 2000. Relation of pathways and transit times of recharge water to nitrate concentrations using stable isotopes. *Ground Water* 38(3): 381–395.
- Liegel, E.A., and L.M. Walsh. 1976. Evaluation of sulfur-coated urea (SCU) applied to irrigated potatoes and corn. *Agron. J.* 68:457–463.
- Mueller, D.K., and D.R. Helsel. 1996. Nutrients in the nation's waters - too much of a good thing? U.S. Geol. Surv. Pub. 1136. p. 24.
- Olsen, R.J., R.F. Hensler, O.J. Attoe, S.A. Witzel, and L.A. Peterson. 1970. Fertilizer nitrogen and crop rotation in relation to movement of nitrate nitrogen through soil profiles. *Soil Sci. Soc. Am. J.* 34:448–452.
- Pack, J.E., C.M. Hutchinson, and E.H. Simonne. 2006. Evaluation of controlled-release fertilizers for northeast Florida chip potato production, *J. Plant Nutr.* 29(7):1301–1313.
- Power, J.F., and J.S. Schepers. 1989. Nitrate contamination of groundwater in North America, *Agric. Ecosys. Environ.* 26:165–187.
- Saffigna, P.G., and D.R. Keeney. 1977. Nitrate and chloride in ground water under irrigated agriculture in central Wisconsin. *Ground Water* 15:170–177.
- Saffigna, P.G., D.R. Keeney, and C.B. Tanner. 1977. Nitrogen, chloride, and water balance with irrigated Russet Burbank potatoes in a sandy soil. *Agron. J.* 69:251–257.
- Spalding, R.F., and M.E. Exner. 1993. Occurrence of nitrate in groundwater - A review. *J. Environ. Qual.* 22:392–402.
- Tomer, M.D., and M.R. Burkart. 2003. Long-term effects of nitrogen fertilizer use on ground water nitrate in two small watersheds. *J. Environ. Qual.* 32:2158–2171.
- Westermann, D.T., and G.E. Kleinkopf. 1985. Nitrogen requirements of potatoes. *Agron. J.* 77:616–621.
- Wilson, M.L., C.J. Rosen, and J.F. Moncrief. 2010. Effects of polymer-coated urea on nitrate leaching and nitrogen uptake by potato. *J. Environ. Qual.* 39:492–499.
- Worthington, C., K. Portier, J. White, R. Mylavarapu, T. Obreza, W. Stall, and C. Hutchinson. 2007. Potato (*Solanum tuberosum* L.) yield and internal heat necrosis incidence under controlled-release and soluble nitrogen sources and leaching irrigation events. *Am. J. Potato Res.* 84:403–413.
- Zvomuya, F., and C.J. Rosen. 2001. Evaluation of polyolefin-coated urea for potato production on a sandy soil, *HortScience* 36:1057–1060.
- Zvomuya, F., C.J. Rosen, M.P. Russelle, and S.C. Gupta. 2003. Nitrate leaching and nitrogen recovery following application of polyolefin-coated urea to potato. *J. Environ. Qual.* 32:480–489.

Appendix A

- Bero, N.J., M.D. Ruark, and B. Lowery. 2013. Controlled-release fertilizer effect on groundwater nitrogen concentration in sandy soil under potato production. *Agronomy Journal* (In review).
- Bero, N.J., M.D. Ruark, and B. Lowery. 2011. Slow-release fertilizer effect on groundwater nitrogen concentration in sandy soils under potato production. *North Central Extension and Industry Soil Fertility Conference Vol. 27, 16-17 Nov., Des Moines, IA.*
- Award : Nick Bero, 2012 Grad Student Award, 2011 North Central Soil Fertility Industry and Extension Conference.

Appendix B

Other available data (e.g. petiole nitrate, potato specific gravity and internal defects) are reported in Nick Bero's MS Thesis (Dept. of Soil Science, University of Wisconsin, 2012). Available as pdf upon request.

Tracer study

Materials and Methods

A Br⁻ tracer field experiment was conducted at the Hancock Agricultural Research Station in a Plainfield loamy sand soil. Two fields were divided into twelve 14.6 m × 15.24 m plots, arranged two plots wide by six plots long. Three wells were placed diagonally across each plot, at a distance of 4.9 m (A well), 7.6 m (B well), and 9.8 m (C well) respectively from the south edge of each plot (Figures 1 and 2). Wells were completed on 17 May 2010 in the first field and on 2 May 2011 in the second field. The average depth to groundwater was 6.7 m at the time of well installation in 2010. Wells were installed approximately 3.1 m below the water table, leaving the top of the screen 1.6 m below the water table. On 14 October 2010, the center well, labeled as the B well, was raised to 7.3 m depth, which was 1.3 m below the water table to allow for sampling at the surface of the water table and assessment of the vertical placement of well screens. On 23 May 2011, all wells in the first field were raised so that the well screens intersected the water table. Wells in the second field in 2011, which were used in the 2012 Br⁻ application, were installed at a depth of 9.1 m with 2.3 m screens at 1.8 m of depth into the water table. Wells in 2012 intersected the water table at all times during the study period. Bromide was applied to plots 202 and 302 at a rate of 112 kg ha⁻¹ (2.72 kg plot⁻¹), and Cl⁻ to plots 103 and 203 at a rate of 224 kg ha⁻¹ (5.44 kg plot⁻¹), on 14 October 2010 (Figure 1). Bromide was applied on 9 March 2012 to the second field in plots 103 and 302 (Figure 2). Chloride was not applied to the second field in the spring of 2012. A CO₂ powered backpack sprayer with a four nozzle spray boom was used to uniformly apply the tracers to the plot. Each plot required two tanks of dissolved tracer, and application was done North-South using the first tank and East-West on the second tank to assure uniform coverage of tracer to plots. Yearly well sampling was such that wells were sampled twice weekly following tracer application from 14 October 2010 until 16 December 2010, monthly until 27 May 2011, then again weekly until 14 October 2011, then monthly until 26 April 2012, where the data set ended. The second replicate in the second field was sampled weekly from 15 March 2012 to **3 August 2012** and analyzed for concentration mg L⁻¹ of Br⁻ tracer.

Infiltration and downward movement of the tracer was driven by irrigation and rainfall in 2010 (Figure 3). If rainfall did not occur within 2 days, approximately 18 to 35 mm of water was applied during the period of 14 October to 28 October 2010 by irrigation. Irrigation was then discontinued after October because of freezing temperatures. In 2012, rainfall and scheduled crop irrigation was the driver for leaching Br⁻ from the soil profile (Figure 4). Contrary to the 2010 application of tracer, the second field in 2012 did not have the irrigation turned on for the growing season as of application date, and could not be used to provide water for immediate leaching.

The Br⁻ microplate analysis used in this study was a modified colorimetric method from Lepore and Barak (2009). Their method capitalizes on the transformation of phenol red to bromine blue in the presence of Br⁻. A Biotek PowerWave XS (BioTek Instruments Inc. Winooski, VT 05404) microplate reader was used to measure absorbances, and concentration of Br⁻ each week's set of samples was based on a standard curve prepared with four replicates of standards from 0-12.5 mg Br⁻ L⁻¹. The Cl⁻ analysis for this study utilized the reaction between mercury thiocyanate, ferric nitrate, and Cl⁻, and absorbances were again read by the Biotek microplate reader. Unknown sample concentrations were calculated from standards that ranged from 0-100 mg Cl⁻ L⁻¹ (Adriano and Donnor, 1982). Secondary Cl⁻ analysis was performed on the two shallow middle B wells of the Cl⁻ applied plots to verify the numbers calculated from the Cl⁻ microplate analysis with the Dionex Ion Chromatograph (Thermo Scientific Sunnyvale, CA 94088). The groundwater BTCs were then constructed from the resulting water concentrations of Br⁻ and Cl⁻.

Results-Bromide

The total amount of water applied during the initial downward leaching of Br in 2012 was 25.7 cm as of 18 July 2012. The cumulative amount of water that was applied during the initial downward

leaching of the tracers from 14 October to 15 December was 17.14 cm in 2010. The plots for which Br⁻ were applied showed breakthrough at the shallow well, but there was no breakthrough in wells that were screened deeper into the water table. The Br⁻ BTCs were characteristic bell shaped for plots 202 and 302 between days 2 November and 10 December 2010 and each plot showed two peaks (Figure 5 and 6). Breakthroughs for wells 202B and 302B occurred on November 2nd, and peak concentration was observed the next sample day of November 5th. The second breakthrough occurred again in wells 202B and 302B approximately three weeks later spanning November 23rd through December 10th. The Br⁻ concentration in plot 302 was greater than that of plot 202 by approximately 6 mg Br⁻ L⁻¹. The peak concentration in plot 302 was about 8 mg Br⁻ L⁻¹ where plot 202 peak reached 1.5 mg Br⁻ L⁻¹. During the initial infiltration of Br⁻ wells in the surrounding plots show no indication of Br⁻ breakthrough during the initial downward leaching (Figures 7 and 8). On the 14 February 2011 sample date, Br⁻ was detected in the raised center well in plots 103 and 203. These plots are to the southwest of the plots to which Br⁻ was applied and concentrations above background persisted for several months (Figures 7 and 8). Bromide reappeared in the wells of plots to which it was applied in concentrations that were greater than the initial breakthrough concentrations and persisted throughout the summer of 2011 and winter of 2012. Concentrations of Br⁻ above background were also detected in the wells in plot 204 during the summer of 2011. At the end of sampling in the field used in 2010, there was Br⁻ in the system in plots 103 and 203. As of the 25 July 2012 sample date, Br⁻ had not been detected in any well in the second field (Figures 9 and 10).

Results - Chloride

Chloride was found in plots 303, 304, 301, 104, and 102. Changes in Cl⁻ concentrations were seen in several non-Cl⁻ applied plots, but the data do not provide a pattern that is useful for solute leaching analysis (Figures 11 and 12). The results from the Dionex Ion Chromatograph show that although the concentrations from the two methods are different, the shape of the Cl⁻ concentration curves for each of the wells are similar to one another (Figure 13).

Figures listed here and below refer to Figure numbers in Bero's MS Thesis.

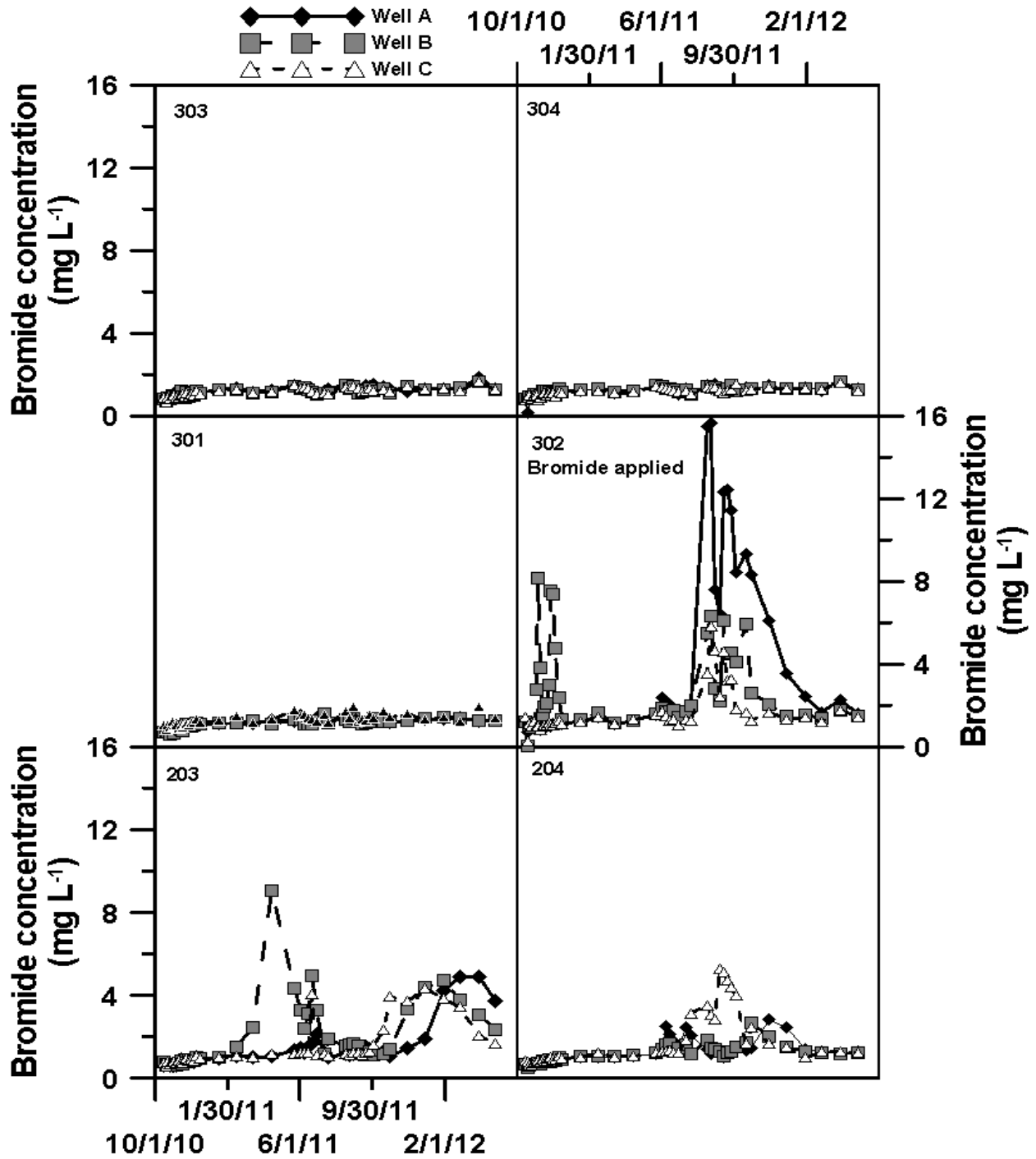


Figure 1. Bromide concentrations in the north six plots of the first field where bromide was applied on 14 October 2010. The first sample date represents the day on which bromide was applied.

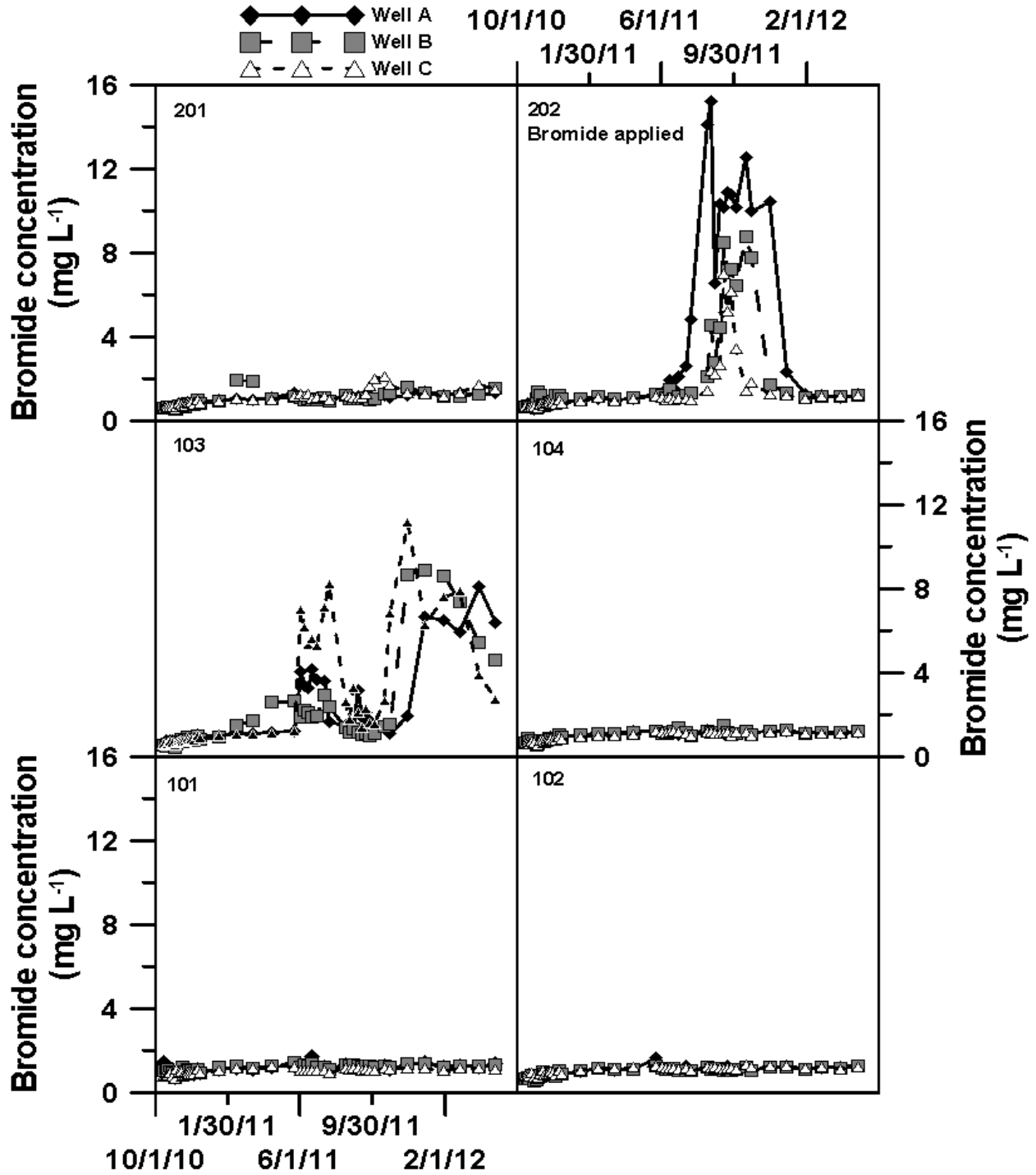


Figure 2. Bromide concentrations in the south six plots of the first field where bromide was applied on 14 October 2010. The first sample date represents the day on which bromide was applied.

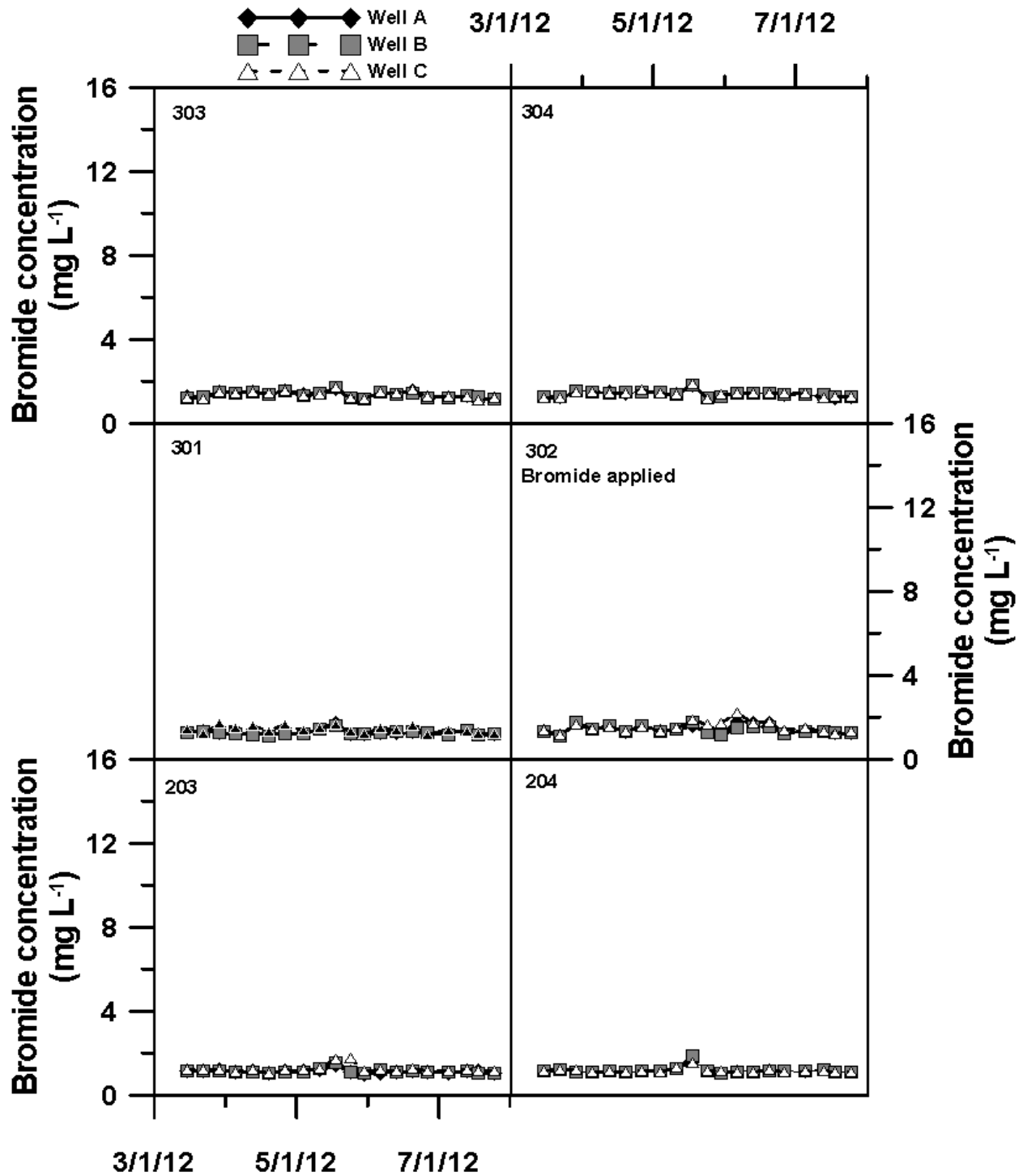


Figure 3. Bromide concentrations in the north six plots of the second field where bromide was applied on 9 March 2012. The first sample date represents the day on which bromide was applied.

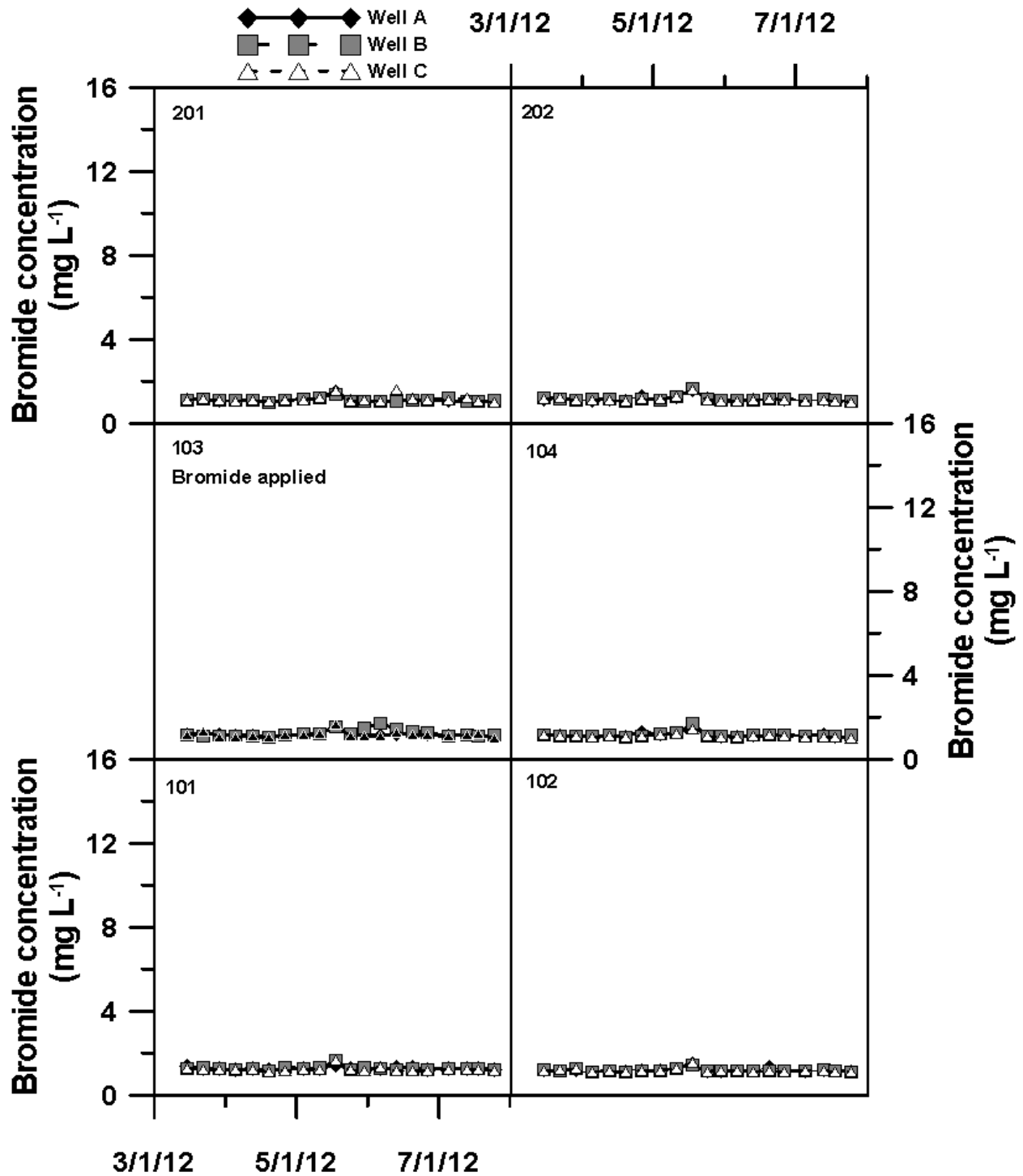


Figure 4. Bromide concentrations in the south six plots of the second field where bromide was applied on 9 March 2012. The first sample date represents the day on which bromide was applied.

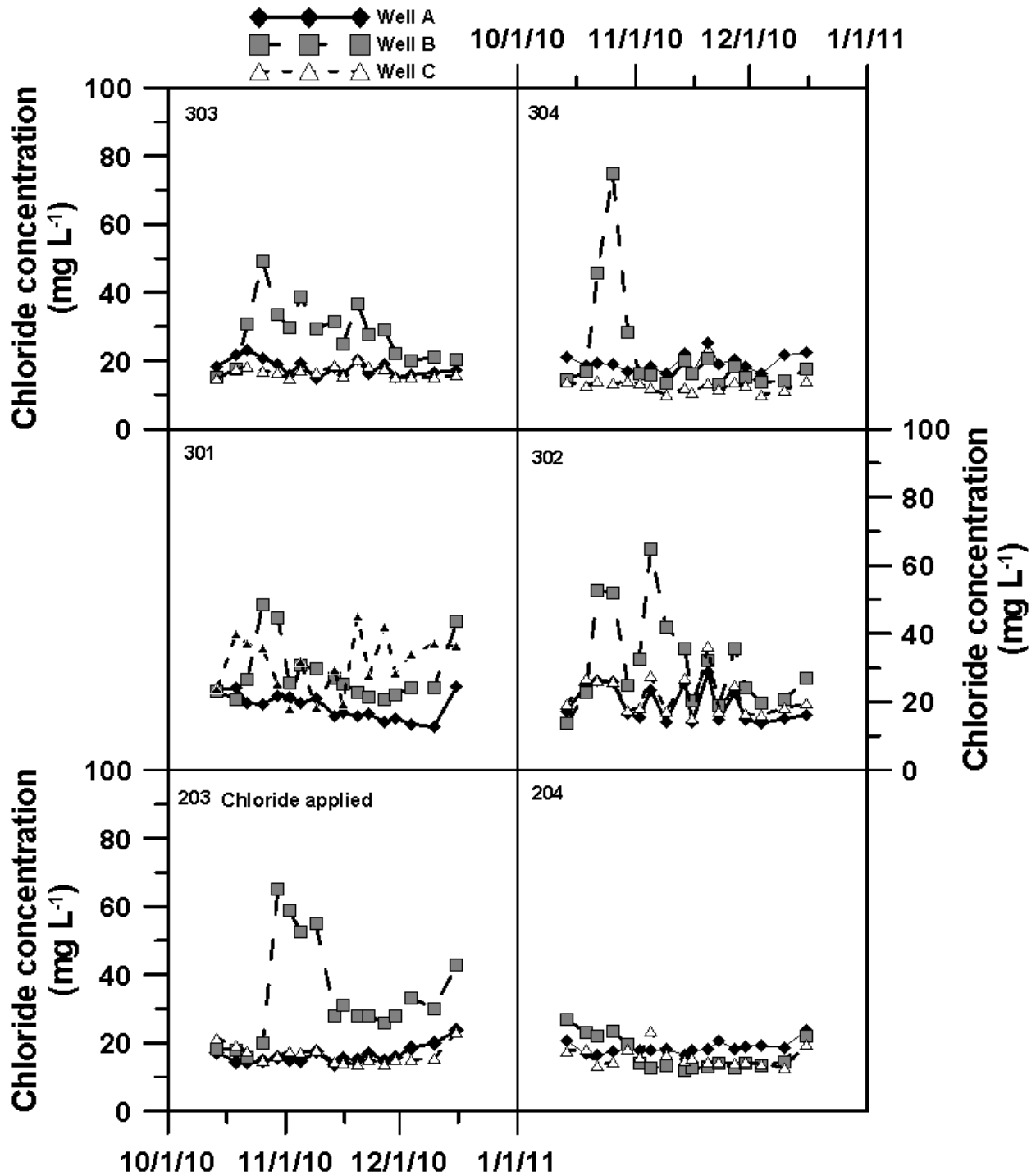


Figure 5. Chloride concentrations in the north six plots of the first field where chloride was applied on 14 October 2010. The first sample date represents the day on which chloride was applied.

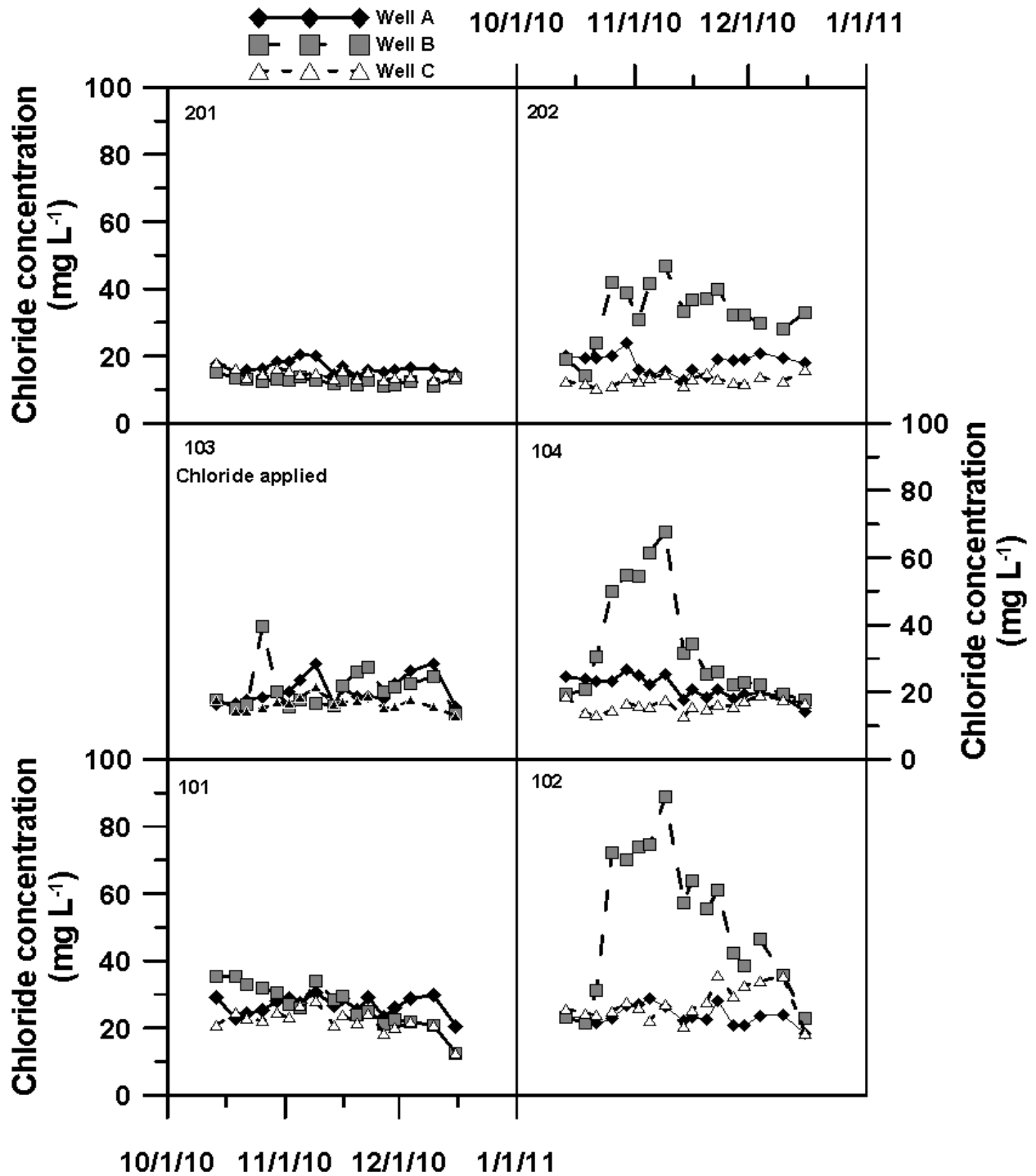


Figure 6. Chloride concentrations in the south six plots of the first field where chloride was applied on 14 October 2010. The first sample date represents the day on which chloride was applied.

Influence of Adsorbed Antibiotics on Water Quality and Soil Microbes

Basic Information

Title:	Influence of Adsorbed Antibiotics on Water Quality and Soil Microbes
Project Number:	2010WI2850
Start Date:	7/1/2010
End Date:	6/30/2013
Funding Source:	Other
Congressional District:	WI 2nd
Research Category:	Ground-water Flow and Transport
Focus Category:	Water Quantity, Geochemical Processes, Sediments
Descriptors:	
Principal Investigators:	Zhaohui Li

Publications

1. Chang, P.-H., Li, Z., Jean, J.-S., Jiang, W.-T., Wang, C.-J., Lin, K.-H. (2012) Adsorption of tetracycline on 2:1 layered non-swelling clay mineral illite, *Appl. Clay Sci.*, 67-68, 158-163. <http://dx.doi.org/10.1016/j.clay.2011.11.004>
2. Wu, Q., Li, Z., Hong, H. (2012) Influence of types and charges of exchangeable cations on ciprofloxacin sorption by montmorillonite, *J. Wuhan Univ. Technol. - Mater. Sci. Ed.*, 27, 516-522. <http://dx.doi.org/10.1007/s11595-012-0495-2>
3. Lv, G., Liu, L., Li, Z., Liao, L., Liu, M. (2012) Probing the interactions between chlorpheniramine and 2:1 phyllosilicates, *J. Colloid Interface Sci.*, 374, 218-225. <http://dx.doi.org/10.1016/j.jcis.2012.01.029>
4. Wu, Q., Li, Z., Hong, H. (2013) Adsorption of the quinolone antibiotic nalidixic acid onto montmorillonite and kaolinite, *Appl. Clay Sci.*, 74, 66-73. <http://dx.doi.org/10.1016/j.clay.2012.09.026>
5. Jiang, W.-T., Wang, C.-J., Li, Z. (2013) Intercalation of ciprofloxacin accompanied by dehydration in rectorite, *Appl. Clay Sci.*, 74, 74-80. <http://dx.doi.org/10.1016/j.clay.2012.07.009>
6. Jiang, W.-T., Chang, P.-H. Wang, Y.-S., Tsai, Y., Jean, J.-S., Li, Z., Krukowski, K. (2013) Removal of ciprofloxacin from water by birnessite, *J. Hazard. Mater.*, 250-251, 362-369. <http://dx.doi.org/10.1016/j.jhazmat.2013.02.015>
7. Wu, Q., Li, Z., Hong, H., Li, R., Jiang, W.-T. (2013) Desorption of ciprofloxacin from clay mineral surfaces, *Water Res.*, 47 (1), 259-268. <http://dx.doi.org/10.1016/j.watres.2012.10.010>

Annual Progress Report

Selected Reporting Period: 7/1/2011 - 6/30/2012

Submitted By: Zhaohui Li
Submitted: 4/30/2013

Project Title

WR10R006: Influence of Adsorbed Antibiotics on Water Quality and Soil Microbes

Project Investigators

Zhaohui Li, University of Wisconsin-Parkside
Maria MacWilliams, University of Wisconsin-Parkside

Progress Statement

The goal of this research is to investigate the influence of adsorbed antibiotics on water quality and soil microbes. To achieve this central goal, we conducted the following experiments.

1. Determined the desorption kinetics of tetracycline (TC) and ciprofloxacin (CIP) from external surfaces of nonswelling clays or from the interlayer of swelling clays at different loading levels and their effect on water quality.
2. Determined the desorption of TC and CIP from the clays under different pH conditions.
3. Determined the influence of the presence of different types of cations on the desorption of TC and CIP.
4. Determined the antimicrobial activity of TC and CIP bond to external surfaces of kaolinite and in the interlayer spaces of montmorillonite against TC sensitive and TC resistant strains.

Principal Findings and Significance

Principal Findings and Significance

Description A swelling clay mineral montmorillonite and a nonswelling clay mineral kaolinite were preloaded with antibiotics tetracycline and ciprofloxacin at varying concentrations and bioassays were conducted to examine whether the antibiotics still inhibited bacterial growth in the presence of montmorillonite. *Escherichia coli* was incubated with montmorillonite or antibiotic-adsorbed montmorillonite, and then the number of viable bacteria per mL was determined. The antimicrobial activity of tetracycline was affected in the presence of montmorillonite, as the growth of non-resistant bacteria was still found even when extremely high TC doses were used. Conversely, in the presence of montmorillonite, ciprofloxacin did inhibit *E. coli* bacterial growth at high concentrations. These results suggest that the effectiveness of antimicrobial agents in clayey soils depends on the amount of antibiotic substance present, and on the interactions between the antibiotic and the clays in the soil, as well.

Awards, Honors & Recognition

Title	Top cited article of the year
Event Year	2012
Recipient	Zhaohui Li
Presented By	Journal of colloids and interfacial Science

Description Awarded for the paper:

Zhaohui Li, Po-Hsiang Chang, Jiin-Shuh Jean, Wei-Teh Jiang, Chih-Jen Wang (2010) Interaction between tetracycline and smectite in aqueous solution. Journal of Colloid and Interface Science. 341(2) pp. 311-319

Journal Articles & Other Publications

Publication Type Journal Article/Book Chapter (Peer-Reviewed)
Title Desorption of tetracycline from montmorillonite by aluminum, calcium and sodium: an indication of intercalation stability
Author(s) Chang, P.-H., Li, Z., Jean, J.-S., Jiang, W.-T., Wu, Q., Lin, K.-H., Kraus, J.
Publication/Publisher Int. J. Environ. Sci. Technol.
Year Published In Press
Volume & Number
Number of Pages
Description <http://dx.doi.org/10.1007/s13762-013-0215-2>
Any Additional Citation Information

.....

Publication Type Journal Article/Book Chapter (Peer-Reviewed)
Title Influence of montmorillonite on antimicrobial activity of tetracycline and ciprofloxacin: a preliminary study
Author(s) Lv, G., Pearce, Gleason, A., C.W., Liao, L., MacWilliams, M.P., Li, Z.
Publication/Publisher J. Asian Earth Sci.
Year Published In Press
Volume & Number
Number of Pages
Description <http://dx.doi.org/10.1016/j.jseaes.2013.04.025>
Any Additional Citation Information

.....

Publication Type Newsletter/Periodical (Peer-Reviewed)
Title Enrofloxacin uptake and retention on different types of clays
Author(s) Wan, M., Li, Z., Hong, H., Wu, Q.
Publication/Publisher J. Asian Earth Sci.
Year Published In Press
Volume & Number
Number of Pages
Description <http://dx.doi.org/10.1016/j.jseaes.2013.02.032>
Any Additional Citation Information

.....

Publication Type Newsletter/Periodical (Peer-Reviewed)
Title Adsorption of the quinolone antibiotic nalidixic acid onto montmorillonite and kaolinite
Author(s) Wu, Q., Li, Z., Hong, H.
Publication/Publisher Appl. Clay Sci.
Year Published In Press
Volume & Number 74

Number of Pages 66-73
Description <http://dx.doi.org/10.1016/j.clay.2012.09.026>
Any Additional Citation Information

.....

Publication Type Newsletter/Periodical (Peer-Reviewed)
Title Intercalation of ciprofloxacin accompanied by dehydration in rectorite
Author(s) Jiang, W.-T., Wang, C.-J., Li, Z.
Publication/Publisher Appl. Clay Sci.
Year Published In Press
Volume & Number 74
Number of Pages 74-80
Description <http://dx.doi.org/10.1016/j.clay.2012.07.009>
Any Additional Citation Information

.....

Publication Type Newsletter/Periodical (Peer-Reviewed)
Title Probing the interactions between chlorpheniramine and 2:1 phyllosilicates
Author(s) Lv, G., Liu, L., Li, Z., Liao, L., Liu, M.
Publication/Publisher J. Colloid Interface Sci.
Year Published 2012
Volume & Number 374
Number of Pages 218-225
Description <http://dx.doi.org/10.1016/j.jcis.2012.01.029>
Any Additional Citation Information

.....

Publication Type Newsletter/Periodical (Peer-Reviewed)
Title Removal of ciprofloxacin from water by birnessite
Author(s) Jiang, W.-T., Chang, P.-H. Wang, Y.-S., Tsai, Y., Jean, J.-S., Li, Z., Krukowski, K.
Publication/Publisher J. Hazard. Mater.
Year Published In Press
Volume & Number 250-251
Number of Pages 362-369
Description <http://dx.doi.org/10.1016/j.jhazmat.2013.02.015>
Any Additional Citation Information

.....

Publication Type Newsletter/Periodical (Peer-Reviewed)
Title Desorption of ciprofloxacin from clay mineral surfaces
Author(s) Wu, Q., Li, Z., Hong, H., Li, R., Jiang, W.-T.
Publication/Publisher Water Res.
Year Published In Press

Volume & Number 47
Number of Pages 259-268
Description <http://dx.doi.org/10.1016/j.watres.2012.10.010>
Any Additional Citation Information

.....

Publication Type Newsletter/Periodical (Peer-Reviewed)
Title Adsorption of tetracycline on 2:1 layered non-swelling clay mineral illite
Author(s) Chang, P.-H., Li, Z., Jean, J.-S., Jiang, W.-T., Wang, C.-J., Lin, K.-H.
Publication/Publisher Appl. Clay Sci.
Year Published 2012
Volume & Number 67-68
Number of Pages 158-163
Description <http://dx.doi.org/10.1016/j.clay.2011.11.004>
Any Additional Citation Information

.....

Publication Type Newsletter/Periodical (Peer-Reviewed)
Title Influence of types and charges of exchangeable cations on ciprofloxacin sorption by montmorillonite
Author(s) Wu, Q., Li, Z., Hong, H.
Publication/Publisher J. Wuhan Univ. Technol. - Mater. Sci. Ed.
Year Published 2012
Volume & Number 27
Number of Pages 516-522
Description <http://dx.doi.org/10.1007/s11595-012-0495-2>
Any Additional Citation Information

Presentations & Public Appearances

Title Interactions of antibiotics with Clay Minerals
Presenter(s) Zhaohui Li
Presentation Type Seminar
Event Name Invited talk to Geosciences department, University of Wisconsin - Milwaukee
Event Location
Event Date 11/10/2011
Target Audience
Audience Size 50
Description

.....

Title Interactions between antibiotics and clays in aqueous system
Presenter(s) Zhaohui Li
Presentation Type Seminar
Event Name Invited talk to China University of Geosciences (Beijing)
Event Location

Event Date 12/21/2011
Target Audience International organization
Audience Size 50
Description

.....

Title Interactions between antibiotics and clays in aqueous system
Presenter(s) Zhaohui Li
Presentation Type Seminar
Event Name Invited talk to China University of Geosciences (Wuhan)
Event Location
Event Date 1/5/2012
Target Audience International organization
Audience Size 30
Description

.....

Title Stabilities of selected pharmaceuticals in the presence of geologic colloids
Presenter(s) Zhaohui Li
Presentation Type Poster session
Event Name AWRA meeting on 3/1/2012
Event Location
Event Date 3/1/2012
Target Audience
Audience Size
Description

.....

Title A Mechanistic Study of Ciprofloxacin removal by Kaolinite
Presenter(s) Roberta A. MacDonald, Zhaohui Li, Caren J. Ackley, Amanda L. Mihelich, Shannon M. Emard, Laura Schulz
Presentation Type Poster session
Event Name AWRA meeting
Event Location
Event Date 3/1/2012
Target Audience
Audience Size
Description

Students & Post-Docs Supported

Student Name Samantha Leick
Campus University of Wisconsin-Parkside

Advisor Name Zhaohui Li
Advisor Campus University of Wisconsin-Parkside

Degree Undergraduate
Graduation Month May
Graduation Year 2012

Department Geosciences
Program Environmental Geosciences
Thesis Title
Thesis Abstract

.....

Student Name Roberta MacDonald
Campus University of Wisconsin-Parkside

Advisor Name Zhaohui Li
Advisor Campus University of Wisconsin-Parkside

Degree Undergraduate
Graduation Month
Graduation Year
Department Geosciences
Program
Thesis Title
Thesis Abstract

Undergraduate Students Supported

New Students: **1**
Continuing Students: **1**

Transport of Manure-Derived, Tetracycline Resistant Escherichia Coli in Unsaturated Soil

Basic Information

Title:	Transport of Manure-Derived, Tetracycline Resistant Escherichia Coli in Unsaturated Soil
Project Number:	2010WI286O
Start Date:	7/1/2010
End Date:	6/30/2012
Funding Source:	Other
Congressional District:	WI 4th
Research Category:	Ground-water Flow and Transport
Focus Category:	Solute Transport, Sediments, Agriculture
Descriptors:	
Principal Investigators:	Shangping Xu

Publications

1. Walczak JJ, SL Bardy, L Feriancikova, S Xu (In Press) Comparison of the Transport of Tetracycline-Resistant and Tetracycline-Susceptible Escherichia coli Isolated from Lake Michigan. Water, Air and Soil Pollution
2. Walczak, J. J.; Bardy, S. L.; Feriancikova, L.; Xu, S. (2011) Comparison of the Transport of Tetracycline-Resistant and Tetracycline-Susceptible Escherichia coli Isolated from Lake Michigan. Water Air and Soil Pollution. 222 (1-4):305-314. doi:10.1007/s11270-011-0825-6

Transport of manure-derived, tetracycline resistant *Escherichia coli* in unsaturated soil

A Report Prepared for Wisconsin Groundwater Coordinating Council

Lucia Feriencikova, Shangping Xu

Department of Geosciences, University of Wisconsin Milwaukee

1. Introduction

As “America’s Dairyland”, Wisconsin is the home to ~15,000 dairy farms and 1.2 million cows, which are producing ~ 4 million tons (dry weight) of manure. Lately, the prevalence of antibiotic resistant bacteria in Wisconsin’s dairy manure was reported (Ray et al. 2006, 2007, Sato et al. 2004, Sato et al. 2005, Halbert et al. 2006, Walczak and Xu 2009). Ray *et al.* (2006), for instance, compared the antibiotic-resistance of *Salmonella* isolated from conventional and organic dairy farms in four states including Wisconsin, Michigan, Minnesota and New York, and found that 1) *Salmonella* isolates from most farms were resistant to at least one of following antibiotics: amoxicillin-clavulanic acid, ampicillin, cephalothin, kanamycin, streptomycin, sulfamethoxazole, and tetracycline, and 2) *Salmonella* isolates that were resistant to 5 or more antibiotics were occurring on 24.6% of conventional farms and 11.5% of organic farms. Halbert *et al.* (2006) reported that out of 2030 *Campylobacter* isolates from both organic and conventional dairy farms, 10% were resistant to ampicillin, and 30-60% were resistant to kanamycin, sulfamethoxazole and tetracycline. Sato *et al.* (2004) studied the antibiotic resistance of *Campylobacter* isolated from Wisconsin dairy farms and found that 45% of *Campylobacter* isolates were resistant to tetracycline and no difference was observed between organic and conventional farms. In another study, Sato *et al.* (2005) tested antibiotic resistance of *E. coli* isolated from manure samples collected from 30 organic and 30 conventional Wisconsin dairy farms, and found prevalence of antibiotic resistance to ampicillin, amoxicillin-clavulanic acid, cephalothin, cefoxitin, ceftiofur, streptomycin, kanamycin, gentamycin, apramycin, chloramphenicol, tetracycline, sulfamethoxazole and trimethoprim-sulfamethoxazole. My group recently tested the antibiotic resistance of *E. coli* isolated from lactating cows of different ages and observed that 1) 99.3%, 25.1%, 98.9%, 59.1% and 0.6% of the *E. coli* isolates were resistant to cephalothin, tetracycline, erythromycin, ampicillin and sulfamethoxazole, respectively; 2) 99.6%, 67.6%, 23.2% and 0.1% of the *E. coli* isolates were resistant to 2, 3, 4 and 5 antibiotics (Walczak and Xu 2011).

Manure produced in dairy farms is usually applied to the crop fields as a source of fertilizer. The spread of manure is performed either daily or following temporary storage in structures that are often not lined (Turnquist et al. 2006, Jackson-Smith et al. 2000). Leakage from manure storage structures and downward infiltration of water through manure-laden soil could lead to groundwater contamination by antibiotic resistant bacteria (Anderson and Sobsey 2006, Mckeon et al. 1995). Sapkota *et al.* (2007) reported that a concentrated animal feeding operation (CAFO) resulted in groundwater pollution by *Enterococci* that were resistant to erythromycin, tetracycline and clindamycin. Anderson and Sobey (2006) observed high percentages of antibiotic-resistant *E. coli* in groundwater samples collected in the vicinity of a CAFO. Mckeon *et al.* (1995) tested antibiotic resistance of more than 250 coliform and noncoliform bacteria isolated from rural groundwater supplies. It was found that 100% of the noncoliforms and 87% of the coliforms were resistant to at

least one of the 16 antibiotics, with resistance most commonly directed toward novobiocin, cephalothin, and ampicillin. Approximately 60% of the coliforms were resistant to multiple drugs.

About 70% of Wisconsin's population depends on groundwater as the source of drinking water (Solley et al. 1998). In rural areas where most of the dairy farms are located groundwater often accounts for 100% of drinking water supply (Ellefson et al. 2002). Contamination of groundwater by antibiotic resistant bacteria associated with dairy manure thus poses a direct and serious public health threat (World Health Organization 2003). Additionally, the health risks associated with the spread of antibiotic resistant bacteria in soil and groundwater are amplified by the phenomenon of horizontal gene transfer, through which antibiotic resistance can be passed to a diverse group of microorganisms, including pathogens (Levy 1998).

Recently, we compared the transport of tetracycline-resistant (tet^R) and tetracycline-susceptible (tet^S) *E. coli* (Walczak et al. 2011a, Walczak et al. 2011b). Our results showed that the tet^R *E. coli* consistently displayed higher mobility than the tet^S *E. coli* within saturated sands (Figure 1, left panel). The surface properties of the *E. coli* isolates were characterized and compared. The profiling of cell outer membrane protein (OMPs) using sodium dodecyl-sulfate polyacrylamide gel (SDS-PAGE) suggested that different proteins existed on the outer membrane of tet^R and tet^S strains (Figure 1, right panel). Specifically, there were at least four proteins present in the outer membrane of the tet^R strains that were absent in the tet^S strains (indicated by arrows in Figure 1). These proteins had approximate molecular masses of 54, 47, 44 and 40 kDa. Additionally, there were three proteins (indicated with arrow heads in Figure 1) that were present in the tet^S strains but were absent in the tet^R strains. The OMP TolC, which has a molecular mass of 52 kDa and represents the OMP component of drug efflux pumps, was identified as an OMP that *coli* strains that were isolated from dairy manure and Lake Michigan water potentially could have enhanced the *E. coli* mobility within saturated sands (Xu et al. 2006, Alekshun and Levy 2007, de Cristobal et al. 2006).

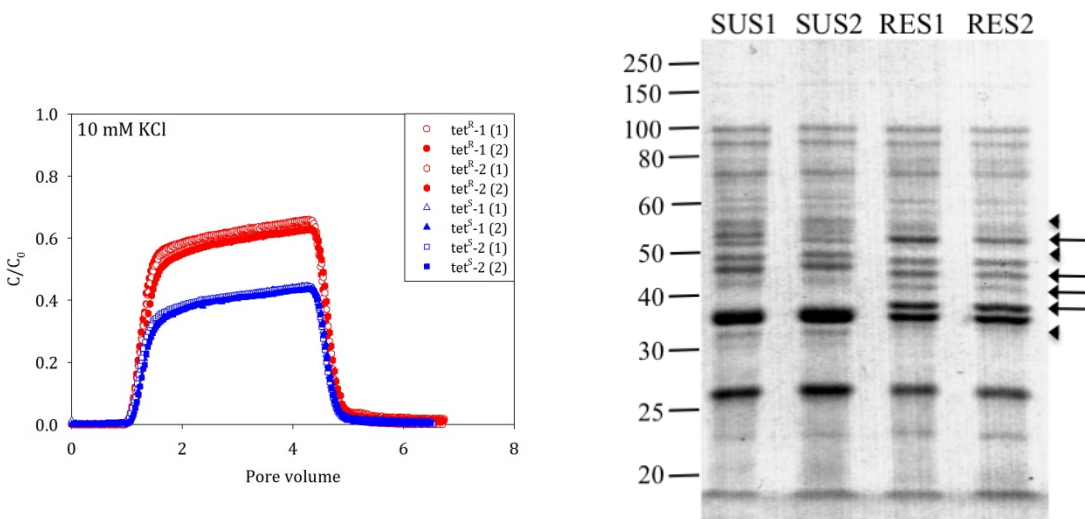


Figure 1. (Left) Comparison of the mobility of the tet^R and tet^S *E. coli* isolated from dairy manure within saturated sands. (Right) Outer membrane protein profiles of the tet^R (RES1 and RES2) and tet^S (SUS1 and SUS2) *E. coli* isolates using SDS-PAGE. Molecular masses (kDa) are indicated on the left. Proteins that are present in the tetracycline resistant strains, but absent in the tetracycline susceptible strains, are indicated with an arrow. Proteins that are present in the tetracycline susceptible strains, but absent in the tetracycline resistant strains are indicated with arrow heads.

2. Research Goals

Based on the previously published research findings, the first goal of this research is to specifically evaluate the effects of OMP TolC on the transport of *E. coli* within saturated sands using mutants that are created through genetic manipulation. The findings from this research will provide valuable insights into the relationship between cell surface structures and *E. coli* mobility.

In saturated porous media, the transport of bacterial cells is primarily controlled by the kinetics of cell deposition at the solid-water interfaces. When the soil is partially saturated, several mechanisms contribute to cell deposition. In addition to the solid-water interface, bacterial cells may adhere to the air-water interface. Bacterial cells can also be strained at the edges of pendular rings that form around adjacent grains or by the thin water film that stretches between the pendulum rings (Denovio et al. 2004). Published experimental results showed that pore water chemistry and soil moisture content are the most important parameters that control the retention of colloid-sized particles in unsaturated soil (Denovio et al. 2004, Lenhart and Saiers 2002). The second goal of this research is to evaluate the influence of pore water chemistry and soil moisture content on the transport of tet^R *E. coli* in unsaturated soil. It was also reported that chemical perturbation, drainage (i.e. drying front) and imbibitions (i.e. wetting front) could mobilize substantial quantities of colloid-sized particles in partially saturated soil (Cheng and Saiers 2009, Saiers et al. 2003). This proposed research will also examine the release of the retained bacterial cells under transient chemical and flow conditions.

3. Effects of OMP TolC on *E. coli* transport¹

3.1. Materials and Methods

In this research, the wild type strain was *E. coli* K12 (strain W25113), which was used to make the Keio Collection of single-gene knockouts (Baba et al. 2006). The strain JW5503 (*tolC::kan*) was obtained from the Keio collection: in this strain the *tolC* open reading frame was replaced with a kanamycin cassette (amplified from plasmid pKD13) flanked by FLP recombination sites (Baba et al. 2006). To construct the markerless deletion of *tolC* (i.e., to excise kanamycin resistance), *E. coli* JW5503 was transformed with plasmid pCP20 and the kanamycin resistant colonies were selected at 30°C. pCP20 has temperature sensitive replication and thermal induction of FLP recombinase expression (Cherepanov and Wackernagel 1995, Datsenko and Wanner 2000). The transformants were cultured at 43°C, after which the loss of both pCP20 and the kanamycin resistance cassette were confirmed via polymerase chain reaction (PCR) and ampicillin/kanamycin sensitivity testing. The markerless strain lacking TolC was referred to as *ΔtolC*.

The *E. coli* cells preserved in 20% glycerol under -80°C was streaked onto Luria-Bertani (LB) (Fisher Scientific) agar plates. After overnight incubation at 37°C, cells from a freshly formed colony were transferred to culture tubes containing 15 ml LB broth. The culture tubes were shaken at 90 rpm and incubated at 37°C for 6 hours. The starter culture was used to inoculate LB broth (1:500 dilution ratio). Following the incubation at 37°C for 18 hours on an orbital shaker (90 rpm), the *E. coli* cells were harvested by centrifugation (4000×g, 10 minutes, 4°C). To remove the growth medium, the bacterial pellet was rinsed 4 times with the appropriate electrolyte solution. The

¹ This research was also supported by UWM Research Foundation through a fellowship to LF. A manuscript has been published in Environmental Science & Technology (doi: 10.1021/es400292x).

concentration of cells was then adjusted to $\sim 4 \times 10^7$ cell/ml for the column transport experiments. The pH of the cell suspensions was ~ 5.7 .

The silica sands used for the column experiments were purchased from US Silica and had a size range of 0.210-0.297 mm. The sands received from the manufacturer were alternately cleaned using concentrated nitric acid to remove metal hydroxides and diluted NaOH solution to remove natural clay particles (Xu et al. 2008), rinsed with deionized water and dried at 80 °C. The porosity of the sand was 0.37 as determined using the bulk density method (Weight 2008).

A pair of glass chromatography columns (Kontes, Vineland, NJ) measuring 15 cm in length and 2.5 cm in diameter were vertically oriented and then wet-packed with the clean silica sands. Care was taken to eliminate the possibility of trapped air bubbles. Once packed, >30 pore volumes (PV) of appropriate background electrolyte (i.e., 1, 5, 20, 50 or 100 mM NaCl) was injected into the columns to equilibrate them. The downward flow was driven by gravity and the Darcy velocity was maintained at 0.31 cm/min using peristaltic pumps (MasterFlex, Vernon Hills, IL). The flow velocity that was employed in the column experiments is on the high end of natural groundwater flow, and is on the same order of magnitude as that encountered in riverbank filtration (Havelaar et al. 1995).

Upon the completion of the equilibration step, the transport experiments were initiated by injecting the *E. coli* cell suspensions to the top of the columns and concentrations of the bacterial cells in the effluent were determined through measuring the absorbance at a wavelength of 220 nm using a Shimadzu UV-1700 spectrophotometer. The injection of *E. coli* cell suspension (~ 3.5 PV) lasted for 60 min, after which the columns were flushed with bacteria-free background electrolyte solution until the absorbance of effluent returned to the background values.

The clean-bed deposition rate coefficients (k_d) of the *E. coli* cells within the saturated sand packs were estimated from the steady-state breakthrough concentrations in the effluent (Walker et al. 2005, Kretzschmar et al. 1997, Castro and Tufenkji 2007):

$$k_d = -\frac{v}{\varepsilon L} \ln \left(\frac{C}{C_0} \right) \quad (1)$$

where ε is porosity, v is the specific discharge, L is the column length and C/C_0 is the normalized breakthrough concentration relevant to clean-bed conditions, which was obtained from the average bacterial breakthrough concentrations between 1.8-2.0 PV (Walker et al. 2005, Castro and Tufenkji 2007).

The retained *E. coli* cells can be remobilized when the ionic strength of the solution is lowered (Redman et al. 2004). For each *E. coli* strain, upon the completion of the column experiments using 100 mM NaCl, the 1 mM NaCl solution was injected to the columns and the concentrations of the released *E. coli* cells were monitored similarly using the spectrophotometer. The results obtained were used to evaluate the reversibility of *E. coli* retention within the sand packs.

The mobility of *E. coli* cells within the saturated sands is determined by the energy interactions between the cells and the surface of the sands. According to the XDLVO theory, the energy interactions between the *E. coli* cells and the surface of quartz sands are the summation of the Lifshitz–van der Waals (LW) interaction, the electrostatic double layer (EDL) interaction and the Lewis acid-base (AB) interaction:

$$\Phi^{\text{Total}} = \Phi^{\text{LW}} + \Phi^{\text{EDL}} + \Phi^{\text{AB}} \quad (2)$$

The LW, EDL and AB interaction energies (Φ^{LW} , Φ^{EDL} and Φ^{AB}) for the cell-sand (sphere-plate geometry) system can be calculated using the following equations (Redman et al. 2004, Ong et al. 1999, Bayouhd et al. 2006, Bayouhd et al. 2009, Farahat et al. 2009, Elimelech 1994, Huang et al. 2010, Morrow et al. 2005a):

$$\Phi^{LW} = -\frac{Aa_b}{6h} \left[1 - \frac{5.32h}{\lambda} \ln \left(1 + \frac{\lambda}{5.32h} \right) \right] \quad (3)$$

$$\Phi^{EDL} = \pi\epsilon_0\epsilon_w a_b \left\{ 2\psi_b\psi_s \ln \left[\frac{1 + \exp(-\kappa h)}{1 - \exp(-\kappa h)} \right] + (\psi_b^2 + \psi_s^2) \ln [1 - \exp(-2\kappa h)] \right\} \quad (4)$$

$$\Phi^{AB} = 2\pi a_b \lambda_w \Delta G_{h_0}^{AB} \exp \left(\frac{h_0 - h}{\lambda_w} \right) \quad (5)$$

where A is the Hamaker constant; a_b is the radius of the bacterial cells; λ is the characteristic wavelength and was set as 42.5 nm; h is the separation distance between the cell and sand surface; ϵ_0 is the dielectric permittivity of vacuum, ϵ_w is the dielectric constant of water; κ^{-1} is the Debye length ($\frac{0.302}{\sqrt{I}}$ nm at 22°C, I =ionic strength); ψ_b and ψ_s are the surface potentials of the bacterial cells and sand, respectively; λ_w ($= 0.6$ nm) is the characteristic decay length of AB interactions in water; h_0 represents the minimum equilibrium distance between the cell and sand surface due to Born repulsion and equals to 0.157 nm; and $\Delta G_{h_0}^{AB}$ represents the hydrophobicity interaction free energies per unit area corresponding to h_0 .

The values of a_b , ψ_b , ψ_s , A and $\Delta G_{h_0}^{AB}$ were required for the interaction energy calculations. To determine cell sizes (a_b), images of the *E. coli* cells suspended in 1 and 100 mM NaCl were obtained using a Nikon Eclipse 50i microscope that was equipped with a Photometric CoolSnap ES digital camera and MetaMorph software. The length and width of ~ 30 cells were determined using the ImageJ software and the equivalent radii of the cells were calculated as $\sqrt{\frac{L_C \times W_C}{\pi}}$, where L_C and W_C represent the length and width of the cell, respectively (Haznedaroglu et al. 2008, Wang et al. 2011). In this research, zeta potential values were used in place of surface potentials for the XDLVO calculations (Walker et al. 2004). *E. coli* cell suspensions were prepared in a similar fashion as the column transport experiments and the quartz sands were pulverized and the colloid-sized quartz particles were suspended in the NaCl solutions (Porubcan and Xu 2011). The zeta potential values of the bacterial cells and quartz particles were then measured using a ZetaPALS analyzer (Brookhaven Instruments Corporation).

The Hamaker constants were calculated from the LW surface tension parameters of bacteria (γ_b^{LW}), water (γ_w^{LW}) and sand (γ_s^{LW}) (van Oss 1993):

$$A = 24\pi h_0^2 \left(\sqrt{\gamma_b^{LW}} - \sqrt{\gamma_w^{LW}} \right) \left(\sqrt{\gamma_s^{LW}} - \sqrt{\gamma_w^{LW}} \right) \quad (6)$$

The values of $\Delta G_{h_0}^{AB}$ can be obtained from the electron-accepting (γ^+) and electron-donating (γ^-) surface tension parameters (van Oss 1993):

$$\Delta G_{h_0}^{AB} = 2 \left[\sqrt{\gamma_w^+} \left(\sqrt{\gamma_b^-} + \sqrt{\gamma_s^-} - \sqrt{\gamma_w^-} \right) + \sqrt{\gamma_w^-} \left(\sqrt{\gamma_b^+} + \sqrt{\gamma_s^+} - \sqrt{\gamma_w^+} \right) - \sqrt{\gamma_b^- \gamma_s^+} - \sqrt{\gamma_b^+ \gamma_s^-} \right] \quad (7)$$

where the subscripts of b , w and s represent bacteria, water and sand, respectively. For water, the values of γ_w^{LW} , γ_w^+ and γ_w^- are 21.8, 25.5 and 25.5 mJ m⁻², respectively (Morrow et al. 2005b). For quartz sands, the previously reported values of γ_s^{LW} (39.2 mJ m⁻²), γ_s^+ (1.4 mJ m⁻²) and γ_s^- (47.8 mJ m⁻²) were used in this research (2005a). To determine the values of γ_b^{LW} , γ_b^+ and γ_b^- for each *E. coli* strain, bacterial lawns were produced by filtering cells onto porous membrane, which was subsequently dried at room temperature for ~15 minutes. The contact angles (θ) of two polar and one non-polar probe liquids with known surface tension parameters on the bacterial lawns were measured using a Rame-Hart goniometer (Ong et al. 1999, Morrow et al. 2005a, van Oss 1993):

$$\gamma_i^L (1 + \cos \theta) = 2\sqrt{\gamma_i^{LW} \gamma^{LW}} + 2\sqrt{\gamma_i^+ \gamma^-} + 2\sqrt{\gamma_i^- \gamma^+} \quad (8)$$

where the subscript i represents water ($\gamma^L=72.8$, $\gamma^{LW}=21.8$ and $\gamma^+=\gamma^- = 25.5$ mJ m⁻²), glycerol ($\gamma^L=64.0$, $\gamma^{LW}=34.0$, $\gamma^+ = 3.92$ and $\gamma^- = 57.4$ mJ m⁻²) or diiodomethane ($\gamma^L=50.8$, $\gamma^{LW}=50.8$ and $\gamma^+=\gamma^- = 0$ mJ m⁻²) (van Oss 1993), respectively.

3.2 Results and Discussion

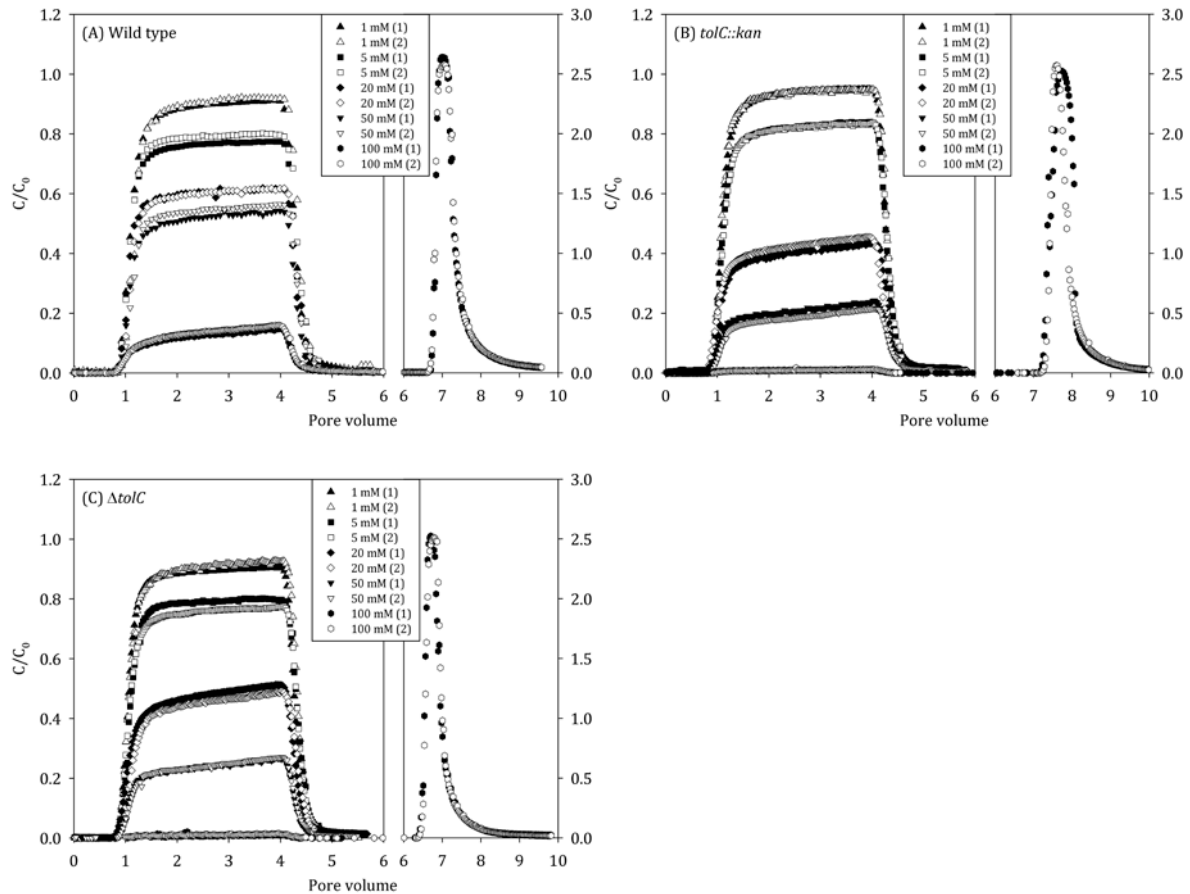


Figure 2. Breakthrough curves of (A) wild type, (B) *tolC::kan* and (C) $\Delta TolC$ *E. coli* cells suspended in 1, 5, 20, 50 and 100 mM NaCl, respectively (left panels). C represents *E. coli*

concentrations in the effluent and C_0 represents influent *E. coli* concentrations. Upon the completion of the 100 mM NaCl experiments, the 1 mM NaCl solution was injected to the columns and the release kinetics of the previously retained bacterial cells are shown in the right panels.

The normalized effluent *E. coli* concentrations under various ionic strength conditions are shown in Figure 2 (left panels). For all the *E. coli* strains, the increase in ionic strength led to lower breakthrough concentrations and lower recovery of bacterial cells in the effluent. For instance, the breakthrough concentrations (between 1.8-2.0 PV) of the wild type strain decreased from 87.0(±1.7)% to 11.2(±0.6)% when ionic strength increased from 1 mM to 100 mM. Accordingly, integration of the breakthrough curves showed that 86.3(±2.9)% and 12.8(±0.6)% of the wild type *E. coli* cells traveled through the sand columns under 1 and 100 mM NaCl conditions, respectively.

Upon the completion of the column experiments using 100 mM NaCl, the 1 mM NaCl solution was injected into the columns and the concentrations of the released *E. coli* cells were monitored (Figure 2, right panels). The pulse-type release of the previously retained *E. coli* cells led to extremely high cell concentrations in the effluent. Integration of the release curves showed that, at the end of the release experiments, 28.0(±2.6)%, 50.9(±7.8)% and 60.4(±0.5)% of the cells remained immobilized for the wild type, *tolC::kan* and $\Delta tolC$ *E. coli* strains, respectively. In comparison, the column experiments performed using 1 mM NaCl showed that ~13.7(±2.9)%, 9.4(±0.9)% and 11.7(±1.7)% of the wild type, *tolC::kan* and $\Delta tolC$ cells were retained, respectively. The fact that higher fractions of the cells remained retained following the release experiments suggested that cell immobilization was only partially reversible.

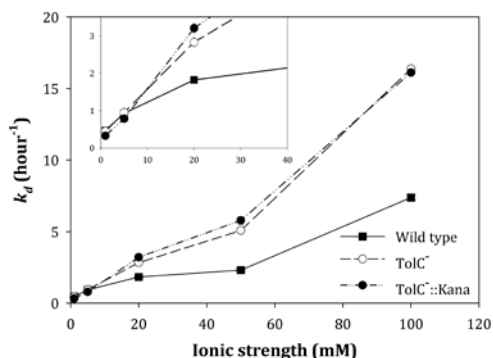


Figure 3. Average deposition rate coefficients (k_d) for the three *E. coli* strains under ionic strength conditions of 1, 5, 20, 50 and 100 mM. The error bars, which represent the standard deviations, are usually smaller than the symbols.

The clean-bed deposition rate coefficients (k_d) were calculated from the early breakthrough concentrations using equation (1) (Figure 3). Student's *t*-test performed using Microsoft Excel showed that the deposition rate coefficients were similar ($p > 0.05$) for the *tolC::kan* and $\Delta tolC$ strains under all ionic strength conditions (1-100 mM NaCl). This indicated that the insertion of the kanamycin resistance cassette into *E. coli* chromosome and the gain of kanamycin resistance had little effects on the mobility of *E. coli* within saturated quartz sands. When the ionic strength was between 1-5 mM, the wild type *E. coli* strain also had similar k_d values as the TolC-deletion *E. coli* strains (Student's *t*-test, $p > 0.05$). The removal of OMP TolC, however, led to significant increase in values of k_d (i.e., decrease in *E. coli* mobility) when the ionic strength was between 20 and 100

mM (Student's *t*-test, $p < 0.05$). This finding was consistent to previously published results that suggested that OMP TolC could enhance the transport of *E. coli* isolated from various natural sources such as dairy manure (Walczak et al. 2011a, Walczak et al. 2011b). To elucidate the mechanisms behind the effects of OMP TolC on the mobility of *E. coli*, we characterized the *E. coli* cells and examined the energy interactions between the *E. coli* cells and quartz sands using the XDLVO theory.

Results from the cell size measurements under 1 and 100 mM NaCl conditions suggested that ionic strength had minimal effects (Student's *t*-test, $p > 0.05$) on the size of the *E. coli* cells. For instance, the equivalent diameter of the wild type *E. coli* cells was $2.04(\pm 0.19)$ μm in 1 mM NaCl and $2.01(\pm 0.17)$ μm in 100 mM NaCl, respectively. For each *E. coli* strain, all the size measurements were thus pooled together and a single diameter value was calculated. The average sizes of the wild type, *tolC::kan* and ΔtolC strains were $2.04(\pm 0.19)$ μm , $1.98(\pm 0.22)$ μm and $2.02(\pm 0.17)$ μm , respectively. The results from Student's *t*-test indicated that the removal of OMP TolC and/or the presence of kanamycin resistance did not significantly alter cell size.

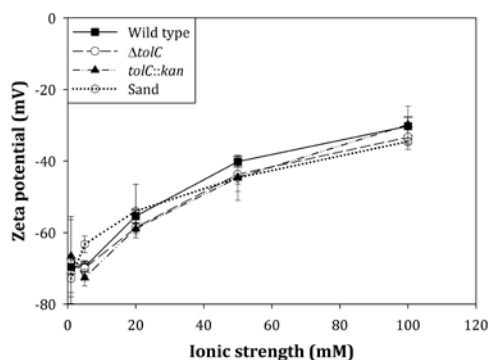


Figure 4. Zeta potential values of the *E. coli* cells and the quartz sands in 1, 5, 20, 50 and 100 mM NaCl. Error bars represent the standard deviation of a minimum of 5 measurements.

When suspended in 1, 5, 20, 50 and 100 mM NaCl (non-buffered, pH ~ 5.7), the zeta potential values of the *E. coli* cells were negative, suggesting that their surfaces were negatively charged (Figure 4). Given the slightly acidic pH of the cell suspensions, these negative charges should originate from the deprotonation of acid-base functional groups such as carboxylic and phosphoric groups (Hong and Brown 2006). With the increase in ionic strength, the zeta potential values of the *E. coli* cells generally became less negative due to the compression of the electric double layer (Wang et al. 2011). Additionally, all three *E. coli* strains displayed comparable zeta potential values under the same ionic strength conditions (Student's *t*-test, $p > 0.05$). The OMP TolC is a 471-residue trimer that contains an α -helical domain, a mixed α/β domain and a β domain (Koronakis et al. 2000). The α -helical domain, which forms a tunnel through the periplasm, is anchored to bacterial wall. The β -barrel, which extends to the outside of the outer membrane, has a length of ~ 4 nm (Koronakis et al. 2000). Because the exterior of the β domain is largely non-polar (Koronakis et al. 2000), it is expected that the deletion of TolC from the outer membrane would not significantly alter cell surface charge and zeta potential. Similarly, because the kanamycin resistance in the *tolC::kan* strain is conferred by the Tn5 neomycin phosphotransferase, an

aminoglycoside modifying enzyme that exists and functions inside the *E. coli* cell (Datsenko and Wanner 2000, Wright 2008), the kanamycin resistance had little effect on cell zeta potential.

Table 1. Contact angle measurements, surface tension components, Hamaker constant (A) and $\Delta G_{h_0}^{AB}$ for the three *E. coli* strains. Numbers in parenthesis are the standard deviations of the contact angle measurements.

Properties		Wild type	<i>tolC::kan</i>	$\Delta tolC$
Contact angle (°) (n≥4)	Water	18.7(±1.4)	19.0(±3.0)	19.6(±1.5)
	Glycerol	21.4(±8.4)	25.9(±2.0)	20.6(±2.8)
	Diiodomethane	67.4(±3.9)	55.4(±8.7)	54.1(±2.8)
Surface tension components (mJ m ⁻²)	γ_b^{LW}	24.33	31.2	32.0
	γ_b^+	6.51	3.63	4.3
	γ_b^-	47.93	48.3	44.8
Hamaker constant, A (10 ⁻²¹ J)		0.78	2.72	2.92
$\Delta G_{h_0}^{AB}$ (mJ m ⁻²)		23.8	26.4	23.8

The results of the contact angle measurements are shown in Table 1. Student's *t*-test indicated that there was significant difference ($p < 0.05$) in the diiodomethane contact angle between the wild type and TolC-deletion *E. coli* strains. It was interesting to note that the wild type, which was able to produce the non-polar OMP TolC, had a higher contact angle of the non-polar diiodomethane than the two TolC-deletion mutants. Similar trend was observed in Ong et al. (Ong et al. 1999) and Johanson et al. (Johanson et al. 2012). Ong et al. observed *E. coli* D21f1, which lacks the charge-containing LPS, had a higher contact angle of diiodomethane than the LPS-producing *E. coli* D21 (Ong et al. 1999). Johanson et al. reported that *Enterococcus faecium* that produced the hydrophobic enterococcal surface protein (*esp*) had a higher contact angle of diiodomethane than the corresponding *esp*-deletion mutant (Johanson et al. 2012). The values of γ_b^{LW} , γ_b^+ and γ_b^- for each *E. coli* strain were then calculated from the contact angle measurements using equation (8) (Table 1). These values, together with the zeta potential values and cell size measurements were then used to quantify the energy interactions between the *E. coli* cells and the quartz sands.

The values of $\Delta G_{h_0}^{AB}$ were 23.8 mJ m⁻², 26.4 mJ m⁻² and 23.8 mJ m⁻² and the Hamaker constants were 0.78×10^{-21} J, 2.72×10^{-21} J and 2.92×10^{-21} J for the wild type, *tolC::kan* and $\Delta tolC$ *E. coli* strains, respectively (Table 1). The values $\Delta G_{h_0}^{AB}$ showed that the AB force between the *E. coli* cells and the surface of quartz sands was repulsive. Equation (6) suggests that the Hamaker constant is a function of the LW surface tension components of the bacterial cell, water and quartz sands. Because the electron-accepting (γ^+) and electron-donating (γ^-) surface tension components for diiodomethane are both zero, the LW surface tension parameter for each *E. coli* strain was calculated from equation (8) that corresponded to diiodomethane. The difference in the Hamaker constants thus was the result of the difference in the diiodomethane contact angles measured on the bacterial lawns of the three *E. coli* strains. The results obtained in this research indicated that variations in cell surface structures such as OMPs could alter cell surface tension components and subsequently the energy interactions between the cells and the surface of quartz sands. Similar relationship was reported in several previous publications (Ong et al. 1999, Johanson et al. 2012). Ong et al. (1999), for instance, observed that the wild type *E. coli* D21 and its LPS-deletion mutant

(strain D21f2) had different surface tension values. As a result, for four different types of surfaces (i.e., mica, glass, polystyrene and Teflon), the Hamaker constants for strain D21 were approximately two times the magnitude of the Hamaker constants for strain D21f2. Johanson et al. (2012) reported that for *Enterococcus faecium*, the removal of the surface protein *esp* increased the Hamaker constant for the cell-water-quartz system from 4.2×10^{-21} J to 4.8×10^{-21} J and the value of $\Delta G_{h_0}^{AB}$ from 24.1 to 31.4 mJ m^{-2} .

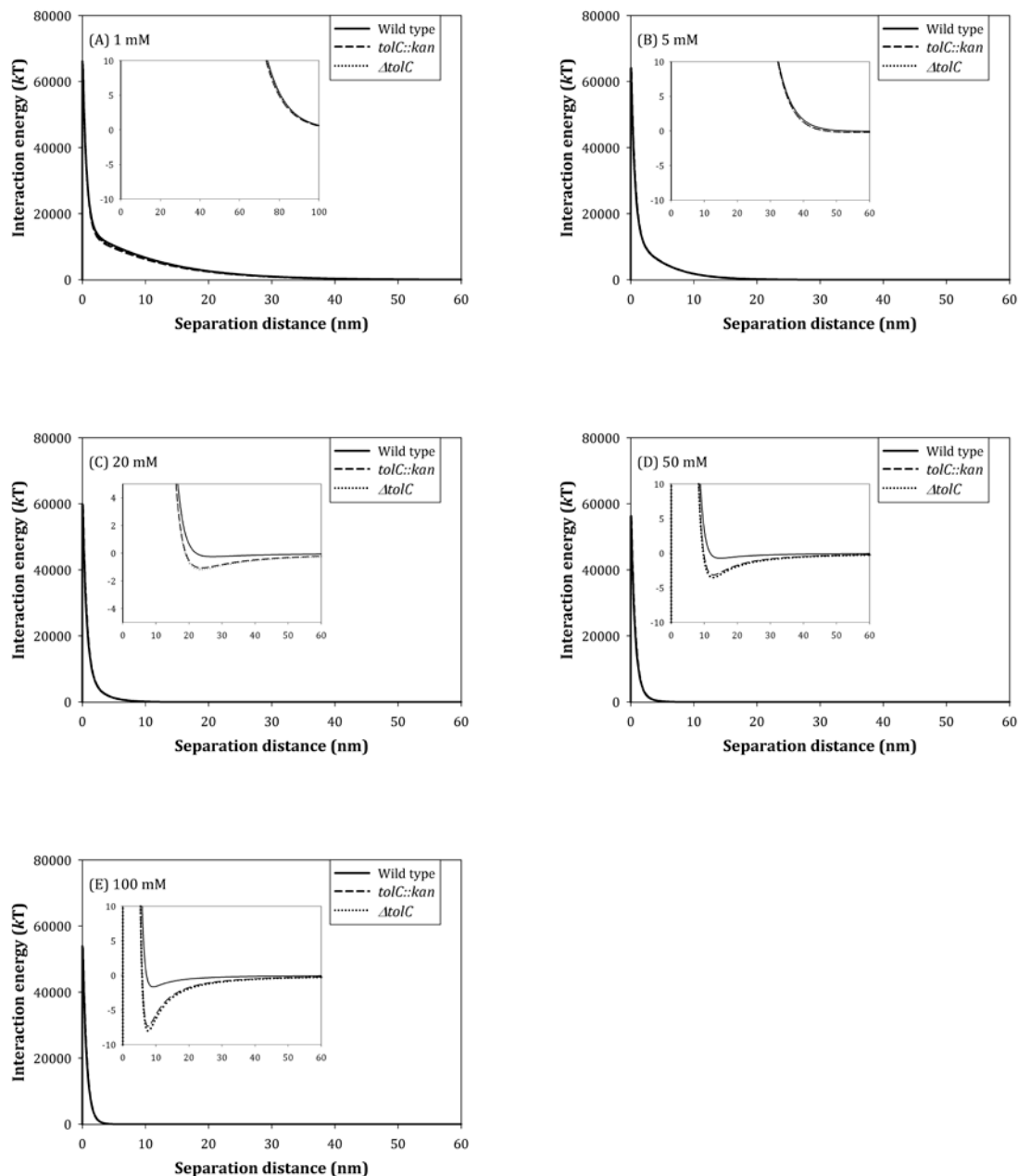


Figure 5. The calculated XDLVO interaction energy profiles as a function of separation distance for (A) 1 mM, (B) 5 mM, (C) 20 mM, (D) 50 mM and (E) 100 mM ionic strength conditions.

The XDLVO energy interactions between the *E. coli* cells and the surface of quartz sands were calculated and shown in Figure 5. For all the ionic strength conditions, there existed sizeable energy barriers for the attachment of *E. coli* cells to quartz sands. The magnitude of the energy barrier was comparable for all three *E. coli* strains under the same ionic strength condition, but decreased from $\sim 6.4 \times 10^4$ kT to $\sim 5.4 \times 10^4$ kT when the ionic strength increased from 1 mM to 100 mM. The presence of the substantial energy barriers made it difficult for the *E. coli* cells to be deposited into the primary energy minimum and the immobilization of the *E. coli* cells should thus occur primarily through their entrapment within the secondary energy minimum (Redman et al. 2004, Wang et al. 2011, Morrow et al. 2005b, Azeredo et al. 1999).

When the ionic strength was within 1-5 mM, the three *E. coli* strains shared similar XDLVO energy interaction profiles (Figures 5A and 5B). For the higher ionic strength range (20-100 mM), the XDLVO calculations showed that the two TolC-deletion strains had similar interaction energy profiles; and their secondary energy minimum was always deeper than the wild type strain. For each *E. coli* strain, the depth of the secondary energy minimum also increased with ionic strength. The XDLVO calculations were thus consistent to the experimental observations that i) the three *E. coli* strains had similar mobility under the low ionic strength conditions; ii) the TolC-deletion strains had higher deposition rates than the wild type strain under high ionic strength conditions; and iii) the deposition of the *E. coli* cells increased with ionic strength (Figure 3). Overall, our data suggested that the deposition rate coefficients (k_d) were negatively related to the depth of the secondary energy minimum.

The XDLVO calculations predicted the absence of the secondary minimum for the ionic strength of 1 mM NaCl (Figure 5A). Inspection of the XDLVO interaction energy profiles revealed that the lowest point was ~ 0.5 kT. In theory, this indicated that there should be no cell immobilization at the secondary energy minimum. The experimental results showed that the transport of the *E. coli* cells was not conservative and $\sim 12\%$ of the *E. coli* cells were immobilized. Similar discrepancies between the interaction energy calculations and particle transport results were previously reported (Farahat et al. 2009, Sharma and Rao 2003). For instance, Farahat et al. observed that *E. coli* cells could attach to quartz under pH > 4.5 when the XDLVO energy calculations showed the absence of secondary energy minimum (Farahat et al. 2009). A wide range of factors such as heterogeneity in cell properties (e.g., the zeta potential of some cell might be less negative than the average values), charge heterogeneity and roughness on the surface of quartz sands, XDLVO forces as well as flow hydrodynamics could have contributed to the deposition of a fraction of *E. coli* cells when the average XDLVO profile predicted the absence of secondary energy minimum (Torkzaban et al. 2008, Dong 2002, Bhattacharjee et al. 1998, Wang and Keller 2009).

The XDLVO calculations were also consistent to the results obtained from the release experiments. When the ionic strength was lowered from 100 mM NaCl to 1 mM, the depth of the secondary energy minimum decreased and a fraction of the *E. coli* cells that were previously retained was remobilized (Redman et al. 2004).

Compared to the DLVO theory, the extra force that is considered by the XDLVO theory is the AB force (equation 5). In this research, the AB force was repulsive and the inclusion of this force significantly increased the magnitude of the energy barrier. However, because the AB force decreased more rapidly with the separation distance than the LW and EDL forces, and because the secondary energy minimum was generally located 7 nm or further away from the sand surface, the AB force has very small effects on the depth of the secondary energy minimum. For *tolC::kan*, the

depth of the secondary energy minimum was $-7.34 kT$ and $-7.57 kT$ for the XDLVO theory and DLVO theory, respectively.

For Gram-negative bacteria such as *E. coli*, outer membrane structures such as LPS and proteins can exert steric interactions for the cell-surface system (Wang et al. 2011, Strauss et al. 2009). Such steric interactions are not considered by the XDLVO calculations and can significantly influence the transport behavior of bacterial cells within porous media (Wang et al. 2011). The *E. coli* K12 strain that was used in this study did not express the O-antigen of the LPS and the length of the LPS was estimated as 3 ± 2 nm (Strauss et al. 2009). The length of OMP TolC that is extended to the outside of the membrane is ~ 4 nm (Koronakis et al. 2000). The XDLVO calculations showed that the secondary energy minimum was usually located >7 nm from the surface of the sands (Figure 4). Therefore, the steric forces could increase the magnitude of the energy barrier, but should have negligible impact on the location and depth of the secondary minimum. Wang et al. (2011) derived the steric force formula from the deGennes equation (Butt et al. 2005, Israelachvili 1991) using the Derjaguin's approximation:

$$\Phi^{steric} = \frac{4}{385h} \pi a_b \frac{kT}{s^3} \left[-20D^3 \left(\frac{h}{L} \right)^{\frac{3}{4}} + 308L^3 \left(\frac{h}{L} \right)^{\frac{3}{4}} - 420hL^2 + 132h^2L \right] \text{ (if } h < L \text{)} \quad (9)$$

where Φ^{Steric} is the steric interaction energy, L is the length of the brush (e.g., LPS or protein), h is separation distance, a_b is the radius of the bacterial cell, k is Boltzmann constant, T is absolute temperature in Kelvin, s average distance between anchoring sites.

Assuming that $L = 5$ nm, and $s = 2.2$ nm (Strauss et al. 2009, Neidhardt 1996), the steric force between the *E. coli* K12 cell and the surface of the sands was calculated (Figure S1A). Because the steric force was 0 beyond 5 nm, the inclusion of the steric force did not alter the location or magnitude of the secondary energy minimum (Figure 6).

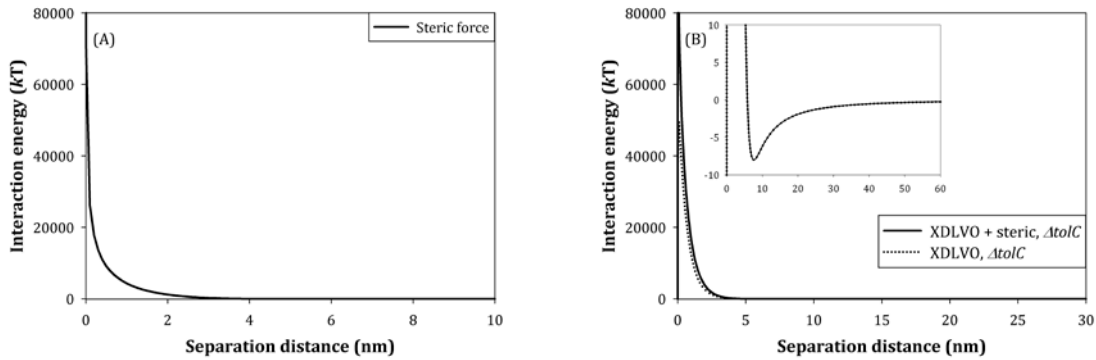


Figure 6. (A) The steric force profile between *E. coli* K12 cells and the surface of sand. (B) The inclusion of the steric force into the XDLVO calculation did not change the location and magnitude of the secondary energy minimum because the steric force diminished beyond 5 nm (i.e., the length of the LPS or protein).

Findings from this research confirmed that OMP TolC, which was firstly identified by Walczak et al. (2011a, 2011b), could enhance the mobility of *E. coli* within saturated sands. Drug efflux pumps represent one of the most effective and widespread mechanisms for antibiotic resistance in bacterial cells (Walsh 2003). Particularly, efflux pumps that span the cytoplasm, periplasm and outer membrane could transport antibiotics to the outside environment and therefore lead to bacterial resistance against high levels of antibiotics. The OMP TolC was reported to be the outer membrane component of several common efflux pumps (e.g., the AcrAB-TolC pump) that are responsible for bacterial resistance to various antibiotics such as tetracycline, macrolide and ampicillin (de Cristobal et al. 2006, Chollet et al. 2004, Fralick 1996, Nishino et al. 2003). It was observed that the total dissolved solid (TDS) of groundwater that was influenced by manure storage and application was often 1000 mg/L or higher (20 mM NaCl is equivalent to a TDS of 1170 mg/L) (Harter et al. 2002). Findings from this research suggested that antibiotic resistant bacteria with the OMP TolC could have higher mobility and display wider spread within sandy aquifers influenced by manure.

4. Transport of tet^R and tet^S *E. coli* isolated from manure within unsaturated soil

4.1 Materials and Methods

The tet^R and tet^S *E. coli* isolates used in this research were from Walczak et al. (2011b), where their mobility within saturated quartz sands were investigated. The results from the *saturated* experiments showed that the tet^R *E. coli* strain exhibited higher mobility than the tet^S *E. coli* strain. For this research, one tet^R and one tet^S *E. coli* isolates were selected for the experiments. The *E. coli* isolates stored in 20% glycerol under -80°C were streaked onto Muller-Hinton (MH) agar plates. After overnight incubation at 37°C, cells from the freshly formed colonies were transferred to culture tubes containing 15 ml Luria-Bertani (LB) broth. The culture tubes were incubated at 37°C for 6 hours with 90 rpm shaking. The starter culture were used to inoculate LB broth (dilution ratio 1:500), which was then be incubated at 37°C with 90 rpm shaking. After 18 hours of incubation, the bacterial cells were harvested using centrifuge (5000g, 10 minutes, 4°C). To remove the growth medium, the bacterial pellet was rinsed 4 times with the appropriate electrolyte solution. The concentration of cells was adjusted to ~10⁷ cells/ml and the suspension is ready for column transport study.

All column transport experiments were run in duplicates. Custom-built acrylic columns, measuring 7.6 cm in diameter and 7.6 cm in length, were used for the transport experiments. Two venting holes were drilled on opposite sides at the top of the vertically oriented column. The venting holes were covered with gas-permeable PTFE membranes which allowed for free air exchange and prevented loss of water from the column. On top of the PTFE membrane, the venting holes could be sealed using PVC tapes when air exchange was not desired (e.g., when a freshly packed column is equilibrated with background electrolyte solution). A moisture probe (ML2x Thetaprobe, Delta-T Devices) were inserted at the middle of the column to determine volumetric moisture content. Readings from the moisture probe were recorded using a datalogger (Delta-T Devices, Model GP1). Plates made from perforated stainless steel sheet were placed at the bottom and top of the column to support the sands within the column and to distribute the influent solution. Nylon membranes with 20 µm openings (Spectrum Laboratories) were placed on top of the stainless steel plates to hold the sand and to maintain capillary pressure inside the column. Both ends of the columns were sealed using butyl rubber O rings. The inflow (top) and outflow (bottom) rates were regulated using two peristaltic pumps (Masterflex, ColeParmer).

The columns were wet-packed by adding natural sands (US Silica, 595-841 μm in diameter) in 50 ml increments into electrolyte solution standing in the column. The porosity of the sand was 0.369. The newly added sands were stirred and mixed with the previously added sands. After each increment, the columns were tapped with hands to allow the newly added sands to settle. The packed sand columns were equilibrated with >4 pore volumes of appropriate electrolyte solution.

The transport of the *E. coli* isolates within the unsaturated soil was investigated under two different soil moisture content levels: $\sim 12(\pm 1)\%$ ($\sim 30\%$ saturation level) and $\sim 25(\pm 1)\%$ ($\sim 68\%$ saturation level), respectively. Following the equilibration step, the saturated sand columns were slowly drained by setting the outflow rate to be $\sim 50\%$ higher than the inflow rate. It was observed that by setting the inflow rate at 0.3 mL/min and 1.0 mL/min, we were able to achieve the $\sim 12\%$ and $\sim 25\%$ of soil moisture contents, respectively. Once the drying front reached the bottom of the column and the desired moisture content was achieved, the inflow and outflow rates were set to equal. The columns were further stabilized for ~ 0.5 hour before they were used for the *E. coli* transport experiments.

The *E. coli* cells suspended in the NaCl solutions (1 mM, 5 mM or 10 mM) were introduced to the top of the column. The concentrations of bacterial cells in the effluent was determined by measuring the light extinction at a wavelength of 220 nm with a UV/Vis spectrophotometer (Shimadzu UV-1700) equipped with 1-cm flow-through cuvettes at 30-second intervals (Walczak et al. 2011a, Walczak et al. 2011b). The injection of the cell suspension usually lasted ~ 2 pore volumes (PV) and then influent was switched to the background, cell-free NaCl solution. The experiments were completed when the cell concentration in the effluent approached zero. During the injection experiments, the soil moisture content remained stable.

The transport of the *E. coli* cells within the unsaturated soil was described by the two-region, dual-porosity model that assumes that the liquid phase could be separated into mobile and immobile zones (Pang et al. 2008). The exchange of *E. coli* cells between θ_m (flowing, inter-aggregate) and immobile θ_{im} (stagnant, intra-aggregate) zones was modeled as a first order process (Note: $\theta = \theta_m + \theta_{im}$). Additionally, we considered the potential detachment of *E. coli* cells that were previously immobilized. The general governing equations for the transport of the tracer and *E. coli* cells within the unsaturated soil were:

$$\theta_{im} \frac{\partial c_{im}}{\partial t} = \omega(c_m - c_{im}) \quad (10)$$

$$\frac{\partial(\theta_m c_m)}{\partial t} + \rho \frac{\partial S}{\partial t} = \frac{\partial}{\partial x} \left(\theta_m D \frac{\partial c_m}{\partial x} \right) - \frac{\partial(q c_m)}{\partial x} - \omega(c_m - c_{im}) \quad (11)$$

$$\rho \frac{\partial S}{\partial t} = \theta_m k_a c_m - k_d \rho S \quad (12)$$

where c_m is the cell ($\text{N}_c \text{L}^{-3}$) concentration in the mobile region, c_{im} is the cell ($\text{N}_c \text{L}^{-3}$) concentration in the immobile region, ω (T^{-1}) is the first-order mass transfer rate between the mobile and immobile regions, ρ ($\text{M} \text{L}^{-3}$) is soil bulk density, S ($\text{N}_c \text{M}^{-1}$) is the quantity of immobilized *E. coli* cells in the solid phase, D ($\text{L}^2 \text{T}^{-1}$) is the dispersion coefficient, k_a is the first-order attachment rate coefficient (T^{-1}), and k_d is the first-order detachment rate coefficient (T^{-1}).

The values of θ_m , θ_{im} , ω , D , k_a and k_d were estimated by inversely solving equations (10) to (12) using HYDRUS-1D. In other words, the HYDRUS-1D solutions were fitted to the breakthrough data using the least-squares algorithm to obtain the best-fit values.

The ionic strength of the soil solution may drop and this change in pore water chemistry could lead to the release of previously retained bacterial cells in unsaturated soil (Jensen et al. 1998).

Such release of the bacterial cells was previously identified as a major mechanism that can lead to groundwater contamination. For this purpose, the transport experiments were firstly carried out using 10 mM NaCl. The 1mM NaCl solution was then introduced to the columns. Once a new steady state was reached (i.e., effluent bacterial cell concentration returns to zero), the experiments was ended.

Soil moisture content constantly changes as a result of rainfall, snowmelt, irrigation and evapotranspiration. It was previously reported that the wetting (imbibitions) fronts can mobilize substantial quantities of colloid-sized particles in unsaturated soil (Cheng and Saiers 2009). To study the mobilization of retained bacterial cells during imbibition, a saturated column was firstly drained to a moisture content of ~12% of soil moisture content using a flow rate of 0.3 mL/min. Bacterial cell suspension was injected into the column under steady flow conditions. Following the flushing step under the same flow rate (i.e., 0.3 mL/min), the inflow rate was increased to 1 mL/min. Once the wetting front reached the bottom of the column and the soil moisture content rose to 25% ($\pm 2\%$), the outflow rate was set at 1 mL/min to maintain steady flow condition. As the moisture content inside the column increased, a fraction of the previously retained bacterial cells were mobilized. The experiment was terminated following the pulse-type release of bacterial cells.

4.2 Results and Discussions

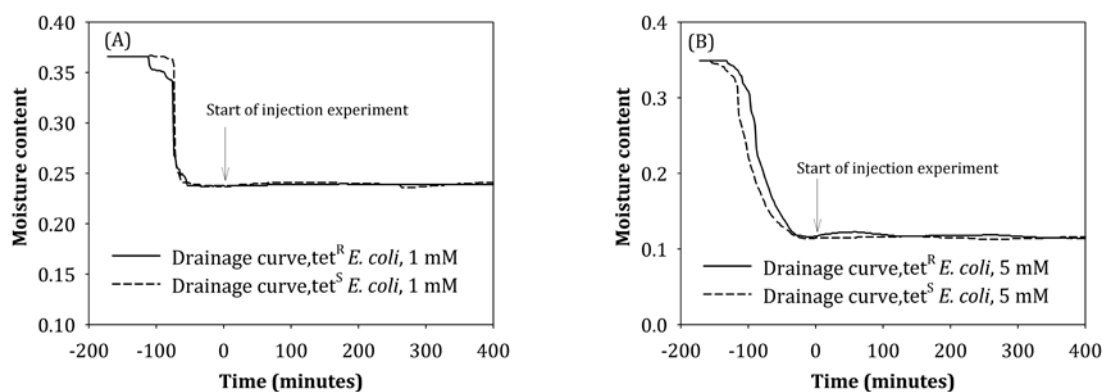


Figure 7. Representative soil drainage curve (soil moisture content vs. time) for the steady-state (i.e., constant soil moisture content) experiments. (A) drainage to ~25% of soil moisture content; (B) drainage to ~12% of soil moisture content. The injection of cell suspensions started at time 0.

From the saturated sand columns, the soil moisture content was lowered to ~12% and ~25% through controlling the inflow and outflow rates (Figure 7). Figure 7 also showed that once the target soil moisture content was reached, it can be maintained steady during the *E. coli* transport experiments.

The breakthrough curves of the *tet^R* and *tet^S* *E. coli* strains under high soil moisture content conditions (i.e., ~25%) are shown in Figure 8. When the ionic strength was 1 mM, the breakthrough concentrations of the *tet^S* *E. coli* strain were slightly higher than those of the *tet^R* *E. coli* strain. When the ionic strength was either 5 mM or 10 mM, the *tet^R* *E. coli* strain consistently displayed higher mobility than the *tet^S* *E. coli* strain (i.e., higher breakthrough concentrations for the *tet^R* *E. coli* strain). The mobility of the *tet^S* *E. coli* strain also decreased more rapidly with increasing ionic strength than the *tet^R* *E. coli* strain. Overall, the results suggested that, consistent to the findings

obtained under saturated conditions, the manure-derived tet^R *E. coli* strain could spread more easily than the corresponding tet^S *E. coli* strain that was isolated from the same source.

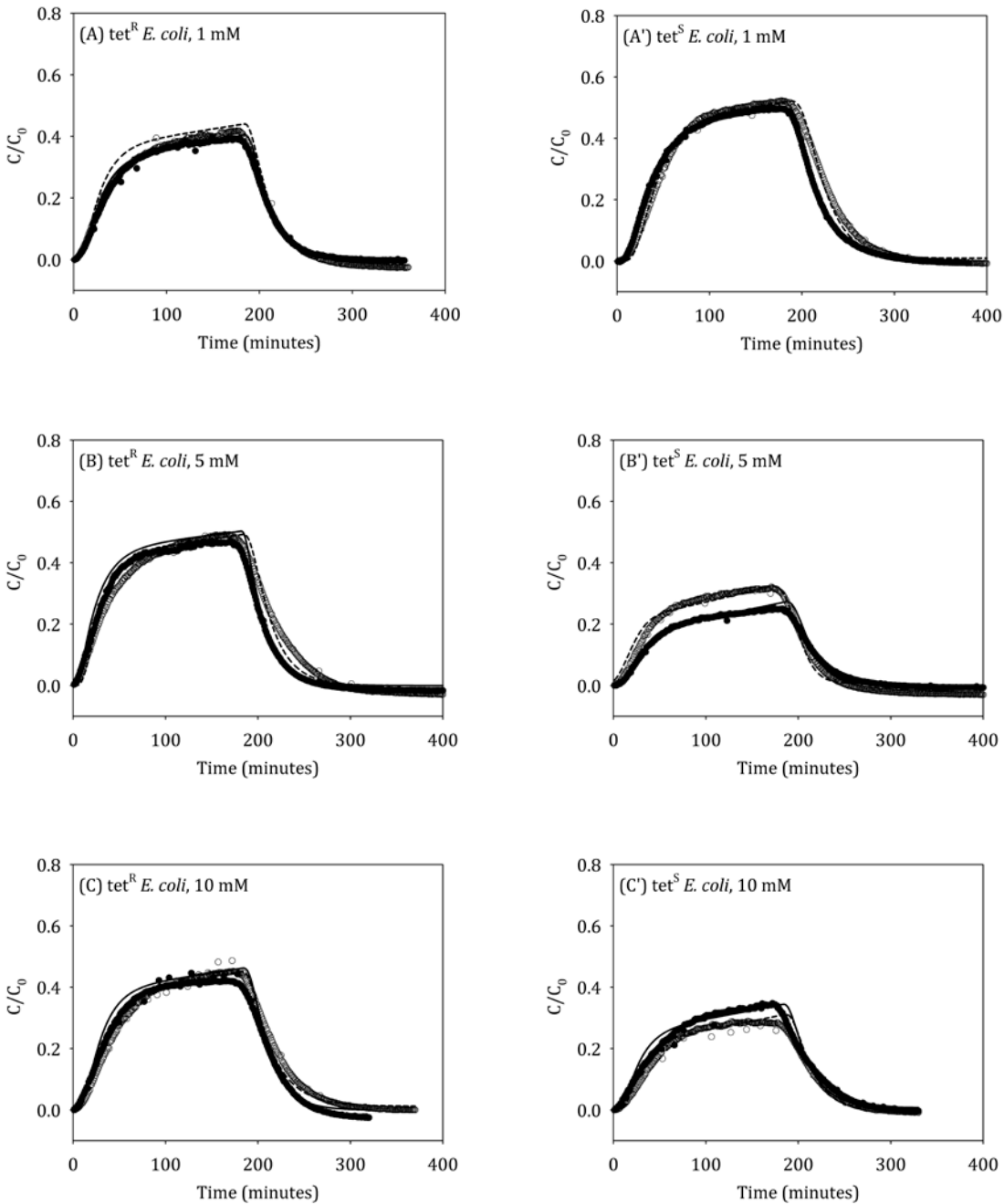


Figure 8. Breakthrough concentrations of the tet^R (A-C) and tet^S (A'-C') *E. coli* strains under ~25% of soil moisture content. Symbols represent experimental observations and lines represent model simulation results.

The mathematical model of equations (10) to (12) was fitted to the breakthrough data using the computer program HYDRUS-1D (Pang et al. 2008). Overall, the dual porosity model could

satisfactorily describe the transport behavior of the tracer under both soil moisture conditions with R^2 values greater than 0.95 (Figure 8). The best-fit values of θ_{im} , D , k_a and k_d were shown in Table 2. The simulation results indicated that the immobile fraction of the aqueous phase is usually less than 3%, suggesting that the aqueous phase was predominantly mobile. Because the values of θ_{im} is relatively small compared to θ , the effects of immobile zone on *E. coli* transport was negligible. Additionally, it was found that the values of k_d were usually two orders of magnitude or more lower than k_a , suggesting that cell detachment was negligible.

Table 2. The best-fit values of θ_{im} , ω , D , k_a and k_d that were estimated from the *E. coli* breakthrough curves using HYDRUS-1D. Note that $\theta = \theta_m + \theta_{im}$. Because the values of θ_{im} is relatively small compared to θ , the effects of immobile zone on *E. coli* transport was negligible.

Moisture content (θ)	<i>E. coli</i> strain	Ionic strength (mM)	θ_{im}	D (cm ² /min)	k_a (min ⁻¹)	k_d (min ⁻¹)
25%	tet ^R	1	2.85(±0.93)%	3.39(±1.67)	0.0273(±0.0014)	<10 ⁻⁴
		5	3.99(±1.24)%		0.0222(±0.0020)	<10 ⁻⁴
		10	2.03(±2.87)%		0.0234(±0.0015)	<10 ⁻⁴
	tet ^S	1	<1%	2.79(±1.65)	0.0166(±0.0016)	<10 ⁻⁴
		5	<1%		0.0346(±0.0087)	<10 ⁻⁴
		10	<1%		0.0347(±0.0017)	<10 ⁻⁴
12%	tet ^R	1	<1%	5.05(±4.25)	0.0175(±0.0055)	<10 ⁻⁴
		5	<1%		0.0169(±0.0084)	<10 ⁻⁴
		10	<1%		0.0228(±0.0020)	<10 ⁻⁴
	tet ^S	1	<1%	2.27(±1.38)	0.0200(±0.0022)	<10 ⁻⁴
		5	<1%		0.0319(±0.0076)	<10 ⁻⁴
		10	<1%		0.0300(±0.0097)	<10 ⁻⁴

Figure 9 shows breakthrough concentrations of the tet^R and tet^S *E. coli* strains under low soil moisture content conditions (i.e., $\theta = \sim 12\%$). In general, the breakthrough concentrations of both *E. coli* strains were lower than those measured under the high soil moisture content conditions. Within partially saturated porous media, the water-air interface provides an important adsorption sites for the immobilization of colloidal sized particles such as *E. coli* cells and the area of the water-air interface usually increases when soil moisture content decreases (Denovio et al. 2004). The decrease in *E. coli* mobility under lower soil moisture content thus reflected the increased adsorption of *E. coli* cell at the water-air interface. The size of *E. coli* cells was found to be 1 μm or greater (Walczak et al. 2011b), *E. coli* cells could also be immobilized as a result of straining within the thin water films that coat the surface of the solid matrix (Wan and Tokunaga 1997). It is also expected that the thin-film straining of *E. coli* cells would increase as soil moisture content was lowered.

Consistent to the observations from the high soil moisture content conditions, the mobility of the tet^R *E. coli* strain was higher than the mobility of the tet^S *E. coli* strain under all three ionic strength conditions, suggesting that the tet^R *E. coli* strain tend to spread more easily within the partially saturated soil. The values of θ_{im} , D , k_a and k_d estimated using HYDRUS-1D showed that, even under the low soil moisture conditions, the fraction of immobile aqueous phase was small and the cell detachment from the solid matrix was slow and negligible (Table 2).

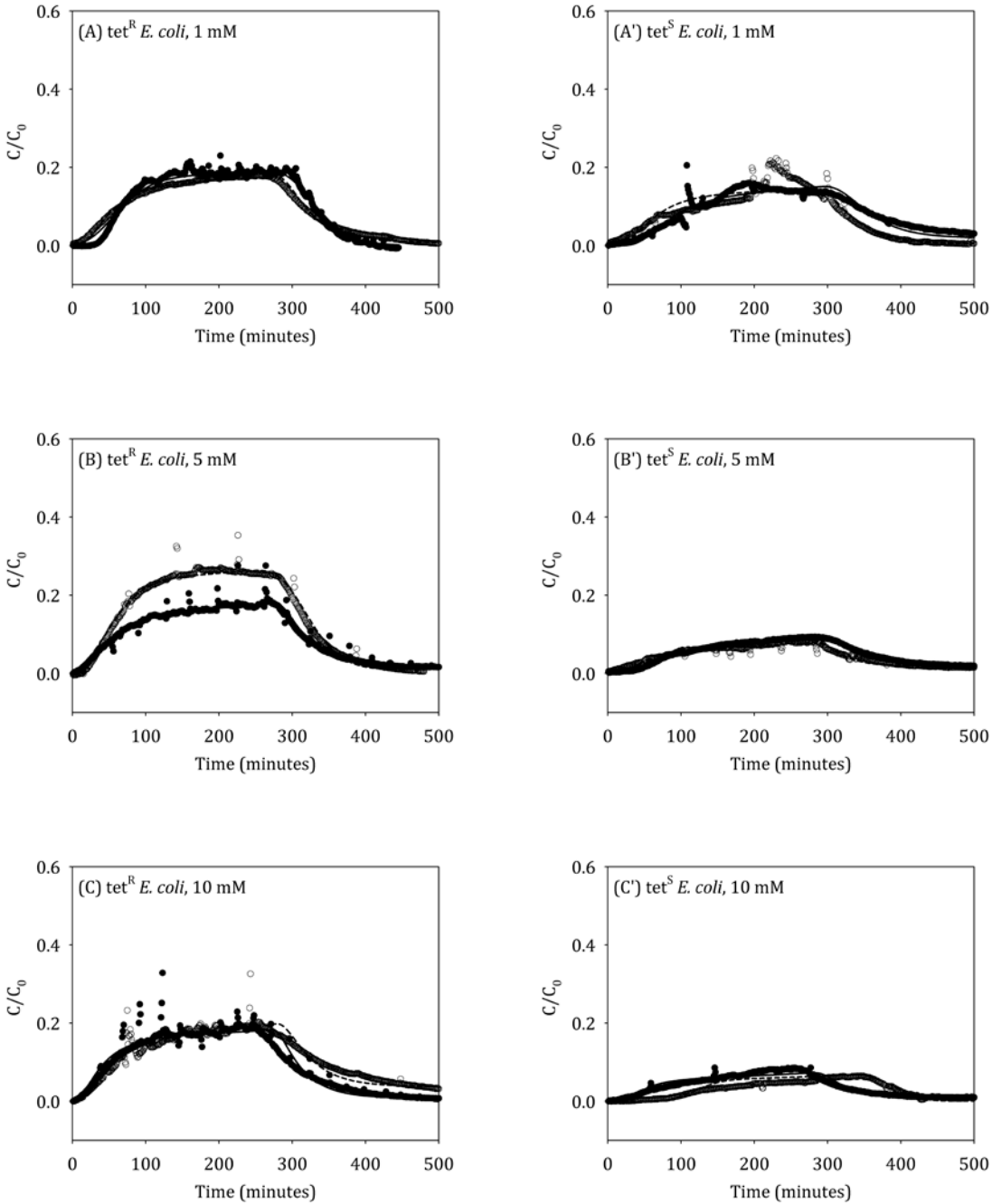


Figure 9. Breakthrough concentrations of the tet^R (A-C) and tet^S (A'-C') *E. coli* strains under 12% of soil moisture content. Symbols represent experimental observations and lines represent model simulation results.

Results from previous studies suggested that change in water chemistry conditions (e.g., a drop in ionic strength) could release the previously immobilized colloid sized particles and this process represents a major mechanism that can transport large quantities of colloids to the underlying groundwater (Denovio et al. 2004). In this research, following a few selected

experiments performed using 10 mM NaCl, the ionic strength was lowered to 1 mM NaCl while the soil moisture content was maintained constant. The effects of chemical perturbation on the transport of *E. coli* cells within partially saturated soil could thus be evaluated.

In general, our results suggested that a small fraction of the immobilized *E. coli* cells under high ionic strength conditions could be remobilized as a result of the drop in NaCl concentration (Figure 10), suggesting that the immobilization of the *E. coli* cells within the unsaturated cells was largely irreversible.

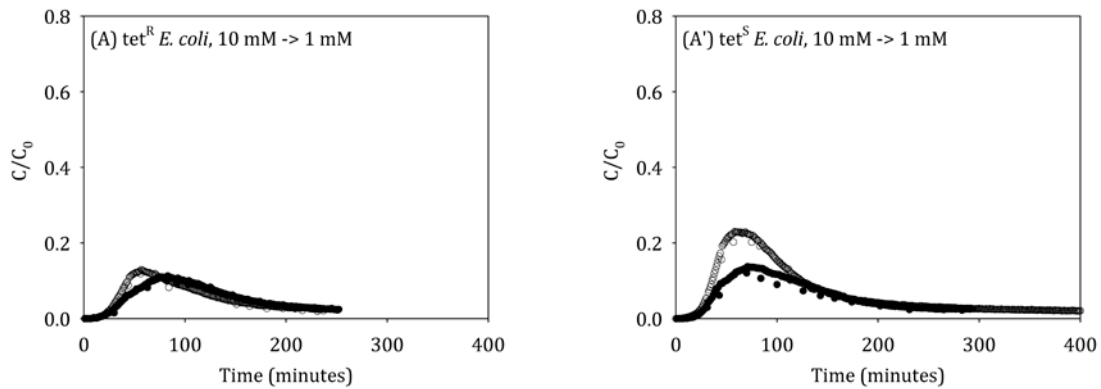


Figure 10. Typical results of the release of tet^R (A) and tet^S (A') *E. coli* cells when the ionic strength was lowered from 10 mM NaCl to 1 mM NaCl. The soil moisture content was maintained at 25%. Time 0 represents the start of the injection of the 1 mM NaCl solution. Lower effluent *E. coli* concentrations were observed during chemical perturbation experiments performed under other ionic strength and/or soil moisture conditions.

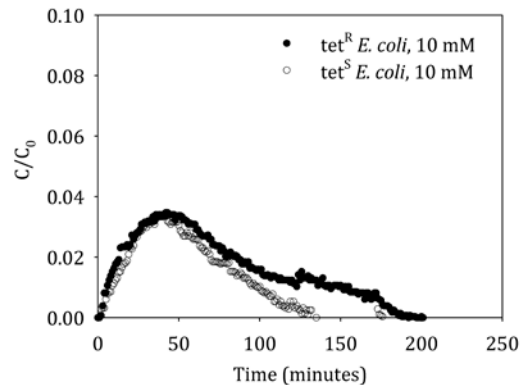


Figure 11. Typical results for the release of tet^R and tet^S *E. coli* cells when the soil moisture content was raised from ~12% to ~25% while the ionic strength was maintained at 10 mM NaCl. Time 0 represents the time when the initiation of the soil moisture content increase. start of the injection of the 1 mM NaCl solution.

It was also suggested that changes in soil moisture contents (i.e., transient flow conditions) could lead to the release of previously immobilized colloid-sized particles (Denovio et al. 2004,

Cheng and Saiers 2009). To evaluate the potential effects of transient flow on the transport of manure-derived *E. coli*, the soil moisture content was raised from 12% to 25% following selected steady-state transport experiments. Similar to the observations from the chemical perturbation experiments, our results indicated that only a small fraction of the *E. coli* cells could be remobilized as a result of imbibition (i.e., increase in soil moisture content) (Figure 11). The effluent concentration of the *E. coli* cells during the imbibition experiments was generally less than 4% of the *E. coli* concentration that was used for the transport experiments (Figure 11).

5. Conclusions

1. The OMP TolC, which is commonly involved in high-level, multi-drug bacterial resistance, could enhance the spread of *E. coli* within the subsurface system.
2. The tet^R *E. coli* strain isolated from dairy manure exhibited higher mobility than then tet^S *E. coli* strain isolated from the same source.
3. The mobility of manure-derived *E. coli* was lower when the ionic strength increased or when the soil moisture content decreased.
4. Only a small fraction of the previously immobilized *E. coli* cells were re-mobilized due to chemical perturbation or transient flow.

References

- Ray, K.A., Warnick, L.D., Mitchell, R.M., Kaneene, J.B., Ruegg, P.L., Wells, S.J., Fossler, C.P., Halbert, L.W. and May, K. (2006) Antimicrobial susceptibility of Salmonella from organic and conventional dairy farms. *Journal of Dairy Science* 89(6), 2038-2050.
- Ray, K.A., Warnick, L.D., Mitchell, R.M., Kaneene, J.B., Ruegg, P.L., Wells, S.J., Fossler, C.P., Halbert, L.W. and May, K. (2007) Prevalence of antimicrobial resistance among Salmonella on midwest and northeast USA dairy farms. *Preventive Veterinary Medicine* 79(2-4), 204-223.
- Sato, K., Bartlett, P.C., Kaneene, J.B. and Downes, F.P. (2004) Comparison of prevalence and antimicrobial susceptibilities of Campylobacter spp. isolates from organic and conventional dairy herds in Wisconsin. *Applied and Environmental Microbiology* 70(3), 1442-1447.
- Sato, K., Bartlett, P.C. and Saeed, M.A. (2005) Antimicrobial susceptibility of Escherichia coli isolates from dairy farms using organic versus conventional production methods. *Journal of the American Veterinary Medical Association* 226(4), 589-594.
- Halbert, L.W., Kaneene, J.B., Ruegg, P.L., Warnick, L.D., Wells, S.J., Mansfield, L.S., Fossler, C.R., Campbell, A.M. and Geiger-Zwald, A.M. (2006) Evaluation of antimicrobial susceptibility patterns in Campylobacter spp isolated from dairy cattle and farms managed organically and conventionally in the midwestern and northeastern United States. *Journal of the American Veterinary Medical Association* 228(7), 1074-1081.
- Walczak, J. and Xu, S. (2009) Antimicrobial susceptibility of *Escherichia coli* from lactating cows of different ages. *Canadian Journal of Microbiology* in review.
- Walczak, J.J. and Xu, S.P. (2011) Manure as a Source of Antibiotic-Resistant Escherichia coli and Enterococci: a Case Study of a Wisconsin, USA Family Dairy Farm. *Water Air and Soil Pollution* 219(1-4), 579-589.
- Turnquist, A., Foltz, J. and Roth, C. (2006) Manure management on Wisconsin farms, p. 23, Program on Agricultural Technology Studies, College of Agricultural and Life Sciences, University of Wisconsin-Madison.
- Jackson-Smith, D., Moon, S., Ostrom, M. and Barham, B. (2000) Farming in Wisconsin at the end of the century: results of the 1999 Wisconsin farm poll, p. 18, Program on Agricultural Technology Studies, University of Wisconsin, Madison.
- Anderson, M.E. and Sobsey, M.D. (2006) Detection and occurrence of antimicrobially resistant E-coli in groundwater on or near swine farms in eastern North Carolina. *Water Science and Technology* 54(3), 211-218.
- Mckee, D.M., Calabrese, J.P. and Bissonnette, G.K. (1995) Antibiotic-resistant Gram-negative bacteria in rural groundwater supplies. *Water Research* 29(8), 1902-1908.
- Sapkota, A.R., Curriero, F.C., Gibson, K.E. and Schwab, K.J. (2007) Antibiotic-resistant enterococci and fecal indicators in surface water and groundwater impacted by a concentrated swine feeding operation. *Environmental Health Perspectives* 115(7), 1040-1045.
- Solley, W.B., Pierce, R.R. and Perlman, H.A. (1998) Estimated use of water in the United States in 1995, U.S. Geological Survey circular 1200, p. 79.
- Ellefson, B.R., Mueller, G.D. and Buchwald, C.A. (2002) Water use in Wisconsin, 2000. U. S. Geological Survey open-file report 02-356.
- World Health Organization (2003) 1st Joint FAO/OIE/WHO Expert Workshop on Non-human Antimicrobial Usage and Antimicrobial Resistance: Scientific assessment, <http://www.who.int/foodsafety/publications/micro/en/amr.pdf>, Geneva.
- Levy, S.B. (1998) The challenge of antibiotic resistance. *Scientific American* 278(3), 46-53.

Walczak, J.J., Bardy, S.L., Feriencikova, L. and Xu, S. (2011a) Comparison of the Transport of Tetracycline-Resistant and Tetracycline-Susceptible *Escherichia coli* Isolated from Lake Michigan. *Water Air and Soil Pollution* 222(1-4), 305-314.

Walczak, J.J., Bardy, S.L., Feriencikova, L. and Xu, S.P. (2011b) Influence of tetracycline resistance on the transport of manure-derived *Escherichia coli* in saturated porous media. *Water Research* 45(4), 1681-1690.

Xu, C.X., Lin, X.M., Ren, H.X., Zhang, Y.L., Wang, S.Y. and Peng, X.X. (2006) Analysis of outer membrane proteome of *Escherichia coli* related to resistance to ampicillin and tetracycline. *Proteomics* 6(2), 462-473.

Alekshun, M.N. and Levy, S.B. (2007) Molecular mechanisms of antibacterial multidrug resistance. *Cell* 128(6), 1037-1050.

de Cristobal, R.E., Vincent, P.A. and Salomon, R.A. (2006) Multidrug resistance pump AcrAB-TolC is required for high-level, Tet(A)-mediated tetracycline resistance in *Escherichia coli*. *Journal of Antimicrobial Chemotherapy* 58(1), 31-36.

Denovio, N.M., Saiers, J.E. and Ryan, J.N. (2004) Colloid movement in unsaturated porous media: recent advances and future directions. *Vadose Zone Journal* 3, 338-351.

Lenhart, J.J. and Saiers, J.E. (2002) Transport of silica colloids through unsaturated porous media: Experimental results and model comparisons. *Environmental Science & Technology* 36(4), 769-777.

Cheng, T. and Saiers, J.E. (2009) Mobilization and transport of in situ colloids during drainage and imbibition of partially saturated sediments. *Water Resources Research* 45, W08414, doi:08410.01029/02008WR007494.

Saiers, J.E., Hornberger, G.M., Gower, D.B. and Herman, J.S. (2003) The role of moving air-water interfaces in colloid mobilization within the vadose zone. *Geophysical Research Letters* 30(21), 2083.

Baba, T., Ara, T., Hasegawa, M., Takai, Y., Okumura, Y., Baba, M., Datsenko, K.A., Tomita, M., Wanner, B.L. and Mori, H. (2006) Construction of *Escherichia coli* K-12 in-frame, single-gene knockout mutants: the Keio collection. *Molecular Systems Biology*, -.

Cherepanov, P.P. and Wackernagel, W. (1995) Gene Disruption in *Escherichia-Coli* - Tcr and Km(R) Cassettes with the Option of Flp-Catalyzed Excision of the Antibiotic-Resistance Determinant. *Gene* 158(1), 9-14.

Datsenko, K.A. and Wanner, B.L. (2000) One-step inactivation of chromosomal genes in *Escherichia coli* K-12 using PCR products. *Proceedings of the National Academy of Sciences of the United States of America* 97(12), 6640-6645.

Xu, S.P., Liao, Q. and Saiers, J.E. (2008) Straining of nonspherical colloids in saturated porous media. *Environmental Science & Technology* 42(3), 771-778.

Weight, W.D. (2008) *Hydrogeology field manual*, McGraw-Hill, New York.

Havelaar, A.H., Vanolphen, M. and Schijven, J.F. (1995) Removal and inactivation of viruses by drinking-water treatment processes under full-scale conditions. *Water Science and Technology* 31(5-6), 55-62.

Walker, S.L., Redman, J.A. and Elimelech, M. (2005) Influence of growth phase on bacterial deposition: Interaction mechanisms in packed-bed column and radial stagnation point flow systems. *Environmental Science & Technology* 39(17), 6405-6411.

Kretzschmar, R., Barmettler, K., Grolimund, D., Yan, Y.D., Borkovec, M. and Sticher, H. (1997) Experimental determination of colloid deposition rates and collision efficiencies in natural porous media. *Water Resources Research* 33(5), 1129-1137.

Castro, F.D. and Tufenkji, N. (2007) Relevance of nontoxigenic strains as surrogates for *Escherichia coli* O157 : H7 in groundwater contamination potential: Role of temperature and cell acclimation time. *Environmental Science & Technology* 41(12), 4332-4338.

Redman, J.A., Walker, S.L. and Elimelech, M. (2004) Bacterial adhesion and transport in porous media: Role of the secondary energy minimum. *Environmental Science & Technology* 38(6), 1777-1785.

Ong, Y.L., Razatos, A., Georgiou, G. and Sharma, M.M. (1999) Adhesion forces between E-coli bacteria and biomaterial surfaces. *Langmuir* 15(8), 2719-2725.

Bayouhdh, S., Othmane, A., Bettaieb, F., Bakhrouf, A., Ben Ouada, H. and Ponsonnet, L. (2006) Quantification of the adhesion free energy between bacteria and hydrophobic and hydrophilic substrata. *Materials Science & Engineering C-Biomimetic and Supramolecular Systems* 26(2-3), 300-305.

Bayouhdh, S., Othmane, A., Mora, L. and Ben Ouada, H. (2009) Assessing bacterial adhesion using DLVO and XDLVO theories and the jet impingement technique. *Colloids and Surfaces B-Biointerfaces* 73(1), 1-9.

Farahat, M., Hirajima, T., Sasaki, K. and Doi, K. (2009) Adhesion of *Escherichia coli* onto quartz, hematite and corundum: Extended DLVO theory and flotation behavior. *Colloids and Surfaces B-Biointerfaces* 74(1), 140-149.

Elimelech, M. (1994) Particle Deposition on Ideal Collectors from Dilute Flowing Suspensions - Mathematical Formulation, Numerical-Solution, and Simulations. *Separations Technology* 4(4), 186-212.

Huang, X.F., Bhattacharjee, S. and Hoek, E.M.V. (2010) Is Surface Roughness a "Scapegoat" or a Primary Factor When Defining Particle-Substrate Interactions? *Langmuir* 26(4), 2528-2537.

Morrow, J.B., Stratton, R., Yang, H.H., Smets, B.F. and Grasso, D. (2005a) Macro- and nanoscale observations of adhesive behavior for several E-coli strains (O157 : H7 and environmental isolates) on mineral surfaces. *Environmental Science & Technology* 39(17), 6395-6404.

Haznedaroglu, B.Z., Bolster, C.H. and Walker, S.L. (2008) The role of starvation on *Escherichia coli* adhesion and transport in saturated porous media. *Water Research* 42(6-7), 1547-1554.

Wang, L., Xu, S. and Li, J. (2011) Effects of Phosphate on the Transport of *Escherichia coli* O157:H7 in Saturated Quartz Sand. *Environmental Science & Technology* 45(22), 9566-9573.

Walker, S.L., Redman, J.A. and Elimelech, M. (2004) Role of cell surface lipopolysaccharides in *Escherichia coli* K12 adhesion and transport. *Langmuir* 20(18), 7736-7746.

Porubcan, A.A. and Xu, S.P. (2011) Colloid straining within saturated heterogeneous porous media. *Water Research* 45(4), 1796-1806.

van Oss, C.J. (1993) Acid-Base Interfacial Interactions in Aqueous-Media. *Colloids and Surfaces a-Physicochemical and Engineering Aspects* 78, 1-49.

Morrow, J.B., Stratton, R., Yang, H.H., Smets, B.F. and Grasso, D. (2005b) Macro- and nanoscale observations of adhesive behavior for several E. coli strains (O157:H7 and environmental isolates) on mineral surfaces. *Environmental Science & Technology* 39(17), 6395-6404.

Hong, Y. and Brown, D.G. (2006) Cell surface acid-base properties of *Escherichia coli* and *Bacillus brevis* and variation as a function of growth phase, nitrogen source and C : N ratio. *Colloids and Surfaces B-Biointerfaces* 50(2), 112-119.

Koronakis, V., Sharff, A., Koronakis, E., Luisi, B. and Hughes, C. (2000) Crystal structure of the bacterial membrane protein TolC central to multidrug efflux and protein export. *Nature* 405(6789), 914-919.

Wright, G.D. (2008) Bacterial Resistance to Antimicrobials. Wax, R.G., Lewis, K., Salyers, A.A. and Taber, H. (eds), pp. 71-101, CRC Press, Boca Raton, FL.

Johanson, J.J., Feriencikova, L. and Xu, S.P. (2012) Influence of Enterococcal Surface Protein (esp) on the Transport of *Enterococcus faecium* within Saturated Quartz Sands. *Environmental Science & Technology* 46(3), 1511-1518.

Azeredo, J., Visser, J. and Oliveira, R. (1999) Exopolymers in bacterial adhesion: interpretation in terms of DLVO and XDLVO theories. *Colloids and Surfaces B-Biointerfaces* 14(1-4), 141-148.

Sharma, P.K. and Rao, K.H. (2003) Adhesion of *Paenibacillus polymyxa* on chalcopyrite and pyrite: surface thermodynamics and extended DLVO theory. *Colloids and Surfaces B-Biointerfaces* 29(1), 21-38.

Torkzaban, S., Tazehkand, S.S., Walker, S.L. and Bradford, S.A. (2008) Transport and fate of bacteria in porous media: Coupled effects of chemical conditions and pore space geometry. *Water Resources Research* 44(4), W04403.

Dong, H.L. (2002) Significance of electrophoretic mobility distribution to bacterial transport in granular porous media. *Journal of Microbiological Methods* 51(1), 83-93.

Bhattacharjee, S., Ko, C.H. and Elimelech, M. (1998) DLVO interaction between rough surfaces. *Langmuir* 14(12), 3365-3375.

Wang, P. and Keller, A.A. (2009) Natural and Engineered Nano and Colloidal Transport: Role of Zeta Potential in Prediction of Particle Deposition. *Langmuir* 25(12), 6856-6862.

Strauss, J., Burnham, N.A. and Camesano, T.A. (2009) Atomic force microscopy study of the role of LPS O-antigen on adhesion of *E. coli*. *Journal of Molecular Recognition* 22(5), 347-355.

Butt, H.J., Cappella, B. and Kappell, M. (2005) Force measurements with the atomic force microscope: Technique, interpretation and applications. *Surface Science Reports* 59(1-6), 1-152.

Israelachvili, J.N. (1991) Intermolecular and surface forces, Academic Press, London ; San Diego.

Neidhardt, F.C. (1996) *Escherichia coli* and *Salmonella* : cellular and molecular biology, ASM Press, Washington, D.C.

Walsh, C. (2003) *Antibiotics : actions, origins, resistance*, ASM Press, Washington, D.C.

Chollet, R., Chevalier, J., Bryskier, A. and Pages, J.M. (2004) The AcrAB-TolC pump is involved in macrolide resistance but not in telithromycin efflux in *Enterobacter aerogenes* and *Escherichia coli*. *Antimicrobial Agents and Chemotherapy* 48(9), 3621-3624.

Fralick, J.A. (1996) Evidence that TolC is required for functioning of the Mar/AcrAB efflux pump of *Escherichia coli*. *Journal of Bacteriology* 178(19), 5803-5805.

Nishino, K., Yamada, J., Hirakawa, H., Hirata, T. and Yamaguchi, A. (2003) Roles of TolC-dependent multidrug transporters of *Escherichia coli* in resistance to beta-lactams. *Antimicrobial Agents and Chemotherapy* 47(9), 3030-3033.

Harter, T., Davis, H., Mathews, M.C. and Meyer, R.D. (2002) Shallow groundwater quality on dairy farms with irrigated forage crops. *Journal of Contaminant Hydrology* 55(3-4), 287-315.

Pang, L., McLeod, M., Aislabie, J., Simunek, J., Close, M. and Hector, R. (2008) Modeling Transport of Microbes in Ten Undisturbed Soils under Effluent Irrigation. *Vadose Zone Journal* 7(1), 97-111.

Jensen, M.B., Hansen, H.C.B., Hansen, S., Jorgensen, P.R., Magid, J. and Nielsen, N.E. (1998) Phosphate and tritium transport through undisturbed subsoil as affected by ionic strength. *Journal of Environmental Quality* 27(1), 139-145.

Wan, J.M. and Tokunaga, T.K. (1997) Film straining of colloids in unsaturated porous media: Conceptual model and experimental testing. *Environmental Science & Technology* 31(8), 2413-2420.

Simulating Lake Responses to Climate Change with a Mechanistic Water Quality Model

Basic Information

Title:	Simulating Lake Responses to Climate Change with a Mechanistic Water Quality Model
Project Number:	2011WI266B
Start Date:	3/1/2011
End Date:	2/28/2013
Funding Source:	104B
Congressional District:	WI-2
Research Category:	Climate and Hydrologic Processes
Focus Category:	Climatological Processes, Water Quality, Models
Descriptors:	None
Principal Investigators:	Trina McMahon

Publications

1. Kara, Emily. 2012. Eutrophication processes and microbial ecology of Lake Mendota, Wisconsin. PhD Thesis. Civil and Environmental Engineering, University of Wisconsin-Madison, Madison, WI. 177p
2. Hawley, Josiah (Jay). 2012. Simulating Lake Responses to Climate Change with a Mechanistic Water Quality Model. MS Thesis. Civil and Environmental Engineering, University of Wisconsin-Madison, Madison, WI.

Annual Progress Report

Selected Reporting Period: 3/1/2012 - 2/28/2013

Submitted By: Katherine McMahon

Submitted: 5/31/2013

Project Title

WR11R001: Simulating Lake Responses to Climate Change with a Mechanistic Water Quality Model

Project Investigators

Katherine McMahon, University of Wisconsin-Madison

Progress Statement

We calibrated and validated our coupled hydrodynamic-ecosystem process water quality model (DYRESM/CAEDYM) based on driver data and observations during the ice-free seasons, for Lake Mendota. We expanded this calibration and validation process beyond the 2008 data set to include years 2009 and 2010. Statistical analyses were done to quantify the closeness of fit between the modeled output and observed data. These analyses were part of the parameter sensitivity analysis to determine the multi-year parameter values to use in the climate change simulations. We identified periods of observation data in the 2001-2010, ten year driver data set that match the conditions of our climate change scenarios. These actual observation data were then merged with other driver data to simulate the entire ice-off period of the climate change scenario. We simulated 84 different scenarios corresponding to spring warming (all day, sun-up hours only, night-time hours only), summer warming (all day, sun-up hours only, night-time hours only), spring drought, summery drought, increased spring intense storm events, and increased summer intense storm events. We evaluated the effect of each scenario on model state variables including hypolimnetic dissolved oxygen, nitrate in the epilimnion and hypolimnion, phosphate in the epilimnion and hypolimnion, chlorophyll-a, total cyanobacteria, and total phytoplankton. The results were compiled in Josiah Hawley's masters thesis.

Josiah successfully defended his thesis in September 2012 and graduated in December 2012. We are currently working on preparing a manuscript based on the results of his work. Craig Snorheim was an undergraduate working on the project and he has decided to stay for an MS in Civil and Environmental Engineering, working on a similar project funded by my collaborator Paul Hanson. Craig will continue to use the calibrated model and driver data for his MS work.

Principal Findings and Significance

Principal Findings and Significance

Description

We report a significant change in knowledge: Graduate students Emily Kara and Josiah Hawley advanced our knowledge on how to perform water quality modeling, including model calibration and validation. A deeper understanding of the impact of key parameters on the model output has been gained by expanding the simulations to include the 2009 and 2010 data sets. Calibrating and validating the models for multiple years is helped us to better constrain the range of reasonable parameter values for Lake Mendota and their effect on key water quality components. The climate change scenarios generated some surprising results that we are still trying to interpret. The driver datasets used for running scenarios are themselves a very valuable dataset and we continue to use them for other modeling purposes.

Description

Participant training and collaborations. Dr. Emily Kara received her PhD in Environmental Engineering in summer 2012. Emily calibrated and validated the water quality model that is the foundation for the project. She also conducted analyses of bacterial community composition data that we continue to interpret using the model outputs. Mr. Josiah Hawley obtained his MS in Environmental Engineering in Fall 2012. Josiah is further calibrating and validating the water quality model that is the

foundation for the project. Collaborators include: Dr. Paul Hanson, Scientist in the Center for Limnology. Dr. Hanson worked closely with Emily to calibrate and validate the model. He also performed spectral analysis on the model output to determine how well it captures variability at different temporal scales. Training and Professional Development: The project provided training and professional development opportunities to Dr.. Kara, Mr. Hawley and three undergraduate students majoring in Civil and Environmental Engineering (Douglas Chalmers, sophomore; Aaron Besaw, junior; and Craig Snortheim, junior). Craig Snortheim is continuing for an MS in Civil and Environmental Engineering, continuing to work with the model and scenarios.

Committees, Memberships & Panels

Group Name	Dane County Lakes and Watershed Commission
Description	PI McMahon is a citizen representative sitting on the Dane County Lakes and Watershed Commission. The findings for this project will be communicated to the commission and factored into policy-level decisions for management of the Yahara watershed in Dane County.
Start Date	7/1/2009
End Date	6/30/2015

Students & Post-Docs Supported

Student Name	Josiah (Jay) Hawley
Campus	University of Wisconsin-Madison

Advisor Name	Katherine McMahon
Advisor Campus	University of Wisconsin-Madison

Degree	Masters
Graduation Month	December
Graduation Year	2012
Department	Civil and Environmental Engineering
Program	Civil and Environmental Engineering
Thesis Title	SIMULATING LAKE RESPONSES TO CLIMATE CHANGE WITH A MECHANISTIC WATER QUALITY MODEL
Thesis Abstract	Many lakes currently experience significant stress due to excessive nutrient influxes and resulting eutrophication. Projected changes in climate could exacerbate these problems by increasing overland runoff and lake water temperatures. The impact of these climate changes on the timing and duration of toxin-producing cyanobacteria blooms are of special concern to both water quality managers and public health officials. We used a one-dimensional coupled hydrodynamic-biogeochemical model (DYRESM-CAEDYM) to simulate the effects of future climate change scenarios for southern Wisconsin on key in-lake response variables. The model was parameterized, calibrated, and validated using observational data from Lake Mendota, Wisconsin during the ice-free period of 2008-10. Climate change scenarios examined include changes in the timing, frequency, and intensity of precipitation events; the timing of ice breakup; and increases in spring nighttime and/or daytime temperatures. Hourly meteorological measurements matching these climate change scenarios were located and used as model drivers. Key response variables examined include the timing and magnitude of cyanobacterial blooms, the timing of epilimnetic phosphorus and nitrate depletion, and the timing of hypolimnetic hypoxia. Results of these simulations improve our understanding of these processes and provide local and regional governments such as the Wisconsin Department of Natural Resources, the Dane County Lakes and Watershed Commission, and the City of Madison with a tool to aid in watershed planning and management

.....

Student Name	Emily Kara
Campus	University of Wisconsin-Madison

Advisor Name	Katherine McMahon
---------------------	-------------------

Advisor Campus University of Wisconsin-Madison

Degree PhD
Graduation Month July
Graduation Year 2012

Department Civil and Environmental Engineering

Program Civil and Environmental Engineering

Thesis Title Eutrophication processes and microbial ecology of Lake Mendota, Wisconsin

Thesis Abstract Eutrophication of Lake Mendota, Wisconsin co-occurred with deforestation of the watershed by settlers in the mid 1850's. The characteristics of this aquatic ecosystem are representative of eutrophication occurring throughout the world in lakes, rivers and marine systems (abundant harmful algal blooms [HABs]), anoxic hypolimnia, and altered food webs). Although the flow of nutrients through lakes and the microbial communities responsible for cycling have been a topic of scientific study for more than a century, our understanding of the efficacy of nutrient management, HAB and heterotrophic bacterial community prediction, and phosphorus speciation at the in-lake level remains limited. Enhanced nutrient management in the watersheds of impaired or threatened surface waters is the most common tool for mitigation of eutrophication, and is understood to be an effective tool to improve or prevent degradation of surface water due to excess nutrients. We used a mass balance approach to determine the net effects of nutrient management changes in the Lake Mendota, Wisconsin watershed occurring between 1995 and 2007, including farmers' adoption of enhanced nutrient management plans, reduced use of chemical feed supplements for dairy cattle, and an urban phosphorus ban. These three factors were attributed to be the cause of reduced, but positive accumulation in 2007, indicating that efforts to improve nutrient management have had limited effect on the overall P budget. We set up, calibrated, and validated an aquatic ecosystem model to test its ability for the short- and long-term prediction of the dynamics of HABs in Lake Mendota. We found biological variables to have the poorest fit with observations, particularly at time scales > 1 month, with the use of high-frequency water quality observations and predictions, and assessed using wavelet analysis. We used numerical simulations to assess the effects of climate change scenarios on water quality, and to identify the most potentially important external factors for HAB dynamics in the lake. Beyond HABs, heterotrophic bacterial communities are responsible for important ecosystem functions in lakes, and the interactions of heterotrophic bacteria with each other, with HABs, and with environmental variables over long time series is unknown. We determined the drivers of bacterial community characteristics (including diversity and co-occurrence network structure) using a decade-long record of bacterial community composition together with a long-term ecological research dataset and local similarity analysis. We found season to drive the complexity of interaction networks and patterns in diversity; variation of environmental variables did not explain the patterns observed. Finally, the chemical structure and dynamics of phosphorus compounds in Lake Mendota across space and time was assessed by ³¹P nuclear magnetic spectroscopy (NMR) to determine the prevalence and nature of non-reactive phosphorus in particulate and dissolved fractions. We found particulate and dissolved fractions from all locations observed had significant temporal variability, while epilimnetic particulate P was more stable over 5 months, and was associated with dissolved reactive P dynamics. This work addresses phosphorus cycling and microbial ecology of a eutrophic lake, leveraging and building upon the body of literature on anthropogenic eutrophication processes and microbial ecology in lakes.

Undergraduate Students Supported

New Students: 0

Continuing Students: 2

Climate Change Impacts on Stream Temperature and Flow: Consequences for Great Lakes Fish Migrations

Basic Information

Title:	Climate Change Impacts on Stream Temperature and Flow: Consequences for Great Lakes Fish Migrations
Project Number:	2011WI267B
Start Date:	3/1/2011
End Date:	2/28/2013
Funding Source:	104B
Congressional District:	WI-2
Research Category:	Climate and Hydrologic Processes
Focus Category:	Climatological Processes, Ecology, None
Descriptors:	None
Principal Investigators:	Peter Biek McIntyre

Publications

There are no publications.

Annual Progress Report

Selected Reporting Period: 3/1/2012 - 2/28/2013

Submitted By: Peter McIntyre

Submitted: 5/30/2013

Project Title

WR11R002: Climate Change Impacts on Stream Temperature and Flow: Consequences for Great Lakes Fish Migrations

Project Investigators

Peter McIntyre, University of Wisconsin-Madison

Progress Statement

Objective 1: Quantifying the historical timing of Great Lakes fish migrations in Wisconsin tributaries.

Large historical data sets are rare for fish migrations and long term analysis of migration phenology has not yet been conducted for the Great Lakes. The US Fish and Wildlife Service collected a unique data set as part of their lamprey control program that includes data for multiple migratory species over a period of six decades. Our goal was to examine trends in migration timing in all migratory species for which there was sufficient data.

Historical fish migration data were obtained from the USFWS. Migrating species were identified from seasonal peaks in abundance from the dataset, which included a total of 17 species. Data on multiple life stages (outmigrating juveniles and spawning adults) were available for three of these species. Analysis of the phenology of migrations was restricted to species and life stages with a minimum of 30 years and 50 stream/year observations of at least 50 fish. Of the 13 species/life stages that met these criteria, nine species had significant ($P < 0.10$) trends in migration timing (Table 1). Eight migrated earlier later in the record (Figure 1), while one (rainbow smelt) migrated later. The earlier migration timing of the majority of the species is consistent with the hypothesis that ever warmer spring temperatures have led to advancement of fish migration phenology. Rainbow smelt populations crashed in 1979 and have not recovered above low levels in most parts of the Great Lakes, which may contribute to the anomalous trend in migration phenology. It is also possible that smelt are responding to a different type of migration cue that is decoupled from temperature patterns.

We are now in the process of refining the analyses above by mining the database for additional metrics of migration phenology beyond the date of peak immigration. We have already georeferenced most of the sites in the USFWS database, and found a significant contribution of site latitude to migration timing. To refine that perspective, we will extract daily time series of lake surface temperature in the region at the mouth of each tributary using the NOAA Coast Watch database (covering 1985 to present). We have obtained the processed Coast Watch data through our collaboration with the GLEAM project at the University of Michigan. Our data refinement will be conducted during summer 2013, and will enable us to associate the timing of migrations with water temperatures across the entire basin. That analysis will obviate the latitudinal analysis, since latitude is primarily acting as a proxy for differences in the timing of spring warming across the basin, and also directly link the putative cue (water temperature) to migration phenology. By directly comparing temperature benchmarks (e.g. first date at 10 degrees C) and migration benchmarks (e.g. first fish observed, peak number of immigrants) in terms of Julian dates, we will have a strong test of the hypothesis that water temperatures are changing and that fish are responding to that aspect of climate change. We will also use our recent data from streams in northern Lake Michigan (see Obj. 2 below) to expand upon the USFWS records wherever possible.

As a side note, this WRI project has also led to a collaboration with WDNR to analyze walleye spawning timing shifts in the open waters of the Great Lakes, using analyses similar to those we are applying in the tributaries.

Objective 2: Monitoring the current migration timing along a latitudinal gradient of Wisconsin tributaries to identify temperature and flow levels that trigger the onset of migrations.

Citizen science is an effective way to engage citizens and educate them about the local impacts of climate change. Additionally, it provides a mechanism for collecting data simultaneously across a broad geographic range. Our goal was to establish a volunteer monitoring network to observe the sucker migration along the Wisconsin shore of Lake Michigan to determine the current migration phenology and evaluate migration cues. Suckers were chosen

because they are ubiquitous, abundant, and easily identifiable.

We collaborated with the WDNR and UW Extension volunteer monitoring program to identify and contact potential volunteers. The USGS provided stream gauges that were installed in each stream along with a temperature logger. Each volunteer was trained in fish identification, and an observation site was chosen to maximize visibility and convenience. In 2011, 20 volunteers monitored sucker arrival, temperature, and flow levels in 15 tributaries spanning over 200 miles of Lake Michigan shoreline.

Arrival was closely linked with temperature but showed no clear pattern relative to flow in 2011. Mean temperature on the day of the first pulse of fish was 7.6° C (SD = 0.6) (e.g., Fig. 1). Despite the variability among sites in the start date of the migration, water temperatures at the start of the migration were highly consistent. In contrast, fish arrival was not associated with any particular hydrograph component. In some streams, fish arrived during high flows, but in others they arrived after long periods of declining flows (Fig. 2). This indicates that migration timing depends primarily on water temperature. In 2012, volunteers were again prepared to monitor, but unfortunately the fish arrived earlier than expected, and we were unable to replicate the 2011 results. In 2013, migration phenologies from eight streams were added to the data set, bringing the total to 30 year-stream phenology observations.

High intensity fish migration monitoring was conducted on three streams in 2012 and two streams in 2013 to enable comparisons of high resolution phenological data with stream temperature and discharge metrics. These comparisons are currently underway, and will provide a basis for detailed analysis of the influence of environmental conditions on fish movements. These high-resolution data will also enable us to ensure that volunteer observations are representative of migration timing and cue data.

Objective 3: Predicting how the timing of migrations is likely to shift with future climate change, and evaluate the implications at the species, community, and ecosystem levels.

Understanding how climate change will influence particular aquatic species is essential for public education and to guide management responses. Our original goal was to leverage the latest USGS modeling of climate change effects on temperature and flow regimes in tributaries by merging forecasted stream patterns with our analysis of migration phenology and cues to determine the ecological consequences for fish migrations.

Our collaborating with John Walker and Randy Hunt at the USGS Wisconsin Water Science Center has been stalled, as their project to predict future stream flow and temperature of Great Lakes tributaries had severe funding cuts. Thus, it no longer appears realistic to project future migration timing into the future.

Nonetheless, we have made good headway in monitoring community and ecosystem roles of fish migrations in 2012 and 2013. In April-May of both years, we have monitored nutrients and productivity in a series of Wisconsin tributaries on the Door Peninsula, where background nutrient loads are relatively modest. Analyses of 2012 samples are completed; analyses of 2013 samples will be completed by July 2013. We found much higher background concentrations of nitrogen (specifically NO₃) in Door County streams than expected, yet we have been able to document a clear NH₄ pulse entering many (but not all) streams at the time that the number of breeding suckers peaks. In addition, in 2013 we made a major investment in using dissolved oxygen loggers to measure whole stream metabolism throughout the sucker migrations. During summer 2013, we will process these data and compare them to the dynamics of both fish numbers and nutrient concentrations.

To connect the timing of fish migrations to the ecology of resident sport fishes, in 2012 we assessed consumption of sucker eggs and larvae by brook trout in these same streams. Trout diets consisted almost entirely of sucker eggs during the height of the migration, indicating strong linkages between these species. As a result, shifts in the timing of sucker migrations could affect both the fundamental productivity of Wisconsin tributaries, and the health of valuable sport fish populations. We attempted to replicate this analysis, but the summer drought in 2012 had killed all the brook trout, so no 2013 data could be collected despite enormous quantities of migratory suckers in the study area.

Principal Findings and Significance

Principal Findings and Significance

Description

Outreach activities:

A daily program educating the public about fish migrations, sucker life history, and the impacts of climate change was developed and implemented at the Crossroads at Big Creek Nature Center in 2011 and 2012 during the sucker migration. We prepared a brief lecture for the staff to present to visitors, after which visitors would observe sucker spawning in a local creek. Brief lectures were given to two volunteer groups about fish migration ecology and climate change. This project has been featured in newsletters for multiple citizen groups, as well as on the WRI Press Room website in August 2011 (<http://wri.wisc.edu/pressroom/Details.aspx?PostID=1138>).

Two unanticipated outreach opportunities have also arisen from this project. First, this project has led to a collaborative agreement with the Shedd Aquarium (Chicago, IL) to support a post-doctoral researcher studying Great Lakes fish migrations

for three years starting in August 2012. The position is based in Chicago but involves close collaboration with my lab group at UW-Madison, thereby expanding the scope and impact of this WRI project enormously. As a result, we anticipate jointly designing a display in the Shedd Aquarium to highlight Great Lakes migratory fishes, and how climate change could impact them. Second, informal presentations of our WRI results to WDNR has led to a collaboration with their researchers to test for coupled trends in lake water temperatures and spawning dates for walleye and yellow perch. Those analyses will be conducted during summer 2013.

Results of this research project were presented by Evan Childress at the American Fisheries Society annual meeting in Minneapolis in September 2012, and by Peter McIntyre in seminars at Tulane University, UW's Wednesday Nite @ the Lab, and the Great Lakes Fishery Commission. We are currently working on developing a project webpage, and discussing how to package the results for publication. We submitted a first paper documenting stream fertilization effects of sucker migrations to Ecology, but it was rejected after review. We plan to resubmit it to Ecosystems.

Supporting students

Doctoral student Evan Childress has received a stipend for Spring and Summer 2012. To conserve WRI funds, I was able to support Evan's work on the project using other sources during Spring 2011. As a result, I have requested a no-cost extension of the project to enable support of Evan for an additional semester. The remaining funds will be used primarily to support a data analyst to assist with extracting migration phenology from the large USFWS database, and developing a counterpart database of lake water temperature from the NOAA Coast Watch database. In addition, the funds will be used to cover the costs of collecting and analyzing water samples to document the ecosystem impacts of sucker migrations in a temporally-explicit way. To assist in processing 2013 field samples, we have recruited the assistance of a minority undergraduate summer student at no cost to the project.

Committees, Memberships & Panels

Group Name Evan Childress graduate advisor
Description I chair Evan's doctoral advisory committee.
Start Date 8/30/2010
End Date 5/30/2013

.....

Group Name LMS program Anna Grant Birge Award Committee
Description In both 2012 and 2013, I have been a member of the selection committee for Birge Awards that support graduate research.
Start Date 4/1/2012
End Date 5/30/2013

.....

Group Name Graduate committee member for McKinley students
Description I am on the graduate committee for 2 of Galen McKinley's graduate students (Jennifer Phillips and Darren Pilcher). I have been invited to serve on these committees specifically because of my ongoing research on climate change in the Great Lakes.
Start Date 4/4/2011
End Date 5/30/2013

Journal Articles & Other Publications

Publication Type
Title Nutrient subsidies from native fish migrations enhance productivity in Great Lakes tributaries
Author(s) Evan Childress, Peter McIntyre, J. David Allan

Publication/Publisher Ecosystems
Year Published In Review
Volume & Number
Number of Pages
Description This paper was rejected by Ecology, and will be resubmitted very soon to Ecosystems.
Any Additional Citation Information

Partners

Name/Organization John Walker & Randy Hunt
Affiliation USGS Water Science Center
Affiliation Type Federal
Email
Description Walker and Hunt are our collaborators to link past and future tributary discharge/temperature to fish migration phenology.



Name/Organization John Lyons & Andrew Rypel
Affiliation Wisconsin DNR
Affiliation Type Local & State
Email
Description Lyons and Rypel are collaborating with us on an analysis of shifts in breeding phenology of yellow perch and walleye in Lakes Michigan and Superior.

Students & Post-Docs Supported

Student Name Evan Childress
Campus University of Wisconsin-Madison

Advisor Name Peter McIntyre
Advisor Campus University of Wisconsin-Madison

Degree PhD
Graduation Month May
Graduation Year 2015
Department Zoology
Program Limnology & Marine Science
Thesis Title
Thesis Abstract

Undergraduate Students Supported

Continuing Students: **1**

WRI Progress Report 30 May 30, 2013

Project title: Climate change impacts on stream temperature and flow: consequences for Great Lakes fish migrations

Investigator: Dr. Peter McIntyre, UW Center for Limnology

Figure 1. Examples of latitude corrected migration timing over the past six decades.

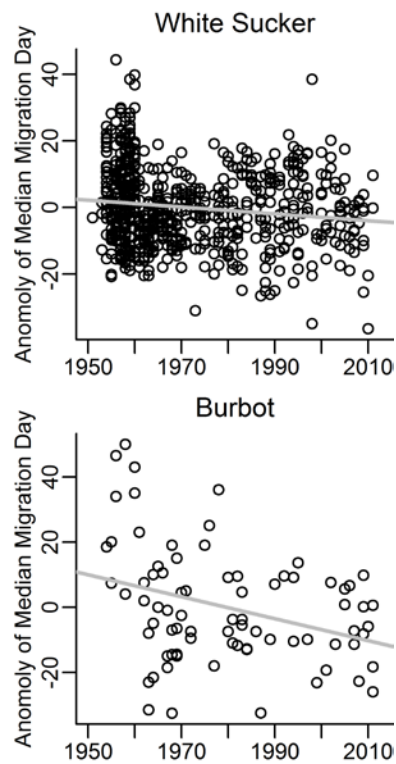


Table 1. Phenological change of latitude corrected fish migration timing in Great Lakes tributaries.

Species	Days of change per decade	P-value	Period of record	n
White Sucker	-0.7	0.001	1951-2011	1027
Silver Lamprey	-1.1	0.056	1954-2011	141
Brown Trout (Adult)	-1.6	0.087	1953-2011	125
Brown Trout (Juvenile)	-7.2	<0.001	1957-2011	61
Rainbow Smelt	3.4	<0.001	1947-2004	379
Redhorse	-3.8	<0.001	1954-2010	58
Burbot	-5.6	<0.001	1954-2004	81
Walleye	1.7	0.379	1954-2004	64
Steelhead (Adult)	0.8	0.287	1954-1995	173
Steelhead (Juvenile)	-2.6	<0.001	1951-2011	393
Alewife	-2.9	<0.001	1957-2009	145
Sea Lamprey	0	0.964	1947-2007	747
Longnose Sucker	-0.1	0.776	1950-2011	516

Uncertainty and Variability of Wisconsin Lakes in Response to Climate Change

Basic Information

Title:	Uncertainty and Variability of Wisconsin Lakes in Response to Climate Change
Project Number:	2011 WI268B
Start Date:	3/1/2011
End Date:	2/28/2014
Funding Source:	104B
Congressional District:	WI-2
Research Category:	Climate and Hydrologic Processes
Focus Category:	Climatological Processes, Water Quality, Geochemical Processes
Descriptors:	
Principal Investigators:	Chin H Wu

Publications

1. Magee M, and CH Wu (In Review) Long-term trends and variability in ice cover and thermal structure in three morphometrically different lakes in response to climate change. Limnology and Oceanography
2. Magee M, and CH Wu (In Review) Hanging climate on three lakes with differing morphometry. Water Research

Project Title:**Uncertainty and Variability of Wisconsin Lakes in Response to Climate Change**

Chin Wu

University of Wisconsin-Madison

Progress Statement

We are investigating the physical responses of ice cover and water temperature in Wisconsin lakes to climate change. During the second year of the project, we focus on three southern lakes, Mendota, Wingra, and Fish Lake in Dane County in Wisconsin to examine physical lake variables in response to changing climate. Specific tasks are (i) the improvement of the one-dimensional lake-ice model, DYRESM-I to simulate ice cover and water temperature at sub-hourly time intervals and added a component to simulate dissolved oxygen levels in the lakes; (ii) the development of a 3D lake ice/snow/hydrodynamic model that can simulate spatial distribution in ice cover and lake thermal structure; (iii) investigation of the importance of climate drivers to water temperature and evaporation; and (iv) study of the effects of climate change on cold-water fish oxythermal stress. Two manuscripts (see below) will be submitted to the peer-review journals. We are currently working on the third manuscript.

Seasonal evaporation of two lakes with different morphometry under changing climate

To better understand how a changing climate affects seasonal evaporation from different sized lakes, a one dimensional lake model is used with historical data to simulate lake evaporation and ice cover throughout the past one hundred years. Lake Mendota, a dimictic lake, and Lake Wingra, a polymictic lake were chosen to examine how lake thermal structure and mixing affect lake evaporation in each season. Results show that (i) spring evaporation is increased due to increased air temperature, (ii) summer evaporation is decreasing due to higher vapor pressure and wind speed decreases, (iii) fall evaporation is decreasing due to lower wind speeds, and (iv) winter evaporation is significantly increasing due to temperature-induced decreases in ice cover duration. In comparison, the dimictic lake experienced greater increases in evaporation in the spring time due to slightly higher sensitivity to increasing temperature. In the fall, dimictic lakes remain warmer, resulting in greater sensitivity to the drops in wind speeds. Finally, the formation of ice at the beginning of winter is more sensitive for deeper lakes, resulting in greater increases in evaporation on deeper lakes.

Response of thermal structure in two dimictic lakes to climate change

DYRESM-I was used to simulate the water temperature of Lake Mendota and Fish Lake to determine historical changes in thermal structure and also changes under potential climate scenarios during the open water season. Under the historical scenario, model results indicate earlier stratification onset, later fall overturn, warming epilimnion water, and cooling

hypolimnion water. The increasing air temperature and decreasing wind speed have a doubling effect on the longer stratification duration, with wind speed playing a dominant role in determining the stratification onset, stratification overturn, and the hypolimnetic water temperatures. Under future climate scenarios, temperature perturbations from -10°C to $+10^{\circ}\text{C}$ indicate that warmer air temperatures lead to earlier stratification onset and later fall overturn for both lakes under all climate scenarios. When considering perturbations of wind speeds from -30% to $+30\%$, decreasing wind speeds lead to earlier stratification onset and later overturn. The magnitude of these changes is larger for each degree or m/s of increase for Fish Lake than for Lake Mendota, indicating that Fish Lake is more susceptible to negative impacts of the changing climate.

Oxythermal stress in a dimictic lake in response to changing climate

Using DYRESM-I, with a newly added dissolved oxygen simulation component, we studied the effect of changing climate on oxythermal stress of a cisco population in Fish Lake, WI, USA. We investigated how the past changing climate has impacted fish stress caused by high temperatures and low dissolved oxygen levels over the last 100 years. A method is developed to quantify the number of days of fish stress per year, and this method applied under the future A1B climate scenario. Results indicate that under future scenarios, the frequency of fish stress and duration of stress will increase dramatically. Furthermore, we used a state-of-the-art 3D hydrodynamic model coupled with a 1D dissolved oxygen model to simulate the spatial extent of dissolved oxygen stress during the year.

USGS Award no. G11AP20226 GLMRIS Water Quality Modeling (Marquette U.)

Basic Information

Title:	USGS Award no. G11AP20226 GLMRIS Water Quality Modeling (Marquette U.)
Project Number:	2011WI288S
Start Date:	9/12/2011
End Date:	9/11/2012
Funding Source:	Supplemental
Congressional District:	
Research Category:	Water Quality
Focus Category:	Surface Water, Water Quality, Management and Planning
Descriptors:	aquatic invasive species, separating watersheds
Principal Investigators:	Anders W. Andren, Charles Steven Melching

Publications

There are no publications.

Annual Progress Report

Selected Reporting Period: 3/1/2012 - 2/28/2013

Submitted By: Charles Melching

Submitted: 5/28/2013

Project Title

WR11R008: GLMRIS Water Quality Modeling

Project Investigators

Charles Melching, Marquette University

Progress Statement

Background

The GLMRIS feasibility study is being undertaken by the U.S. Army Corps of Engineers (Corps) to develop a long-term solution to prevent aquatic invasive species from traveling between the Great Lakes and Mississippi River watersheds. One primary goal of the study is to assess the feasibility of hydrologically separating the two watersheds, which are currently connected via the manmade Chicago Sanitary & Ship Canal and Cal-Sag Channel. These waterways were constructed in the early 20th Century, which allowed the Chicago River and other area waterways to flow to the Illinois River, instead of to Lake Michigan. Re-separating the watersheds will radically alter the existing flow patterns in the system, and is expected to cause significant water quality changes. Modeling and analysis of water quality impacts to both the CAWS and Lake Michigan are needed to ensure any selected alternative will be in compliance with Illinois water quality standards and with the Clean Water Act.

Objective

The existing DUFLOW model (developed by Marquette University for the Metropolitan Water Reclamation District of Greater Chicago, MWRDGC) will be utilized to provide supporting data to quantify water quality impacts to area waterways resulting from hydrologic separation alternatives.

Tasks and Progress

The existing DUFLOW model shall be updated and recalibrated to model water quality in the Chicago Area Waterways System (CAWS). Waterways within the scope of this project include:

- North Shore Channel (NSC)
- North Branch Chicago River (NBCR) downstream of confluence with NSC
- Chicago River Main Stem
- South Branch Chicago River (SBCR)
- South Fork of South Branch Chicago River (SFSBCR) or Bubbly Creek
- Chicago Sanitary & Ship Canal (CSSC)
- Cal-Sag Channel
- Little Calumet River (LCR) from Cal-Sag Channel to junction with Calumet and Grand Calumet Rivers
- Little Calumet River from Cal-Sag Channel to South Holland
- Calumet River

The capability of modeling the stretch of the Calumet River from the lakefront to O'Brien Lock and Dam shall be added to the DUFLOW model.

Progress: The channel geometry and layout data for the Calumet River have been added to the DUFLOW model, appropriate boundary conditions for this reach have been determined, and hydraulic and water quality runs for the Calumet River have been made. The accuracy of the DUFLOW model of the Calumet River was tested for the flow reversal to Lake Michigan during the storm of September 13-16, 2008.

Modeling Scenarios

Five distinct hydrologic scenarios shall be modeled. Additional scenarios may be identified as the GLMRIS study progresses, in which case these scenarios may be added to the modeling scope of work as options to the contract.

Progress: Because the time period for the GLMRIS study was shortened from ending in 2016 to ending in 2013, the number of distinct hydrologic scenarios to be simulated was reduced from five to three. These three scenarios are the (1) "No Project" scenario where no separation of the watersheds is applied, (2) the "Lakefront Separation" scenario in which impenetrable barrier is assumed to be constructed at the Wilmette Pump Station, the Chicago River Controlling Works, and a point on the Little Calumet River (north) just upstream of the junction with the Grand Calumet River, and (3) the "Midsystem Separation" scenario wherein the impenetrable barriers are placed near the original watershed divides in the Chicago and Calumet river systems. By the reporting deadline the "No Project" scenario had been completed for Water Years (WYs) 2003 and 2008 for both baseline and future conditions and the "Lakefront Separation" scenario had been completed for WY 2008 for both baseline and future conditions.

Flow Conditions

Water quality for each hydrologic scenario shall be modeled for wet (2008), dry (2003), and average (2001) year flow conditions in the waterways. Additionally, the system shall be modeled both with and without all MWRDGC TARP reservoirs (currently under construction) in operation. Expected flow data necessary for modeling reservoirs in operation shall be provided by the Corps.

Progress: All needed flow data and stage for WYs 2001, 2003, and 2008 were obtained from the MWRDGC and U.S. Geological Survey (USGS). Also, the Corps provided to the project team simulated gravity combined sewer overflow (CSO) flows reflecting current, baseline conditions (Thornton Reservoir and McCook Reservoir Stage 1 operational), and future conditions (Thornton Reservoir and McCook Reservoir Stages 1 and 2 operational) for each of the three years. Table 1 lists the percentage of CSO flows captured by the McCook Reservoir Stage 1 and Stages 1+2 for WYs 2001, 2003, and 2008, and Table 2 lists the percentage of CSO flows captured by the Thornton Reservoir for WYs 2001, 2003, and 2008. This high capture of CSO flows results in a substantial reduction in storm caused drops in DO concentrations for "No Project" conditions relative to current conditions. The lower percentage capture in WY 2008 results because storms earlier in September filled the reservoirs so that the large storm on September 13-16, 2008, was minimally captured by the reservoirs.

Table 1. Percentage of combined sewer overflow (CSO) flows captured by the McCook Reservoir Stages 1 and 2 for gravity CSO flows and CSO flows from the Racine Avenue Pumping Station (NAPS) and North Branch Pumping Station (NBPS).

Year	Gravity CSOs	RAPS	NBPS
2001	90.0	94.0	98.3
2003	83.6	96.4	95.7
2008	60.2	73.2	85.4

Table 2. Percentage of combined sewer overflow (CSO) flows captured by the Thornton Reservoir for gravity CSO flows and CSO flows from the 125th Street Pumping Station (125PS).

Year	Gravity CSOs	125PS
2001	99.8	100.0
2003	95.7	96.8
2008	49.9	76.5

Water Quality Parameters

The following water quality parameters are required for modeling. If the DUFLOW model did not originally model a parameter it is indicated with a * below, the capability of modeling the parameter was added during the first six months of the project and improved during the reporting period as detailed in the subsequent "Progress" sections.

- DO
- Ammonia
- Nitrate/Nitrite
- BOD
- TSS
- Total Phosphorus
- Fecal Coliform*
- Temperature*
- pH*
- Chloride*

A version of the DUFLOW model that simulates fecal coliform concentrations did exist at the start of this project, but it needed to be updated to consider the extension of the downstream boundary from Romeoville to the Lockport Controlling Works, the increase in representative combined sewer overflow (CSO) locations from 28 to 43, and any new fecal coliform data collected by the MWRDGC since 2005 (when the original fecal coliform model was developed).

In the original DUFLOW model of the CAWS, temperature is not simulated, rather hourly temperatures measured at the MWRDGC continuous measurement sondes are used in the model. Experience filling in missing temperature data has indicated that temperatures at all sonde locations in the CAWS can be reasonably estimated from the temperatures measured at nearby sondes. Thus, the changes in temperature along the waterways may be reliably estimated via statistical models. Such statistical models will be developed for each sonde location and mass balance model principles will be applied at each proposed separation point to consider the reduction in cooler Lake Michigan water (daily Lake Michigan temperature data are available from the Chicago Department of Water Management) reaching various reaches of the CAWS after separation. After the change in water temperature in the vicinity of the point of separation is determined by mass balance, the temperature changes will propagate downstream through the CAWS using the statistical relations between points.

Modeling of chloride in the CAWS will be difficult for the following reasons.

- 1) Chloride is measured only once per 7 days at the outfalls of the Stickney and North Side Water Reclamation Plants (WRPs) and no chloride data are available for the outfall of the Calumet WRP.
- 2) Chloride concentration data for the CSOs is sparse, i.e. single samples during a CSO event are available for the three CSO pumping stations as opposed to event mean concentrations.

Progress:

Fecal Coliform Modeling

The necessary revisions to the domain of the model and the number of CSO input points were made and fecal coliform concentrations were simulated for WYs 2001 and 2003 in the first six months of the project. In the current reporting period, fecal coliform concentrations were simulated for WY 2008, and generally good agreement between simulated and measured fecal coliform concentrations was obtained at all measurement locations for WY 2008. In the past fecal coliform modeling no fecal coliform data were available for post-TARP CSOs in Chicago. Thus, Milwaukee data was applied because Milwaukee also has a deep tunnel system.

- a) The median value for grab samples in Milwaukee was 170,000 CFU/100 mL.
- b) For storms causing flow reversals to Lake Michigan the MWRDGC takes intensive bacteria measurements near the lakefront structures. For these events in 2001 and 2002, a fecal coliform concentration of 1,100,000 CFU/100 mL yielded good agreement between simulated and measured values.

In 2007, the MWRDGC took a large number of fecal coliform measurements in the flows at the NBPS (70) and RAPS (119). The statistics of these measurements are listed in Table 3, and the median value was used in the modeling done here (with the NBPS value also applied to the CSOs discharging to the Calumet River system). The results shown in Figure 1 illustrate the reasonableness of the assumed fecal coliform concentrations for CSOs.

Table 3. Statistics of fecal coliform concentrations measured in 2007 for the combined sewer overflows at the North Branch and Racine Avenue pumping stations in coliform forming units per 100 mL.

Pumping Station	Minimum	Maximum	Mean	Median
North Branch	160,000	4,700,000	862,000	485,000
Racine Avenue	38,000	18,000,000	1,696,000	810,000

Chloride Modeling

Researchers have found a strong correlation typically exists between total dissolved solids (TDS) and chloride in water. Thus, a linear regression relation was derived between chloride and TDS for the Stickney WRP effluent and this relation was used to estimate the chloride concentration in the Calumet WRP effluent. Similarly, a limited amount of data on chloride concentrations and conductivity values were available for storm sewers in Evanston and Crestwood, IL. From these data, linear regression relations between chloride and conductivity were developed that were used to estimate chloride concentrations in CSO flows on the basis of available conductivity data for CSOs in snow and non-snow periods throughout the year.

Using the foregoing estimates for the chloride concentrations for the Calumet WRP and the CSOs, chloride concentrations throughout the CAWS were simulated for WYs 2001 and 2003 in the first six months of the project. During the current reporting period, these regression relations were applied to WY 2008, and generally good agreement between simulated and measured chloride concentrations was obtained at all measurement locations for WY 2008.

pH

Available pH data on CSOs and flows in the TARP drop shafts were used to estimate typical pH values for the northern (to the NSC and NBCR), central (to the Chicago River Main Stem, SBCR, and CSSC), and southern (to the LCR and Cal-Sag Channel) CSOs. Daily pH data were obtained from the Chicago Department of Water Management for 1998 and 1999 and 2005 through 2011. Simulation of pH for WY 2008 using Lake Michigan data for that year and data for other years showed that using the typical annual fluctuation in Lake Michigan pH yielded nearly equal quality results to those obtained using the daily values for WY 2008. The relative percent error in simulated pH values generally is less than 5% at all locations in the CAWS.

Temperature

In the early 1990s, the University of Iowa developed the CHARIMA Model to simulate temperature for 55 miles of waterway from Roosevelt Road on the SBCR to Dresden Island Dam on the Illinois River in a project done for Commonwealth Edison. Short segments of Bubbly Creek, Cal-Sag Channel, Des Plaines River, Hickory Creek, DuPage River, and Kankakee River are included in the model where they flow into the waterway. The CHARIMA model computed the flows using the de Saint Venant Equations (also used in DUFLOW) solved on a one-mile spatial grid at a 30 min time step and computed temperature using an Advection-Diffusion-Source equation for unsteady transport of a fully mixed, dissolved constituent. A key part of the temperature model was the Source/Sink Term for Heat Exchange Between Water and the Atmosphere, which comprised detailed expressions for the physical processes of water heating due to incoming short-wave and long-wave radiation and condensation, water cooling due to outgoing long-wave radiation and evaporation, and water heating due to conduction. Also, time-dependent discharges and water temperatures were specified at the primary model inflow point and all tributary inflows, including the Stickney WRP. The 6 generating stations were modeled as links that withdraw the condenser flow rate from the main channel, heat it by an amount proportional to the temperature rise at full load using the specified time-dependent generation schedule, and return it to the channel. This complex, physics-based model yielded results typically with errors on the order of $\pm 1^\circ\text{F}$ (0.556°C). Thus, it was hoped that the statistical model could yield predictions with similar standard errors (i.e. $\leq 0.556^\circ\text{C}$).

Statistical relations to estimate daily temperature at 29 monitoring locations internal to the CAWS have been developed. For 16 of these locations the standard error of the predicted temperature was less than 0.556°C , indicating that the simple statistical temperature model could yield similar results to the much more complex, physics-based CHARIMA model. These results indicate that the statistical models are adequate for the purposes of the GLMRIS study. Further, periods were identified during which the Fisk Power Plant or Crawford Power Plant were shut down and regression relations were developed to reflect the rise in temperatures across these plants when they are not operational. These relations are very important because the Fisk and Crawford plants were retired in 2012, and, thus, the simulation of baseline and future conditions in this study must reflect temperatures in the CAWS with these plants shut down.

Summary

Simulations of all three scenarios for baseline and future flow conditions for all three water years will be completed by early June 2013 and a draft summary report will be provided to the Corps by the middle of July. The project report will be revised as per the Corps' review comments and the final report will be provided to the Corps by September 30 (the requested, revised ending date for this project).

Principal Findings and Significance

Principal Findings and Significance

Description	Because the project was still in progress at the end of the reporting period and no comparisons of all three scenarios had been completed the "Applications, Impacts, and Benefits" of this project cannot yet be reported. A draft summary report was provided to the U.S. Army Corps of Engineers (Corps) in January 2013 titled "Comparison of Current, Baseline, and Future Dissolved Oxygen Concentrations in the Chicago Area Waterways System for Without Project Conditions" that focused on the results for WY 2008. Also, in February 2013, a summary of the loads to Lake Michigan during the flow reversal of September 13-16, 2008, was provided to the Corps in order for the Lake Michigan modelers to test their models. The draft report, Lake Michigan loading information, periodic progress report meetings (discussed later), and other responses to information requests have met the Corps' needs to date.
--------------------	---

Interactions

Description	GLMRIS Water Quality Modeling—Progress Report Meeting with the U.S. Army Corps of Engineers in Chicago, IL
Event Date	4/6/2012



Description GLMRIS Water Quality Modeling—Progress Report Meeting with the U.S. Army Corps of Engineers in Chicago, IL
Event Date 10/2/2012



Description GLMRIS Water Quality Modeling—Progress Report Meeting with the U.S. Army Corps of Engineers in Chicago, IL
Event Date 2/12/2013

Presentations & Public Appearances

Title Modeling the Water Quality Impacts of the Potential Ecological Separation of the Great Lakes and Mississippi River Basins at Chicago for Invasive Species Control
Presenter(s) Charles S. Melching
Presentation Type Professional meeting
Event Name Wisconsin Section Meeting of the American Society of Civil Engineers
Event Location Pewaukee, WI
Event Date 9/7/2012
Target Audience Regional organization
Audience Size 40
Description The presentation summarized the goals of the GLMRIS project in general and the specific goals of the water-quality modeling study and the steps that must be executed to achieve these goals.

Students & Post-Docs Supported

Student Name Jin Liang
Campus Marquette University

Advisor Name Charles Melching
Advisor Campus Marquette University

Degree PhD
Graduation Month December
Graduation Year 2010
Department Civil and Environmental Engineering
Program Civil and Environmental Engineering
Thesis Title Evaluation of Runoff Response to Moving Rainstorms
Thesis Abstract

Establishing Paleoclimate Records from Spring Tufa Deposits in the Driftless Area of Wisconsin

Basic Information

Title:	Establishing Paleoclimate Records from Spring Tufa Deposits in the Driftless Area of Wisconsin
Project Number:	2011WI2950
Start Date:	7/1/2011
End Date:	6/30/2012
Funding Source:	Other
Congressional District:	6th
Research Category:	Climate and Hydrologic Processes
Focus Category:	Groundwater, Hydrology, Water Quantity
Descriptors:	
Principal Investigators:	Maureen Muldoon, Susan Swanson

Publication

1. Swanson, S.K., Muldoon, M.A., 2010, The geology and ecohydrology of springs in the Driftless Area of southwest Wisconsin, in de Wet, A., ed., Proceedings of the Twenty-third Annual Keck Research Symposium in Geology, Houston, Texas, pp. 96-102

**ESTABLISHING PALEOCLIMATE RECORDS FROM SPRING TUFA DEPOSITS IN THE
DRIFTLESS AREA OF WISCONSIN**

TABLE OF CONTENTS

PROJECT SUMMARY	4
INTRODUCTION	6
Project Objectives	6
Background	7
<i>Hydrogeologic Setting</i>	7
<i>Paleoclimatic Reconstructions</i>	7
PROCEDURES AND METHODS.....	8
Stratigraphic Sections	8
Borehole Geophysics	8
Geochemistry of Spring Water	9
Geochemistry of Tufa Deposits	9
RESULTS AND DISCUSSION.....	9
Stratigraphic Controls on Shallow Groundwater Flow.....	9
Geochemistry Results	11
<i>Geochemistry of Spring Waters</i>	11
<i>Geochemistry of Tufa Deposits</i>	12
<i>Regional Paleoclimatic Records</i>	13
CONCLUSIONS AND RECOMMENDATIONS	13
REFERENCES	14
APPENDIX A: Awards, Publications, Reports, Patents, and Presentations.	16
APPENDIX B. Detailed stratigraphic section near the Potosi spring.	17
APPENDIX C. Geophysical logs for GR1541 and AD099.....	18
APPENDIX D. Records of physicochemical conditions at the tufa-depositing springs.	20
APPENDIX E. Summary of spring water geochemistry results.....	21
APPENDIX F. U-Th dating results.	22

LIST OF FIGURES

Figure 1. (a.) The location of tufa-depositing and other springs in southwestern Wisconsin (Macholl, 2007) and (b.) the distribution of bedrock (WGNHS, 2006; Mudrey et al., 2007).

Figure 2. The Potosi tufa-depositing spring and the associated spring mound. Person for scale on left.

Figure 3. Measured stratigraphic section near the Potosi spring along with outcrop natural gamma values.

Figure 4. Correlation of natural gamma profiles from outcrop measurements and boreholes logs.

Figure 5. Calcite saturation indices at the (a.) Potosi and (b.) Platteville mounds.

Figure 6. Temporal variation of carbon and oxygen isotopic compositions and elemental ratios in the Platteville (PLC3, PLC4-5) and Potosi (POC8) tufa cores.

Figure 7. Temporal variation of carbon isotopic compositions in Coldwater Cave, IA stalagmite 1S (CWC-1S) (Denniston et al., 1999) and the Potosi tufa core (POC8).

PROJECT SUMMARY

Title: ESTABLISHING PALEOCLIMATE RECORDS FROM SPRING TUFA DEPOSITS IN THE DRIFTLESS AREA OF WISCONSIN

Project I.D.: WR11R004

Investigators: Maureen A. Muldoon, Associate Professor of Geology, University of Wisconsin – Oshkosh; Susan K. Swanson, Associate Professor of Geology, Beloit College

Period of Contract: 07/01/11 – 07/31/12

Background/Need: Water at two tufa-depositing springs in Grant County, Wisconsin emanates from stratigraphic positions similar to a laterally-extensive perched aquifer that was identified in the eastern Driftless Area and shown to be stable under current climate conditions (Carter et al., 2010). Due to the similarity in hydrogeologic setting, the tufa-depositing springs may be supplied by a similar shallow groundwater flow system. If geochemical records from the tufa deposits correlate with other proxy climate data in the region, this may suggest that tufa deposition, and therefore spring flow from the shallow flow system, has been continuous throughout the Holocene, even during climate regimes that differ from the present. Few domestic wells in the study area are installed at the stratigraphic interval of interest, but the headwaters of streams throughout the Driftless Area are fed by water discharging from the shallow groundwater flow system. Therefore, an understanding of the potential effects of climate change and variability on shallow groundwater levels and flow is important in maintaining aquatic diversity and stream habitat.

Objectives: The objectives of this study are 1) to gain a better understanding of how regional variations in the lithostratigraphy of the Sinipee Group (Platteville, Decorah, and Galena Formations) affect shallow groundwater flow patterns in the southern Driftless Area of Wisconsin and, specifically, in the vicinity of the tufa-depositing springs and 2) to use the tufa-depositing spring systems to better understand changes in Holocene climate in this region and the effects that climate change had on groundwater levels and flow.

Methods: To address the first objective, detailed measurements and descriptions of a stratigraphic section near the Potosi spring were made, and borehole geophysical logs were collected from existing domestic wells that are in close proximity to each spring site and open to the appropriate stratigraphic interval. Measurements of outcrop natural gamma allowed correlation to subsurface geophysical and hydrogeological data. In order to assess which, if any, of the many lithologic contrasts observed in outcrop functions as a high-permeability flow feature in the subsurface, we also examined existing natural gamma and hydrologic logs from wells where the Decorah Formation, in particular, was saturated.

To address the second objective, it was necessary to first gain an understanding of seasonal variations in tufa deposition. If tufa is deposited year-round, geochemical signatures are likely to represent mean annual conditions, whereas if tufa is deposited seasonally, the record may reflect mean summer or mean winter conditions. Monthly water samples were collected from the spring orifice and the dripface of each tufa mound and analyzed for major ion concentrations. These data were used to calculate calcite saturation indices at each orifice and dripface throughout the year. Continuous measurements of fluid temperature, conductivity, and water level with Levelloggers® provided context for the monthly samples.

Three one-inch tufa cores, each approximately 4m in length, were used to develop a paleoclimatic record based on variations in stable isotopes ($\delta^{18}\text{O}$ and $\delta^{13}\text{C}$) and elemental molar ratios (Mg/Ca). ^{234}U - ^{230}Th

dating was used to constrain the age of the tufa deposits. The paleoclimatic record developed from the tufa cores was then compared to existing proxy climate records for the region.

Results and Discussion: This distinct gamma signature of the Platteville and Decorah Formations is present in all of the logs we collected or examined and was used to correlate the units across the study area. The lithologic contrast between the shaley Spechts Ferry and the overlying Guttenberg limestone, which compose the Decorah Formation, seems to control the location of the tufa-depositing springs as well as seepage in the valley where the Potosi section was measured. Positions of seepage and vegetation growth in other nearby outcrops coincide with this interval and suggest that there are several additional discrete discontinuities that are in close stratigraphic proximity to the Spechts Ferry shale, have developed at zones of contrasting lithology, and may also function as high-permeability features in the subsurface.

Spring monitoring results suggest that physicochemical conditions do not vary widely at the springs, and the lack of variation in calcite saturation at each spring orifice and dripface supports the consistency of tufa deposition throughout the year. This indicates that geochemical results for the tufa deposits are more likely to represent mean annual conditions than seasonal conditions. Three of the seven ^{234}U - ^{230}Th dates that were obtained are thought to be reliable on the basis of their lower levels of detrital thorium and/or higher levels of uranium. Subsequent correlation of geochemical results among the tufa cores and other proxy climate records for the region lends further support for the reliability of the dates. Oxygen isotopes do not show increasing or decreasing trends within the cores. However, carbon isotopic trends in the Platteville cores are similar, in that the $\delta^{13}\text{C}$ in each core decreased by about 2 per mil between 2.4 ka and 1.8 ka. The Potosi core also shows a 2 per mil decrease in $\delta^{13}\text{C}$ between 2.4 ka and 1.8 ka; however, because it represents a longer time period, it is clear that the positive $\delta^{13}\text{C}$ excursion existed prior to 2.4 ka. Mg/Ca excursions correspond to $\delta^{13}\text{C}$ excursions in all three cores. Knox (2000) shows an episode of especially small floods in rivers in southwestern Wisconsin from about 5.5 ka to 3.3 ka, which he attributes to warmer and drier conditions. This interval corresponds to the maximum positive $\delta^{13}\text{C}$ and Mg/Ca excursions in the Potosi core. Carbon isotopic trends in the Potosi core also generally correspond to the $\delta^{13}\text{C}$ records for the Coldwater Cave stalagmites from northeastern Iowa (Denniston et al., 1999).

Conclusions/Implications/Recommendations: Perched groundwater in the Driftless Area was shown to be laterally-extensive and broadly associated with the Decorah, Platteville, and Glenwood Formations, and it is thought to be stable over decadal time scales (Carter et al., 2010). We provide further evidence of the significance of the sequence to shallow groundwater flow in the region, but refine the interval to several high-permeability zones that are concentrated near the upper contact of the Spechts Ferry shale or within one unit above or below the shale. We also favor a conceptual model for the shallow groundwater flow system that includes perched groundwater beneath some ridges and fully saturated conditions beneath others. The low-resolution age control on the tufa cores does not allow for detailed paleoclimatic reconstruction, but broad patterns that agree with other proxy climate records for the region are evident, suggesting that tufa deposition, and therefore spring flow, has been mostly continuous for at least the last five thousand years. This implies that the shallow groundwater flow system has been stable over time frames of thousands of years, even during warmer and drier periods.

Related Publications:

Swanson, S.K., Muldoon, M.A., 2010, The geology and ecohydrology of springs in the Driftless Area of southwest Wisconsin, *in de Wet, A., ed., Proceedings of the Twenty-third Annual Keck Research Symposium in Geology*, Houston, Texas, pp. 96-102.

Key Words: springs, tufa, Driftless Area

Funding: University of Wisconsin System

INTRODUCTION

Project Objectives

Where groundwater dissolves limestone and dolomite and becomes saturated with calcium carbonate, CO₂ degassing can cause tufa deposition near a spring orifice. Paleoclimate records can be constructed from tufa depositional sequences using stable isotope ratios and major and trace element concentrations (Andrews, 2006). Used in association with hydrogeologic information, these records provide insights into the effects of climate change and variability on groundwater levels and flow patterns. Springs that deposit tufa and create mounds are rare in Wisconsin. However, at least two, one near Platteville and another near Potosi, are known to emanate from the Sinnipee Group in the southern Driftless Area of Wisconsin (Figure 1) (Heller, 1988). Both springs discharge at mid-slope positions, well above the level of the receiving streams (Figure 2).

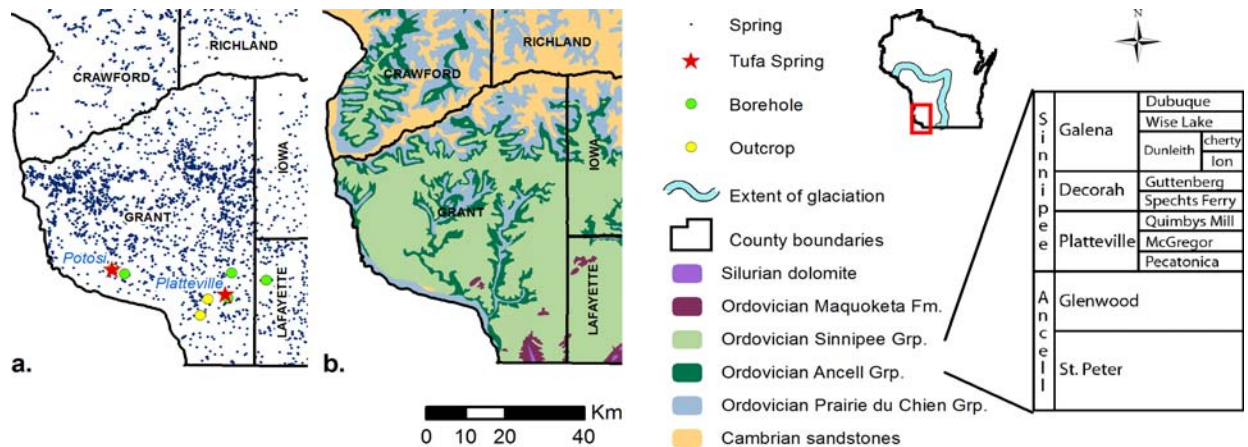


Figure 1. (a.) The location of tufa-depositing and other springs in southwestern Wisconsin (Macholl, 2007) and (b.) the distribution of bedrock (WGNHS, 2006; Mudrey et al., 2007).



Figure 2. The Potosi tufa-depositing spring and the associated spring mound. Person for scale on left.

Water at the tufa-depositing springs emanates from stratigraphic positions similar to a laterally-extensive perched aquifer that was identified in the eastern Driftless Area and shown to be stable under current climate conditions (Carter et al., 2010). Due to the similarity in hydrogeologic setting, the tufa-depositing springs may be supplied by a similar shallow groundwater flow system. If the geochemical records from the tufa deposits correlate with other proxy climate data in the region, this may suggest that tufa deposition, and therefore spring flow from the shallow flow system, has been continuous throughout the Holocene, even during climate regimes that differ from the present. The objectives of this study are 1) to gain a better understanding of how regional variations in the

lithostratigraphy of the Sinnipee Group affect shallow groundwater flow patterns in the southern Driftless Area of Wisconsin and, specifically, in the vicinity of the tufa-depositing springs and 2) to use the tufa-depositing spring systems to better understand changes in Holocene climate in this region and the effects that climate change had on groundwater levels and flow.

Background

Hydrogeologic Setting

Cambrian and Ordovician age strata generally thicken to the west and south in southwestern Wisconsin. They are deeply dissected and regularly exposed in narrow valleys (Figure 1). The Sinnipee Group, composed of the Platteville, Decorah and Galena Formations (Figure 1), is the uppermost bedrock unit in much of Grant County and is highly heterogeneous with abundant dissolution voids, horizontal and vertical fractures, and zones of shale strata. Pleistocene deposits are absent except for layers of loess on ridges, hillslope sediment on valley sides, and stream sediment in valley bottoms (Clayton and Attig, 1997; Mudrey et al., 2007). Local flow systems, with short groundwater flow paths, are common in the layered bedrock uplands. Perched aquifers, some of which may be laterally-extensive, also occur in the region (Krohelski et al., 2000; Hunt et al., 2003; Runkel et al., 2003; Carter et al., 2010). Therefore, the potential for complex groundwater flow paths exists.

Springs provide evidence of heterogeneity of permeability and discrete groundwater flow. As such, their occurrence can reveal important hydrogeologic controls on groundwater flow (Manga, 2001). Although thousands of springs occur in southwestern Wisconsin, the relationship of springs to the groundwater flow system is not well understood. Groundwater is generally thought to flow preferentially along bedding plane fractures or along lithologic contacts between units with differing hydraulic conductivity. Where these features intersect stream valleys, groundwater is discharged at contact springs. De Geoffroy et al. (1967; 1970) note that many of the springs in the historic lead-zinc mining district of southwestern Wisconsin (Iowa, Grant, and Lafayette Counties) emanate from fractures and along zones of contrasting permeability in the Platteville, Decorah, and Galena Formations (Sinnipee Group) (Figure 1). In Iowa County, Wisconsin, approximately 60% of 407 historically-mapped springs are thought to emanate from the Sinnipee Group (Swanson et al., 2007), and recent work suggests that some of these springs may be supplied by a laterally-extensive aquifer that is stable under current climate conditions and perched above the Decorah, Platteville, and Glenwood Formations (DPG aquitard) (Carter et al., 2010). An improved understanding of the hydrostratigraphic positions of springs in other parts of the Driftless Area may lend further evidence to the regional nature and stability of shallow groundwater flow systems under current climate conditions. Geochemical records from tufa deposits may extend the evidence to climate conditions that differ from the present.

Paleoclimatic Reconstructions

The Holocene climatic history of the upper midwestern United States has been reconstructed using a variety of physical and biological data sets including, for example, the analysis of cave stalagmites in northeastern Iowa (Dorale, 1992; Denniston et al., 1999), varved sediments from lakes in central Minnesota (Dean et al., 1984), floods reconstructed from the alluvial records of rivers in southwestern Wisconsin (Knox, 2000), and pollen from across the region (Webb et al., 1983; Bartlein et al., 1984; Baker et al., 1996; Clark et al., 2001; Williams et al., 2009). These studies generally agree that, due to changes in the frequency and duration of the Pacific, Gulf of Mexico, and Arctic air masses, an increase in mean July temperature and a reduction in mean annual precipitation took place from the early to mid-Holocene. Proxy climate data suggest that from the mid Holocene to present, the region became cooler and wetter, with some areas experiencing abrupt changes in temperature and moisture (Knox, 2000; Williams et al., 2009). While a large variety of Holocene proxy records exist for the upper midwestern USA (Williams et al., 2010), relatively few are available for the Driftless Area of Wisconsin. This is largely due to the lack of lakes and bogs typically used in pollen studies (Baker et al., 1996).

Stable isotope and elemental variation in active tufa-depositing systems and accumulated tufa deposits have been shown to reveal paleo-temperature and -moisture conditions (e.g., Andrews et al., 1997; Ihlenfeld et al., 2003; Garnett et al., 2004). Therefore, tufa sequences offer an opportunity not only to better understand current and past groundwater flow conditions, but also to augment climate reconstructions for this region. Variability in the $\delta^{18}\text{O}$ of tufa deposits reflects changes in temperature and

the $\delta^{18}\text{O}$ of water that recharges the aquifer and flows to the spring. Variability in the $\delta^{13}\text{C}$ of tufa deposits reflects the sources of carbon that contribute to dissolved inorganic carbon (DIC) in groundwater. CO_2 with lower $\delta^{13}\text{C}$ is often derived from soil organic matter, whereas higher $\delta^{13}\text{C}$ is often derived from the dissolution of the carbonate aquifer. Variation in $\delta^{13}\text{C}$ can also reflect the dominant type of plant metabolism. Where C3 plants dominate, $\delta^{13}\text{C}$ is typically lower. In drier regions, where C4 plants dominate, $\delta^{13}\text{C}$ is higher (Andrews, 2006). Ratios of Mg to Ca, or other elements such as Sr and Ba, in groundwater are known to increase with aquifer residence time due to differences in dissolution rates of dolomite versus calcite. Low Mg to Ca ratios in tufa have been shown to be associated with short residence times during wet periods and high Mg to Ca ratios with longer residence times during dry episodes (Garnett et al., 2004).

PROCEDURES AND METHODS

Stratigraphic Sections

The lithostratigraphy of the Sinnipee Group has been well characterized, as these strata serve as the host rock for the lead-zinc deposits within the tri-state mining district. Detailed descriptions of the members of the Platteville, Decorah, and Galena Formations can be found in numerous publications (e.g., Agnew et al., 1956; Heyl et al., 1959; Agnew, 1963; Agnew, 1966). One of the goals of this project was to investigate how lithostratigraphic variations affect groundwater flow patterns within the vicinity of the tufa-depositing springs. To accomplish this goal we 1) measured a detailed stratigraphic section of the rocks outcropping near the Potosi spring, 2) collected outcrop natural gamma measurements at both spring sites, and 3) used these data to correlate the outcrop lithostratigraphy near the springs to the regional subsurface stratigraphy. Poor exposure near the Platteville spring precluded measuring a detailed stratigraphic section at that site.

At the Potosi site, the stratigraphic units are exposed along the Grant River and in a small gully that cuts the hillside near the tufa mound. The exposed section extends from the upper St. Peter Formation through the base of the Galena Formation. Unit thicknesses were measured using a Jacob staff, and lithologic units were described noting composition, bedding characteristics, texture, Munsell color, and presence of fossils. These data were used to construct a detailed stratigraphic column. Location of groundwater seepage was also noted. Natural gamma measurements were collected approximately every 0.5 m at the Potosi exposure using a GF Instruments GRM-260 hand-held gamma-ray spectrometer. Additional gamma measurements were taken approximately every 0.1 m within the Decorah Formation which contains the Spechts Ferry and Guttenberg Members.

Borehole Geophysics

We examined well construction reports (WCRs) located within several miles of each spring site in order to identify existing domestic wells that were open to the Sinnipee Group, and specifically the Decorah Formation. For both the Potosi and Platteville sites we were able to identify a suitable well and obtain permission from the owners. We hired certified pump installers to pull the pumps from the wells prior to logging and then reinstall the pumps and disinfect the well upon completion of the logging process. In order to minimize inconvenience to the well owners, the logging was conducted immediately after the pump was pulled. Geophysical logs were collected using the Mount Sopris Matrix wireline logging system owned by the Wisconsin Geological and Natural History Survey (WGNHS). Geophysical data collected from each well include caliper, which measures borehole diameter and can help identify fractures and dissolution zones; natural gamma, which measures natural radiation and can be used for stratigraphic correlation as well as to identify zones with shale or clay; and single-point resistivity, normal resistivity, and spontaneous potential, which are useful for stratigraphic correlation. We also collected optical borehole image (OBI) and acoustic borehole image (ABI) logs for each well. In both wells, the static water level was well below the Decorah Formation, thus precluding the collection of any borehole flow measurements within that unit.

Geochemistry of Spring Water

Paleoclimate information is recorded only during times of active tufa deposition. If tufa is deposited year-round, geochemical signatures are likely to represent mean annual conditions, whereas if tufa is deposited seasonally, the record may reflect mean summer or mean winter conditions. To assess the seasonal consistency of tufa deposition, springs were sampled at the orifice and dripface on a monthly basis for one year. Temperature, specific conductance, pH, alkalinity, and dissolved oxygen were measured in the field, and samples were collected and sent to the University of Wisconsin - Stevens Point Water and Environmental Analysis Laboratory for analysis of major ions. These data were used to calculate monthly calcite saturation indices for each spring orifice and dripface. Lack of variation in the level of calcite saturation would support consistency in tufa deposition throughout the year.

Leveloggers® installed in the pool at each spring orifice were used to record water level, fluid temperature, and fluid conductivity at 30-minute intervals to provide additional context for the monthly water samples. Measurements of water levels in the spring pool allowed assessment of the seasonal variability in spring flow in lieu of actual discharge measurements, which are not possible due to shallow water depths and complex flow patterns across the mounds. A Barologger® installed at the Potosi site recorded barometric pressure and air temperature, allowing correction of water levels for barometric fluctuations. Hourly precipitation measurements for the duration of the study were obtained from the National Climate Data Center for the National Weather Service Cooperative Station at Cuba City, WI.

Geochemistry of Tufa Deposits

Three cores were collected from the two tufa mounds, two from the Platteville mound (3.85 m and 4.13 m) and one from the Potosi mound (3.95 m), using a handheld Tanaka 262DH Engine Drill with a one-inch diameter, diamond-encrusted bit. Each core was sampled at approximately 5 cm intervals using a Dremel drill. Samples were analyzed for stable isotopes of oxygen and carbon using an automated carbonate preparation device (KIEL-III) coupled to a gas-ratio mass spectrometer (Finnigan MAT 252) at the Environmental Isotope Laboratory in the Department of Geosciences at the University of Arizona. The cores were also cut and sampled at approximately 10 cm intervals. These samples were analyzed by X-ray Fluorescence (XRF) for 10 major and 19 trace element abundances at the GeoAnalytical Laboratory at Washington State University.

^{234}U - ^{230}Th dating was used to constrain the age of the tufa deposits. U and Th isotopes for seven samples were measured using a Thermo Neptune multi-collector inductively coupled plasma mass spectrometer (MC-ICPMS) at the University of New Mexico Radiogenic Isotope Laboratory. Although seven samples were analyzed, only three yielded reasonable ages. High levels of detrital Th and/or low levels of U rendered the other four samples questionable.

RESULTS AND DISCUSSION

Stratigraphic Controls on Shallow Groundwater Flow

The stratigraphic section from the Potosi site is presented in Figure 3; a more detailed section is presented in Appendix B. The section exposes 1.7 m of St. Peter Sandstone which is conformably overlain by 0.3 m of Glenwood Shale. The section extends through the Platteville, Decorah, and Galena Formations of the Sinipee Group. The Pecatonica Member consists of 6.0 m of irregularly bedded dolomite that is overlain by 7.25 m of limestone of the McGregor Member. The Quimbys Mill Limestone, as well as part of the overlying Spechts Ferry Member, are covered by talus. By digging into the gully walls, we were able to expose the base of the Quimbys Mill Member which we estimated as 0.2 m thick. The upper Spechts Ferry, exposed under a resistant ledge of the overlying Guttenberg Limestone Member, consists of interbedded gray-green shale layers and thin, fine-grained limestone layers. There is considerable groundwater seepage at the top of the Spechts Ferry Member (18.1 m in Figure Y) and we believe that this stratigraphic contact controls the location of the tufa-depositing springs. The Spechts Ferry Member

is overlain by 4.9 m of the irregularly bedded Guttenberg Limestone Member of the Decorah Formation. The section extends 2.0 meters into the base of the Galena Formation.

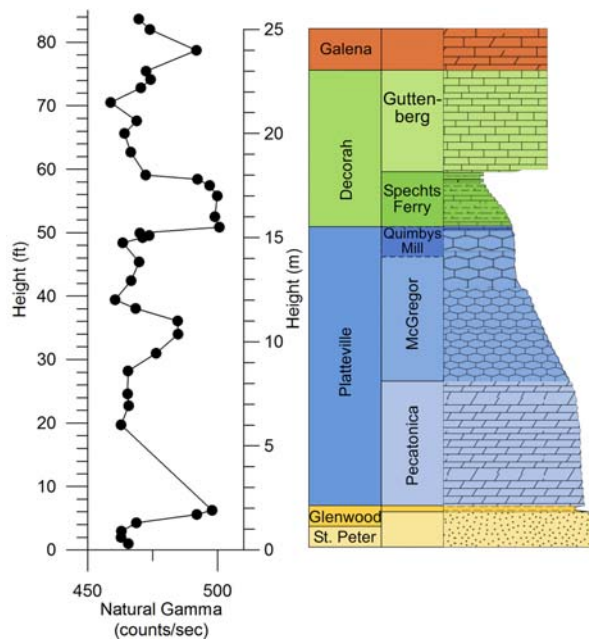


Figure 3. Measured stratigraphic section near the Potosi spring with outcrop natural gamma values.

The domestic well (WUWN GR1541), located near the Potosi spring and logged as part of this project, illustrates the natural gamma profile that is characteristic for the Ancell and Sinnipee Group stratigraphic units. The St. Peter Formation near the base of the log has a characteristically low gamma signature followed by the distinct gamma peak caused by the Glenwood shale. The Platteville Formation exhibits a somewhat variable natural gamma signature that is elevated above St. Peter values. The distinctive peak that extends from ~155 to 180 ft marks the location of the shaley Spechts Ferry Member of the Decorah Formation. This distinct gamma signature is present in all of the logs in Figure 4 and can be used to correlate this stratigraphic unit across the study area. In well GR1541 the Guttenberg lies directly above the Spechts Ferry and it is characterized by generally low gamma values, whereas the Ion submember of the Galena Formation has elevated gamma near the base that decreases as it grades into the overlying Galena members, which have quite low natural gamma signatures.

The lithologic contrast between the shaley Spechts Ferry and the overlying Guttenberg limestone seems to control the location of both tufa-depositing springs as well as the seepage in the valley where the Potosi section was measured. Doherty (2010) notes that the lithology of the backwall at each spring is composed of limestone with brown shale interbeds (Guttenberg) and that at some locations green shale (Spechts Ferry) is visible beneath the limestone. Positions of seepage and vegetation growth in outcrops along Highway 151 and the nearby Church Road quarry coincide with this interval and suggest that there are several additional discrete discontinuities, often developed at zones of contrasting lithology, that may also function as high-permeability features in the subsurface. Specifically, seepage is seen at the contact of the McGregor with the overlying Quimbys Mill, a zone of enhanced vegetation growth was noted in the Church Road quarry at the base of Spechts Ferry, and a large discontinuity with significant seepage was noted at the contact between the Guttenberg and the overlying Ion submember, which lie above the Spechts Ferry.

In the OBI logs collected from both domestic wells near the tufa springs (GR1541 and AD099) we noted that the borehole walls appear wet (dashed line, Figure 4) well above the static water level in the well (solid line, Figure 4). These observations could indicate one of the following hydrogeologic conditions: 1) a strong downward hydraulic gradient where the static water level in the well is not representative of the water table or 2) a perched water table that lies above the regional water table. It is impossible to assess which of these hydrogeologic conditions is present without installing short-interval piezometers at several depths; which was beyond the scope of this project. Logs for both wells are included in Appendix C.

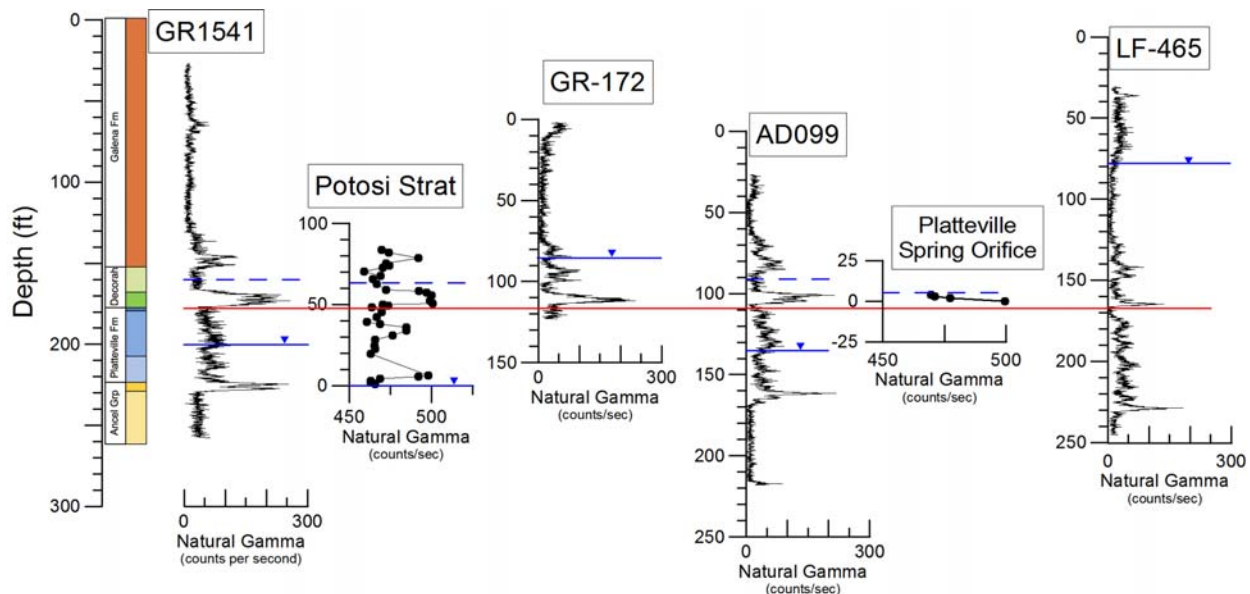


Figure 4. Correlation of natural gamma profiles from outcrop measurements and boreholes logs. The red line indicates the base of the Spechts Ferry Member. For the spring locations, the dashed blue lines indicate spring position whereas the solid blue line indicates the stream level which is assumed to represent the regional water table. For the wells, the solid blue line is the static water level whereas the dashed line indicates the position in the borehole where the walls appeared wet (as seen in the OBI logs).

In order to assess which, if any, of these lithologic contacts functions as a high-permeability flow feature in the subsurface, we also examined existing natural gamma and hydrologic logs from wells where the Decorah Formation was saturated. The WGNHS collected fluid temperature/resistivity data from wells GR-172 (UW-Platteville campus) and LF-465 (UW-Platteville Farm). In addition, an OBI log is available for hole GR-172 and a spinner flowmeter log is available for well LF-465. Sharp changes in a fluid temperature/resistivity profile have been used to identify high-permeability flow features in the subsurface (Muldoon and others, 2001). In GR172, there is a sharp inflection in both fluid temperature and resistivity at 106 ft depth, which lies just above the elevated natural gamma values that characterize the Spechts Ferry. Examination of the OBI log, indicates that this high-permeability feature lies between the Spechts Ferry and the Guttenberg. In LF-465 the fluid temperature and resistivity values showed little variation, however, an inflection in the spinner flow log at about 170 ft depth suggests that a high-permeability feature may be present at the base of the Spechts Ferry in this borehole.

Geochemistry Results

Geochemistry of Spring Waters

Spring monitoring results suggest that physicochemical conditions do not vary widely at the tufa-depositing springs. Concentrations of major ions were consistent throughout the sampling period. Between sampling events, the specific conductance of the spring waters decreased after some large or extended precipitation events, but consistently returned to just below 800 $\mu\text{S}/\text{cm}$ within a few days of an event. Fluid temperature was consistent at both springs, with a slight (< 0.3 $^{\circ}\text{C}$) decrease and increase lagging behind the seasonal transitions to winter and summer, respectively. Furthermore, the water depth in the Potosi spring pool did not vary widely over the monitoring period, averaging 3.7 cm. The water depth in the Platteville spring pool appears to have varied more; however, because these water levels were corrected using atmospheric data recorded at the Potosi mound, some of the variation in the recorded values is clearly due to uncorrected barometric pressure fluctuations. Therefore, it appears as though spring pool water depths do not vary widely at either mound, suggesting that discharge is also fairly

consistent at these springs. Records of physicochemical conditions for both springs for the duration of the monitoring period are included in Appendix D.

Throughout the sampling period and at each mound, calcite saturation indices and pH values increased, from spring orifice to dripface whereas the calcium concentration, alkalinity, and partial pressure of CO₂ decreased (Appendix E). These results provide support for CO₂ off-gassing as the driving mechanism for tufa precipitation at the Platteville and Potosi mounds, although mosses that cover the mounds probably enhance precipitation of tufa by providing a substrate that aids calcite nucleation (Andrews, 2006).

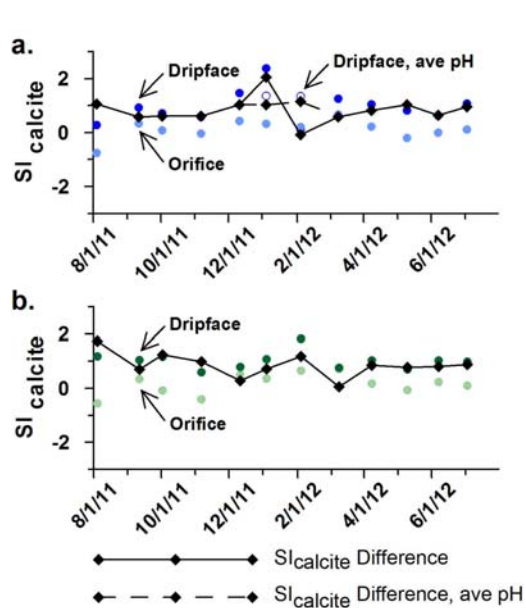


Figure 5. Calcite saturation indices at the (a.) Potosi and (b.) Platteville mounds.

Calcite saturation indices did not vary widely over the sampling period, aside from the January and February results for the Potosi dripface (Figure 5). Challenging winter field conditions at the Potosi dripface and cold air temperatures influenced the reliability of pH measurements for these samples. Water was collected at the dripface and then carried across the Grant River prior to measuring pH. Because it was necessary to traverse the river slowly, the pH meter was exposed to cold temperatures for a longer time period than at other sampling sites. To account for suspect measurements from a malfunctioning pH meter, the average of the pH values for December and March was used to calculate a second calcite saturation index for January and February. These indices are more in line with results for other dates. The overall lack of variation in the level of calcite saturation at each spring orifice and dripface, as well as the lack of variation in monthly differences between orifice and dripface calcite saturation indices, support the consistency of tufa deposition throughout the year. This indicates that geochemical results for the tufa deposits are more likely to represent mean annual conditions than seasonal conditions.

Geochemistry of Tufa Deposits

Three of the seven ²³⁴U-²³⁰Th dates are thought to be reliable on the basis of their lower levels of detrital thorium and/or higher levels of uranium (Appendix F). Subsequent correlation of geochemical results among the three cores and other proxy climate records for the region lends further support for the reliability of these ²³⁴U-²³⁰Th dates. Figure 6 shows the temporal variation of carbon and oxygen isotopic compositions and elemental ratios in the Platteville (PLC3, PLC4-5) and Potosi (POC8) tufa cores. Oxygen isotopes do not show increasing or decreasing trends throughout the depth of the cores. However, carbon isotopic trends in the two Platteville cores are similar, in that the δ¹³C in each core decreased by approximately 2 per mil between 2.4 ka and 1.8 ka. The similarity of the δ¹³C trends for the two Platteville cores suggests that water infiltrating the soil zone had time to reach isotopic equilibrium with soil CO₂ and/or that groundwater reached equilibrium with bedrock carbonate. The carbon isotopic trend in the Potosi core also shows a 2 per mil decrease between 2.4 ka and 1.8 ka. Because this core represents a longer time period, it is clear that the positive δ¹³C excursion existed prior to 2.4 ka.

If tufa δ¹³C is influenced by bedrock carbon and groundwater residence time, then trends in molar ratios of Mg to Ca should be similar to carbon isotopic trends. In all three cores, the molar ratios of Mg to Ca mimic the trends in δ¹³C. Although the δ¹³C records may also be influenced by regional vegetation changes, changes in contributions to DIC from bedrock carbon due to variations in groundwater residence times likely occurred, suggesting that the records can be used to infer paleo-moisture conditions.

Regional Paleoclimatic Records

The low-resolution age control on the tufa cores does not allow for detailed paleo-climatic reconstruction, but broad patterns that agree with other proxy climate records for the region are evident. The results in Figure 6 suggest that the region experienced conditions that were drier than the present until approximately 1.8 ka. Using alluvial records of rivers in southwestern Wisconsin, Knox (2000) shows an episode of especially small floods from about 5.5 ka to 3.3 ka, which he attributes to warmer and drier conditions. This interval corresponds to the maximum positive $\delta^{13}\text{C}$ and Mg/Ca excursions in POC8 (Figure 6). Carbon isotopic trends in POC8 also generally correspond to the $\delta^{13}\text{C}$ records for the Coldwater Cave stalagmites from northeastern Iowa (Figure 7) (Denniston et al., 1999). Overall agreement with these well-established records suggests that tufa deposition, and therefore spring flow, has probably been continuous for at least the last 5,000 years, even during warmer and drier periods.

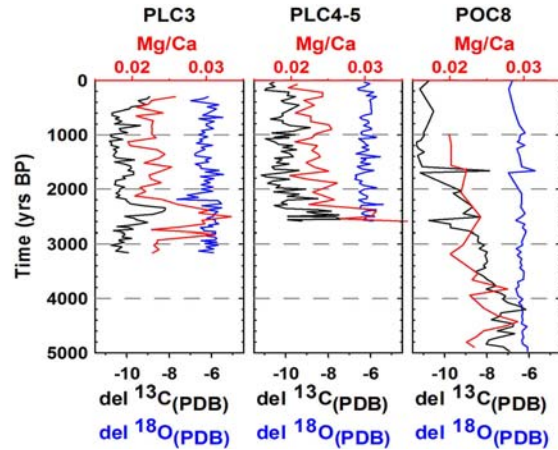


Figure 6. Temporal variation of carbon and oxygen isotopic compositions and elemental ratios in the Platteville (PLC3, PLC4-5) and Potosi (POC8) tufa cores.

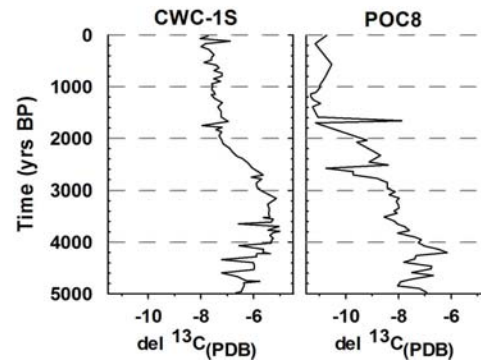


Figure 7. Temporal variation of carbon isotopic compositions in Coldwater Cave, IA stalagmite 1S (CWC-1S) (Denniston et al., 1999) and the Potosi tufa core (POC8).

CONCLUSIONS AND RECOMMENDATIONS

Used in association with the hydrogeologic data, the tufa records from the Platteville and Potosi mounds provide new insights into shallow groundwater flow conditions under climate regimes that differ from the present. Perched groundwater in the Driftless Area has recently been shown to be laterally-extensive and broadly associated with an Ordovician carbonate-siliciclastic sequence (Decorah, Platteville, and Glenwood Formations). Groundwater levels are thought to be stable over decadal time scales (Carter et al., 2010). This study provides further evidence of the significance of the sequence to shallow groundwater flow in the region, but we refine the interval to several high-permeability zones that are concentrated near the upper contact of the Spechts Ferry shale or within one unit above (Guttenberg limestone) or below (Quimby's Mill limestone) the shale. The increasing thickness of the Spechts Ferry shale to the west and southwest in southern Wisconsin (Agnew et al., 1956) may account for its greater relative influence on shallow groundwater flow within the study area. Although both tufa-depositing springs are associated with the high-permeability zone at the top of the Spechts Ferry shale and both discharge well above the level of the receiving streams, without short-interval piezometers, we cannot definitively say that shallow groundwater is perched above the Spechts Ferry shale near the springs. Furthermore, although the static water level lies below this unit in some open boreholes, it lies above this unit in others, so it is unlikely that a laterally-extensive perched system exists. It is more likely that perched systems do exist beneath some of the narrow ridges in the region where wedge-shaped unsaturated zones associated with one or more seepage faces extend to groundwater divides beneath the layered uplands (Rulon et al., 1985), but that fully saturated conditions across the interval have developed

in wider ridges. Therefore, the shallow groundwater flow system is best characterized as one that is complex and influenced by the laterally-extensive lithostratigraphy and by the existing topography.

Few domestic wells in the study area are installed at this stratigraphic interval, but the headwaters of streams throughout the Driftless Area are fed by water discharging from the shallow groundwater flow system. Therefore, an understanding of the potential effects of climate change and variability on shallow groundwater levels and flow is important in maintaining aquatic diversity and stream habitat. All three tufa cores show similar isotopic trends and trends in molar ratios of Mg to Ca. Furthermore, the tufa $\delta^{13}\text{C}$ records are similar to well-established proxy climate records from elsewhere in the Driftless Area, suggesting that tufa deposition, and therefore spring flow, has been mostly continuous for at least the last five thousand years. This implies that the shallow groundwater flow has been stable over time frames of thousands of years, even during warmer and drier periods.

REFERENCES

- Agnew, A. F.; Heyl, A. V.; Behre, C. H., Jr.; Lyons, E. J., 1956. Stratigraphy of Middle Ordovician rocks in the zinc-lead district of Wisconsin, Illinois, and Iowa: USGS Professional paper 274-K.
- Agnew, A. F., 1963, Geology of the Platteville Quadrangle, WI: USGS Bull 1123E, pp. 245-277.
- Agnew, A. F., 1966, Geology of the Potosi Quadrangle, Grant County Wisconsin and Dubuque County, Iowa: USGS Bull 1123I, pp. 533-567.
- Andrews, J.E., 2006, Paleoclimatic records from stable isotopes in riverine tufas; synthesis and review: *Earth-Science Reviews* 75 (1-4), pp.85-104.
- Andrews, J.E., Riding, R., Dennis, P.F., 1997, The stable isotope record of environmental and climatic signals in modern terrestrial microbial carbonates from Europe: *Palaeogeography, Palaeoclimatology, Palaeoecology* 129, pp.171-189.
- Baker, R.G., Bettis, E.A., Schwert, D.P., Horton, D.G., Chumbley, C.A., Gonzalez, L.A., Reagan, M.K., 1996, Holocene paleoenvironments of northeast Iowa: *Ecological Monographs* 66(2), pp. 203-234.
- Bartlein, P.J., Webb, T., Fleri, E., 1984, Holocene climatic change in the northern Midwest: pollen-derived estimates: *Quaternary Research* 22, pp.361-374.
- Carter, J.T.V., Gotkowitz, M.B., Anderson, M.P., 2010, Field verification of stable perched groundwater in layered bedrock uplands: *Ground Water*, doi: 10.1111/j.1745-6584.2010.00736.x.
- Clark, J.S., Grimm, E.C., Lynch, J., Mueller, P.G., 2001, Effects of Holocene climate change on the C4 grassland/woodland boundary in the northern plains, USA: *Ecology* 82(3), pp.620-636.
- Clayton, L., and Attig, J.W., 1997, Pleistocene geology of Dane County, Wisconsin: *Wisconsin Geological and Natural History Bulletin* 95, 64p.
- Dean, W.E., Bradbury, J.P., Anderson, R.Y., Barnosky, C.W., 1984, The variability of Holocene climate change: evidence from varved lake sediments: *Science* 226, pp. 1191-1194.
- De Geoffroy, J., Wu, S.M., and Heins, R.W., 1967, Geochemical coverage by spring sampling method in the southwest Wisconsin zinc area: *Economic Geology* v. 67, p. 679-697.
- De Geoffroy, J., Wu, S.M., and Heins, R.W., 1970, Some observations on springs in southwest Wisconsin: *Water Resources Research*, v.6, no. 4, p.1235-1238.
- Denniston, R.F., Gonzalez, L.A., Asmerom, Y., Baker, R.G., Reagan, M.K., Bettis, E.A., 1999, Evidence for increased cool season moisture during the middle Holocene: *Geology* 27, pp. 815-818.
- Doherty, Hannah, 2010, Lithostratigraphic Controls on groundwater flow and spring location in the Driftless Area of southwest Wisconsin, *in de Wet, A., ed., Proceedings of the Twenty-third Annual Keck Research Symposium in Geology*, Houston, Texas, pp. 103-109.
- Dorale, J.A., Gonzalez, L.A., Reagan, M.K., Pickett, D.A., Murrell, M.T., Baker, R.G., 1992, A high-resolution record of Holocene climate change in speleothem calcite from Cold Water Cave, Northeast Iowa: *Science* 258: pp. 1626-1630.

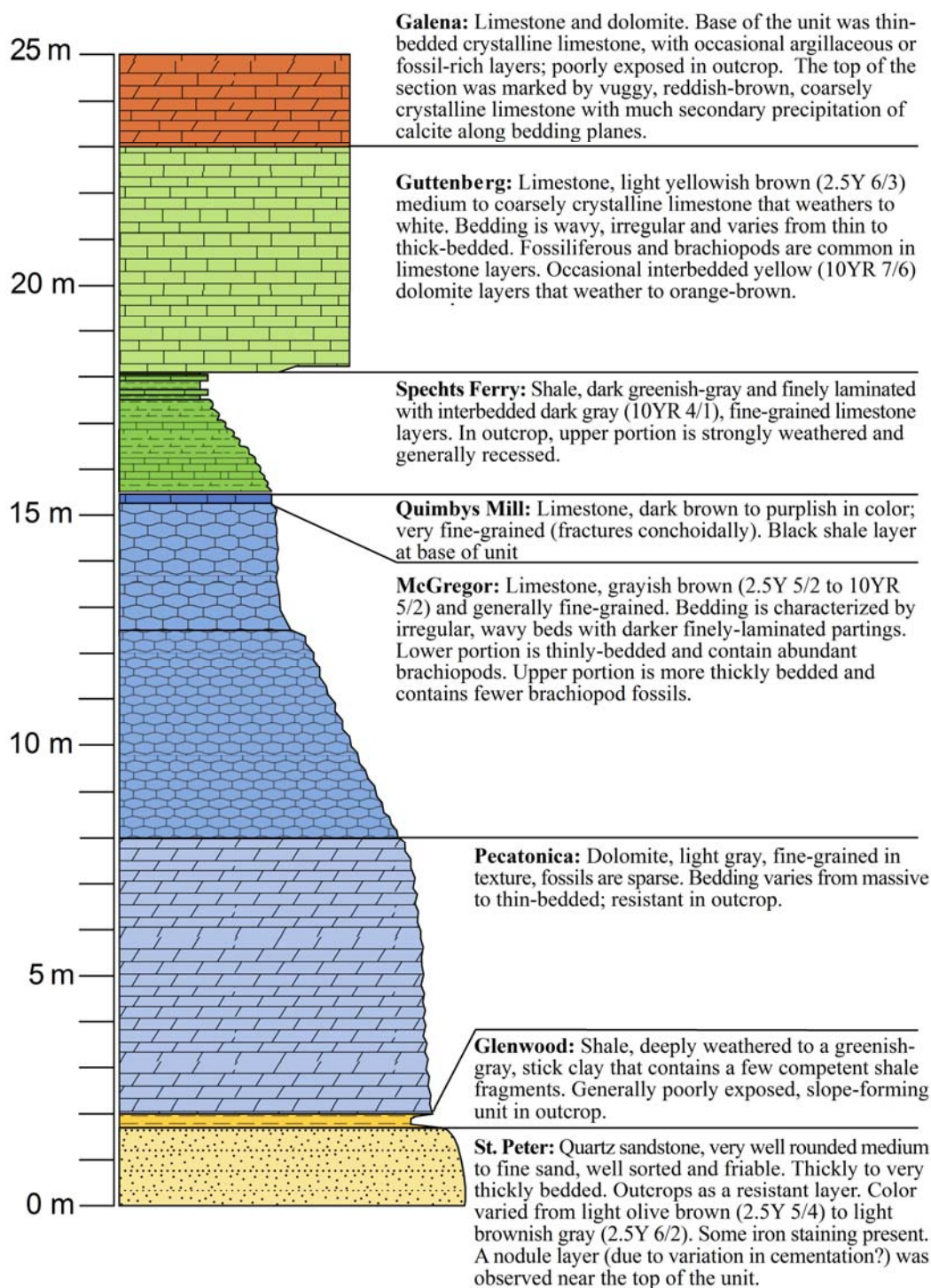
- Garnett, E.R., Andrews, J.E., Preece, R.C., Dennis, P.F., 2004, Climatic change recorded by stable isotopes and trace elements in a British Holocene tufa: *Journal of Quaternary Science* 19(3), pp. 251-262.
- Heller, S.A., 1988, Seasonal geochemistry of two tufa-depositing springs in southwestern Wisconsin: *Geoscience Wisconsin* 12, pp.77-83.
- Heyl, A. V., A. F. Agnew, E. J. Lyons, and A. E. Behre, 1959. The geology of the Upper Mississippi Valley zinc-lead district, USGS Professional Paper 309, 310 p.
- Hunt, R.J., Saad, D.A., Chapel, D.M., 2003, Numerical simulation of ground-water flow in La Crosse County, Wisconsin and into nearby pools of the Mississippi River: U.S. Geological Survey Water-Resources Investigations Report 03-4154, 36 p.
- Ihlenfeld, C., Norman, M.K., Gagan, M.K., Drysdale, R.N., Maas, R., Webb, J., 2003, Climatic significance of seasonal trace element and stable isotope variations in a modern freshwater tufa: *Geochimica et Cosmochimica Acta* 67 (13), pp. 2341-2357.
- Knox, J.C., 2000, Sensitivity of modern and Holocene floods to climate change: *Quaternary Science Reviews* 19, pp. 439-457.
- Krohelski, J.T., Bradbury, K.R., Hunt, R.J., and Swanson, S.K., 2000, Numerical simulation of groundwater flow in Dane County, Wisconsin: *Wisconsin Geological and Natural History Survey Bulletin* 98, 31p.
- Macholl, J.A., 2007, Inventory of Wisconsin's springs: *Wisconsin Geological and Natural History Survey Open File Report 2007-03*, 20 p. plus appendices.
- Manga, M., 2001, Using springs to study groundwater flow and active geologic processes. *Annual Review of Earth and Planetary Sciences* 29, pp.201-228.
- Mudrey, M.G., Jr., Brown, B.A., and Greenberg, J.K., 2007, Bedrock Geologic Map of Wisconsin: *Wisconsin Geological and Natural History State Map 18-DI*, version 1.0, 1 CD-ROM.
- Muldoon, M.A., Simo, J.A., Bradbury, K.R., 2001, Correlation of high-permeability zones with stratigraphy in a fractured-dolomite aquifer, Door County, Wisconsin. *Hydrogeology Journal* 9 (6), pp. 570-583.
- Rulon, J.J., R. Rodway, Freeze R.A., 1985, The development of multiple seepage faces on layered slopes. *Water Resources Research* 21, (11), pp. 1625–1636.
- Runkel, A.C., Tipping, R.G., Alexander Jr., E.C., Green, J.A., Mossler, J.H., Alexander, S.C., 2003, Hydrogeology of the Paleozoic bedrock in southeastern Minnesota: *Minnesota Geological Survey Report of Investigations* 61, 105p.
- Swanson, S.K., Bradbury, K.R., Hart, D.J., 2007, Assessing the ecological status and vulnerability of springs in Wisconsin. *Wisconsin Geological and Natural History Survey Open File Report 2007-04*, 15p. plus appendices.
- Webb III, T., Cushing, E.J., Wright Jr., H.E., 1983, Holocene changes in the vegetation of the Midwest. In: Wright Jr., H.E. (Ed.), *Late-Quaternary Environments of the United States*. University of Minnesota Press, Minneapolis, pp. 142–165.
- Williams, J.W., Shuman, B., Bartlein, P.J., 2009, Rapid responses of the prairie-forest ecotone to early Holocene aridity in mid-continental North America: *Global and Planetary Change* 66, pp.195-207.
- Williams, J.W., Shuman, B., Bartlein, P.J., Diffenbaugh, N.S., Webb III, T., 2010, Rapid, time-transgressive, and variable responses to early Holocene midcontinental drying in North America: *Geology* 38, pp. 135-138.
- WGNHS, 2006, *Bedrock Stratigraphic Units in Wisconsin: Wisconsin Geological and Natural History Survey Open File Report 2006-06*.

APPENDIX A: Awards, Publications, Reports, Patents, and Presentations.

Swanson, S.K., and Muldoon, M.A., March 2012. Evaluating the persistence of perched groundwater using the stratigraphic position and geochemistry of spring tufa deposits in the Driftless Area of Wisconsin, American Water Resources Association – Wisconsin Section Annual Meeting, Wisconsin Dells, Wisconsin.

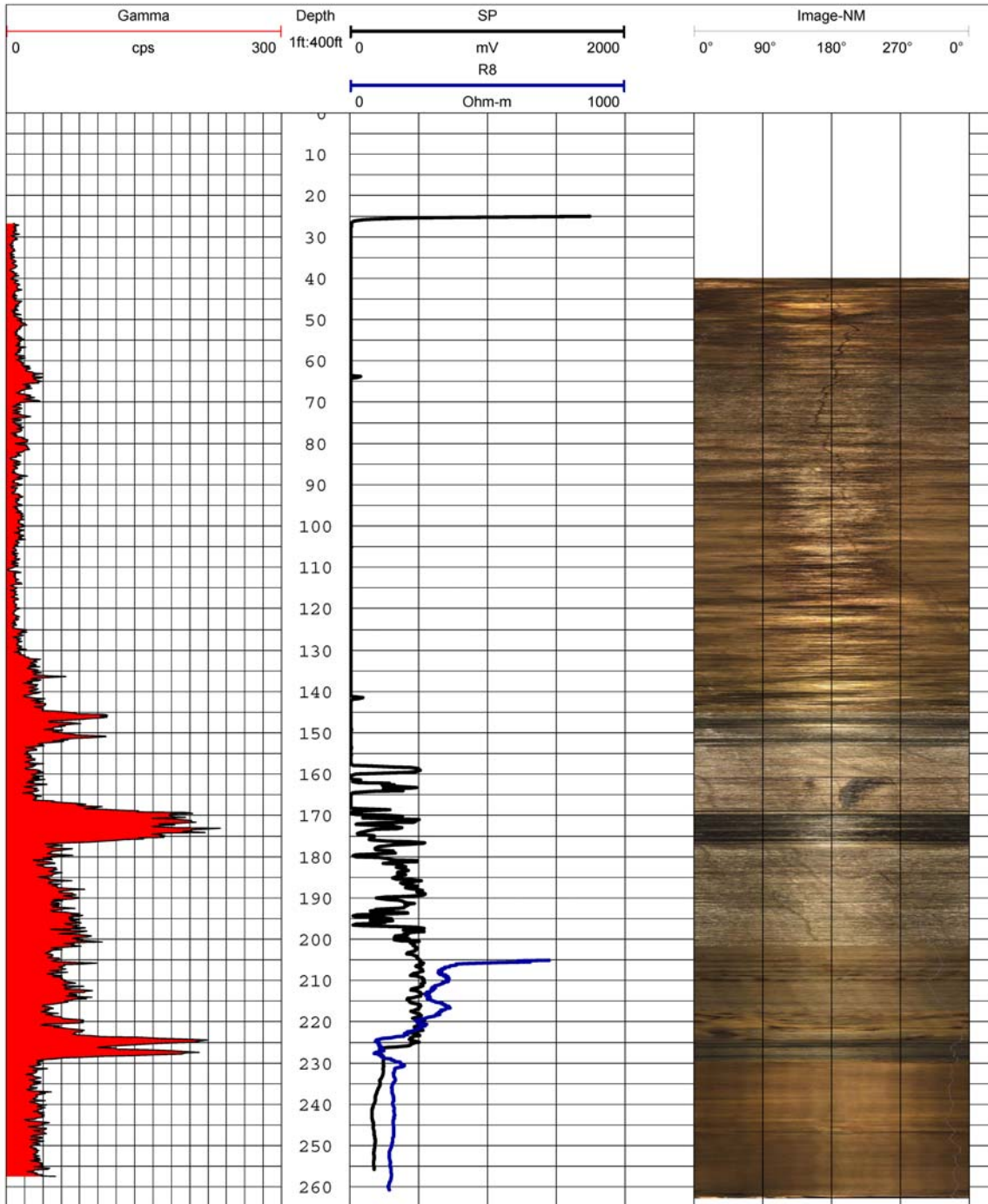
Swanson, S.K., and Muldoon, M.A., October 2011. Hydrostratigraphic and climate controls on spring flow and perched groundwater in the Driftless Area of Wisconsin, Geological Society of America Annual Meeting, Minneapolis, Minnesota.

APPENDIX B. Detailed stratigraphic section near the Potosi spring.

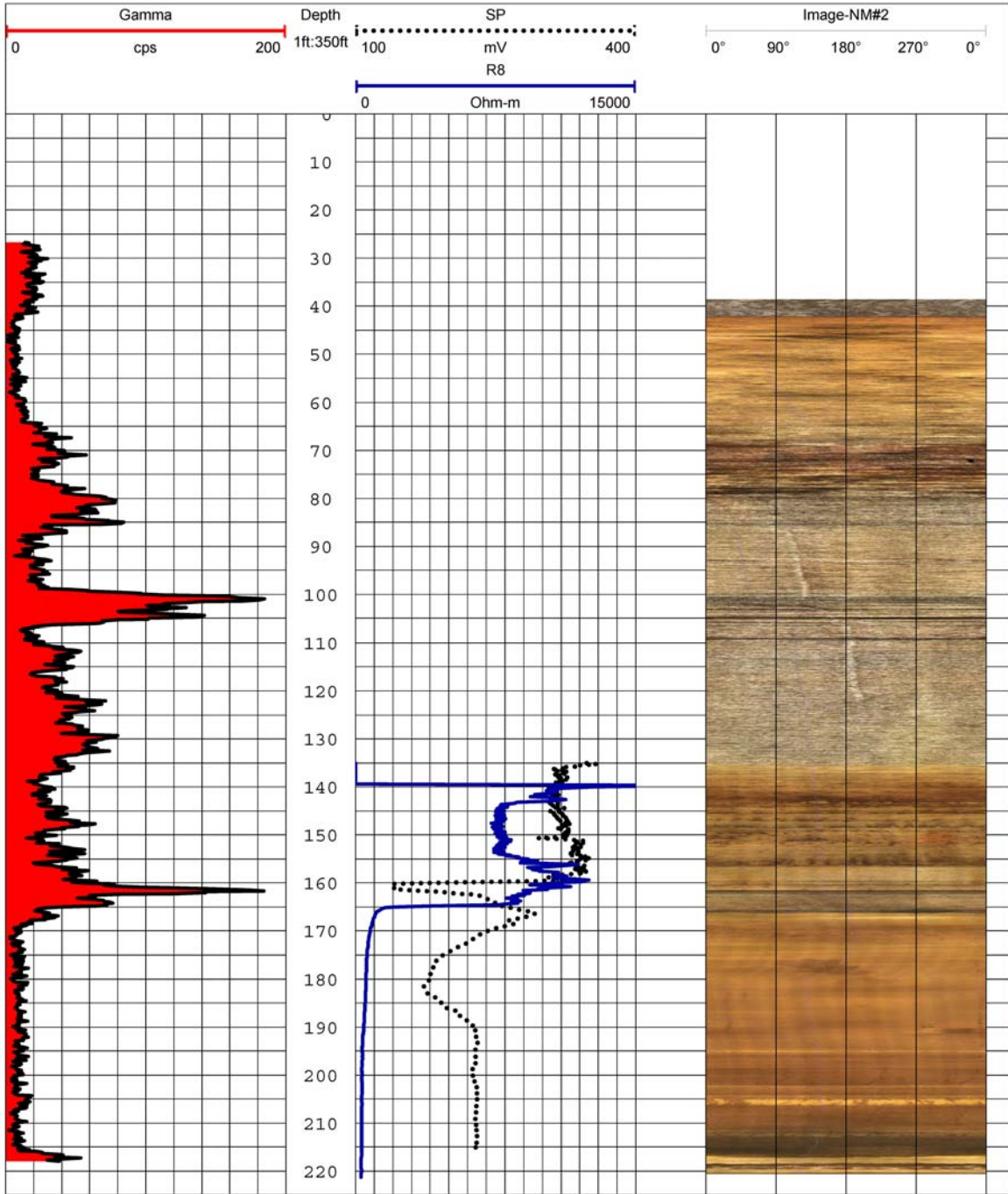


APPENDIX C. Geophysical logs for GR1541 and AD099

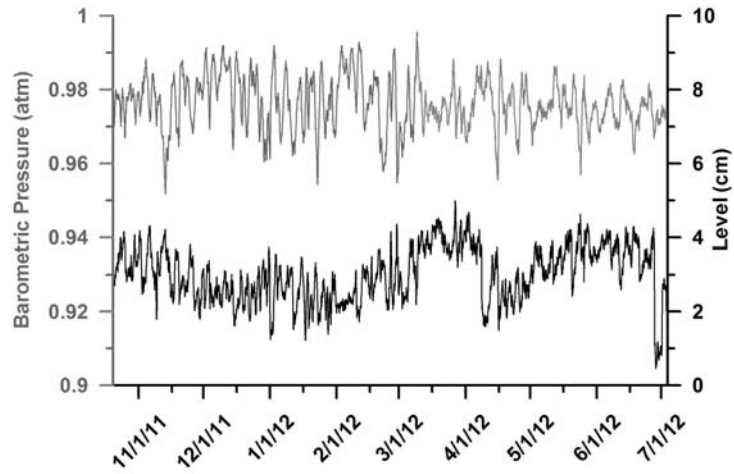
GR1541



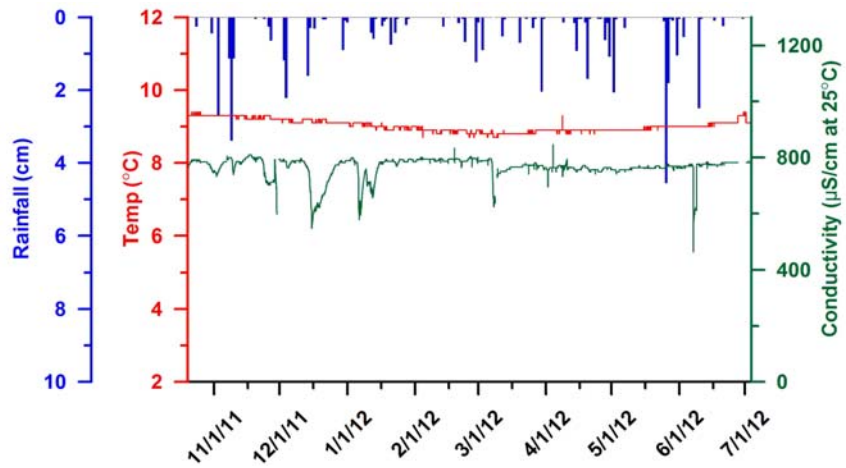
AD099



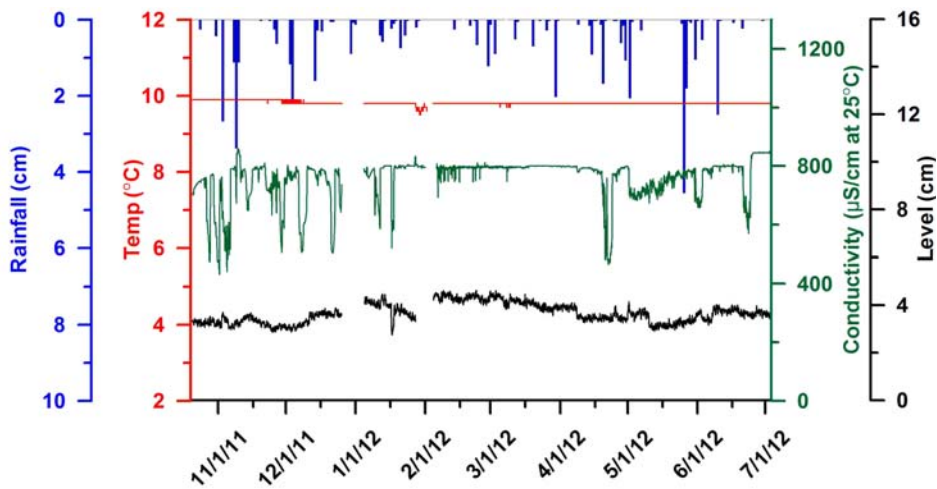
APPENDIX D. Records of physicochemical conditions at the tufa-depositing springs.



Water levels and barometric pressure records for the Platteville spring.



Precipitation, temperature, and conductivity records for the Platteville spring.



Physicochemical conditions at the Potosi spring

APPENDIX E. Summary of spring water geochemistry results.

		Potosi orifice	Potosi dripface	Platteville orifice	Platteville dripface
Calcium (mg/L)	Mean	88.1	75.4	89.1	73.1
	Std. Dev.	3.1	5.9	5.3	14.9
Magnesium (mg/L)	Mean	45.9	45.4	48.3	48.1
	Std. Dev.	1.2	1.2	2.1	1.9
Potassium (mg/L)	Mean	1.1	1.1	0.5	0.6
	Std. Dev.	0.1	0.4	0.2	0.1
Sodium (mg/L)	Mean	5.7	5.5	7.8	7.5
	Std. Dev.	0.4	0.4	0.6	0.7
Chloride (mg/L)	Mean	7.9	7.9	16.3	16.3
	Std. Dev.	0.3	0.3	1.2	1.3
Nitrate (mg/L)	Mean	3.7	3.7	1.1	1.1
	Std. Dev.	0.1	0.3	0.1	0.1
Sulfate (mg/L)	Mean	18.5	18.3	23.6	23.7
	Std. Dev.	0.7	0.5	1.6	1.4
Alkalinity (mg/L CaCO ₃)	Mean	386	348	393	349
	Std. Dev.	7	9	19	38
pH	Mean	7.05	7.98	7.10	8.09
	Std. Dev.	0.36	0.66	0.41	0.42
Conductivity (μS/cm, 25°C)	Mean	755	707	795	718
	Std. Dev.	12	14	44	63
Temperature (°C)	Mean	9.8	10.9	9.2	10.2
	Std. Dev.	0.1	3.4	0.9	4.3
SI _{calcite}	Mean	0.12	0.94	0.17	1.02
	Std. Dev.	0.36	0.59	0.39	0.32
PCO ₂	Mean	5.0E-02	7.0E-03	4.6E-02	3.9E-03
	Std. Dev.	6.5E-02	7.1E-03	4.9E-02	3.5E-03

APPENDIX F. U-Th dating results.

Sample	^{238}U (ppb)	^{232}Th (ppt)	$^{230}\text{Th}/^{232}\text{Th}$ activity ratio	$^{230}\text{Th}/^{238}\text{U}$ activity ratio	Measured $\delta^{238}\text{U}$ (‰)	Initial $\delta^{234}\text{U}$ (‰)	Uncorrected age (yr B.P.)	Corrected age (yr B.P.)
PLC3-308A	137.3±0.1	1126±29	15.994±0.468	0.0429±0.0006	719±2	725±2	2755±37	2617±78
PLC3-389A	119.1±0.1	1549±40	11.288±0.371	0.0480±0.0010	719±2	655±2	3222±67	2993±132
POC8-368A	141.5±0.1	8800±38	4.443±0.044	0.0904±0.0008	791±2	801±2	5637±52	4629±506
PLC5-101	79.0±2.4	102,413±419	1.384±0.099	0.5875±0.0453	1632±67	1689±78	26873±2442	12053±7495
PLC4-220A	80.3±0.1	1964±23	11.311±0.214	0.0905±0.0013	763±2	775±2	5735±87	5334±219
PLC4-220	79.4±0.1	6907±22	2.337±0.028	0.0665±0.0008	599±2	606±2	4629±55	3838±399
PLC4-347	117.8±0.1	12,397±15	1.971±0.012	0.0679±0.0004	1452±2	1459±4	3058±19	1807±624

Notes:

Corrected ages use a calculated initial $^{230}\text{Th}/^{232}\text{Th}$ atomic ratio 4.4 ppm ±50%.

Years before present = yr B.P., where present is AD 2011.

All errors are absolute 2σ .

Subsample sizes range from 50 to 250 mg.

Bold = samples that were more carefully selected to insure visually clean, nonporous carbonate.

Preferential flow paths in heterogeneous glacially-deposited aquitards

Basic Information

Title:	Preferential flow paths in heterogeneous glacially-deposited aquitards
Project Number:	2011 WI296O
Start Date:	7/1/2011
End Date:	6/30/2012
Funding Source:	Other
Congressional District:	2nd
Research Category:	Ground-water Flow and Transport
Focus Category:	Hydrology, Water Quantity, Models
Descriptors:	
Principal Investigators:	David J. John Hart

Publications

There are no publications.

Preferential Flow Paths in Heterogeneous Glacially-Deposited Aquitards
(WRI Project Number WR11R005)

Principal Investigator: David J. Hart, Wisconsin Geological and Natural History Survey

Table of Contents

Table of Contents	2
List of Figures and Tables	3
Project Summary	4
Introduction	6
Procedures and Methods	8
Results and Discussion	11
Conclusions and Recommendations	13
References	14
Appendix A: Awards, Presentations, Reports, Patents and Presentations	16
Appendix B: Electrical Resistivity Imaging	17
Appendix C: Geoprobe Logs	22
Appendix D: Hydrostratigraphic Model Design	26
Appendix E: CONNEC3D Overview	32
Appendix F: Selection of Representative Set of Models	34
Appendix G: Groundwater Flow and Transport Models	42
Appendix H: Additional References in Appendices	53

List of Figures and Tables

Figure 1: Location Map	7
Figure 2: Electrical Resistivity	9
Figure 3: Sand Body Elevations	9
Figure 4: 3-D Well Construction Reports	10
Figure 5: Particle Tracking, Deep Areas of Bedrock Valley	12
Figure 6: Particle Tracking, Shallow Areas of Bedrock Valley	12
Figure 7: Pie Chart for Percent Particle Movement	12
Table 1: Preferential flow examples from individual particles	13

Title: *Preferential Flow Paths in Heterogeneous Glacially-Deposited Aquitards*

Project I.D.: WRI Project Number WR11R005

Investigators: Principal Investigator- *David J. Hart, Hydrogeologist, Wisconsin Geological and Natural History Survey, University of Wisconsin–Extension, 3817 Mineral Point Road, Madison, WI 53705*
Research Assistant- *Kallina M. Dunkle, Graduate Student, Department of Geoscience, University of Wisconsin-Madison, 1215 West Dayton Street, Madison, WI 53706*

Period of Contract: July 1, 2011- June 30, 2012

Background/Need: Preferential flow paths allow for faster movement of fluids than the surrounding matrix due to their hydraulic properties and connectivity. They are important to both groundwater flow and contaminant transport, but are difficult to detect and quantify, especially in aquitards. Preferential flow paths may be caused by fractures and lenses of sediment with high hydraulic conductivity (K) such as sand bodies within a clay matrix. Researchers have discovered that even thick aquitards (greater than 150 ft) may have fractures that are capable of transporting contaminants (Cherry *et al.*, 2006; Gerber *et al.*, 2001) and affecting underlying aquifers. However, few researchers have documented preferential flow paths created by connected sand lenses/bodies. Techniques to delineate preferential flow paths in aquitards are key to determining recharge to underlying confined aquifers and for protection of underlying aquifers.

This project focuses on delineating preferential flow paths in a heterogeneous glacially-deposited aquitard. A representative site has been selected in Outagamie County, Wisconsin where a bedrock valley has been filled with a thick sequence of sediment, dominated by lake sediment with some glacial till and sand lenses of uncertain deposition. This sediment appears to form an extensive aquitard comprised of very low conductivity sediment, occasionally surrounding sand lenses of unknown extent and continuity. Results of this project will be useful to both the municipal and private well owners in Outagamie County. The results can be used in a variety of ways including groundwater management such as siting municipal wells, land use planning such as siting landfills, and public information regarding Wisconsin glacial history.

Objectives: The main objective of this study was to delineate preferential flow paths using multiple-point geostatistics and groundwater flow models for a representative site in Outagamie County, Wisconsin. Additional objectives included demonstrating the use of multiple-point geostatistics, understanding the flow system in Outagamie County, and reviewing and revising the depositional history of glacial Lake Oshkosh.

Methods: Multiple-point geostatistics (Guardino & Srivastava, 1993) was used to create 300 three-dimensional hydrostratigraphic models for the representative site in Outagamie County, Wisconsin, using as input data a combination of well construction reports, electrical resistivity imaging, geoprobe sampling, and reasonable depositional histories. Multiple-point geostatistics uses training images, either 2-D or 3-D, that represent the general features of the subsurface (i.e., channels, lenses). Training images have advantages over variograms, the more traditional geostatistical approach, because training images can include soft data, such as outcrops or geophysics, and can maintain geologic structure and continuity. All 300 hydrostratigraphic models were analyzed for statistics of connectivity and a representative set of six hydrostratigraphic models was selected and imported into groundwater flow and transport models based on these analyses. The groundwater flow models were calibrated to head data, the calibration was checked with streamflow measurements, and particle tracking was performed and compared to statistics of connectivity.

Results and Discussion: Analysis of well construction reports, digital elevation models, and information on the known outlets of glacial Lake Oshkosh indicated the origin of sand and gravel deposits is most likely a combination of beach and underflow deposits, making up to 20% by volume of the total sediments. All 300 models had at least one connected high K zone in the horizontal and vertical directions (percolating pathway), as indicated by statistics of connectivity. Results of the particle tracking indicated that 6% of the particles moved through the glacial deposits and exited into the surrounding bedrock in fewer than 100 years, indicating preferential flow may be occurring. Also, examples of individual particles traced through high K units in faster time than nearby particles moving through low K units were found in every model. Analyses indicated a general lack of correlation between the particle tracking results and the statistics of connectivity. This is probably due to all of the hydrostratigraphic models being geologically plausible and well-connected; thus the statistics and particle tracking have little variation.

Conclusions/Implications/Recommendations: This is one of the first examples demonstrating the use of multiple-point geostatistics in three-dimensions with a variety of data, including surface geophysics and depositional environment information. This work demonstrates that preferential flow can occur in a glacially-deposited aquitard through connected sand bodies without the presence of fractures. Overall, results of the statistics of connectivity and particle tracking indicate that a hydrostratigraphic model with fewer, longer pathways or one with many shorter pathways can create preferential flow paths and can calibrate to head and streamflow data. Finally, preferential flow is likely occurring in glacial Lake Oshkosh sediment as indicated by the analysis of the connectivity statistics for the hydrostratigraphic models and results of the particle tracking. However, the groundwater flow models should be better calibrated in order to use them for purposes of groundwater management in Outagamie County. This will require a joint calibration of groundwater flow and transport models (with oxygen isotope data) as well as collection of additional head, stream flux, and isotope targets.

Related Publications:

- 1) Dunkle, K.M., Hart, D.J., and Anderson, M.P., 2013. Groundwater flow model calibration difficulties in areas with glacially-deposited aquitards: An example from glacial Lake Oshkosh, Geological Society of America *Abstracts with Programs*, vol. 45, no. 4, p. 53.
- 2) Dunkle, K.M., Hart, D.J., and Anderson, M.P., 2012. Preferential flow paths in glacial Lake Oshkosh sediment, Outagamie County, WI, Geological Society of America *Abstracts with Programs*, vol. 44, no. 7, p. 145.
- 3) Dunkle, K.M., Hart, D.J., and Anderson, M.P., 2011. Hydrostratigraphic & groundwater flow models for glacial Lake Oshkosh sediment, Outagamie County, WI, Geological Society of America *Abstracts with Programs*, vol. 43, no. 5, p.560.
- 4) Dunkle, K.M., Hart, D.J., and Anderson, M.P., 2011. Multiple-point geostatistics for creation of 3D hydrostratigraphic models, Outagamie County, WI, Three Dimensional Geological Mapping: Workshop Extended Abstracts, Geological Survey of Canada, Open File 6998.

Key Words: *aquitard, glacial hydrostratigraphy, glacial Lake Oshkosh, groundwater flow modeling, multiple-point geostatistics, preferential flow*

Funding: University of Wisconsin Water Resources Institute

INTRODUCTION

Preferential flow paths allow for faster movement of fluids than the surrounding matrix due to their hydraulic properties and connectivity. They are important to both groundwater flow and contaminant transport, but are difficult to detect and quantify, especially in aquitards. Preferential flow paths may be caused by fractures and lenses of sediment with high hydraulic conductivity (K) such as sand bodies within a clay matrix. Researchers have discovered that even thick aquitards (greater than 150 ft) may have fractures that are capable of transporting contaminants (Cherry *et al.*, 2006; Gerber *et al.*, 2001) and affecting underlying aquifers. However, few researchers have documented preferential flow paths created by connected sand lenses/bodies. Techniques to delineate preferential flow paths in aquitards are key to determining recharge to underlying confined aquifers and for protection of underlying aquifers.

The main objective of this study was to delineate preferential flow paths using multiple-point geostatistics and groundwater flow and transport models for a representative site in Outagamie County, Wisconsin. The Wisconsin Geological and Natural History Survey has done extensive work in Outagamie County to define the distribution and type of glacial deposits. As part of this work, a thick sequence of fine-grained glacial sediment consisting mainly of lake sediment and till was delineated in an east-west trending buried bedrock valley (Fig.1). Outside of this valley, the fine-grained sediment is significantly thinner but appears to drape over the bedrock surface. Given that bedrock aquifers are one of the primary resources for drinking water in Outagamie County, a groundwater investigation was conducted to identify potential recharge areas in the county (Hooyer *et al.*, 2008). As part of this project four rotosonic boreholes were drilled along the axis of the valley and multilevel wells were installed in two of them (RS-17 and RS-18). Two other boreholes were also drilled where the fine-grained sediment was much thinner over bedrock (<50 ft). These boreholes, located at the Riehl and Lorenz Farms, were drilled using a hollow-stem auger. Three multilevel wells were installed in each of these boreholes. With the exception of RS-17, water Leveloggers® were installed and have continuously recorded in every well since 2007 to monitor the pressure heads in the aquitard. The RS-18 location contained a sand body at a depth of 40-60 feet, and sand bodies of similar thicknesses have been noted in multiple private well logs in the study area. Intact core samples from RS-18 and other rotosonic boreholes drilled through the fine-grained sediment were collected for consolidation testing, which determines preconsolidation stress, hydraulic diffusivity (D), and specific storage (S_s) (Grisak and Cherry, 1975; Hooyer *et al.*, 2008). The vertical K can then be calculated from D and S_s . Slug tests performed in the wells at RS-18, Riehl, and Lorenz Farms revealed that K values range from 1×10^{-8} to 5×10^{-14} m/s for the fine-grained sediment, and 2.5×10^{-4} to 6.0×10^{-5} m/s for the sand bodies.

Pore and well water samples from RS-17, RS-18, and RS-14 were analyzed for oxygen ($\delta^{18}\text{O}$) and hydrogen ($\delta^2\text{H}$) isotopes and well water was analyzed for tritium and the following major ions: calcium, magnesium, potassium, sodium, chloride, bicarbonate, sulfate, nitrite, and nitrate. These wells have modern $\delta^{18}\text{O}$ values at the surface, then gradually decrease with depth (indicating older water) and then increase toward more modern values near the bedrock surface. The modern values near the bedrock surface are surprising, given that studies of stable isotope geochemistry of the Cambrian Ordovician aquifer system (Perry *et al.*, 1982; Siegel and Mandle, 1984) show a significant portion of the groundwater in these aquifers may be as much as hundreds of thousands of years old. Hooyer *et al.* (2008) believe this difference in $\delta^{18}\text{O}$ values is due to recharge occurring to the bedrock aquifer where the glacial sediment is thin (<50 ft). However, recharge could be occurring through preferential flow paths such as sand lenses where the sediment is thick (~200-300 ft), allowing for faster movement of groundwater and contaminants. Thus, it is important to determine the connectedness of the sand bodies within this thick sequence of sediment.

As part of Kallina Dunkle's dissertation research approximately 2,200 Wisconsin Well Construction Reports (WCRs) with driller described lithologies were used to analyze the unconsolidated sediment. These sediments were categorized into distinct hydrofacies ranging from dominantly clay or silty clay to

coarse sand or gravel. Most drillers lack formal geologic training and often subtle differences in sediment are not reflected in cuttings. Thus the quality of these data varies considerably. For example, terms such as "hardpan" usually refer to glacial till, but so can "stoney clay" or "clayey gravel", among other designations. Considerable effort was made to be consistent and as accurate as possible in transforming the driller's descriptions into geologic categories. Analysis of the WCRs indicated the presence of four distinct units and their corresponding percentage of unconsolidated material by thickness as: 52.6% clay/silt, 20.1% till, 20.9% sand, and 3.1% gravel, with the remaining 3.3% unknown due to lack of description in the WCRs. Percents were calculated by the following equation: $(\Sigma \text{ sediment type thickness}) / (\Sigma \text{ unconsolidated sediment thickness})$. Analyzed WCR data was then displayed in 3-D using Rockworks to get a general picture of the subsurface geology. Additionally, four geophysical methods: seismic, radar, time-domain electromagnetics, and electrical resistivity imaging (ERI), were tested at the RS-18 site along a 200m transect. ERI was the only tested method that successfully identified the sand body in this geologic setting.

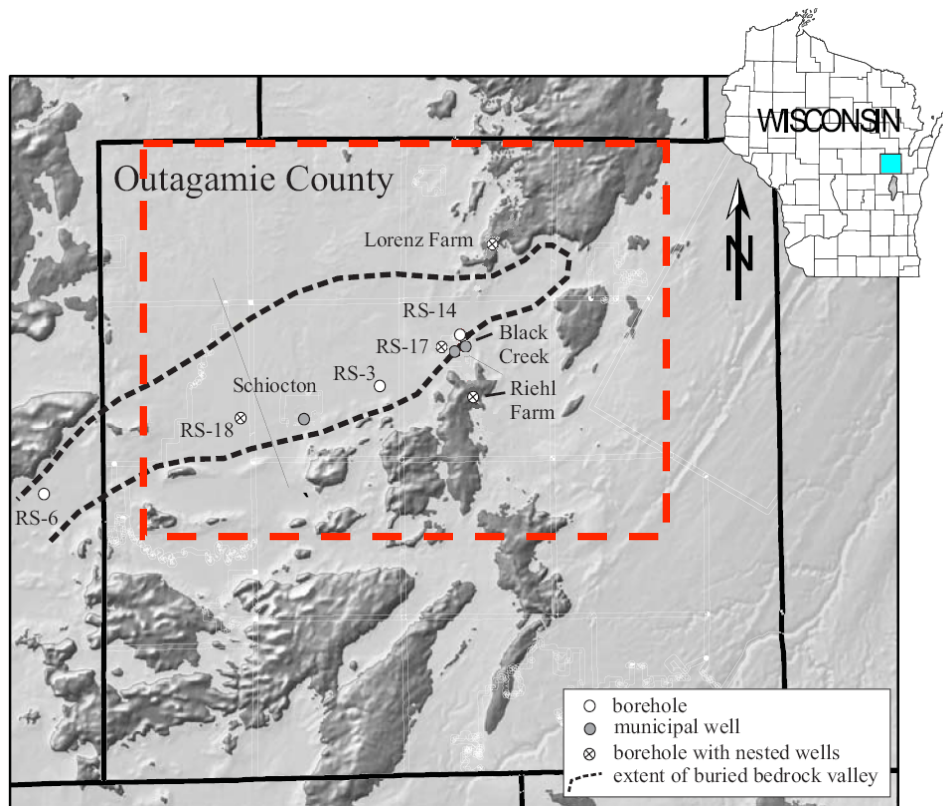


Figure 1. Shaded relief map of Outagamie County showing the lateral margins of the buried bedrock valley and locations of boreholes and wells drilled by the WGNHS. The dashed red box indicates the approximate location of the hydrostratigraphic and groundwater flow models. The light gray regions approximate the area covered by glacial Lake Oshkosh during the last glaciation. The inset shows the location of Outagamie County in WI. (modified from Hooyer *et al.*, 2008)

As part of this project, ERI was used at an additional eight sites, with geoprobe sampling at two of the sites confirming the geophysical interpretations. Then multiple-point geostatistics (Guardino & Srivastava, 1993) was used to create 300 three-dimensional hydrostratigraphic models for the representative site in Outagamie County, Wisconsin (Fig. 1), using as input data a combination of WCRs, electrical resistivity imaging, geoprobe sampling, and reasonable depositional histories determined from WCRs and five known outlets of glacial Lake Oshkosh. Multiple-point geostatistics uses training images, either 2-D or 3-D, that represent the general features of the subsurface (i.e., channels, lenses).

Training images have advantages over variograms, the more traditional geostatistical approach, because training images can include soft data, such as outcrops or geophysics, and can maintain geologic structure and continuity. All 300 hydrostratigraphic models were analyzed for statistics of connectivity using CONNEC3D (Pardo-Igúzquiza & Dowd, 2003) and a representative set of six hydrostratigraphic models was selected and imported into groundwater flow and transport models based on these analyses. The United States Geological Survey's (USGS) Modular Ground-Water Flow Model, MODFLOW-2000 (Harbaugh *et al.*, 2000), was used to simulate groundwater flow in the six selected hydrostratigraphic models. The groundwater flow models were calibrated to head data, the calibration was checked with streamflow measurements, and particle tracking was performed and compared to statistics of connectivity. In addition to delineating preferential flow paths in a glacially-deposited aquitard, objectives included demonstrating the use of multiple-point geostatistics, understanding the flow system in Outagamie County, and reviewing and revising the depositional history of glacial Lake Oshkosh.

PROCEDURES AND METHODS

The hydrostratigraphic models incorporated hard and soft data to represent the possible range of deposits in the subsurface. Hard data are generally geologic or hydrogeologic data at point locations, such as boring logs or hydraulic conductivity measurements, while soft data are generally non-point data and include geophysical logs, outcrop information, or knowledge of the depositional environment. Additionally, these data were used to interpret the provenance of the sand bodies. While glacial in origin, their provenance is unknown. They could be beach deposits, underflow/subaqueous fan type deposits, or perhaps both are present in different areas of the lacustrine sediments.

As described above, ERI was used at an additional 8 sites, with analysis of the imaging used to determine the average and range of sizes of the sand bodies. Several of the sites had more than one ERI transect performed, for a total of 14 ERI transects (See Appendix B and Fig. 2). Every transect had higher resistivity values at depth and three of the transects also had higher values at the surface, indicating the presence of sand (Fig. 2). Hand augering to a depth of 5 ft at both sites with higher surface resistivity values confirmed the presence of sand. The three transects with sand at the surface also had higher resistivity values than the other transects, indicating sand at these sites may be coarser. All of the ERI was done with 5 m (16.4 ft) spacing and a Wenner alpha array, and all transects were 115 m (~377 ft) in length, except for RS-18 transect 1b, which was 195 m (~640 ft). The inversions were performed with the RES2DINV software (Geotomo Software, Malaysia), using a standard Gauss-Newton inversion. The following parameters were used for the inversion process: initial damping factor of 0.160, minimum damping factor of 0.015, relative changes in root mean square (RMS) error for convergence of 5, minimum change in RMS error for line search of 0.4, and the maximum number of iterations was 20. Geoprobe sampling at two sites confirmed the geophysical interpretations, including coarser sand present at sites with higher resistivity values. See Appendix C for the core logs.

Present day elevations of 1,629 sand and gravel bodies were determined from WCR location data and digital elevation models (DEMs), with the use of ArcGIS software. Then using results from the Clark model (Clark *et al.*, 2007; Clark *et al.*, 2008) to account for rebound, the elevations of the sand and gravel bodies were compared to the five known outlets of glacial Lake Oshkosh (Fig. 3). The Clark model uses predictions of glacial isostasy and digital elevation data to determine the paleo-topography, and to create a paleo DEM. Extensions of the ArcGIS and GRASS (Geographic Resources Analysis Support System) software that determine drainage basins from DEMs were used to define the lake size and outlet. It is important to note that the predicted shorelines determined by the Clark model represent a minimum lake extent. Therefore, if the sand body elevations match up with those of the outlets or are higher than the outlet, this would indicate that the sand bodies are most likely beach deposits. If the sand body elevations are lower than the outlets, then the sand bodies are likely underflow deposits, although it should be noted that much lower sand bodies could be beach deposits from an earlier lake level. Analysis of the high K

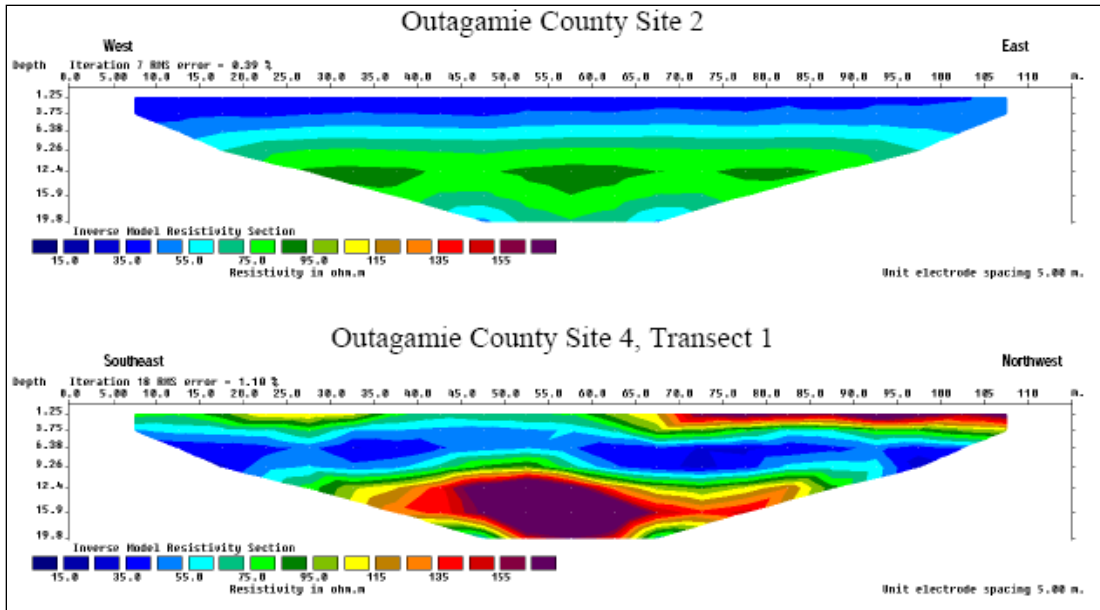


Figure 2. Electrical Resistivity Image for two of the additional sites: OU-2, located in the central western portion of the buried bedrock valley and OU-4, located in the northern central portion of the buried bedrock valley. Note the higher resistivity units at the surface at OU-4 and at depth at both sites, most likely sand. At OU-4 hand augering to a depth of 5 ft (1.5 m) confirmed sand in the near surface and geoprobe sampling to a depth of 55 ft (16.8 m) confirmed sand at depth. Units are in meters and ohm-meters.

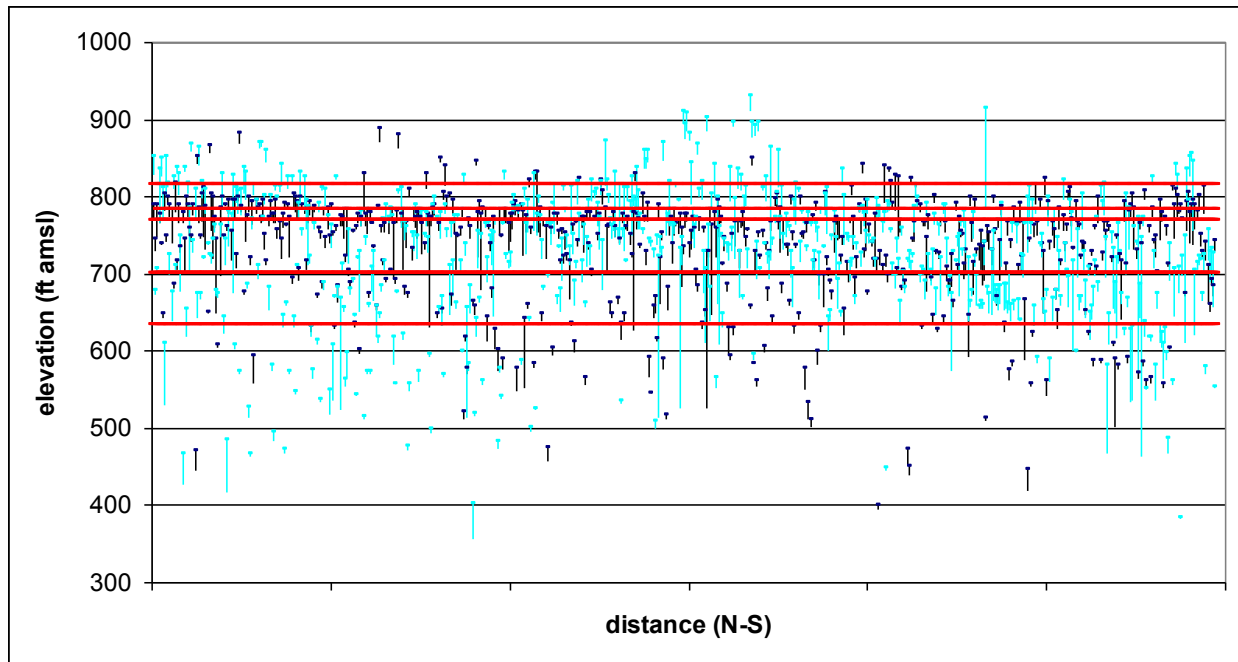


Figure 3. Comparison of the elevations of the sand (dark blue) and gravel (light blue) bodies to the elevations of the five known lake outlets (red). Note that the majority of the deposits below the lowest lake elevation are gravel, indicating underflow type deposits.

deposits (sand and gravel) indicates 10% of the total number of deposits are above the highest lake level (785 ft), while 26% are below the lowest lake level (636 ft). The majority of the deposits are less than 30 ft above the highest lake level, but a few may be dune deposits as they are nearly 100 ft above the highest

lake level. Overall, these analyses indicated the deposits are likely a combination of beach and underflow deposits. Additionally, the 3-D display of WCRs (Fig. 4) indicates there may be slightly more gravel to the east and deeper than the sand bodies, which suggests underflow or subaqueous fan type deposits.

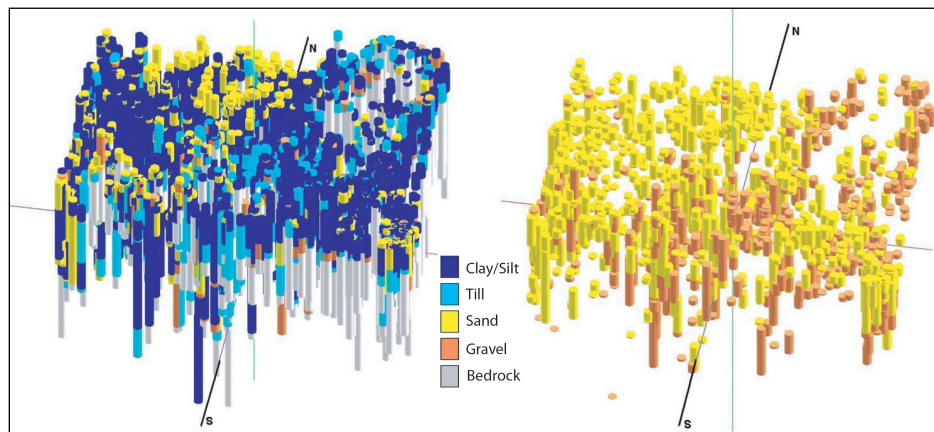


Figure 4. WCRs displayed in 3-D for the area shown in Fig. 1 (dashed red box). All units displayed on left, high K units only displayed on right (created in Rockworks, 2006).

The hard and soft data were used to create 300 hydrostratigraphic models using the Stanford Geostatistical Modeling Software (SGeMS) (Remy et al., 2009), which has the algorithm for multiple-point geostatistics and has a training image generator (TIGENERATOR). Multiple-point geostatistics, which was first suggested to model subsurface heterogeneity by Guardiano and Srivastava (1993), but not used much until the single normal equation simulation (snesim) algorithm was developed by Strebelle (2000, 2002), reducing the computation time. Multiple-point geostatistics uses one or more training images, which can be either 2-D or 3-D, to represent the general features of the subsurface (i.e., channels, lenses), rather than a variogram. Each node is then simulated by conditional probabilities based on the probability of occurrences of data events (patterns of a defined size) within the training image, hard data (if available), and previously simulated nodes. Thus, the training image must be scanned for each node, a computationally intensive procedure. The snesim algorithm reduces computation time by scanning the training image only once and saving the distributions of patterns in a search tree. Details of multiple-point geostatistics and the snesim algorithm can be found in the above cited papers as well as a review paper by Hu and Chugunova (2008). To create the 300 hydrostratigraphic models several steps had to be performed. First, a model grid was defined. Then 80 training images were created, with a subset of these selected for use in the snesim algorithm based on visual comparison with the 3-D WCR display (Fig. 4) and general geologic plausibility. Finally, hard data were imported and parameters were defined and analyzed during the running of the snesim algorithm. Details of the process are described in Appendix D.

All 300 hydrostratigraphic models were analyzed for connectivity statistics using CONNEC3D (Pardo-Igúzquiza & Dowd, 2003), which calculates a number of connectivity statistics and writes these to several output files (see Appendix E for more details). Statistics from all 300 models were imported into an Excel file and analyzed. Of the 300 models, 240 have statistically and geologically acceptable parameters (see Appendix D for more details) and were considered in the selection process for a representative set of models that were imported into groundwater flow models. Selection of the six representative models was based on analyses of the connectivity statistics, especially three connectivity statistics with more variability than the others. Details of the model selection are in Appendix F.

The USGS Modular Ground-Water Flow Model, MODFLOW-2000 (Harbaugh *et al.*, 2000), was used to simulate groundwater flow in the six selected hydrostratigraphic models. This code was chosen because of its capabilities to simulate three-dimensional groundwater flow in steady-state and incorporate the

hydrostratigraphic model data. The pre- and post-processor Groundwater Vistas (GWV) Version 6.15 (Rumbaugh & Rumbaugh, 2012) was used to set up and run the models. The code PEST (Doherty, 2004), which is a parameter estimation routine, was used to calibrate the models. The modular three-dimensional multispecies transport model, MT3DMS, (Zheng & Wang, 1999) was used to model $\delta^{18}\text{O}$ movement in the calibrated groundwater flow models to determine if the anomalous recent water found at depth (Hooyer *et al.*, 2008) could be explained by preferential flow paths. The particle tracking code MODPATH (Pollock, 1994) was used to determine groundwater flow pathways through the glacial Lake Oshkosh sediments, particularly in the deepest parts of the buried bedrock valley. The MODFLOW models were solved using the PCG2 solver (Hill, 1990), which uses both head change and mass-balance as convergence criteria. Details of the groundwater flow and transport models are in Appendix G.

RESULTS AND DISCUSSION

Connectivity statistics had one or more percolating paths (a single connected component that connects from one end to the other in a specific direction) in the z-direction for every hydrostratigraphic model, indicating preferential flow is likely occurring vertically through the glacial sediments. Particle tracking results confirmed this. One particle was placed at the top of each cell in the approximate horizontal extent of the bedrock valley of layer 2 and tracked forward in time, for a total of 2,108 particles. Every model had particles exit in the deeper regions of the bedrock valley (layers 60-83). Also, every model had 42-58% of the total particles exit in the first layer. The percent of particles to exit the constant head boundary in layers 40-83 after traveling at least halfway through the valley vertically varied from 10-18%. Only a small percent (0.33-1.66%) of particles moved vertically into the deepest portions of the bedrock valley (layer 60-83) before exiting (Fig. 5). There also was vertical movement in shallower areas of the valley, often through clay (Fig. 6).

Particles were also placed in every non-boundary cell at the top of layer 2 of the model and tracked forward in time. Results were analyzed for total travel time to a bedrock head boundary. In order to do this, all particles exiting the model at a non-bedrock boundary were removed from the analysis. Among all six models, a total of 25,906 particles traveled through the glacial sediment in the bedrock valley and exited into the bedrock. Results confirmed that flow is largely vertical, with a maximum horizontal particle movement of 11 cells and only 5.2% of the total particles moving horizontally. Results indicated that preferential flow may be occurring, as 6.77% of the particles take fewer than 100 years to move to the bedrock. Percents for eight different time periods are displayed in Figure 7. Since the majority of the particles take between 100 and 10,000 years to move through the model, the small percent moving faster may be indicative of preferential flow. Previous isotope measurements, in particular $\delta^{18}\text{O}$, found anomalous recent water at depth (Hooyer *et al.*, 2008). Preferential flow paths could explain these measurements, but with the majority of particles moving through the valley in fewer than 10,000 years, glacial age water would be largely flushed out of the valley deposits. However, approximately 28% of the simulated isotope values from the MT3DMS simulations (Appendix G) are glacial age values. This discrepancy is likely due to the majority of the particles either moving through the shallower regions of the bedrock valley or through preferential flow paths in the deeper regions of the bedrock valley. There could be additional factors contributing to the overall particle travel times being too fast for glacial age water to remain in the lacustrine deposits, including: the lateral and bottom boundary conditions, lack of understanding recharge in the system, cell size too large, clay K too high, or perhaps there should be more preferential pathways with less overall vertical flow in the clay matrix.

Additional evidence for preferential flow was provided by running a model with a uniform value of K equal to the volumetrically weighted mean K and analyzing travel times for particles placed in every non-boundary cell of layer 2. Compared to the statistics for the six hydrostratigraphic models, travel times are much more uniform, with 90% of particles taking 100-1,000 years. Visual analysis of particles confirms all particles are moving at the same rate.

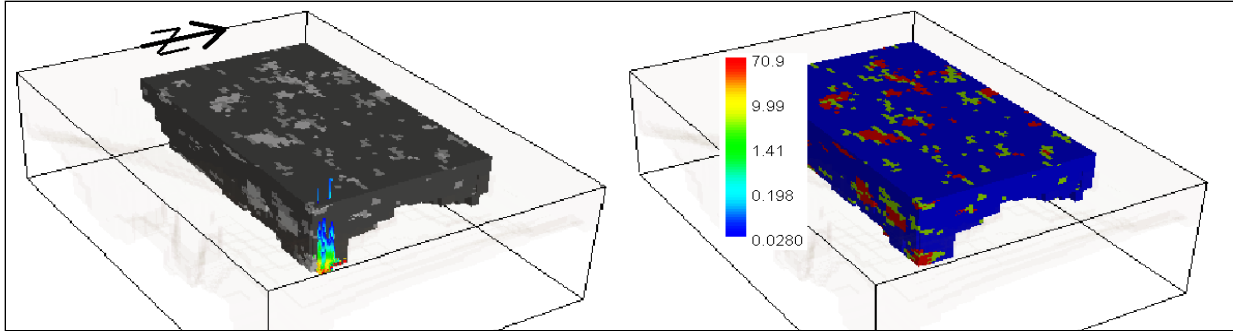


Figure 5. Examples of particle tracking shown as pathways in deeper areas of the bedrock valley for model 10_7. The particles are shown on the left, with blue indicating earlier times, yellow and red later. All particles shown moved through the valley in 1,000 years or less. North is indicated on the particle diagram. The same region is shown on the right, with K values (ft/d) indicating the fine-grained glacial are blue, with coarser deposits yellow and red. 50x vertical exaggeration.

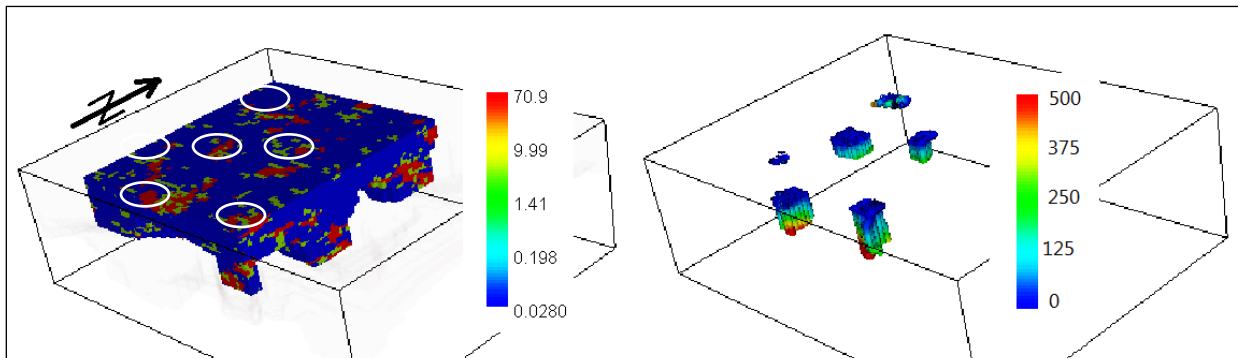


Figure 6 Examples of particle tracking shown as pathways in shallower areas of the bedrock valley for model 10_7. On the left, K values (ft/d) indicate the fine-grained glacial deposits are blue, with coarser deposits yellow and red. On the right, particles tracks are displayed by time in years. North is indicated on the K value image. White ovals on the K figure indicate approximate locations of particle clusters. Note that comparing these two indicates the higher K units are allowing faster movement of particles. 50x vertical exaggeration.

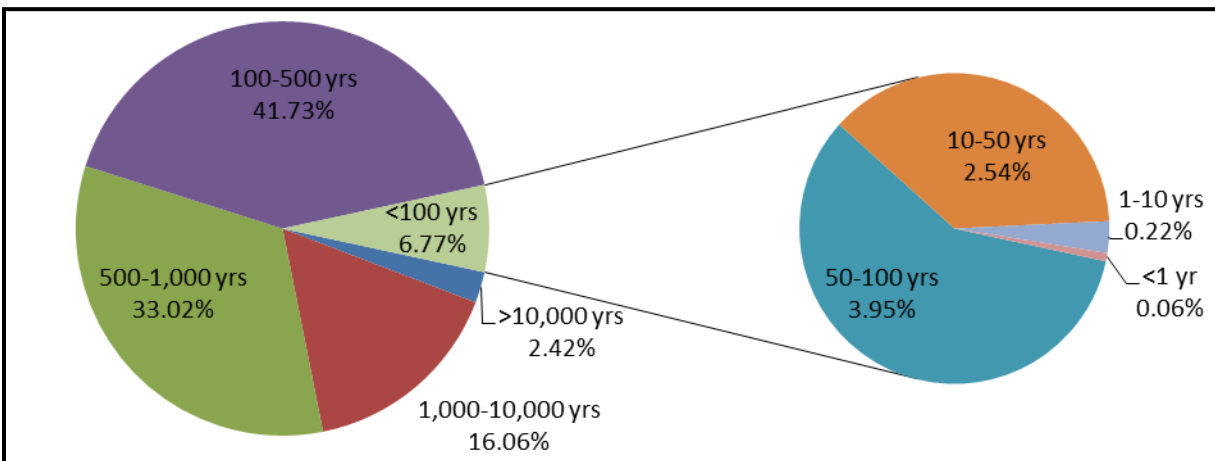


Figure 7. Pie chart of percent of particles taking a given length of time to move through the glacial sediments and into the surrounding bedrock. The chart on the right breaks down the travel times for particles taking fewer than 100 years. Results are combined for all six models.

In addition to the particle travel times and isotope evidence for preferential flow, individual flow paths can be traced vertically through the valley in all six models (Table 1). As an example, in model 10_7 two

particles, 62 and 94 are 1.3 miles apart in layer 2 and both exit into the bedrock in layer 44. However, particle 62 takes 3,425 years, while particle 94 takes only 96 years. Examination of the hydrostratigraphy indicates that particle 62 moves vertically through clay 3,311 of these years, before finding a high K unit and eventually exiting the valley, while particle 94 is in a high K unit for most of its pathway.

Table 1. Examples of preferential flow through comparison of individual particles. Starting and ending separation is the distance between particles at their starting and ending locations. All particles start in layer 2. Lithology is described in percent by cells traveled through, with only the dominant lithology listed as a percent.

Model	Particle #	Starting Separation (mi)	Exiting Layer	Ending Separation (mi)	Travel Time (yrs)	Lithology
10_7	94	1.3	44	0	96	92.9 % sand/gravel (clay at surface)
10_7	62				3,425	97.6% clay (gravel at depth)
18_7	3153	2.9	82	2.4	2,487	61.9% clay (sand interspersing)
18_7	3454				32,247	100% clay
18_7	5753	1.3	33	0.3	4	100% sand
18_7	6049				2,129	56.3% clay (sand at depth)
19_8	2509	0.5	23	0.5	62	100% sand
19_8	2510				235	81.8% sand (clay at surface)
19_8	2511				500	100% clay
22_6	5173	1.2	29	1.1	46	92.9% sand/gravel (clay at depth)
22_6	4686				1,627	92.9% clay (sand at surface)
25_9	4243	0.9	33	0.9	10	100% sand/gravel
25_9	4630				1,036	100% clay
29_4	190	0.45	19	0.45	3	64.7% sand/gravel (clay interspersing)
29_4	188				232	100% clay

CONCLUSIONS AND RECOMMENDATIONS

This is one of the first examples demonstrating the application of multiple-point geostatistics in three-dimensions to a field site using a variety of field data, including geophysics. Previous work either used synthetic data (Feyen & Caers, 2005; Liu, 2006; Michael *et al.*, 2010), was used in mining applications and incorporated traditional geostatistics into the training images (Bastante *et al.*, 2008), was used to model at the pore scale (Lu *et al.*, 2009), only modeled in two-dimensions (Huysmans & Dassargues, 2009), or focused on combining multiple-point simulations with other types of data and models (Michael *et al.*, 2010).

Preferential flow is likely occurring in glacial Lake Oshkosh sediment as indicated by the analysis of the connectivity statistics for the hydrostratigraphic models and results of the particle tracking. All 300 hydrostratigraphic models had one or more percolating components in the z-direction. Also, the particle tracking indicated that for all six groundwater flow models, over 6% of the particles were moving through the bedrock valley in fewer than 100 years; examples of particles moving faster through high K units were found in each model. Additionally, this work demonstrates that preferential flow can occur in a

glacially-deposited aquitard through connected sand bodies without the presence of fractures, and is likely occurring in similar types of deposits, especially those that are more fractured, such as clayey tills. Overall, results of the statistics of connectivity and particle tracking indicate that a hydrostratigraphic model with fewer, longer pathways or one with many shorter pathways can create preferential flow paths and can calibrate to head and streamflow data. Additionally, the origin of the sand and gravel deposits is most likely a combination of beach and underflow deposits as demonstrated by the WCR data.

Based on the calibrations to the head targets and check on the calibration with the stream fluxes, the six models are all equally likely representations of the sediments. However, the groundwater flow models should be better calibrated in order to use them for purposes of groundwater management in Outagamie County. This will require a joint calibration of groundwater flow and transport models (with oxygen isotope data) as well as collection of additional head, stream flux, and isotope targets.

REFERENCES

- Bastante, F.G., Ordóñez, C., Taboada, J., and Matias, J.M., 2008. Comparison of indicator kriging, conditional indicator simulation and multiple-point statistics used to model slate deposits. *Engineering Geology*, vol. 98, p. 50-59.
- Cherry, J.A., Parker, B.L., Bradbury, K.R., Eaton, T.T., Gotkowitz, M.G., Hart, D.J., and Borchardt, M. 2006. Contaminant Transport through Aquitards: A State-of-the-Science Review. Denver, Colorado: American Water Works Association Research Foundation.
- Clark, James A., Zylstra, Deborah J., and Befus, Kevin M., 2007. Effects of Great Lakes Water Loading upon Glacial Isostatic Adjustment and Lake History. *Journal of Great Lakes Resources*, vol. 33. p. 627-641.
- Clark, James A., Befus, Kevin M., Hooyer, Thomas S., Stewart, Peter W., Shipman, Taylor D., Gregory, Chris T., and Zylstra, Deborah J., 2008. Numerical simulation of the paleohydrology of glacial Lake Oshkosh, eastern Wisconsin, USA. *Quaternary Research*, vol. 69, p. 117-129.
- Doherty, J. 2004. PEST, Model-Independent Parameter Estimation: Watermark Numerical Computing.
- Feyen, L. and Caers, J., 2005. Multiple-point geostatistics; a powerful tool to improve groundwater flow and transport predictions in multi-modal formations. Proceedings-European Conference on Geostatistics for Environmental Applications, vol. 5, p. 197-207.
- Gerber, Richard E., Boyce, Joseph I., and Howard, Ken W.F. 2001. Evaluation of heterogeneity and field-scale groundwater flow regime in a leaky till aquitard. *Hydrogeology Journal*. Vol. 9, p. 60-78.
- Grisak, G.E. and Cherry, J.A., 1975. Hydrologic characteristics and response of fractured till and clay confining a shallow aquifer. *Canadian Geotechnical Journal*, vol. 12, p. 23-43.
- Guardiano, F. and Srivastava, M. 1993. Multivariate geostatistics: Beyond bivariate moments, in *Geostatistics Troia '92*, ed. A. Soares. P. 133-144.
- Harbaugh, A.W., Banta, E.R., Hill, M.C., and McDonald, M.G. 2000. MODFLOW-2000, The U.S. Geological Survey modular ground-water model- user guide to modularization concepts and the ground-water flow process. U.S. Geological Survey Open-File Report 00-92.
- Hill, M.C. 1990. Preconditioned Conjugate-Gradient 2, A Computer Program for Solving Ground-Water Flow Equations: U.S. Geological Survey, Water-Resources Investigations Report 90-4048.

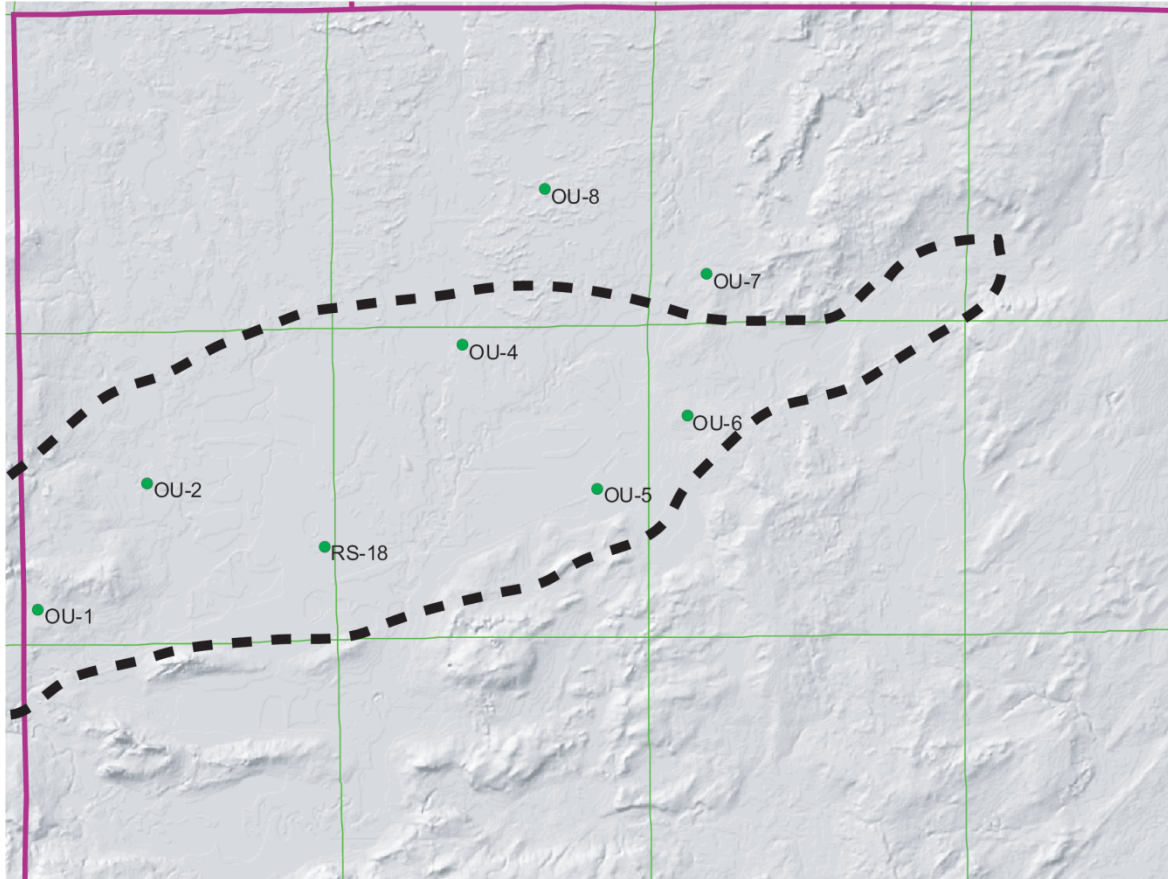
- Hooyer, T.S., Hart, D.J., Bradbury, K.R., and Batten, W.G., 2008. Investigating groundwater recharge to the Cambrian-Ordovician Aquifer through fine-grained glacial deposits in the Fox River Valley: Final Report to the Wisconsin Department of Natural Resources.
- Hu, L.Y. and Chugunova, T., 2008. Multiple-point geostatistics for modeling subsurface heterogeneity: A comprehensive review. *Water Resources Research*, vol. 44, W11413.
- Huysmans, Marijke and Dassargues, Alain, 2009. Application of multiple-point geostatistics on modelling groundwater flow and transport in a cross-bedded aquifer (Belgium). *Hydrogeology Journal*, vol. 17, p. 1901-1911.
- Liu, Yuhong, 2006. Using the *Snesim* program for multiple-point statistical simulation. *Computers & Geosciences*, vol. 32, p. 1544-1563.
- Lu, DeTang, Zhang, Ting, Yang, JiaQing, Li, DaoLun, and Kong, XiangYan, 2009. An Improved Reconstruction Method for Porous Media Based on Multiple-point Geostatistics. *Chinese Science Bulletin*, vol. 54, no.11, p 1876-1885.
- Michael, H.A., Li, H., Boucher, A., Sun, T., Caers, J., and Gorelick, S.M., 2010. Combining geologic-process models and geostatistics for conditional simulation of 3-D surface heterogeneity. *Water Resources Research*, vol. 46, W05527, 20 pages.
- Pardo-Igúzquiza, Eulogio and Dowd, Peter A., 2003. CONNEC3D: a computer program for connectivity analysis of 3D random set models. *Computers and Geosciences*, vol. 29, p. 775-785.
- Perry, E.C. Jr., Grundl, T., and Gilkeson, R.H., 1982. H, O, and S isotopic study of the groundwater in the Cambrian-Ordovician aquifer system of northern Illinois. In: Perry, E.C. Jr. and Montgomery, C.W., Eds. *Isotopic Studies of Hydrologic Processes*. Northern Illinois Univ. Press, p. 35-43.
- Pollock, D.W. 1994. User's Guide for MODPATH/MODPATH-PLOT, Version 3: A particle tracking post-processing package for MODFLOW, the U.S. Geological Survey finite-difference groundwater flow model: U.S. Geological Survey, Open-File Report 94-464.
- Remy, Nicolas, Boucher, Alexandre, and Wu, Jianbing, 2009. *Applied geostatistics with SGeMS; a user's guide*, Cambridge University Press, New York, 110 p.
- Rumbaugh, J. O., and Rumbaugh, D. B. 2007. *Groundwater Vistas*, version 5. Environmental Solutions Inc., Reinholds, PA, www.groundwatermodels.com.
- Siegel, D.I. and Mandle, R.J., 1984. Isotopic Evidence for Glacial Meltwater Recharge to the Cambrian-Ordovician Aquifer, North-Central United States. *Quaternary Research*, vol. 22, p. 328-335.
- Strebelle, 2000. *Sequential simulation drawing structures from training images*: Ph.D. diss., Stanford.
- Strebelle, 2002. Conditional simulation of complex geological structures using multiple-point statistics. *Mathematical Geology*, vol. 34, no. 1, p 1-21.
- Zheng, Chunmiao and Wang, P. Patrick, 1999. *MT3DMS: A Modular Three-Dimensional Multispecies Transport Model for Simulation of Advection, Dispersion, and Chemical Reactions of Contaminants in Groundwater Systems; Documentation and User's Guide*; U.S. Army Engineer Research and Development Center Contract Report SERDP-99-1, Vicksburg, Mississippi, 202 p.

APPENDIX A: Awards, Presentations, Reports, Patents and Presentations

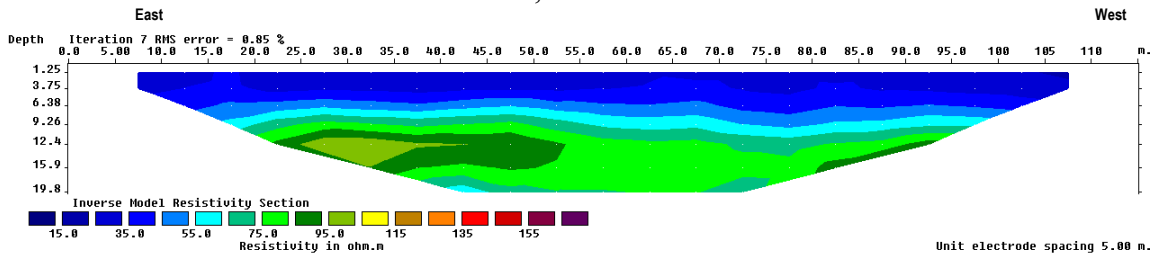
- 1) Dunkle, K.M., Hart, D.J., and Anderson, M.P., 2013. Groundwater flow model calibration difficulties in areas with glacially-deposited aquitards: An example from glacial Lake Oshkosh, Geological Society of America *Abstracts with Programs*, vol. 45, no. 4, p. 53.
Presented: May 3, 2013 in Kalamazoo, Michigan
- 2) Dunkle, K.M., Hart, D.J., and Anderson, M.P., 2012. Preferential flow paths in glacial Lake Oshkosh sediment, Outagamie County, WI, Geological Society of America *Abstracts with Programs*, vol. 44, no. 7, p. 145.
Presented: November 4, 2012 in Charlotte, North Carolina
- 3) Dunkle, K.M., Hart, D.J., and Anderson, M.P., 2011. Hydrostratigraphic & groundwater flow models for glacial Lake Oshkosh sediment, Outagamie County, WI, Geological Society of America *Abstracts with Programs*, vol. 43, no. 5, p.560.
Presented: October 12, 2011 in Minneapolis, Minnesota
- 4) Dunkle, K.M., Hart, D.J., and Anderson, M.P., 2011. Multiple-point geostatistics for creation of 3D hydrostratigraphic models, Outagamie County, WI, Three Dimensional Geological Mapping: Workshop Extended Abstracts, Geological Survey of Canada, Open File 6998.
Presented: October 8, 2011 in Minneapolis, Minnesota

APPENDIX B: Electrical Resistivity Imaging

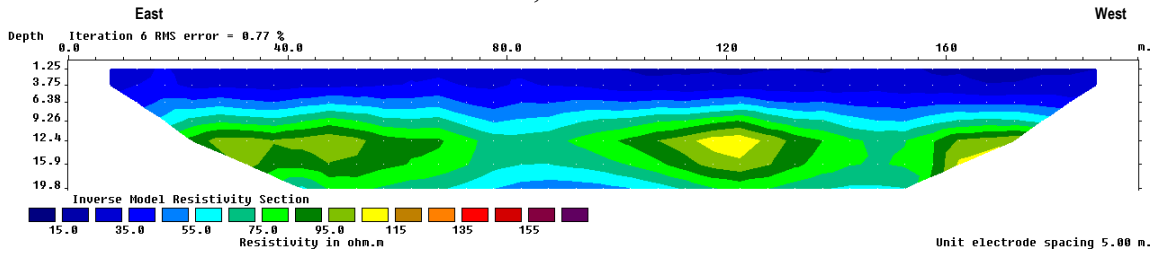
Location of Electrical Resistivity Imaging sites in modeling area (Fig. 1: dashed red box). Dashed line is approximate extent of pre-glacial buried bedrock valley. Pale green lines outline the townships, which are 6 x 6 miles.



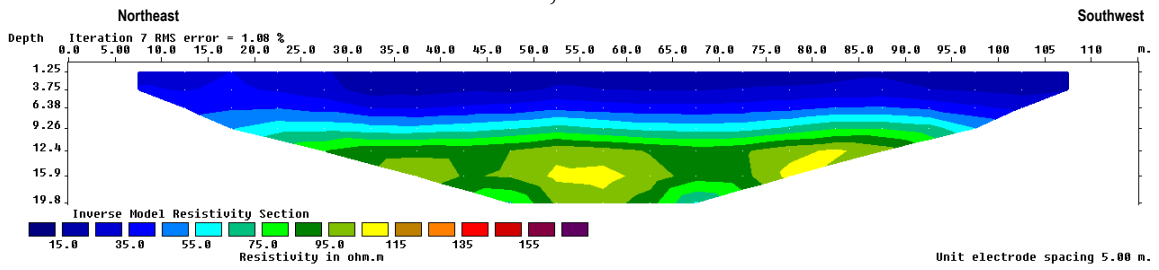
RS-18, Transect 1a*



RS-18, Transect 1b*

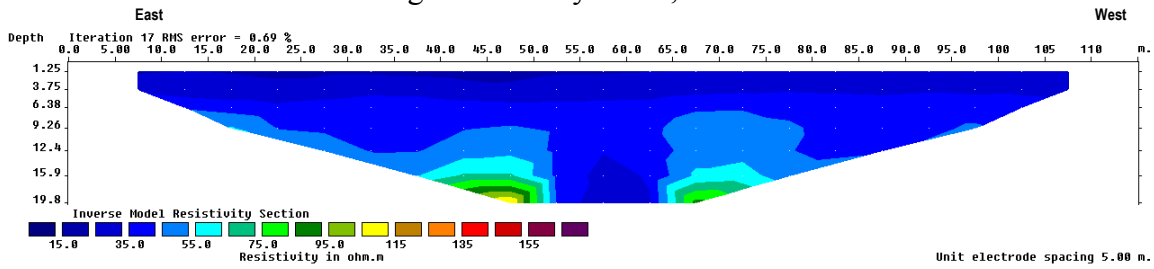


RS-18, Transect 2

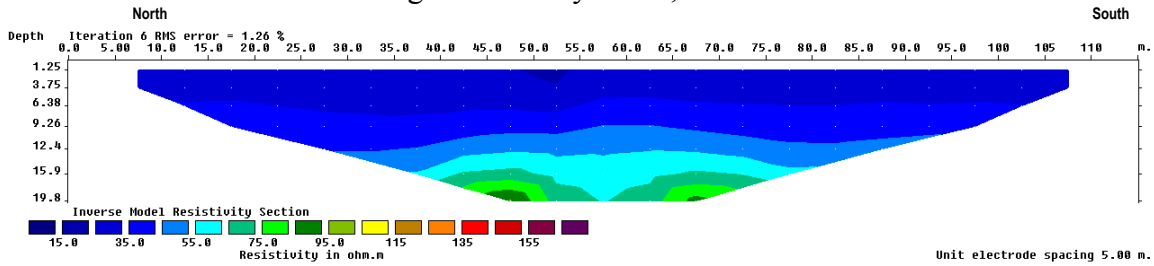


*Note that transects 1a and 1b have the same starting location and direction.

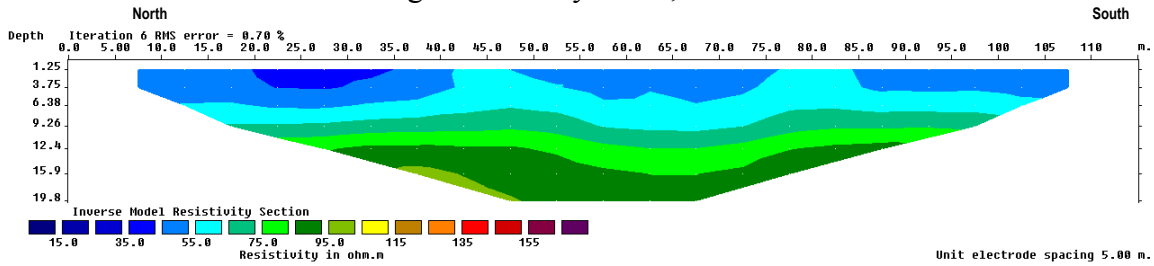
Outagamie County Site 1, Transect 1



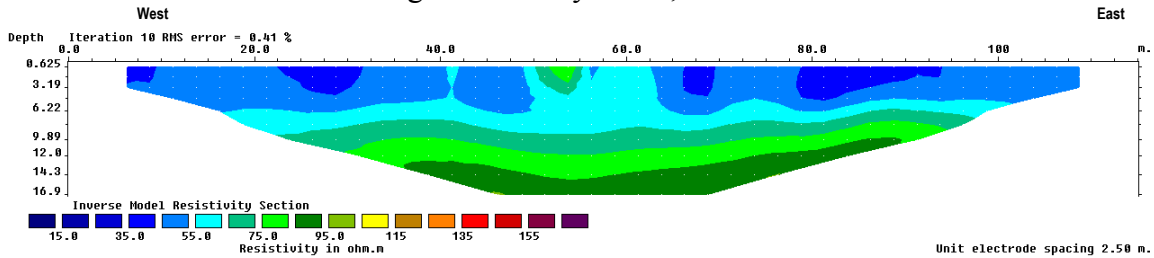
Outagamie County Site 1, Transect 2



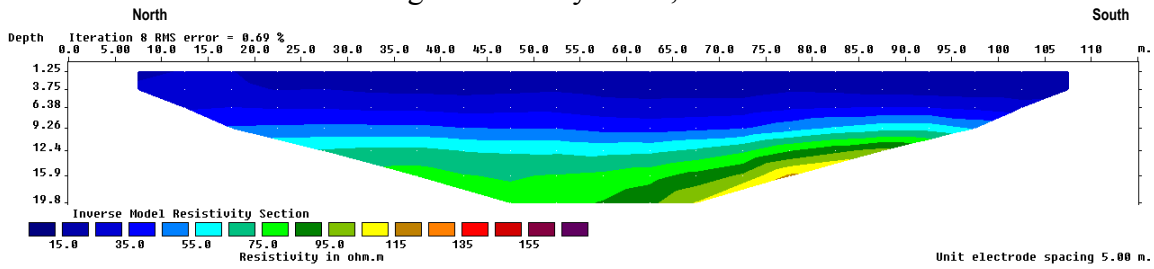
Outagamie County Site 6, Transect 1



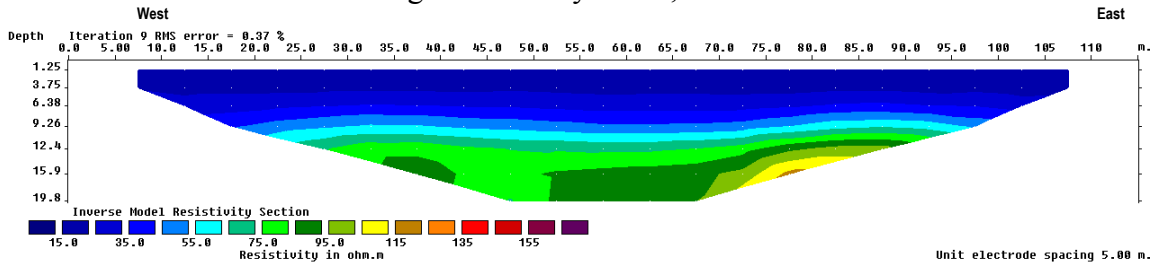
Outagamie County Site 6, Transect 2



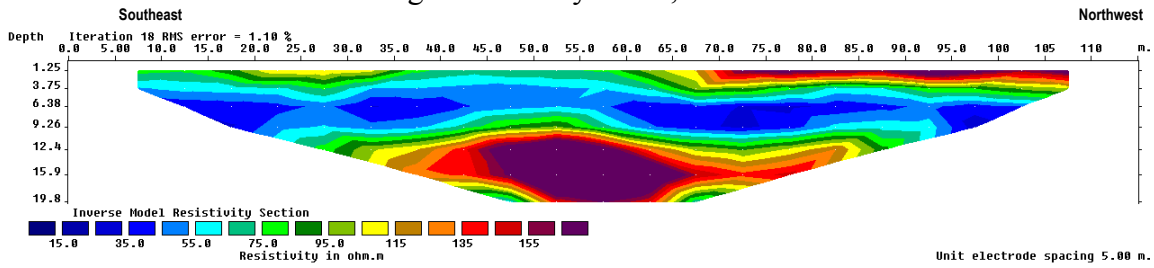
Outagamie County Site 7, Transect 1



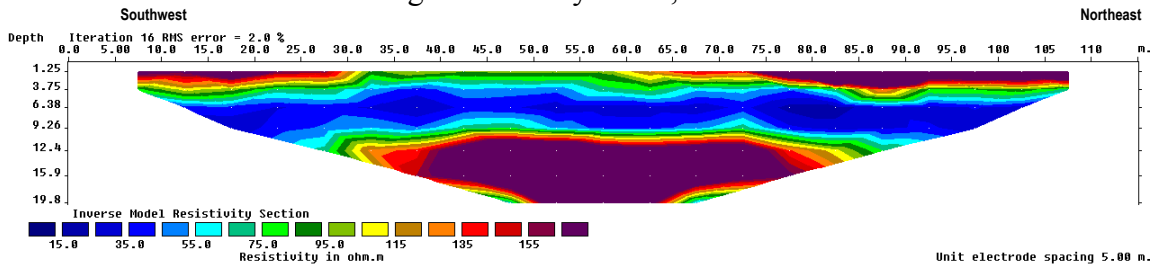
Outagamie County Site 7, Transect 2

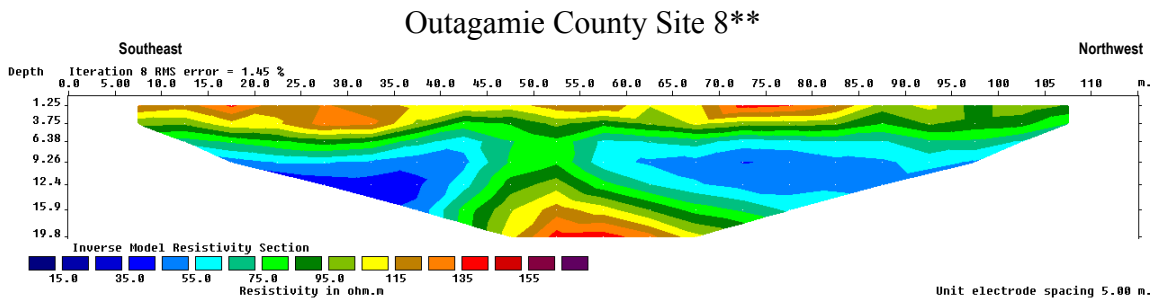
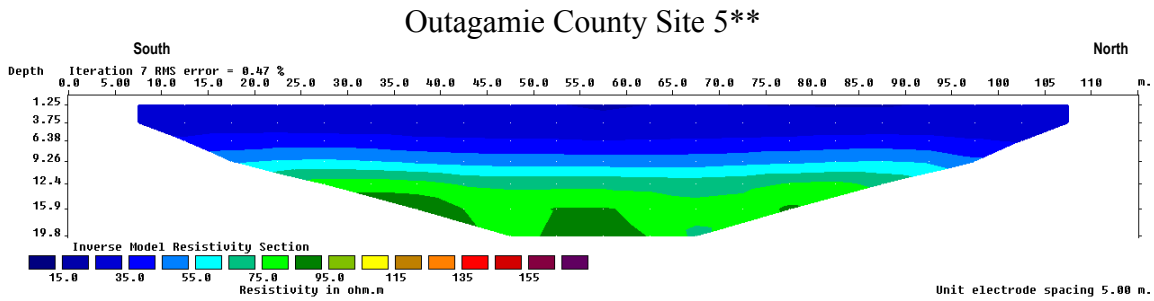
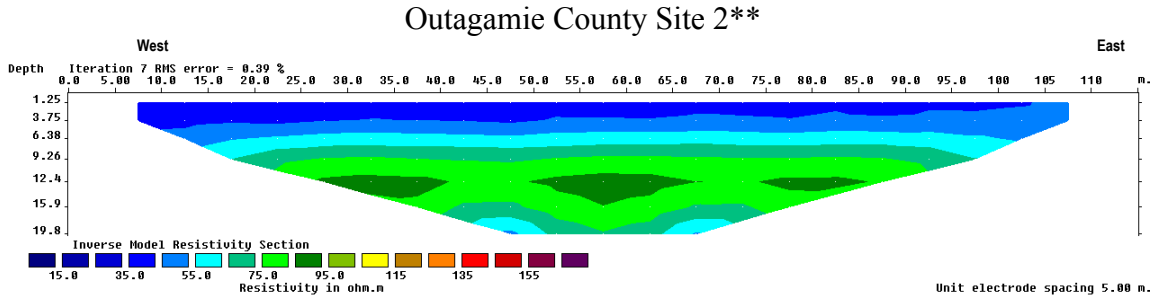


Outagamie County Site 4, Transect 1



Outagamie County Site 4, Transect 2





**Only one transect done at each of these sites due to various field settings:
 OU-2: road and railroad at this location
 OU-5: stream running through the property
 OU-8: frozen/partially frozen ponds through woods; note hand augering confirmed sand in the near surface

APPENDIX C: Geoprobe Logs

Note sampling done in 5 ft increments for all cores.

RS-18 Core #1

Depth (ft)	Description
0-5	40% recovery, all at bottom of sleeve
3-3.3	Gasket
3.3-3.6	Very fine sand, dark matter (organics?), abrupt contact at 3.6 ft
3.6-5	Fine to very fine sand, well to very well rounded, laminations (dark); from 4.05-4.3 ft, soft, little clayey
5-10	100% recovery, lots of water in the bottom
5-6	Fine to very fine sand with dark spots
6-7.5	Fine to very fine sand
7.5-8.2	Transition
8.2-10	Clay with fine sand; sticky clay layer from 9.25-9.35 ft
10-15	100% recovery
10-12.7	Clay with fine sand
12.7-15	Clay, sticky; few black organics at end (possibly sluff)
15-20	96% recovery, missing bottom
15-15.9	Clay with fine sand (less sand than above)
15.9-19.8	Clay, sticky
20-25	100% recovery
20-21.05	Clay with fine sand; abrupt contact at 21.05 ft
21.05-25	Clay, sticky
25-30	100% recovery
25-26.05	Clay with varves; few dark spots 25.45-25.9 ft (organics or mineral core?)
26.05-28.7	Clay with lower fine to very fine sand; harder than sticky clay
28.7-30	Clay, sticky
30-35	100% recovery
30-35	Clay, sticky with few varves
35-40	100% recovery
35-37.05	Clay, sticky, abrupt contact at 37.05
37.05-37.32	Upper fine to lower medium sand with organics; microscope examination indicated mostly quartz (~90%), with few dark fragments
37.32-40	Upper fine to lower medium sand; some patches upper medium
40-45	92% recovery, bottom is sluff
40-44.6	Upper fine to medium sand; lamination at 42.25 ft
45-50	100% recovery
45-48.05	Sandy-clay, coarsens downward from fine to upper fine; clay laminations/layers from 45.8-46.05 ft
48.05-50	Upper fine to lower medium sand

RS-18 Core #1-continued

Depth (ft)	Description
50-55	100% recovery; maybe some sluff on top
50-50.6	Upper fine to lower medium sand; abrupt contact at 50.6 ft; microscope examination indicated mostly quartz (~90%), with few dark fragments
50.6-51.2	Fine grained sandy discolorations
51.2-54.2	Sand clay/clayey sand; slowly coarsening upward
54.2-54.65	Clay (darker color) with sand (lighter color) laminations
54.65-55	Clay with fine sand

RS-18 Core #2

Depth (ft)	Description
0-30	No sample taken.....geoprobe pushed through to only sample sand transition
30-35	88% recovery
30.1-32.84	Clay, sticky; abrupt contact at 32.84 ft
32.84-34.32	Upper fine to lower medium sand (mostly lower)
34.32-35	Mostly missing, upper fine to lower medium sand on edges; microscope examination indicated mostly quartz (~90%), with few dark fragments
35-40	100% recovery
35-40	Upper fine to lower medium sand; few dark spots (organics/minerals); saturated; microscope examination indicated mostly quartz (~90%), with few dark fragments
40-45	100% recovery
40-41.11	Upper fine to medium sand; more fine than above
41.11-41.8	Upper fine to medium sand; more gray than brown; maybe some clay
41.8-43.1	Fine sand
43.1-43.4	Fine sand with clay; harder; orange in color
43.4-45	Fine sand
45-50	100% recovery
45-47.4	Fine sand; few dark spots; microscope examination indicated mostly quartz (~90%), with few dark fragments
47.4-48.6	Fine sandy clay
48.6-50	Fine sandy clay; more clay content than above; sticky clay interspersed

RS-18 Core #3

Depth (ft)	Description
0-30	No sample taken.....geoprobe pushed through to only sample sand transition
30-35	96% recovery
30.2-35	Clay, sticky
35-40	100% recovery
35-36.51	Clay, sticky; abrupt contact at 36.51 ft
36.51-36.78	Fine sand; very dark
36.78-38.4	Fine to lower medium sand with clay skins
38.4-40	Fine to lower medium sand; microscope examination indicated mostly quartz (~90%), with few dark fragments
40-45	100% recovery

40-45	Fine to lower medium sand; darker spots from 40-41.6 ft
45-50	100% recovery
45-46.85	Fine to lower medium sand (maybe some upper medium)
46.85-48.18	Fine to medium sand; darker brown color
48.18-49.5	Fine sandy clay
49.5-50	Clay, hard, with some fine sand (less than above)

OU-4 Core #1

Depth (ft)	Description
0-5	54% recovery
2.3-3	Dark, clayey topsoil
3-5	Very fine to fine sand, occasional organics (roots)
5-10	66% recovery
6-6.6	Very fine to fine sand, occasional organics (roots)
6.6-7.5	Fine sand, transitioning to medium sand
7.5-9.3	Medium sand, clean; mostly quartz
10-15	100% recovery
10-11.5	Fine to medium sand
11.5-12.5	Medium sand
12.5-13	Fine sand
13-13.5	Clayey fine sand
13.5-15	Clay with silt or very fine sand; sticky; ribbons poorly
15-20	76% recovery
16-16.6	Clay with silt or very fine sand
16.6-19.8	Clay, sticky, gray-brown, some brown zoning
20-25	96% recovery
20-20.5	Clay with fine sand
20.5-23	Clay, sticky, gray-brown
23-24.8	Clay, sticky, transitioning to reddish-brown
25-30	98% recovery
25-29.9	Clay, sticky, with laminations/layers of clay with trace very fine sand; Clay with sand found from 25-25.4 ft, 24.9-25 ft, 27.1-27.3 ft, and 28.7-28.9 ft
30-35	0% recovery; sleeve stuck in pipe
	Sand at bottom of plug (probably medium); appeared to be all sand falling out of sleeve

OU-4 Core #2

Depth (ft)	Description
0-5	72% recovery
1.4-2.1	Dark topsoil
2.1-2.9	Very fine to fine sand
2.9-5	Transitions to medium sand; some fine, dark laminations with slight yellow to red changes
5-10	100% recovery
5-5.4	Fine to medium sand; few organics (possibly sluff)
5.4-9.2	Medium sand, clean
9.2-10	Clay with trace very fine sand
10-15	98% recovery
10-10.7	Fine to medium sand
10.7-12	Medium sand
12-14.9	Clay with silt or very fine sand
15-20	98% recovery
15-17.4	Clay with silt; ribbons poorly
17.4-19.9	Clay, sticky, buff brown with some reddish-brown zoning
20-25	98% recovery
25-29.9	Clay, sticky; some brown/reddish-brown color zonation and possible laminations visible
25-30	98% recovery
25-25.9	Clay with very fine sand
25.9-26.2	Clay, sticky, with brown/reddish-brown color zonation
26.2-26.7	Clay with silt or very fine sand
26.7-29.4	Clay, sticky, with brown/reddish-brown color zonation
30-35	68% recovery
31.6-32.1	Fine to medium sand
32.1-35	Medium sand, clean, quartz; darker sand from 34-35 ft
35-40	90% recovery; sleeve stuck so lost some off both ends
35.4-39.9	Medium sand, some dark spots (organics?); 15mm diameter Limestone Pebble at 39 ft
40-45	34% recovery; sleeve stuck so only grab sample from bottom
43.3-45	Medium sand
45-50	68% recovery; sleeve stuck so lost some off both ends
46.5-47.2	Clay with very fine sand (sluff?)
47.2-48	Fine to medium sand
48-49.9	Fine sand with clay
50-53	100% recovery; note only drilled to 53 ft
50-51.2	Clay with silt or very fine sand
51.2-52.8	Fine sand or silt with clay
52.8-53	Clay, sticky, brown

APPENDIX D: Hydrostratigraphic Model Design

To create the hydrostratigraphic models several steps had to be performed. First, a model grid was defined. Then 80 training images were created, with a subset of these selected for use in the *snesim* algorithm. Finally, hard data were imported and parameters were defined and analyzed during the running of the *snesim* algorithm. Details of this process are described in the following sections.

Model Grid and Layers

The size of the area in Outagamie County to be modeled (Fig. 1) is approximately 22.5 miles (E-W) by 16 miles (N-S). The size of the grid was based on data from the WCRs and ERI. The horizontal spacing was chosen to be 1200 x 1200 ft, in order to allow for small enough grid spacing to account for horizontal sand body lengths identified from the ERI and to keep the hydrostratigraphic model from being too large and thereby increasing computational time. Since sand was present along the entire length of each of the ERI transects, ranging from approximately 375 to 650 ft, with no indication of pinching out near the ends of the transect, it can be assumed that a slightly larger grid spacing is an approximate minimum size for the sand bodies. The vertical spacing was chosen to be 5 ft because the mode thickness from the WCR analysis for the high K units was 10 ft, allowing for units to be thinner than the mode. The model grid has 99 cells in the x-direction (E-W), 71 cells in the y-direction (N-S), and 160 layers, for a total of just over 1.1 million nodes.

Training Image Creation & Selection

SGeMS TIGENERATOR was used to create 80 training images, of which 12 were selected for use in the creation of the hydrostratigraphic models with the *snesim* algorithm. The TIGENERATOR generates shapes to represent the pattern distribution of a depositional environment using a non-iterative, unconditional Boolean simulation. This is basically an object generator, which places a set of objects that are not constrained to local data onto a grid. Parameters that have to be defined to create a training image include geobody type, proportion, geobody interaction, and geobody parameters. Eight parameter sets were chosen, with 10 realizations for each, for a total of 80 training images.

Geobody type is basically a shape, and can be sinusoid, ellipsoid, half-ellipsoid, or cuboid. One or more types can be used for each parameter set. Shapes were based on the depositional environment, as well as visual comparison of the training images to the WCR data shown in Figure 4. The first four training image parameter sets were each run with a different set of geobodies. Visual examination excluded two of them (cuboid/sinusoid, ellipsoid/half-ellipsoid), as geologically unreasonable and a combination of visual examination and lack of data for added complexity excluded a third (lower half-ellipsoid/ellipsoid/sinusoid). A realization for each of these is shown in Figure D1. The remaining three training image parameter sets were then run with the selected geobodies (lower half-ellipsoid/sinusoid) that were judged to best represent the likely depositional environment of underflow type deposits (gravel) and beach deposits (sand).

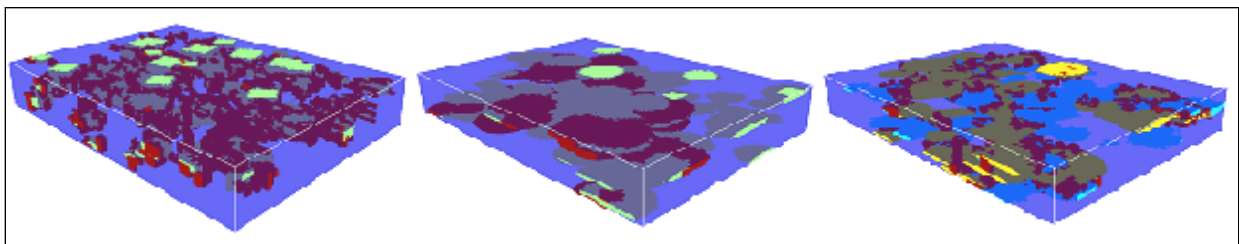


Figure D1. Training images from the geobody types not selected due to visual examination lack of comparison to WCRs in 3-D and geologic plausibility. From left to right the geobodies used are cuboid/sinusoid, ellipsoid/half-ellipsoid, and lower half-ellipsoid/ellipsoid/sinusoid.

Proportion is the total volume that a geobody type should fill. A proportion of 0.2 (20%) was used for each parameter set based on the calculated percent by thickness from the WCRs (high K units were 19.5%). Because sand was present along the entire length of each of the ERI transects, it is likely the thickness can be projected into volume.

Geobody interaction is the way the second or subsequent geobodies are placed in space with regards to the previous geobodies, and includes three parameters: erosion, minimum overlap, and maximum overlap. All geobodies erode the background, but have the option to either erode or be eroded by previously simulated geobodies. Seven of the eight parameter sets were set to erode the previous geobodies, as during the last glaciation the ice sheet would have advanced and retreated several times, eroding some of the earlier deposits and then depositing other sediment. Minimum and maximum overlap constrains the fraction of volumetric overlap between two geobodies. For seven of the eight parameter sets a minimum of 0.01 and maximum of 0.8 was used, allowing for geobodies to be “deposited” above previous geobodies. The eighth parameter set used a minimum of zero to allow the geobodies to either be deposited or not deposited above the previous geobodies. However, this causes the placement of subsequent geobodies to be more random, resulting in training images that are not representative of the depositional environment.

Geobody parameters are assigned for each geobody type and include orientation and dimensions (dependent on geobody type). The parameters can be defined as constant (mean), uniform (minimum, maximum), or triangular (minimum, mode, maximum). Orientation is the direction in which the geobody is “deposited”. Since the ice sheet moved in a east-northeast direction (Clark *et al.*, 2008), the deposits will generally be oriented in the same direction as the ice sheet; thus, a triangularly defined orientation was used for all geobody types in every parameter set of 15, 45, 95 (in degrees). The maximum orientation was extended to be approximately due south since in Outagamie County the curvature of the edge of the ice sheet was such that not all deposits coming off the ice sheet were necessarily deposited in the overall ice sheet direction. Dimensions are defined by number of nodes, and were based on information from the WCR analyses, ERI, and the depositional environment. Table D1 lists the dimensions used for the eight training image parameter sets.

Selection of the training images was based on visual comparison with the 3-D WCR display and general geologic plausibility. Of the 80 images, 12 were selected to be run with the *snesim* algorithm (Fig. D2). Note that these 12 were realizations from only four of the eight training image parameter sets; specifically training images 3, 5, 6, and 7 (Table D1).

Hard Conditioning Data

The hard conditioning data for the hydrostratigraphic models are mainly from the WCRs, but also include well reports from previously drilled rotosonic boreholes (Hooyer *et al.*, 2008). The data must be in point form for multiple-point geostatistics; thus, the center point of each unit was taken as a data point. For example, if clay were present from 700-720 ft elevation, the hard data point would be clay at 710 ft elevation. The total number of hard data was 5,153. During simulation, the hard data are assigned to the nearest grid node and kept constant.

Table D1. Dimensions for geobodies used in the training image generator. Ten realizations were run for each training image. Dimensions are listed as constant, uniform, or triangular (1, 2, or 3 values; see above text for explanation) and in number of nodes (not length measurements). Maxrad, medrad, and minrad, are the maximum, median, and minimum radii for ellipsoid objects. For sinusoidal objects thick is thickness, amp is amplitude, and wave is wavelength.

Training Image	Geobody Type	Geobody Dimensions
1	cuboid	Length 1,10; Width 1,10; Height 1,2,40
	sinusoid	Length 1,4; Width 1,2; Thick 1,2,40; amp 2; wave 2,15
2	ellipsoid	Maxrad 2,10; medrad 1,10; minrad 1,2,40
	lower half-ellipsoid	Maxrad 2,10; medrad 2,10; minrad 1,2,40
3	lower half-ellipsoid	Maxrad 2,10; medrad 2,10; minrad 1,2,40
	sinusoid	Length 1,4; Width 1,2; Thick 1,2,40; amp 2; wave 2,15
4	lower half-ellipsoid	Maxrad 2,10; medrad 2,10; minrad 1,2,40
	ellipsoid	Maxrad 2,10; medrad 1,10; minrad 1,2,40
	sinusoid	Length 1,4; Width 1,2; Thick 1,2,40; amp 2; wave 2,15
5	lower half-ellipsoid	Maxrad 2,10; medrad 2,10; minrad 1,2,40
	sinusoid	Length 1,4; Width 1,2; Thick 1,2,40; amp 1,3; wave 2,4
6	lower half-ellipsoid	Maxrad 2,10; medrad 2,10; minrad 1,2,40
	sinusoid	Length 1,4; Width 1,2; Thick 1,2,40; amp 1,3; wave 2,4
7	lower half-ellipsoid	Maxrad 2,5; medrad 2,5; minrad 1,2,40
	ellipsoid	Length 1,4; Width 1,2; Thick 1,2,40; amp 2; wave 2,15
8	lower half-ellipsoid	Maxrad 2,10; medrad 2,10; minrad 1,2,40
	ellipsoid	Length 1,4; Width 1,2; Thick 1,2,40; amp 2; wave 2,15

Parameters Analyzed

Certain parameters were kept the same for all *snesim* simulations, while others were varied in addition to varying the training image used. Using the 12 selected training images (Fig. D2), 30 simulations were run, with 10 realizations for each, for a total of 300 hydrostratigraphic models. Eight of the simulations were run with the same training image but varying other parameters. After analysis of the effects of these parameters, the remaining simulations were run with the other 11 selected training images.

Liu (2006) performed sensitivity analyses on many of the *snesim* input parameters using a 2-D case. Although the models for this research are in 3-D, many of the 2-D results can be extended into 3-D. A correction factor, named the servosystem correction, is used to bring the simulated target proportion closer to the target, but this loses structural information from the training image. The servosystem parameter must be set between 0 and 1, with higher values causing a larger correction to the target proportion. For all simulations in this research the servosystem parameter was set to 0.5, to allow a balance between the training image geometry and the target proportion. The target distribution itself was one of the parameters that was tested as will be described below. Liu (2006) determined that the program was not very sensitive to the minimum number of replicates parameter, and an empirical value between 10 and 20 should be used, with a smaller value needed for increasing number of multi-grids (discussed below). Thus a value of 10 was used for all simulations in this research. Liu (2006) also analyzed the search template geometry, and determined it was most robust to use an isotropic search ellipsoid. The size of the ellipsoid was tested, but all were horizontally isotropic (circle). Since the z-direction is of a much shorter length, a fully isotropic search ellipsoid is impractical. The final parameter that was tested for this research was the number of multi-grids. Multi-grids allow for large scale structures to be simulated by first simulating nodes on the coarsest grid with a large rescaled template, then simulating nodes on the second coarsest grid with a smaller rescaled template, and so on until the finest grid is

simulated using the original template. Liu (2006) found that increasing the number of multi-grids to 5 and 6 does not improve large scale structure, and only having 1 multi-grid is unacceptable as it only captures small-scale structures.

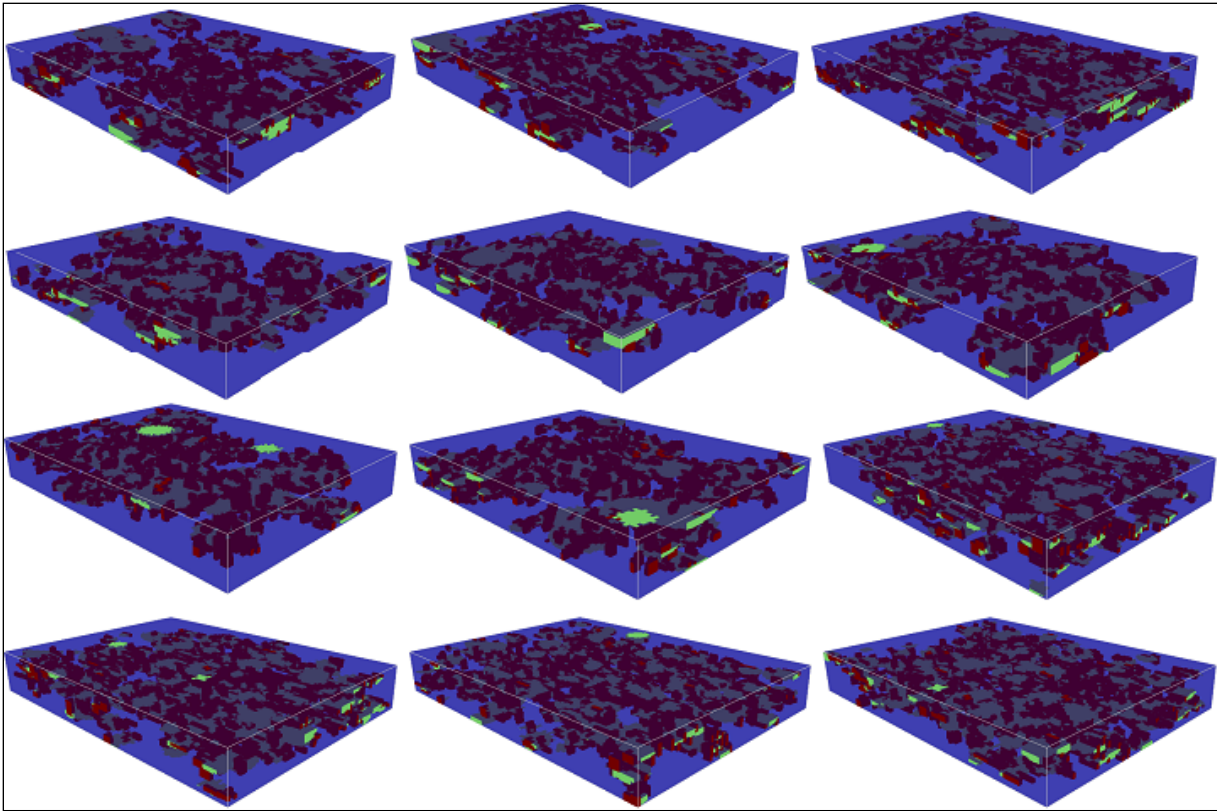


Figure D2. The twelve training images selected for use in the *snesim* algorithm.

Three parameters were tested by running simulations with the same training image. These parameters are the target marginal distribution (or proportion), the size of the search template, and the number of multi-grids. As described in the introduction, the percent by thickness for the units was approximately 20% for the high K units, so this value was used for the proportion in the hydrostratigraphic model. However, one model was tested with a lower percentage of 10%. The two sets of tested values for the target marginal distribution (given as a ratio) for low K units, sand, and gravel, respectively, are as follows: 0.8, 0.1, 0.1 and 0.9, 0.05, 0.05. Analysis of connectivity statistics (see Appendix F for more information) indicated similar connectivity despite having a lower percentage (10%) of high K material; thus, 20% was used. Furthermore, the values of 0.8, 0.1, 0.1 were used for the remaining models as these are the values suggested by the WCR data. Two sizes of search template were tested, with values in feet in the x, y, and z directions, respectively, as follows: 12000, 12000, 50 and 24000, 24000, 100. Analysis of connectivity statistics indicated slightly higher connectivity in the second of the two templates, which is not surprising given that Liu (2006) found that the search template size should be adapted to the dimensions of the structures. Since the maximum size of these sand bodies is unknown, the smaller size of 12000, 12000, 50 was used for all other simulations so as to not add additional connectivity that may not be present. Finally, the number of multi-grids was tested by running models with 1 through 5 multi-grids. Connectivity statistics showed little change in connectivity with models using 1, 2, or 3 multi-grids. However, visually the models with 1 or 2 multi-grids were not geologically plausible as they only captured small structures (Fig. D3). Connectivity statistics changed with 4 multi-grids, indicating greater connectivity in the z-direction and fewer, but longer connected pathways. Additionally, the average

proportion of high K units increased slightly from 0.17 to 0.18. When 5 multi-grids were used this proportion increased to 0.19, with even fewer and longer pathways. However, the connectivity in the z- and y-directions actually decreased, while x-direction connectivity increased. Additionally, the models visually began to have structures that were too large, particularly near the surface; thus, only 3 and 4 multi-grids were used in the other simulations.

Statistics from all 300 models were imported into an Excel file and analyzed. Results from initial simulations with the same training image aided in the determination of parameters (as described above) used in later simulations. Of the 300 models, 240 have acceptable parameters as discussed above and were considered in the selection process. Table D2 displays the averages, standard deviations, and maximum and minimum values for all 300 models and also the subset of 240 acceptable models.

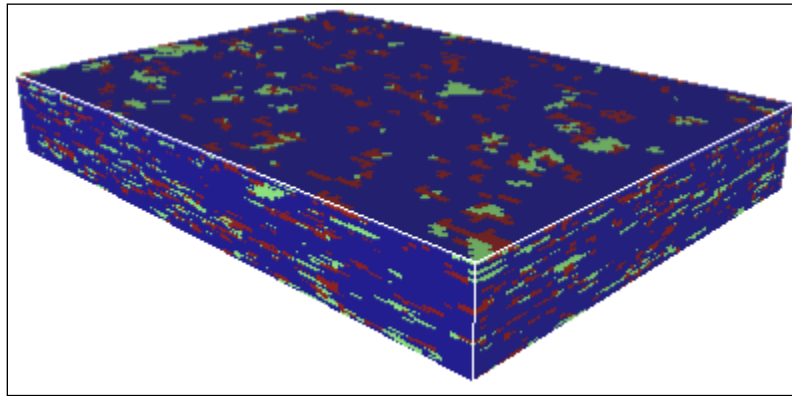


Figure D3. Hydrostratigraphic model using only 1 multi-grid. Note the lack of large scale structures.

Table D2. Average (AVG), standard deviation (SD), maximum value (MAX) and minimum value (MIN) for all 220 models (all) and the subset of 240 models with acceptable parameters (okpar). Note that the pixel size is 1200 ft in the x and y directions, and 5 ft in the z direction.

Model	Proportion	Number of connected components	Mean size (pixels)	Mean length-x (pixels)	Mean length-y (pixels)	Mean length-z (pixels)
AVG_all	0.16	10971	17.68	1.50	1.52	3.28
SD_all	0.02	2038	4.89	0.08	0.08	0.33
MAX_all	0.19	15274	31.49	1.69	1.69	4.47
MIN_all	0.09	6673	6.77	1.28	1.29	2.37
AVG_okpar	0.16	11192	17.31	1.51	1.53	3.34
SD_okpar	0.01	1942	4.42	0.07	0.07	0.29
MAX_okpar	0.19	15209	30.89	1.69	1.69	4.47
MIN_okpar	0.14	6824	10.23	1.30	1.34	2.69

Model	Max size (pixels)	Max length-x (pixels)	Max length-y (pixels)	Max length-z (pixels)	Min size (pixels)	Min length-x (pixels)	Min length-y (pixels)	Min length-z (pixels)
AVG_all	105352	57.95	71.00	160.00	1.00	1.00	1.00	1.00
SD_all	27437	22.00	0.00	0.00	0.00	0.00	0.00	0.00
MAX_all	177015	99.00	71.00	160.00	1.00	1.00	1.00	1.00
MIN_all	45400	29.00	71.00	160.00	1.00	1.00	1.00	1.00
AVG_okpar	104107	53.99	71.00	160.00	1.00	1.00	1.00	1.00
SD_okpar	23226	19.02	0.00	0.00	0.00	0.00	0.00	0.00
MAX_okpar	177015	99.00	71.00	160.00	1.00	1.00	1.00	1.00
MIN_okpar	66215	35.00	71.00	160.00	1.00	1.00	1.00	1.00

Model	Number of percolating components-x	Number of percolating components-y	Number of percolating components-z
AVG_all	0.16	1.36	1.55
SD_all	0.37	0.51	0.71
MAX_all	1.00	3.00	5.00
MIN_all	0.00	1.00	1.00
AVG_okpar	0.10	1.36	1.58
SD_okpar	0.29	0.50	0.72
MAX_okpar	1.00	3.00	5.00
MIN_okpar	0.00	1.00	1.00

APPENDIX E: CONNEC3D Overview

All 300 hydrostratigraphic models were analyzed for connectivity statistics using CONNEC3D (Pardo-Igúzquiza & Dowd, 2003), which calculates a number of connectivity statistics and writes these to several output files. This free program was used as a post-processor by de Vries et al., (2009) to create training images with all channel features connected, and Pardo-Igúzquiza & Dowd (2003) demonstrated its capabilities with a randomly generated model, but it has not been used as a quantitative measure of connectivity with a model created from field data.

Two input files need to be written for CONNEC3D (Pardo-Igúzquiza & Dowd, 2003). First the hydrostratigraphic model output must be categorized into two units based on a threshold value of K so that all high K values (sand and gravel bodies) are assigned a value of 1 and all low K values (glacio-lacustrine and till deposits) are assigned a value of 0. This information must be saved as a .dat file. The other input file is a nine-line parameter file containing the names of the .dat file and output files, the grid size and spacing, and two adjustable parameters: connectivity analysis and lag. The connectivity analysis is the number of adjacent cells used in the determination of the connectivity statistics (Fig. E1) and can be either 6 (defined by cells that share a face), 18 (defined by cells that share a face or an edge), or 26 (defined by cells that share a face, edge, or vertex). The lag is the number of cells over which the connectivity statistics are calculated in any direction. All hydrostratigraphic models were run with a connectivity analysis of 18 and a lag of 30 cells.

The program calculates the following connectivity statistics: proportion of unit that is being analyzed (high K units for this research), number of connected components, mean size of a connected component (cc), mean length in the x, y, and z directions of a cc, size of the largest and smallest cc, length in the x, y, and z directions of the largest and smallest cc, and number of percolating components in the x, y, and z directions. A percolating component is a single connected component that connects from one end to the other in a specific direction, for example a percolating component in the z-direction would indicate a connected pathway from the top to the bottom of the model. Additionally, the connectivity function (for this research estimated by the number of high K cells within the lag distance that are connected divided by the total number of high K cells within the lag distance) is calculated for 13 directions (x, y, z, four 3-D diagonals, and six diagonals of planes). Also the average of the x, y, and z directions and the average of the four 3-D diagonals are calculated.

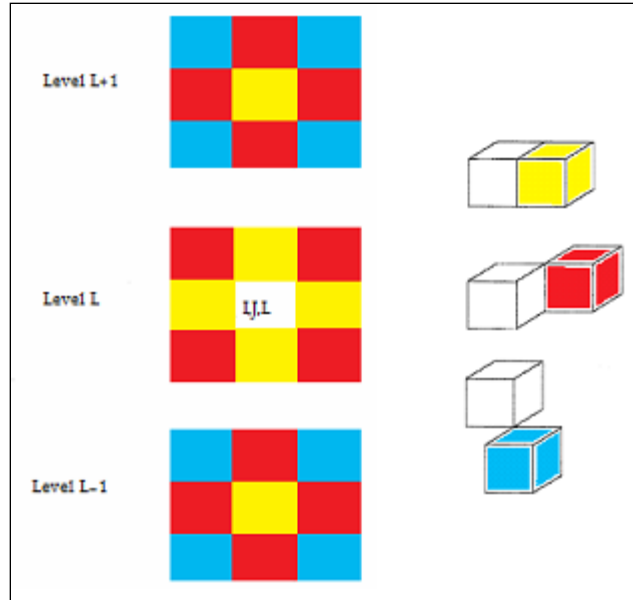


Figure E1. Connectivity analysis demonstrated for cell I,J,L (on left). Shown are the six neighbors of 6-connectivity analysis (yellow), 18 neighbors of 18-connectivity analysis (yellow plus red) and 26 neighbors of 26-connectivity analysis (yellow plus red plus blue). On the right: face (yellow), edge (red), and vertex (blue) connectivity are demonstrated with two nodes. Adapted from Pardo-Igúzquiza & Dowd (2003).

APPENDIX F: Selection of Representative Set of Models

A representative set of models was selected from the 240 models with acceptable parameters, based on analyses of the connectivity statistics. Several of the statistics, such as the minimum size and lengths in all directions had a standard deviation of zero and were not considered in selecting a representative set. Three of the connectivity statistics had variability that needed to be considered in selecting models: proportion, number of connected components, and maximum size in pixels.

The overall range of each of these three statistics was analyzed graphically (Figs. F1-F3). As the proportion of high K material increases (Fig. F1), the number of connected components decreases (Fig. F2), indicating that there are fewer but longer connected pathways. Additionally, there is some correlation with the longest maximum size (in pixels; Fig. F3) occurring for those models having fewer connected components, further indicating that fewer but longer pathways are generally occurring in these models.

In addition to the graphical analysis, every model was analyzed for each of these connectivity statistics and assigned a categorical value of three letters based on the value of each individual statistic. Each statistic was assigned a range for low (L), average (A), and high (H) values (Table F1). Then each model was categorized based on its statistics for proportion, number of connected components, and number of percolating components. For example, a model with low values for each of these would be categorized as an LLL model.

The final selection took into account the overall range of the three statistics and the categorical values of all the models, as well as ensuring selection of models with different training images and number of multi-grids (3 & 4). Additionally, the number of percolating components in the x-, y-, and z-directions and the maximum length in the x-direction were considered. After analysis of all of these factors, six models were selected as a representative set.

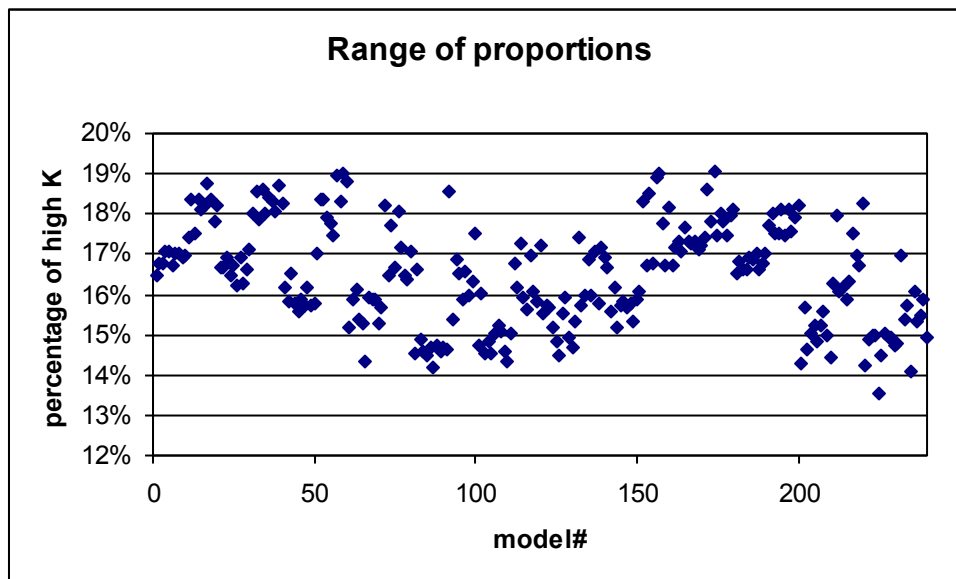


Figure F1. Proportion values for the 240 models. Note that although the proportion was set at 20% for the simulations, the simulated values vary from approximately 13.5-19% due to the servosystem correction being set at 0.5, which allows for the training image geometry to also be observed.

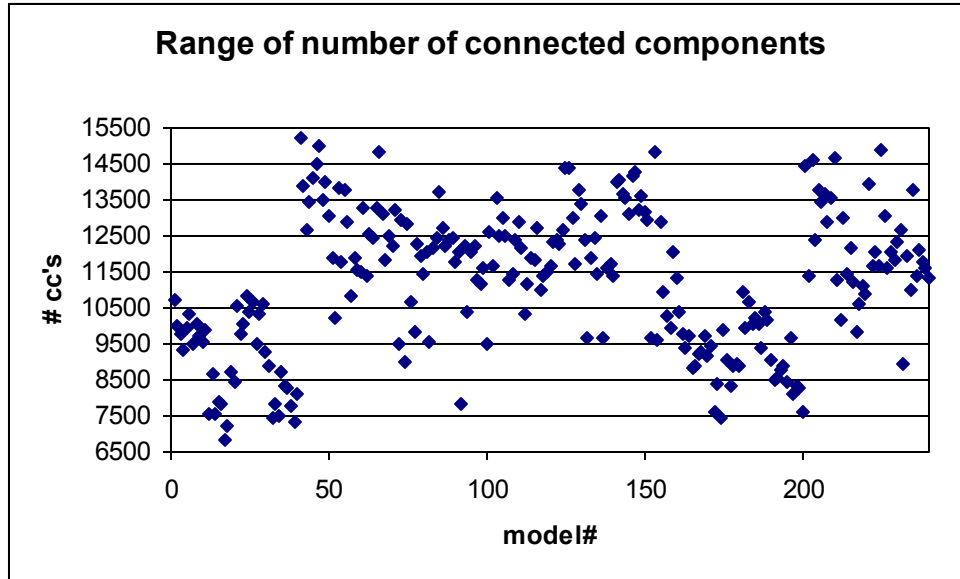


Figure F2. The number of connected components for the 240 models. Note that the model number is the same for the proportion graph (Fig. 2.9), and comparison indicates generally fewer connected components with increasing proportion (i.e., models 1-40, 161-200)

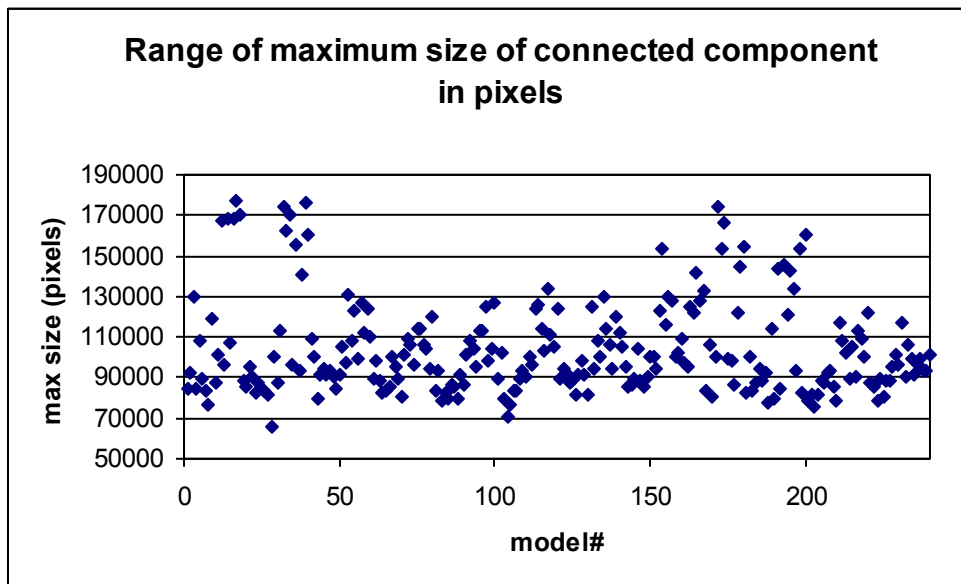


Figure F3. Values of maximum size of connected components measured in pixels for the 240 models.

Table F1. Values for each statistic that were used to assign low, average, and high ranges to each model.

Statistic	Low	Average	High
proportion	<0.155	0.155-0.175	>0.175
number of connected components	<10000	10000-12000	>12000
maximum size of connected component (pixels)	<90000	90000-115000	>115000

Initial analyses were based on the categorical values for the models. Certain categories, such as LLL, LLA, and LLH did not have any models. For other categories, including LHL and AHA, over 10% of the models fit in this category. Through analysis of the percentage of each category, and taking into account that models of categories with only one difference in letter (e.g. HAA and HAH) were often identical in the two categories with only a minor difference in the third, it was determined that five to seven models would be necessary for a representative set.

Selecting the representative set, including determining the exact number necessary, was done iteratively. One model was selected for a category with a high percentage, then a second selected from another category, until five to seven models were selected. Throughout the process each set of models was compared for number of multi-grids and training images, as well as insuring that individual values for the three statistics represented the full range of values. Certain sets would not work because more than one model would be from the same training image, or all of the models would be realizations from the same training image parameter set. Eventually, the six selected models were determined through this process. Figures F4-F6 graphically show that the selected models represent the range of each of the connectivity statistics. Figure F7 demonstrates that the selected models represent the range of models based on the 27 possible categories (e.g., LLL). Graphs for the connectivity function in the x, y, and z directions indicate a range of connectivities are represented by these models (Figs. F8-F10). Table F2 displays statistics for each of the selected models, as well as the averages of these statistics compared to the averages of the 240 acceptable models. These figures and tables demonstrate that the six selected models truly are a representative set. Finally, Figure F11 shows a 3-D image of each of the selected models.

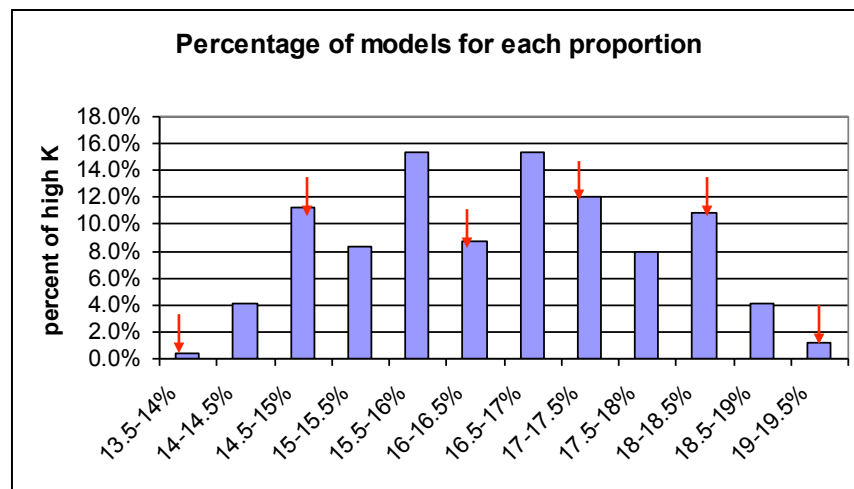


Figure F4. Percentage of models for each proportion (listed as percent by volume). The red arrows indicate the proportion of the six selected models.

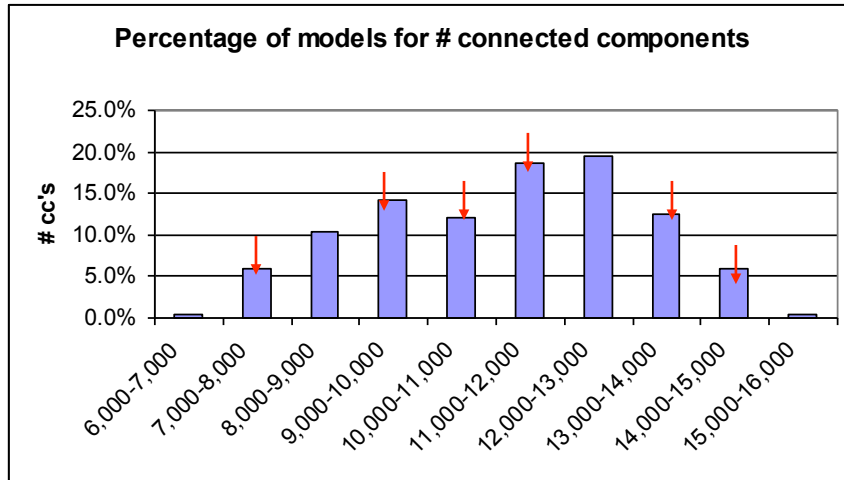


Figure F5. Percentage of models for number of connected components. The red arrows indicate the number of connected components of the six selected models.

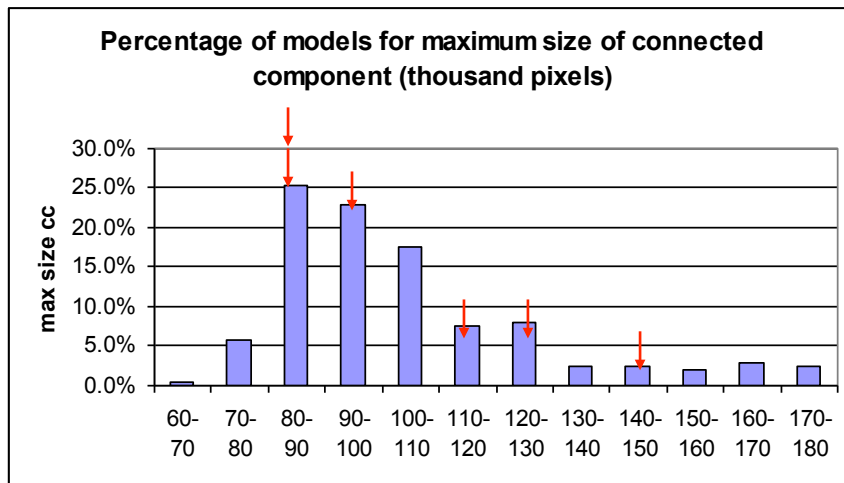


Figure F6. Percentage of models for maximum size of connected component (in thousands of pixels). The red arrows indicate the maximum connected component size of the six selected models.

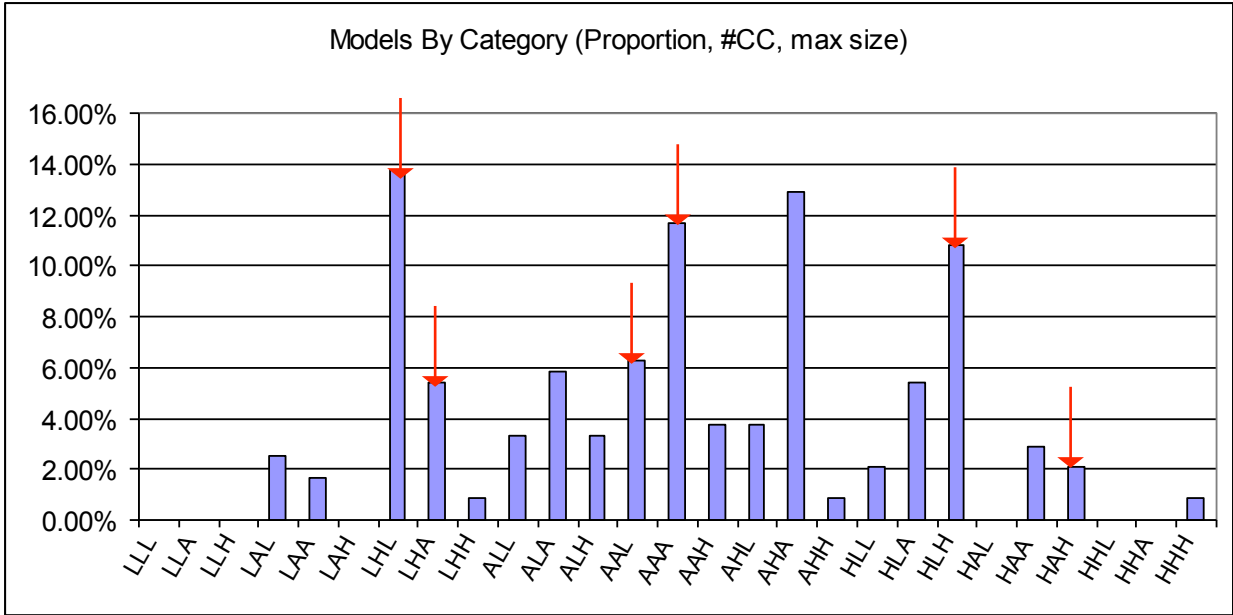


Figure F7. Percentage of models by category (see text and table F1 for details). The red arrows indicate the category of the six selected models.

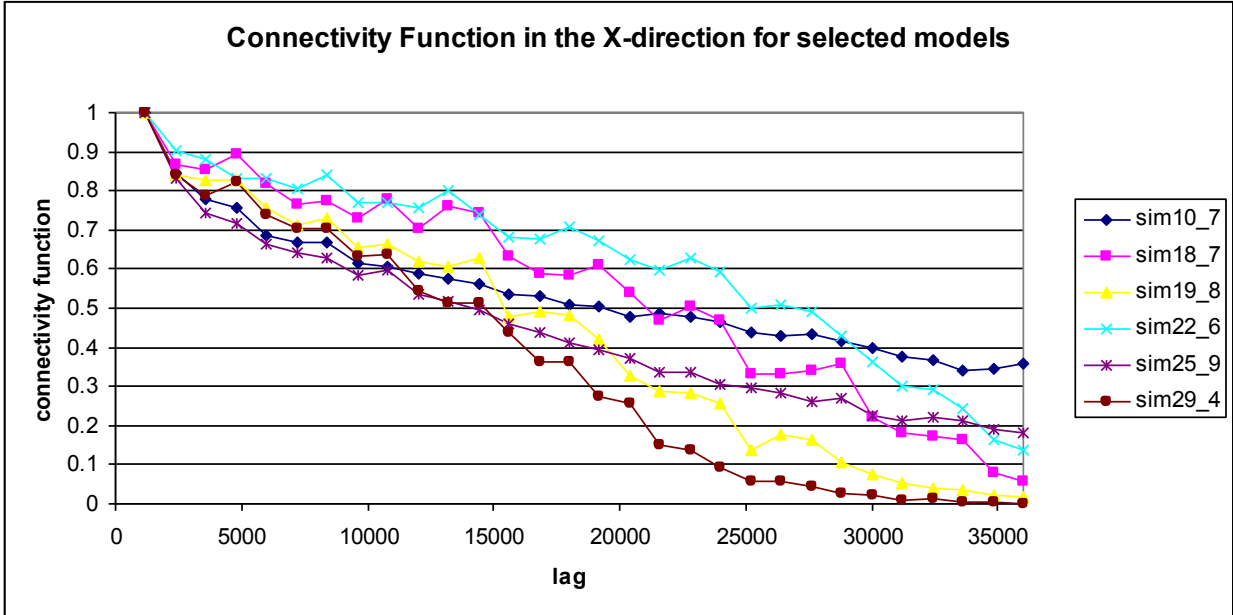


Figure F8. Connectivity function (number of connected high K cells within the lag distance / total number of high K cells within the lag distance) in the x-direction for each of the selected models. Model sim10_7 has a percolating component in the x-direction, and thus maintains a higher connectivity function at larger lag distances.

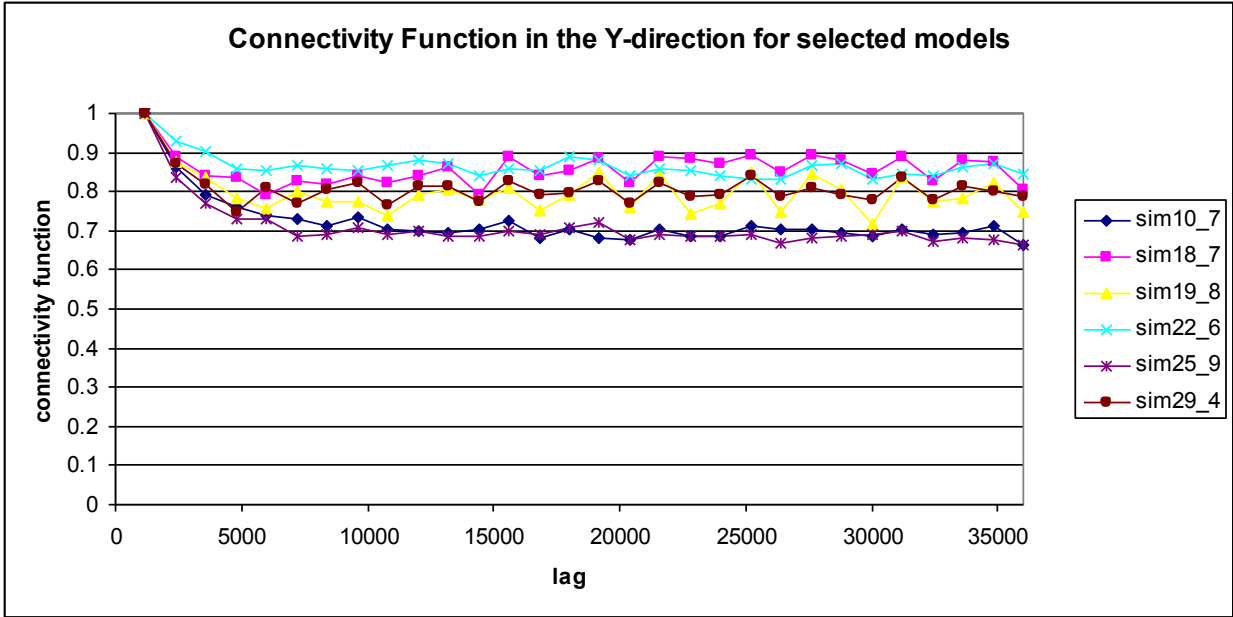


Figure F9. Connectivity function (number of connected high K cells within the lag distance / total number of high K cells within the lag distance) in the y-direction for each of the selected models.

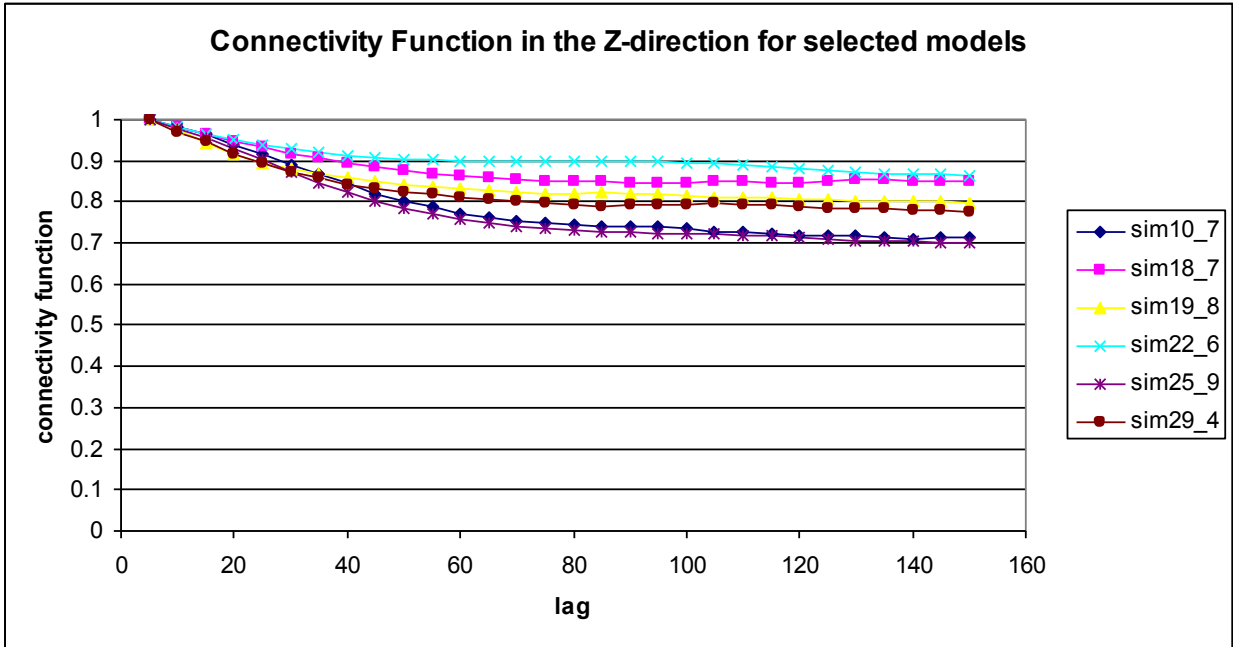


Figure F10. Connectivity function (number of connected high K cells within the lag distance / total number of high K cells within the lag distance) in the z-direction for each of the selected models.

Table F2. Selected models and their corresponding training image (TI), number of multi-grids, and connectivity statistics that did not have a standard deviation of zero for all models. The last two rows list the average of these statistics for the selected models and the 240 possible models. Note that the averages of the representative set are nearly identical to those of all the possible models. Model names are given by simnumber_realization number and training images by training image number_realization number. Pixel size is 1200 ft in the x and y directions, and 5 ft in the z direction.

Model	TI	# multi-grids	proportion	#cc's	Mean size (pixels)	Mean length-x (pixels)	Mean length-y (pixels)	Mean length-z (pixels)
sim10_7	7_2	4	0.1808	7753	26.2326	1.5184	1.5443	3.2602
sim18_7	3_3	4	0.1607	11406	15.8407	1.3839	1.4295	3.8511
sim19_8	5_6	3	0.1492	13800	12.1569	1.5143	1.5214	3.2954
sim22_6	6_6	4	0.1903	10274	20.8331	1.4963	1.5742	3.0993
sim25_9	7_1	3	0.1703	9052	21.1548	1.5166	1.5104	3.1130
sim29_4	3_9	3	0.1352	14868	10.2273	1.4531	1.4875	3.1776
AVG-selected			0.16	11192	17.74	1.48	1.51	3.30
AVG-all plausible (240)			0.16	11192	17.31	1.51	1.53	3.34

Model	Max size (pixels)	Max length-x (pixels)	# perc comp-x	# perc comp-y	# perc comp-z
sim10_7	140420	99	1	1	1
sim18_7	110996	42	0	1	3
sim19_8	91895	41	0	1	1
sim22_6	127871	40	0	2	2
sim25_9	79940	56	0	2	2
sim29_4	80439	37	0	1	1
AVG-selected	105260	53	0.17	1.33	1.67
AVG-all plausible (240)	104107	54	0.10	1.36	1.58

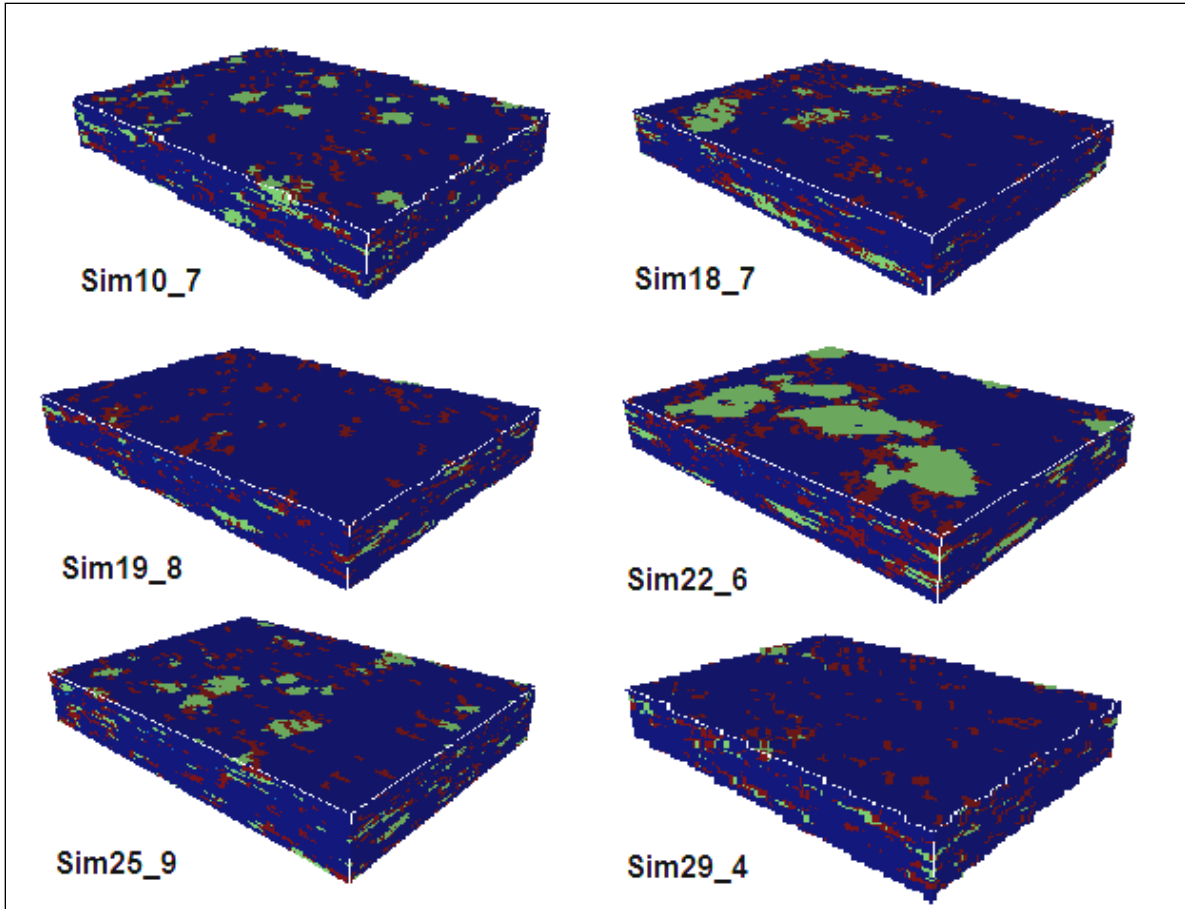


Figure F11. Selected models, names for each are to the bottom left corner of the model and correspond to those listed in Table F2. The view shows the southern and eastern edges of the model on the left and right sides, respectively. Red and green (sinusoids/sand and lower-half ellipsoids/gravel, respectively) are the high K units.

APPENDIX G: Groundwater Flow and Transport Models

Model Design

Regional groundwater flow in Outagamie County is mainly to the east (Fig. G1). However, in the glacial Lake Oshkosh sediment, flow is mainly vertical (Hooyer *et al.*, 2008). As will be described in more detail in this appendix, the model grid and boundary conditions have been adjusted to simulate this vertical flow.

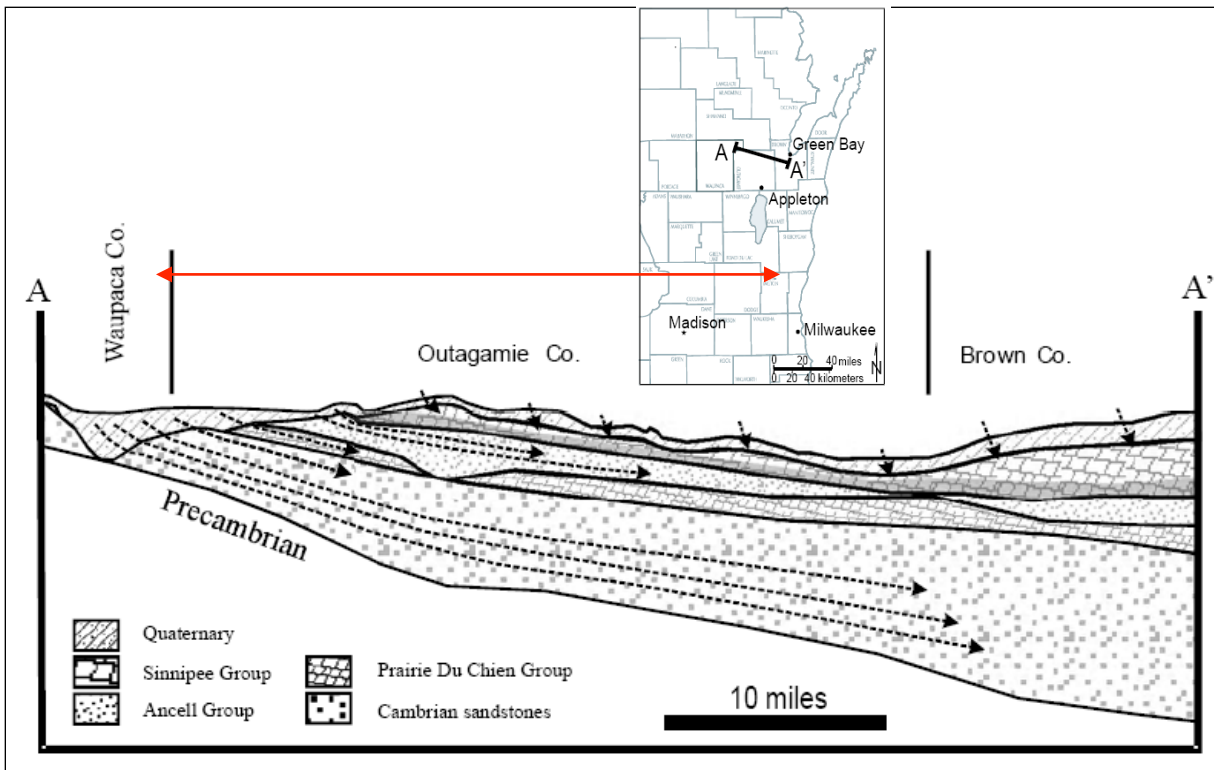


Figure G1. Idealized cross section showing the bedrock units and groundwater flow in the study area (Outagamie Co.). General location of the cross section is shown in the inset. Red arrow indicates approximate extent of groundwater flow models in the direction of the cross-section. (from Hooyer *et al.*, 2008)

Model Grid & Layers

The Lake Michigan Basin Model (LMBM, Feinstein *et al.*, 2010), which has horizontal grid spacing of 5,000 by 5,000 feet in the area of interest and 20 layers of variable thickness, was initially used to define the Outagamie County groundwater flow models using the telescopic mesh refinement (TMR, Ward *et al.*, 1987) option in Groundwater Vistas. The groundwater flow models have the same uniform horizontal grid spacing (1,200 by 1,200 feet, with 71 rows and 99 columns) as the hydrostratigraphic models. Except for layer 1, the 98 layers in the groundwater flow models have uniform thickness of 5 ft, which is the same as the hydrostratigraphic models. The top twenty layers of the hydrostratigraphic models were removed because they were either above the maximum land surface elevation or the maximum water table elevation. The bottom sixteen layers of the hydrostratigraphic models were also removed because they are entirely within the Precambrian bedrock. The top and bottom elevations of layer 1 are 940 and 755 ft above mean sea level (amsl), respectively. This layer is very thick because upland areas exist in the eastern corners of the model; however, the maximum surface water feature elevation outside of these areas is only 795 ft. Since the minimum surface water feature elevation is 760 ft amsl, this thicker layer allows for all surface water features to be modeled in layer 1.

Whereas the hydrostratigraphic models included only the glacial sediments, the groundwater flow models initially were designed to include the bedrock units shown in Fig. G1. Therefore, the hydrostratigraphic model data and the bedrock elevation data from the LMBM (Feinstein *et al.*, 2010) were compared in a spreadsheet in order to determine whether a particular node contained glacial deposits, bedrock, or both. If a node contained both glacial deposits and bedrock it was assigned to whichever unit had the greater volume of material in that node. If a node was in bedrock, it was assigned to a bedrock unit. Bedrock units are the Ancell Group, Prairie du Chien Group, and Cambrian sandstones (Fig. G1). Then the walls of the bedrock valley were further modified to correct for the lack of detail in the valley due to the large grid size of the LMBM. This was done by comparing the WCR data and mapping of the bedrock valley by Hooyer *et al.* (2008) in order to define the bedrock valley more accurately. The addition of the bedrock valley resulted in “losing” some of the high K units. The groundwater models have 10-16% sand and gravel.

Boundary Conditions

Initially, in early test models, head values were taken from the LMBM model along the four sides of the Outagamie County groundwater flow models in every layer and used to specify heads along the side boundaries. However, all six models had very poor calibrations, with every head target simulated higher than the observed, up to a 350 ft difference. Comparison of the LMBM head values with elevations of local surface water features from topographic maps and the head targets indicated the head values from the LMBM were all too high. Additionally, Feinstein *et al.* (2010) indicated few calibration points in this area of Outagamie County.

Because there are insufficient data to set the lateral boundaries, the layer 1 lateral boundaries were based on the surface water features, interpolating head between them. These boundaries were then used in every layer of the model as vertical hydraulic gradient information was not available near the boundaries. It was also found that the basal boundary condition needed adjustment. Initially, the bottom boundary, at the base of layer 98, was a no-flow boundary set in the Precambrian bedrock; the lower most layer containing glacial deposits is 83. The model was initially run with all 98 layers active. In order to simulate only the glacial deposits, head values based on values computed by the model with a no-flow boundary in the Precambrian bedrock were then assigned to all bedrock nodes, which effectively moved the lower boundary to the top of the bedrock valley. However, boundary heads proved to be too high, producing a thousand feet of water mounding on the surface. Therefore, during calibration, PEST determined one head value to be used as the lower boundary condition set at the bedrock valley walls. The top layer (upper boundary condition) has a specified flux equal to the recharge rates. Two recharge zones were specified based on conclusions drawn by Hooyer *et al.* (2008) that regions with 50 ft or less of glacial sediment have more recharge. The initial recharge rate was assigned as 1 in/yr in zone 1 and 6.4 in/yr in zone 2 (Fig G2), following Hooyer *et al.* (2008). Initial head values were set to 850 ft amsl for all cells.

The River Package was used to simulate major surface water features in the model area and the Drain Package to simulate minor surface water features (Fig. G3). Initially, only major surface water features were simulated, but this did not move enough water as indicated by the mounds of water found over large areas of the model. This problem was alleviated by adding minor water features as drain cells. Surface water features were digitized from a Geographic Information System (GIS) coverage of surface waters in Wisconsin imported to Groundwater Vistas as a map. River cells were defined as either lakes/wetlands or streams. Each lake/wetland cell was assigned a length and width so as to encompass the entire surface area of the cell. All stream cells were assigned a length of 1,200 ft and a width between 30-50 or 100 ft, based on average stream widths from topographic maps. Drain cells were assigned a length and width so as to encompass the entire surface area of the cell. Thickness of the streambed and lakebed sediment was arbitrarily set to 1 ft for all river cells and the vertical hydraulic conductivity of the bed was assigned a value of 4.5 ft/day for all river and drain cells, the average measured value for sand deposits (Freeze and

Cherry, 1979), which are prevalent along the major surface water features in the area. Literature values were assigned since local K values for fluvial sand deposits were not available. Streambed and lakebed elevations were estimated from topographic maps.

Model Properties

Porosity values (Table G1) were taken from the literature, including consolidation testing data from Hooyer *et al.* (2008). Hydraulic conductivity (K) is the only parameter that is different among the six models, as each is based on a different hydrostratigraphic model. Three different zones of K were used, one zone for each of the glacial deposits (fine-grained lacustrine/till, sand, and gravel). Locations of the glacial deposit zones were from the selected hydrostratigraphic models. Initial values of K (Table G1) for the glacial deposits were taken from Hooyer *et al.* (2008).

Table G1. Porosity and initial hydraulic conductivity values for each of the six models. Note that K_x indicates horizontal hydraulic conductivity for both the x and y directions, and K_z vertical hydraulic conductivity.

Unit	Porosity	Kx (ft/day)	Kz (ft/day)
<i>lacustrine/till</i>	0.3	2.83E-02	2.83E-04
<i>sand</i>	0.2	4.54	0.45
<i>gravel</i>	0.2	70.9	7.09

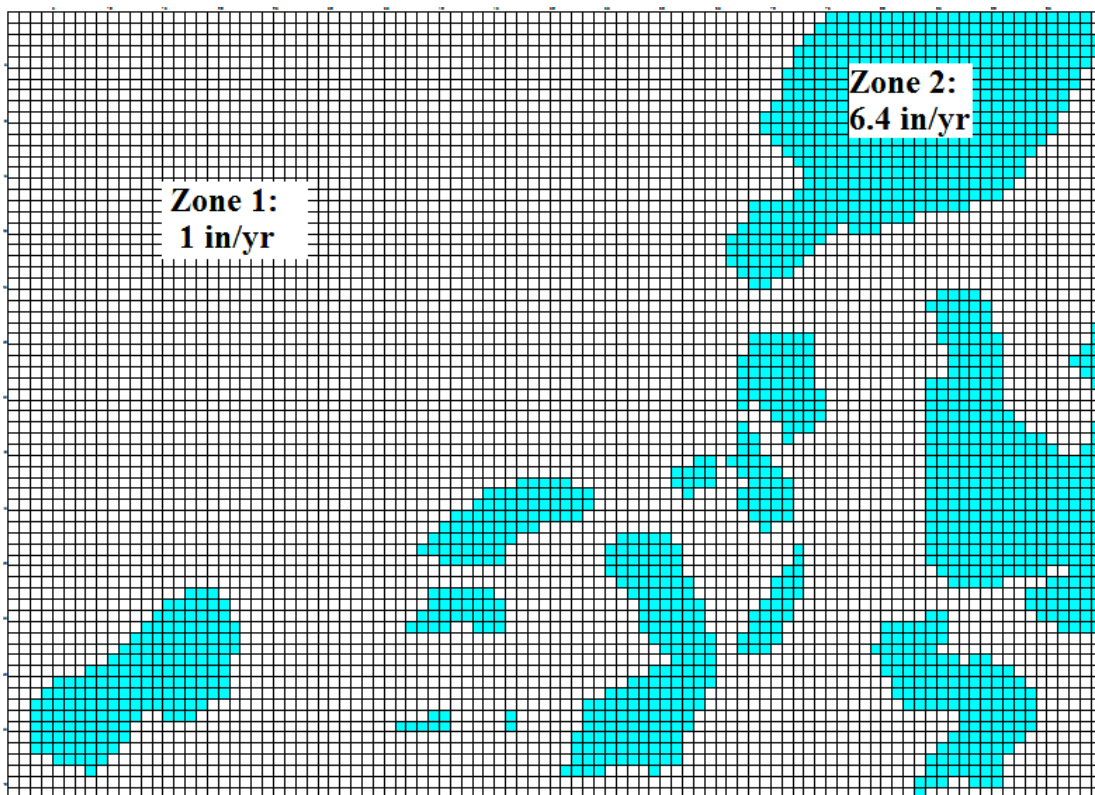


Figure G2. Initial estimates of recharge used in the groundwater flow models, taken from Hooyer *et al.* (2008).

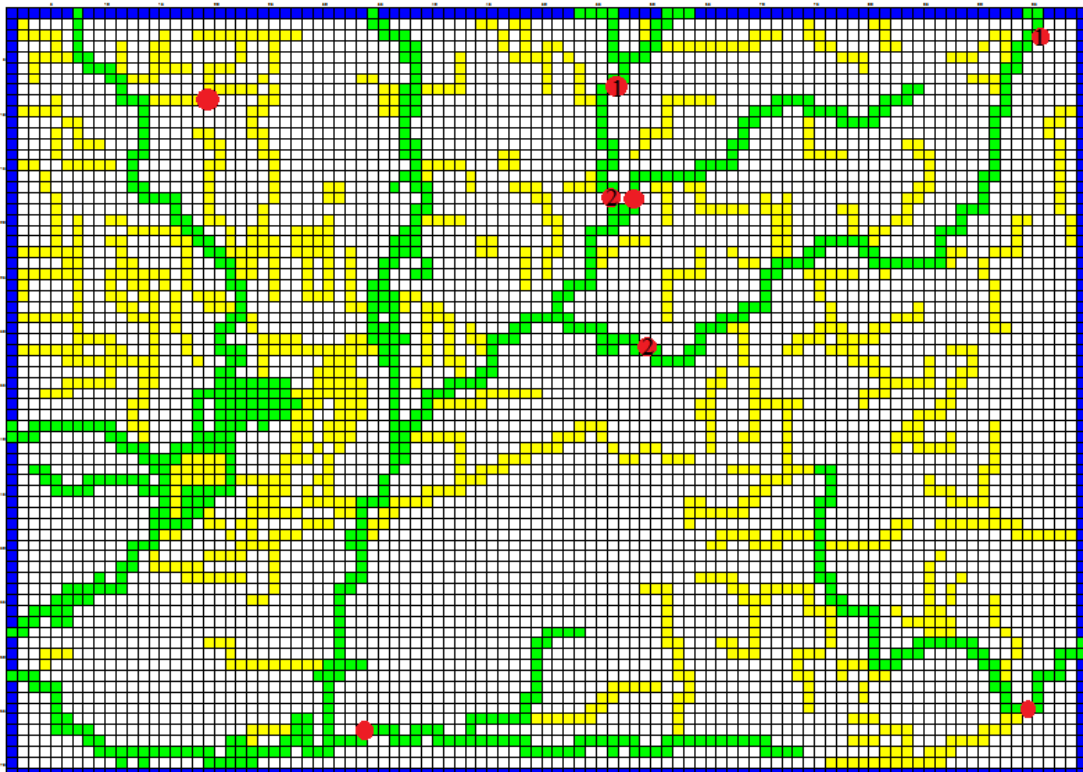
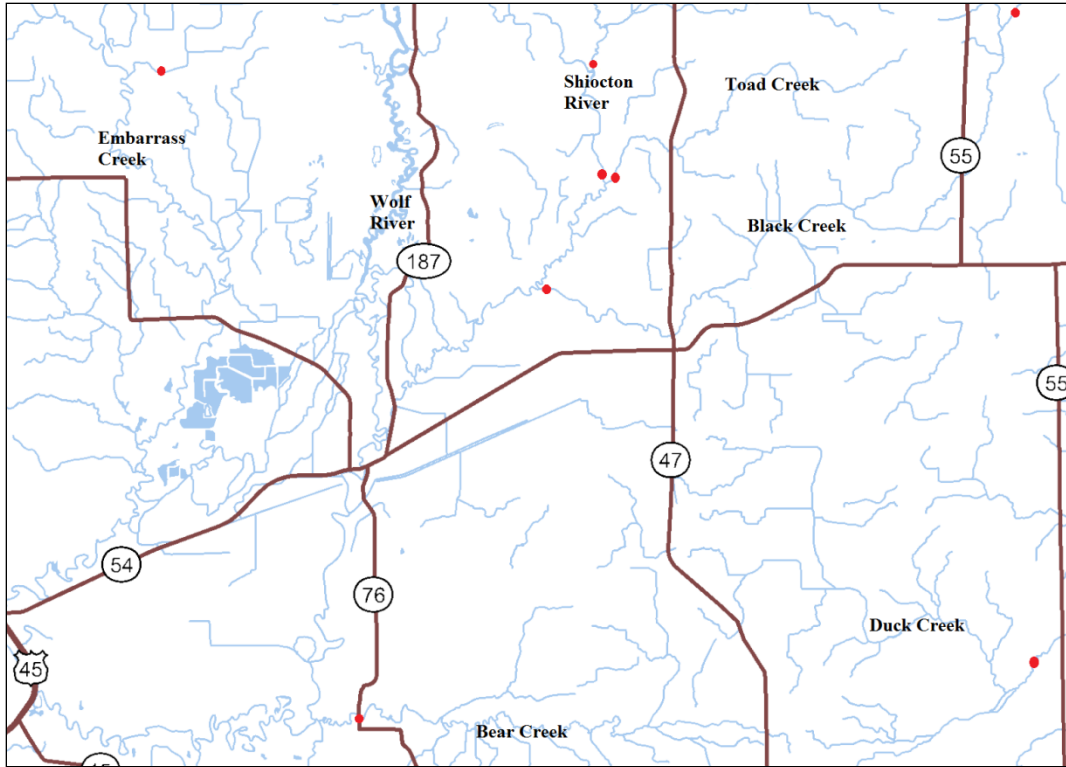


Figure G3. Location map of surface water features in the modeling area and layer 1 of the model showing the cells in the River Package (in green) and Drain Package (in yellow) used to simulate lakes, streams, and wetlands. Blue cells are specified head boundaries. Red dots indicate location of stream flux targets.

Calibration

Calibration of the six models was performed using the inverse code PEST (Doherty, 2004). PEST was used to determine optimal values of horizontal hydraulic conductivity (K_x), vertical hydraulic conductivity (K_z), recharge rates, and a constant head value for the bedrock nodes that formed the lower boundary. Note that initially PEST was run with five bedrock constant head zones, based on the bedrock units present in the study area (Fig. G1). However, this proved to be too many parameters for the available targets as PEST determined sand K to be lower than clay K and/or minimized recharge and maximized clay K for all six models.

Targets and Weights

Twenty head targets (Fig. G4) were used to calibrate the groundwater flow models, one of which was from a USGS long term monitoring well, nine from WCRs used in the geophysics site selection, and ten from Hooyer *et al.* (2008). The head targets were located throughout the model, with two targets in each of layers 1, 10, and 18, and one target each in layers 3, 4, 9, 15, 19, 21, 28, 29, 33, 34, 39, 44, 57, and 60. In addition to the head targets, six stream flux targets were used as a final check of the calibration (Fig. G3).

Weights were determined based on the credibility of the targets, with locations having lower measurement uncertainty receiving higher weights. The numbers were selected arbitrarily, with RS-18 values an order of magnitude higher than the WCRs. All RS-18 targets were given a weight of 10; all WCRs a weight of 1. The remaining targets from the Lorenz, Riehl, and USGS sites were given a weight of 5 as these targets were considered more uncertain due to their shallow locations (Lorenz/Riehl) or anomalously low head value (USGS).

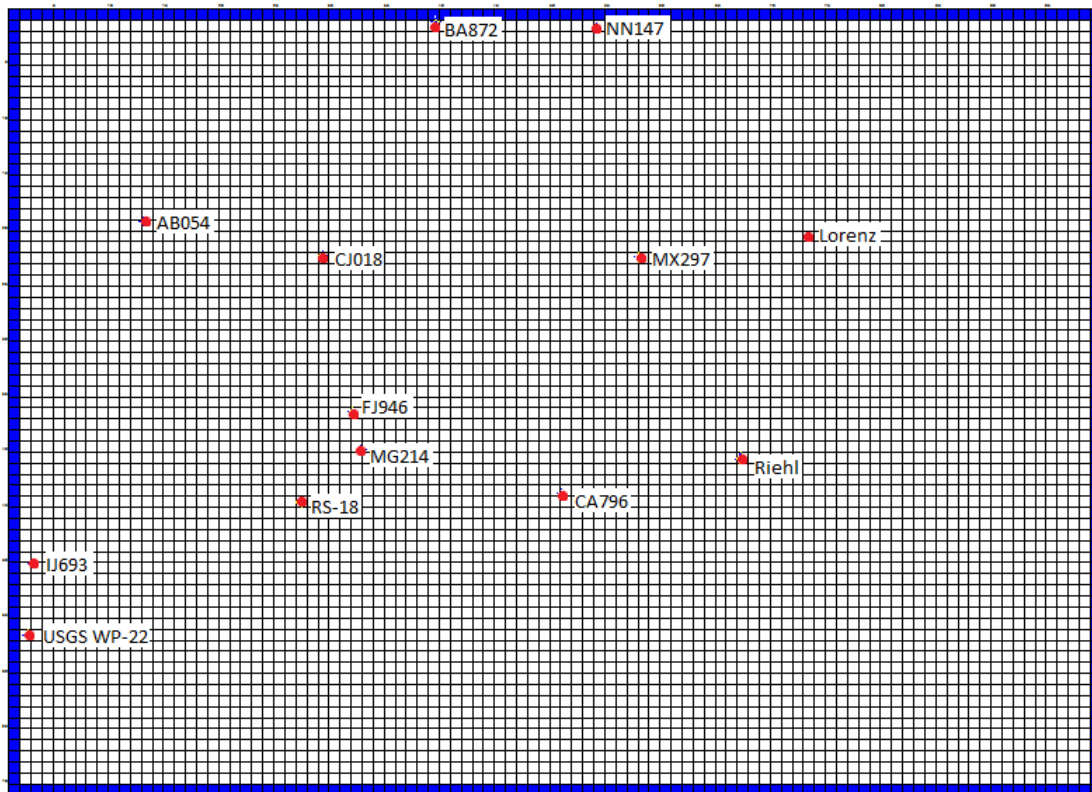


Figure G4. Location of head targets. Twenty targets are used from thirteen locations, with multiple targets at the RS-18 and Riehl sites. Note that targets labeled with two letters and three numbers are the WCRs.

Final Parameter Values

The final K_x and K_z values for the six models are shown in Table G2. The constant head value at the lower boundary was 760.28 in all six models. Except for zone 2 in model 10_7, which has a value of 6.4 in/yr, the value for both recharge zones is 1 in/yr for all six models. However, in model 10_7 the water table is above the land surface in the southwest corner of the model. The PEST determined value for recharge in zone 2 is less than that determined by Hooyer *et al.* (2008), who calculated the rate at only two sites and their value may not be representative of the entire area. Additionally, recharge results do not match the soil-water balance model recharge rates calculated by Hart & Schoephoester (2011), who estimated a mean recharge of 6.2 in/yr for Outagamie County, with some areas over 10 in/yr. Gebert *et al.* (2007) estimated mean recharge rates for Wisconsin based on streamflow measurements at gaging stations with long-term records. They estimated a mean recharge of 8.5 in/yr for all but the eastern edge of the modeling area, which they estimate at 1.6 in/yr.

Table G2. Final hydraulic conductivity values for each of the six models. K_x indicates horizontal hydraulic conductivity for both the x and y directions, and K_z vertical hydraulic conductivity.

Model:	10_7	18_7	19_8	22_6	25_9	29_4
Kx (ft/day)						
<i>lacustrine/till</i>	0.028	0.100	0.100	0.100	0.100	0.100
<i>sand</i>	4.535	4.536	4.536	4.538	4.536	4.535
<i>gravel</i>	70.866	70.866	70.866	70.866	70.866	70.866
Kz (ft/day)						
<i>lacustrine/till</i>	3.20E-03	1.11E-03	5.69E-04	1.55E-03	9.51E-04	5.60E-03
<i>sand</i>	0.454	0.454	0.454	0.454	0.454	0.454
<i>gravel</i>	7.087	7.087	7.087	7.087	7.087	7.087

In general, to improve calibration in cases where simulated heads are higher than observed values, recharge can be decreased or effective K (clay K for this site) can be increased to generate a better fit. For these six models, PEST determined the K_x of the clay to be 10^{-1} to 10^{-2} ft/day and K_z of the clay to be 10^{-3} to 10^{-4} ft/day. The determined K_z values are near the upper limit of the range of values of 10^{-3} to 10^{-7} ft/day determined by Hooyer *et al.* (2008); therefore, the recharge needed to be decreased in order to maintain measured values of K and have a better calibration. The difference in recharge rates between the soil-water balance model and the groundwater flow models could be due to the soil-water model accounting only for soil characteristics and not characteristics of glacial deposits. The WCRs indicated the presence of 0.5-1 ft of soil and 50-350 ft of glacial sediment throughout the modeled area. If recharge to the bedrock aquifers is more controlled by the thicker glacial sediment, the majority of which is fine-grained clay and till, lower recharge values would be expected. In addition to estimating mean recharge for Wisconsin based on streamflow measurements at long-term gaging stations, Gebert *et al.* (2007) also estimate mean recharge for low-flow partial-record stations in three major Wisconsin river basins. They found the overall basin estimate comparable to estimates based on data from the long-term streamflow-gaging stations, but found a wider range in recharge values (0.01 to 16.5 in/yr for the three studied basins). They note that it is likely this basin variability is typical in all the major drainage basins with calculated mean recharge from streamflow-gaging stations, and demonstrate this in a more recent report (Gebert *et al.*, 2009). Their estimate for the entire Wolf River Basin, which covers approximately 3,690 mi^2 , is 8.5 in/yr. However, low-flow partial record analysis determined a range of 0.1 to 34.4 in/yr in the Wolf River Basin. Furthermore, available records in the eastern half of the study area ranged from 0.1 to 2.2 in/yr, indicating it is likely that lower recharge values may be representative of the entire study area.

Calibration Results

The calibrated models varied in their ability to match the head targets (Table G3, Fig. G5). Generally, the RS-18 head targets had the best fit for all of the models (Fig. G6), which is expected given these were weighted higher during calibration. The shallow targets (Lorenz/Riehl) had the largest range of simulated values, likely due to a thicker layer 1. The absolute residual mean (arm) was between 10.93 ft and 12.50 ft for all six models, which is less than the arm value of 25.21 ft reported for the LMBM. Additionally, the mass balance was within 0.6% for all six models.

Eight measurements of stream flux data used to check the PEST calibrations (Fig. G3, Table G3). These measurements were made under approximately baseflow conditions. Two measurements were made for both Black Creek and the Shiocton River, in order to calculate a flux for one reach. The ditch feeding into the Embarrass River and Duck Creek had no measurable flows. All but one model simulated losing streams for both of these locations. For locations with measurable flow, a flow was considered to be simulated correctly if it was within one order of magnitude of the observed, due to the uncertainty in streamflow measurements. For Black Creek and the Shiocton River three of the models correctly simulated both streams, two correctly simulated flows for one of the streams, and only model 10_7 failed to correctly simulate either measured flow. With the exception of model 19_8, flows were simulated correctly for Toad Creek. Only two of the models correctly simulated flows for Bear Creek. However, Bear Creek runs nearly parallel to the southern model boundary; thus simulated fluxes may be affected by the specified head boundary. Individually, every model matched at least three of the six stream fluxes, with two matching a fourth target and three of them matching a fifth target. Thus results of the stream flux check indicate the PEST calibrations are acceptable, and any of the six models are equally plausible representations of glacial Lake Oshkosh sediment. However, none of these are highly calibrated models; thus they should not be used for groundwater management in Outagamie County.

Table G3. Calibration statistics for all six models. Note that only the heads were used as calibration targets with PEST, the stream flux data were used to check the calibrations. Stream fluxes are in ft³/d, with positive numbers for gaining streams and negative for losing. The Shiocton River and Black Creek were calculated for one reach from two stream flux measurements (measurement 1 was subtracted from measurement 2, see Fig. G3 for locations).

Model:		10_7	18_7	19_8	22_6	25_9	29_4
Head Targets							
Residual Mean (ft)		-10.37	-6.74	-6.80	-5.59	-5.80	-3.61
Absolute Residual Mean (ft)		12.50	11.94	11.31	12.12	10.93	11.99
Root Mean Squared Error (ft ²)		5044	4277	3977	4170	3673	4421
Minimum Residual (ft)		-39.33	-26.96	-32.17	-24.27	-30.12	-27.90
Maximum Residual (ft)		15.00	19.51	21.90	26.35	21.22	27.61
Stream Flux Calibration Check							
Duck Creek	No Flow	-1.49E+05	-6.54E+04	-9.11E+04	-4.65E+04	1.20E+04	-3.05E+03
Ditch-Embarrass	No Flow	-1.05E+05	-1.90E+04	-1.33E+05	-3.00E+04	-8.38E+04	-5.98E+04
Black Creek	5.66E+05	-1.25E+04	3.26E+04	-4.38E+04	6.00E+04	3.07E+05	2.30E+05
Shiocton River	-1.12E+05	8.54E+03	-2.04E+04	-4.41E+04	-1.44E+04	-1.97E+04	4.72E+03
Toad Creek	5.66E+04	2.82E+05	4.87E+04	-1.66E+04	2.13E+04	1.95E+04	1.25E+05
Bear Creek	3.76E+05	1.02E+05	-2.86E+04	-4.89E+04	-1.54E+04	-2.28E+04	3.58E+04

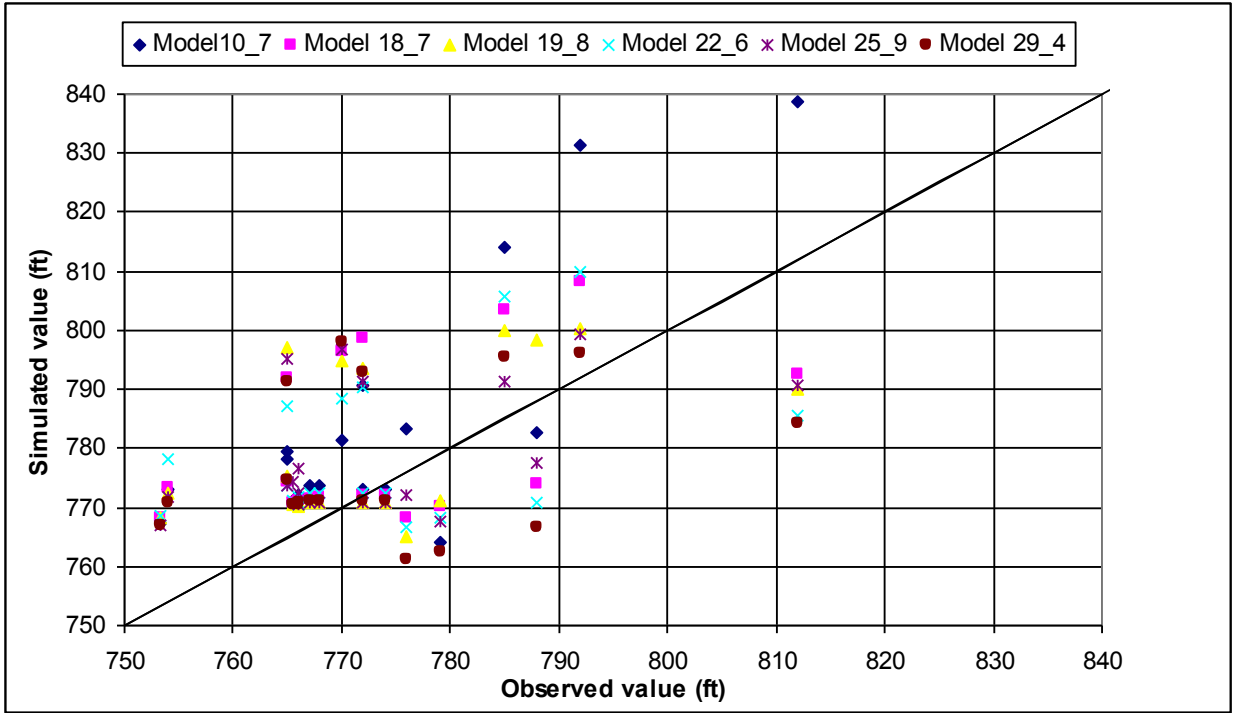


Figure G5. Observed versus simulated head values by model.

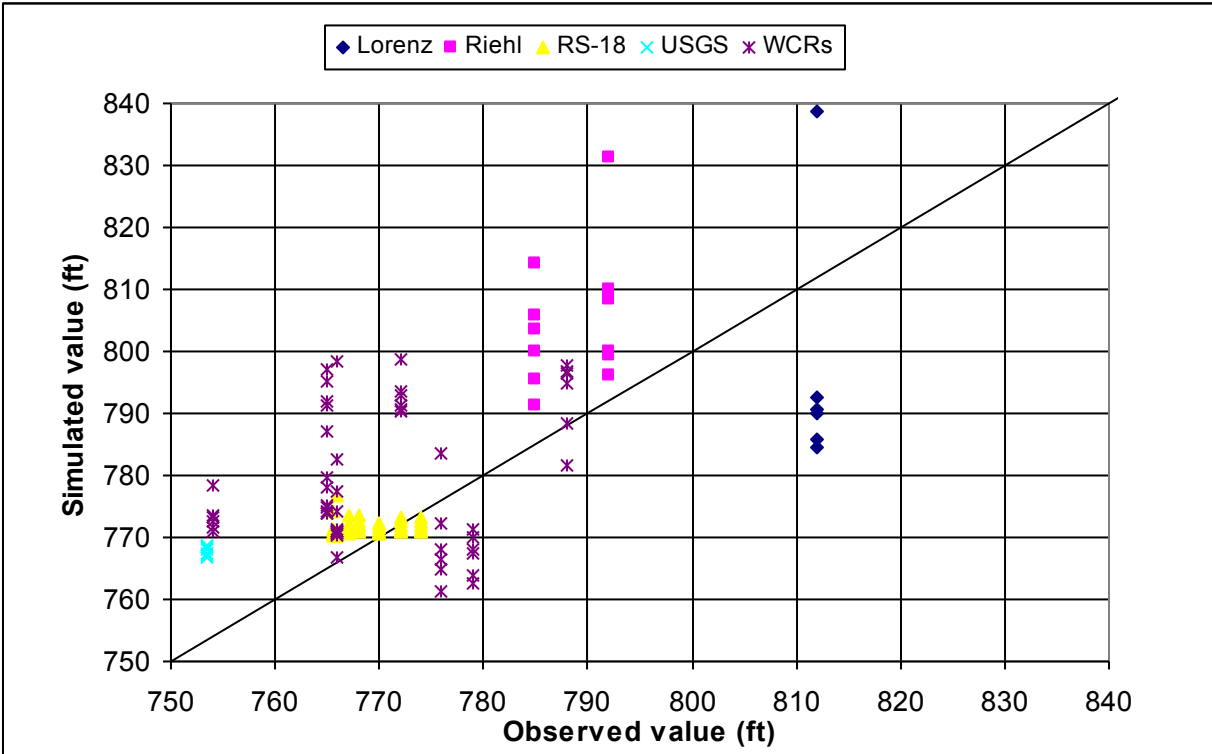


Figure G6. Observed versus simulated head values by target. Targets are grouped by location for the Lorenz, Riehl, RS-18, and USGS sites. All WCR target locations are grouped together. Note that the RS-18 targets have much better matches than the other sites.

MT3DMS

The groundwater flow models are run to steady-state and those heads are imported to MT3DMS (Zheng & Wang, 1999). A single stress period of 12,000 years (4.38×10^6 days) was selected for the MT3DMS simulations because this is the approximate length of time the entire model area was no longer glaciated and glacial Lake Oshkosh was fully drained and the area would likely start receiving modern day recharge values of $\delta^{18}\text{O}$. MT3DMS was run with an initial transport time step of 1,000 days with a 1.1 time-step multiplier and a maximum time step of 20,000 days, for a total of 241 transport time steps to reach the 12,000 years. The implicit finite difference solution with upstream weighting was used to solve for advection and dispersion.

Initial concentration of $\delta^{18}\text{O}$ for all cells was set at -30 ‰, a value typical of glacial-age water, and recharge set at -8‰, which represents modern day recharge values of $\delta^{18}\text{O}$ (Hooyer *et al.*, 2008). Dispersivity values of 100, 10^{-2} , and 10^{-4} ft were taken from Zheng and Bennett (2002) and assigned for longitudinal, transverse, and vertical dispersivity, respectively. Figures 11.4, 11.5, and 11.6 in Zheng and Bennett (2002) graphically display each of the dispersivities versus scale of observation, classifying the data by reliability. Values were selected from these figures, so that both the scale of observation and reliability were taken into account. It should be noted that dispersivity values are highly uncertain guesses at best.

Thirty $\delta^{18}\text{O}$ values from Hooyer *et al.* (2008) were used as an additional calibration check and to determine if the anomalous recent water found at depth could be explained by preferential flow paths. These targets are from four sites: Riehl, RS-18, RS-17, and RS-14 (Fig. 1). Each target is in a different layer, with the deepest located in layer 60.

The $\delta^{18}\text{O}$ values were matched the best by model 22_6 (Fig. G7, Table G4). Overall the best fit for all six models were the $\delta^{18}\text{O}$ values at RS-17 (Fig. G8). Figure G7 indicates that some of the models are allowing more recharge through certain areas of the bedrock valley so that the values are those of modern day recharge, while other models are restricting recharge so the values remain at the initial glacial water values. This difference is likely due to the presence of vertical preferential flow paths near the observation locations. Additionally, at seven of the targets modern $\delta^{18}\text{O}$ values were measured deep in the system while glacial values of $\delta^{18}\text{O}$ were measured in the shallow system. This suggests that present day recharge is being transported deep into the system via preferential flow paths. Overall, 76% of the simulated values at these anomalous seven targets for all six models are modern values; models 10_7 and 29_4 simulated modern $\delta^{18}\text{O}$ values for all seven targets.

The two models (18_7, 19_8) with the lowest percentage of particles exiting more than halfway vertically through the buried valley (Table 1) also had the most simulated $\delta^{18}\text{O}$ values remain at glacial values, indicating preferential flow is not occurring near the observations. Model 10_7 was the only model to have all simulated $\delta^{18}\text{O}$ values reach modern recharge values, indicating preferential flow is occurring near all observations. Also, as shown in Table 1, model 10_7 has a much higher percentage of particles exit the bedrock valley in fewer than 100 years (20.39%; all other models are less than 6%).

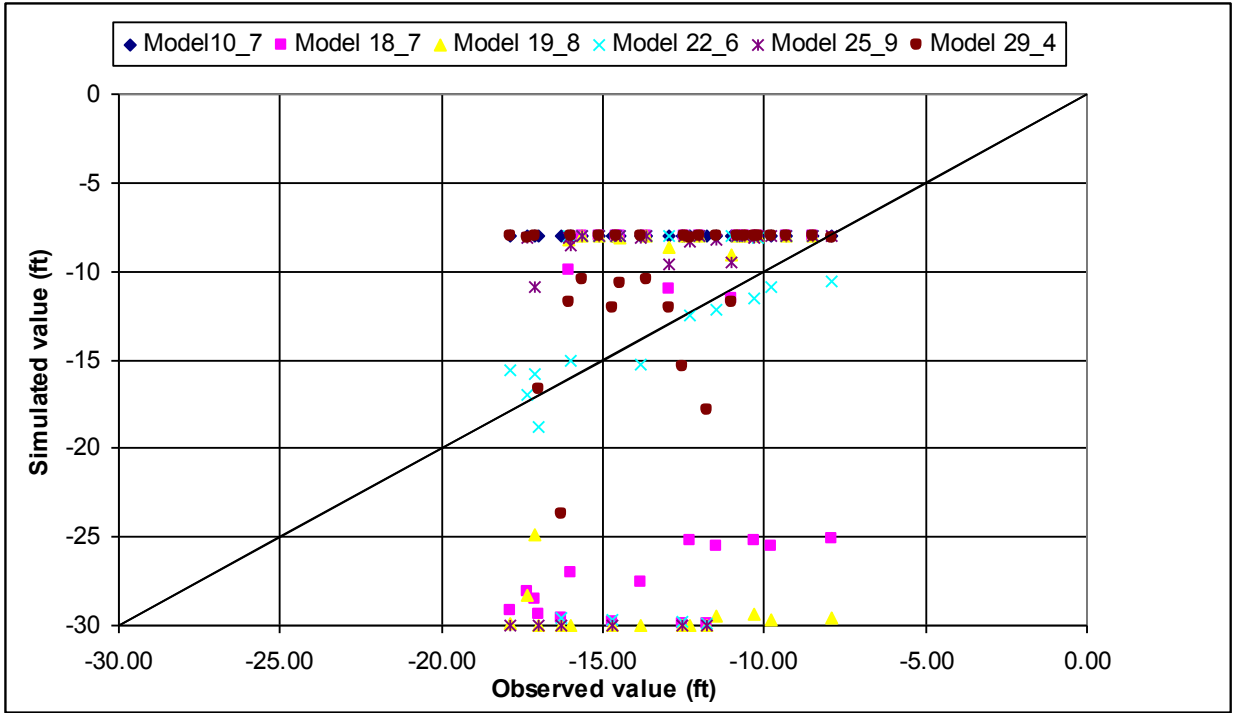


Figure G7. Observed versus simulated $\delta^{18}\text{O}$ values by model. Note the variation in models allowing more (e.g. 29_4) or less (e.g. 18_7) recharge to move through the deposits, likely due to the presence or lack of preferential flow paths near the observation locations, respectively. Also, model 22_6 matches the observed values much better than the other five models, indicated statistically in Table A4.1.

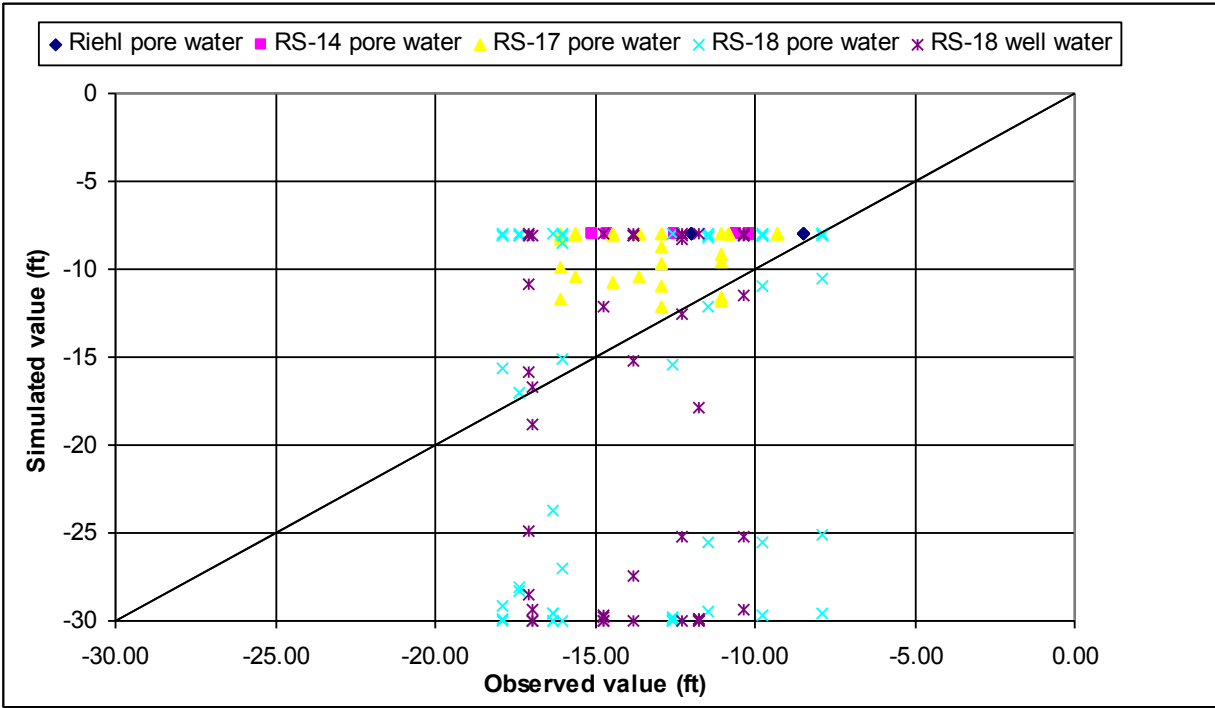


Figure G8. Observed versus simulated $\delta^{18}\text{O}$ values by location. Note that RS-18 is separated into pore and well water groups.

Table G4. Calibration statistics for all six models for the $\delta^{18}\text{O}$ values.

Model:	10 7	18 7	19 8	22 6	25 9	29 4
$\delta^{18}\text{O}$ Calibration Check						
Residual Mean (‰)	-5.16	5.00	5.65	-0.06	-0.47	-3.40
Absolute Residual Mean (‰)	5.17	8.97	10.00	4.90	6.46	4.56
Minimum Residual (‰)	-9.88	-7.63	-7.83	-8.07	-9.22	-10.26
Maximum Residual (‰)	0.09	18.11	21.69	18.12	18.24	7.44

APPENDIX H: Additional References in Appendices

- de Vries, Luis Manuel, Carrerra, Jesus, Falivene, Oriol, Gratacós, Oscar, and Slooten, Luit Jan, 2009. Application of Multiple Point Geostatistics to Non-stationary Images. *Mathematical Geosciences*, vol. 41, p. 29-42.
- Feinstein, D.T., Hunt, R.J., and Reeves, H.W., 2010, Regional groundwater-flow model of the Lake Michigan Basin in support of Great Lakes Basin water availability and use studies: U.S. Geological Survey Scientific Investigations Report 2010-5109, 379 p.
- Freeze, R.A. and Cherry, J., 1979. *Groundwater*. Hemel Hempstead: Prentice Hall International, 660 p.
- Gebert, Warren A., Radloff, Mandy J., Considine, Ellen J., and Kennedy, James L, 2007. Use of streamflow data to estimate base flow/ground-water recharge for Wisconsin. *Journal of the American Water Resources Association*, vol. 43, no. 1, p. 220-236.
- Gebert, Warren A, Walker, John F., and Kennedy, James L., 2009. Estimating 1970-99 Average Annual Groundwater Recharge in Wisconsin Using Streamflow Data. U.S. Geological Survey Open-File Report 2009-1210, 118 p.
- Hart, David and Schoepfoester, Peter, 2011. Groundwater recharge in Calumet, Outagamie, and Winnebago Counties, Wisconsin, estimated by a GIS-based water-balance model: Wisconsin Geological and Natural History Survey, Open-file Report 2011-05, 26 p.
- Ward, David S., Buss, David R., Mercer, James W., and Hughes, Shereen S., 1987. Evaluation of a groundwater corrective action at the Chem-Dyne Hazardous Waste Site using a telescopic mesh refinement modeling approach. *Water Resources Research*, vol. 23, no. 4, p. 603-617.
- Zheng, Chunmiao and Bennett, Gordon D., 2002. Applied Contaminant Transport Modeling, John Wiley and Sons, Inc., New York, 621 p.

The Effects of Particulate Organic Carbon Quantity and Quality on Denitrification of Groundwater Nitrate

Basic Information

Title:	The Effects of Particulate Organic Carbon Quantity and Quality on Denitrification of Groundwater Nitrate
Project Number:	2011WI297O
Start Date:	7/1/2011
End Date:	6/30/2013
Funding Source:	Other
Congressional District:	6th
Research Category:	Ground-water Flow and Transport
Focus Category:	Hydrogeochemistry, Sediments, Water Quality
Descriptors:	
Principal Investigators:	Robert Scott Stelzer

Publications

There are no publications.

Annual Progress Report

Selected Reporting Period: 7/1/2011 - 6/30/2012

Submitted By: Robert Stelzer

Submitted: 5/27/2013

Project Title

WR11R006: The Effects of Particulate Organic Carbon Quantity and Quality on Denitrification of Groundwater Nitrate

Project Investigators

Lynn Bartsch, Other

J. Thad Scott, Other

Robert Stelzer, University of Wisconsin-Oshkosh

Progress Statement

During the period between July 1, 2011 and June 30, 2012 we made significant progress on the project "WR11R006: The effects of particulate organic carbon quantity and quality on denitrification of groundwater nitrate". One experiment funded by this award was successfully completed and the details of the experiment and stage of completion are provided in more detail below.

Experiment 1- 2011 The effects of particulate carbon quantity on nitrogen processing deep stream sediments.

The interface between groundwater and surface water in streams is known to be a hotspot for nitrogen processing. However, the role of buried organic carbon in nitrogen transformation at this interface is not well understood, and inferences have been largely based on descriptive studies. Our main objective was to determine how buried particulate organic carbon (POC) affected denitrification and nitrate retention in groundwater of an upwelling reach within a sand plains stream in Wisconsin. POC was manipulated in mesocosms inserted in the sediments. Treatments included Low and High quantities of conditioned red maple leaves (buried beneath combusted sand), Ambient sediment (sand containing background levels of POC), and a Control (combusted sand). Denitrification rate in sediments was measured by acetylene block assays in the lab and by changes in N₂ concentrations in the field using membrane inlet mass spectrometry. Nitrate, ammonium, and dissolved organic nitrogen (DON) retention were measured by changes in concentrations and fluxes along groundwater flow paths within the mesocosms. POC addition drove oxic groundwater to severe hypoxia, led to large increases in dissolved organic carbon (DOC) and strongly increased denitrification rates and nitrogen (nitrate and total dissolved nitrogen) retention relative to the Control. In situ denitrification accounted for 30 to 60 % of nitrate retention. Collectively, our results suggest that buried POC stimulated denitrification and nitrate retention by producing DOC and by creating favorable redox conditions for denitrification.

All of the tasks for this experiment have been completed, with the exception of revision of a manuscript that stems from this work (see below)

Dr. Stelzer was invited to submit a manuscript about this work in a special issue of Freshwater Science about groundwater-surface water interaction in streams and rivers. The manuscript, entitled "Buried particulate organic carbon stimulates denitrification and nitrate retention in stream sediments at the groundwater-surface water interface" will be submitted to Freshwater Science in 2013 for the special issue.

Principal Findings and Significance

Principal Findings and Significance

Description

The principle finding from our project is that buried particulate organic matter quantity had positive effects on nitrate retention and denitrification in stream sediments. We think these results will impact the fields of biogeochemistry and aquatic

ecology because they suggest mechanisms by which nitrate in groundwater can be removed along upwelling flow paths in sediments. Our results reinforce the importance of linked biogeochemical cycles, in this case the carbon and nitrogen cycles. Furthermore, our results suggest that intact riparian zones and forested watersheds can promote nitrate retention at the groundwater-stream water interface by providing a supply of fixed carbon to support nitrate retention (including denitrification). Our results may have implications for stream restoration. Restoration techniques in the watershed and stream channel that promote the accumulation of terrestrial fixed carbon and deposition and burial of this carbon in stream sediments will likely increase nitrate retention.

Committees, Memberships & Panels

Group Name Wisconsin AWRA Board of Directors
Description Dr. Stelzer served as Vice President of the Wisconsin Section of the American Water Resources Association during the dates indicated below
Start Date 3/8/2011
End Date 3/7/2012

Presentations & Public Appearances

Title Buried particulate organic carbon stimulates denitrification and nitrate retention in stream sediments
Presenter(s) R.S. Stelzer, J. T. Scott, L.A. Bartsch
Presentation Type Professional meeting
Event Name Society for Freshwater Science Annual Meeting
Event Location Louisville, KY
Event Date 5/21/2012
Target Audience Scientific audience
Audience Size 100
Description Invited presentation in a Special Session on sediment processes

Students & Post-Docs Supported

Student Name Jennifer Krueger
Campus University of Wisconsin-Oshkosh

Advisor Name Robert Stelzer
Advisor Campus University of Wisconsin-Oshkosh

Degree Undergraduate
Graduation Month August
Graduation Year 2011
Department Biology
Program
Thesis Title
Thesis Abstract

.....

Student Name Michael Louison
Campus University of Wisconsin-Oshkosh

Advisor Name Robert Stelzer

Advisor Campus University of Wisconsin-Oshkosh

Degree Expected Masters

Graduation Month December

Graduation Year 2013

Department Biology

Program MS

Thesis Title

Thesis Abstract



Student Name Alyssa McCumber

Campus University of Wisconsin-Oshkosh

Advisor Name Robert Stelzer

Advisor Campus University of Wisconsin-Oshkosh

Degree Undergraduate

Graduation Month December

Graduation Year 2012

Department Biology

Program

Thesis Title

Thesis Abstract

Silage Leachate: Waste Quality Assessment and Treatment

Basic Information

Title:	Silage Leachate: Waste Quality Assessment and Treatment
Project Number:	2011WI298O
Start Date:	7/1/2011
End Date:	6/30/2013
Funding Source:	Other
Congressional District:	2nd
Research Category:	Ground-water Flow and Transport
Focus Category:	Groundwater, Solute Transport, Nitrate Contamination
Descriptors:	
Principal Investigators:	, Rebecca A Larson

Publications

There are no publications.

Annual Progress Report

Selected Reporting Period: 7/1/2011 - 6/30/2012

Submitted By: Rebecca Larson

Submitted: 5/29/2013

Project Title

WR11R007: Silage Leachate: Waste Quality Assessment and Treatment

Project Investigators

Rebecca Larson, University of Wisconsin-Madison

John Panuska, University of Wisconsin-Madison

Progress Statement

Three silage storage sites for monitoring silage runoff have been identified and equipment installed to collect samples from each. Runoff samples from 6+ storm events have been collected and analyzed at each site. The sites will continue to be monitored throughout the next year. The two side by side filter strips were established at the Dairy Forage Research Center in Prairie du Sac, WI. Collection and application of silage runoff will continue for these two filter strips over the next year.

Principal Findings and Significance

Principal Findings and Significance

Description In the initial data collection phases of the project researchers are seeing significant changes in runoff quality from storm to storm and from site to site. Additional data will be required to determine significance of these changes throughout the next year. However, the collection information has been used to design additional studies throughout the state for additional data collection in conjunction with UW Discovery Farms.

Students & Post-Docs Supported

Student Name Michael Holly
Campus University of Wisconsin-Madison

Advisor Name Rebecca Larson
Advisor Campus University of Wisconsin-Madison

Degree Masters
Graduation Month July
Graduation Year 2013
Department Biological Systems Engineering
Program
Thesis Title Silage Runoff Characterization and Treatment Using Agricultural Filter-strips
Thesis Abstract

Identifying the Controls on Flow and Contaminant Distribution in Siliciclastic Bedrock Aquifer Systems.

Identifying the Controls on Flow and Contaminant Distribution in Siliciclastic Bedrock Aquifer Systems.

Basic Information

Title:	Identifying the Controls on Flow and Contaminant Distribution in Siliciclastic Bedrock Aquifer Systems.
Project Number:	2012WI3200
Start Date:	7/1/2012
End Date:	6/30/2014
Funding Source:	Other
Congressional District:	WI-2
Research Category:	Ground-water Flow and Transport
Focus Category:	Water Quality, Hydrology, Water Supply
Descriptors:	distributed temperature sensing, Cambrian sandstone
Principal Investigators:	David J. John Hart

Publications

There are no publications.

WRI: FY 2013 State of Wisconsin Groundwater Research and Monitoring Proposals

Proposal Number:

13-CTP-02

Title:

Identifying the Controls on Flow and Contaminant Distribution in Siliciclastic Bedrock Aquifer Systems.

Abstract:

This proposed research will advance characterization of groundwater flow in aquifers and aquitards in siliciclastic bedrock systems. Improved understanding of flow and contaminant transport in these hydrogeologic systems will allow for better water supply well siting and design. The research includes investigation of heterogeneity within siliciclastic aquifers and aquitards, and examines how heterogeneity is related to the distribution of anthropogenic and naturally occurring contaminants.

The selected study area for this research, the Cambrian sandstone aquifer in south-central Wisconsin, is traditionally described as a relatively homogeneous hydrogeologic unit with a notable lack of differentiation within Cambrian formations. However, recent evidence suggests significant variability in hydraulic conductivity, including fracture flow pathways, within these units. We will use distributed temperature sensing (DTS) technology, straddle packers, borehole flow logging, and traditional pumping tests to measure variation in hydraulic properties with depth in the aquifer. Such measurements, including evaluation of transmissive fractures, will determine the relative influence of fracture flow and intergranular flow in sandstone aquifers.

Aquitards play a significant role in groundwater flow and contaminant distribution and are often assumed to be perfect barriers to contaminant transport, yet are often poorly characterized. The proposed work includes improvements to in situ hydraulic conductivity tests in low-permeability strata. We will refine a shut-in pressure test that will allow for more rapid and accurate assessment of hydraulic properties of low hydraulic conductivity sedimentary layers.

Finally, this project includes assessment of groundwater chemistry to link physical heterogeneity of the system with chemical heterogeneity. This will be accomplished by sampling groundwater from discrete intervals of interest for major ions, trace metals, radioactivity, and indicators of redox conditions. The geochemistry data will support improved conceptual models of the effects of physical heterogeneity on water chemistry.

Location of Research:

South-central Wisconsin (Columbia, Dane, Dodge, and Sauk Counties)

Investigator(s):

David Hart, UW-Extension (Principal Investigator)

Madeline Gotkowitz, UW-Extension (Associate Investigator)

Jean Bahr, UW-Madison (Associate Investigator)

Effects of Nuanced Changes in Lot Layout and Impervious Area Connectivity on Urban Recharge

Basic Information

Title:	Effects of Nuanced Changes in Lot Layout and Impervious Area Connectivity on Urban Recharge
Project Number:	2012WI321O
Start Date:	7/1/2012
End Date:	6/30/2014
Funding Source:	Other
Congressional District:	WI-2
Research Category:	Ground-water Flow and Transport
Focus Category:	Water Supply, Management and Planning, Hydrology
Descriptors:	infiltration
Principal Investigators:	Steven Loheide

Publications

There are no publications.

WRI: FY 2013 State of Wisconsin Groundwater Research and Monitoring Proposals

Proposal Number:

13-HDG-02

Title:

Effects of Nuanced Changes in Lot Layout and Impervious Area Connectivity on Urban Recharge

Abstract:

The water balance in urban watersheds is strongly controlled by precipitation patterns and the large-scale presence and arrangement of impervious area, within the watershed. While it is well known that the configuration of impervious area within an urban catchment has a predictable impact on the catchment's rainfall-runoff response, the response of groundwater recharge to urbanization is difficult to estimate. Recent studies have found both increases and decreases when examining recharge's response to the gross arrangement of impervious surface in the watershed. Very little work has been done to identify how nuanced, small-scale changes in impervious area configuration and connectivity, such as downspout disconnection distance and driveway pitch, impact recharge rates. The objective of this study is to determine the extent to which the amount, arrangement, and connectivity of impervious area in urban residential lots impacts recharge in urban watersheds. We hypothesize that there are some layouts and connectivity schemes that will promote recharge by concentrating infiltration and developing strong, fast-moving wetting fronts that are able to penetrate through the root zone without entirely being extracted by roots. Because existing hydrological models do not capture the arrangement of impervious area at the parcel scale, we will address our research questions by constructing our own, physically-based model of water movement through urban lots. Using our model, we will conduct a factorial experiment wherein we determine how recharge responds to lot layout, connectivity between impervious areas, soil types, and rainfall patterns. Our results will suggest ideal layouts of urban residential lots for achieving various recharge management goals, and our work will also contribute to the larger body of literature that seeks to quantify how urbanization impacts groundwater recharge. Empirical relationships we develop in this study will be useful for scaling up the effects of parcel-level configuration on hydrology to the larger, catchment scale.

Location of Research:

Madison, WI Sun Prairie, WI

Investigator(s):

Steven Loheide, UW-Madison (Principal Investigator)

Jeffrey Miller, UW-Madison (Associate Investigator)

Transport of Manure-derived Escherichia coli within Naturally-Fractured Dolomite

Basic Information

Title:	Transport of Manure-derived Escherichia coli within Naturally-Fractured Dolomite
Project Number:	2012WI3220
Start Date:	7/1/2012
End Date:	6/30/2014
Funding Source:	Other
Congressional District:	WI-4
Research Category:	Ground-water Flow and Transport
Focus Category:	Water Quality, Agriculture, Toxic Substances
Descriptors:	carbonate aquifers, remobilization kinetics, Laboratory experiments
Principal Investigators:	Shangping Xu

Publications

There are no publications.

WRI: FY 2013 State of Wisconsin Groundwater Research and Monitoring Proposals

Proposal Number:

13-CTP-05

Title:

Transport of Manure-derived Escherichia coli within Naturally-Fractured Dolomite

Abstract:

In Northeastern Wisconsin, the unconfined dolomite aquifer represents a major source of drinking water. Well monitoring data showed that microbial contamination is prevalent in this aquifer. In general, manure is considered the most likely source of the microbial contamination. However, little is known about the transport behavior of manure-derived bacteria within the dolomite fractures under varying water chemistry and flow conditions. The primary goal of this proposed research is to fill this knowledge gap through a series of laboratory-scale experiments using naturally-fractured dolomite samples. Specifically, I plan to examine the transport behavior of manure-derived E. coli within natural dolomite fractures under a range of water chemistry and flow conditions. I will also investigate the remobilization kinetics of previously retained E. coli cells due to water chemistry and flow perturbations. Findings from this proposed research will advance our understanding of the mechanisms that control the retention and release of E. coli, a representative indicator bacterium, within natural dolomite fractures and will provide useful kinetics parameters for the future development, refinement and validation of predictive mathematical models. Combined with field observation data, the results obtained from this research will also provide a basis for evaluating the public health risks associated with the application of manure as a fertilizer in agricultural fields (e.g., to identify the private wells that are most susceptible to microbial contamination). Additionally, the findings can lead to improved manure management practices, such as the timing of manure application and the selection of agricultural fields for manure application, which can potentially reduce the risks of groundwater contamination by manure-derived bacteria. Because fractured carbonate aquifers represent important sources of drinking water in areas beyond the state of Wisconsin and bacterial contamination of fractured rock aquifers by livestock manure has been documented in many other places, the expected findings from this project will have broad applications by advancing our understanding of the spread of bacteria in saturated fractured geological formations.

Location of Research:

UW-Milwaukee

Investigator(s):

Shangping Xu, UW-Milwaukee (Principal Investigator)

An Evaluation of the Distribution and Sources of Dissolved Strontium in the Groundwater of Eastern Wisconsin, with a Focus on Brown and Outagamie Counties

Basic Information

Title:	An Evaluation of the Distribution and Sources of Dissolved Strontium in the Groundwater of Eastern Wisconsin, with a Focus on Brown and Outagamie Counties
Project Number:	2012WI3230
Start Date:	7/1/2012
End Date:	6/30/2013
Funding Source:	Other
Congressional District:	WI-8
Research Category:	Ground-water Flow and Transport
Focus Category:	Water Quality, Hydrogeochemistry, Solute Transport
Descriptors:	municipal wells, Piper Plots,
Principal Investigators:	John Luczaj, Michael Edward Zorn

Publications

There are no publications.

WRI: FY 2013 State of Wisconsin Groundwater Research and Monitoring Proposals

Proposal Number:

13-GCP-01

Title:

An Evaluation of the Distribution and Sources of Dissolved Strontium in the Groundwater of Eastern Wisconsin, with a Focus on Brown and Outagamie Counties

Abstract:

Groundwater in hundreds of eastern Wisconsin wells contains dissolved strontium (Sr) at levels that exceed lifetime and short-term EPA Health Advisories of 4 mg/L and 25 mg/L, respectively. The most widely recognized adverse health effect from Sr ingestion is a musculoskeletal disease known as "strontium rickets".

Affected wells include many municipal wells from suburban Milwaukee north to Green Bay. In addition, an anomaly of high Sr in domestic wells exists in Brown County in the Town of Lawrence. An analysis of groundwater Sr concentrations, local bedrock geochemistry, well construction, and hydrostratigraphy is needed to understand the scope of the problem.

Our study will determine the regional and stratigraphic distribution of dissolved Sr in the groundwater of eastern Wisconsin, with a focus on Brown and Outagamie counties. In addition, we will identify mineral sources of Sr in bedrock aquifers. Our research will include an analysis of existing and new water quality data, well construction data, whole-rock samples from drill cores, and isotopic "fingerprinting" of strontium sources. New water quality data (Sr²⁺, general chemistry) will be collected from 100-200 wells in Brown and Outagamie counties and used to construct Piper Plots and cross plots to understand the geochemistry of Sr in the groundwater system in this part of Wisconsin.

We also propose to drill a bedrock core in the Town of Lawrence through the Ordovician carbonate section to evaluate bedrock Sr concentrations and host minerals in this anomalous area. Additional data from water well cuttings and rock quarries in western Brown and eastern Outagamie counties will be gathered.

Solid minerals such as calcite, dolomite, strontianite, and celestite will preserve a ⁸⁷Sr/⁸⁶Sr-isotopic signature indicative of their mode of origin. Strontium-isotopic analysis of mineral phases and dissolved Sr in groundwater will allow us to "fingerprint" the specific source of strontium in the groundwater.

Location of Research:

The main focus is on Brown and Outagamie Counties, with a general data analysis for available statewide data.

Investigator(s):

John Luczaj, UW-Green Bay (Principal Investigator)

Michael Zorn, UW-Green Bay (Principal Investigator)

Joseph Baeten, UW-Green Bay (Associate Investigator)

Hexavalent Chromium (Cr(VI)) in WI Groundwater: identifying factors controlling the natural concentration and geochemical cycling in a diverse set of aquifers

Hexavalent Chromium (Cr(VI)) in WI Groundwater: identifying factors controlling the natural concentration and geochemical cycling in a diverse set of aquifers

Basic Information

Title:	Hexavalent Chromium (Cr(VI)) in WI Groundwater: identifying factors controlling the natural concentration and geochemical cycling in a diverse set of aquifers
Project Number:	2012WI324O
Start Date:	7/1/2012
End Date:	6/30/2014
Funding Source:	Other
Congressional District:	WI-2
Research Category:	Ground-water Flow and Transport
Focus Category:	Water Quality, Solute Transport, Geochemical Processes
Descriptors:	kinetics, dissolution rates
Principal Investigators:	Patrick Gorski, Martin Shafer

Publications

There are no publications.

WRI: FY 2013 State of Wisconsin Groundwater Research and Monitoring Proposals

Proposal Number:

13-GCP-02

Title:

Hexavalent Chromium (Cr(VI)) in WI Groundwater: identifying factors controlling the natural concentration and geochemical cycling in a diverse set of aquifers.

Abstract:

This proposal addresses the specific problem that detectable concentrations of hexavalent chromium (Cr(VI)) have been measured in drinking water sourced from Wisconsin groundwater. Although chromium (Cr) is a naturally occurring in groundwater, Cr(VI) - Cr in the +6 oxidation state - is a known carcinogen. The biogeochemical cycling of Cr between the +6 oxidation state and the more benign +3 oxidation state (Cr(III)), as well as interaction with aquifer material at ambient groundwater conditions, needs to be fully assessed to determine potential human health concerns within certain aquifers of Wisconsin. We hypothesize that mineralized edges of three major geological basins of Wisconsin provide conditions favorable to the formation of Cr(VI). Our objective is to characterize the major aquifers of Wisconsin as to their natural background concentrations and release rates of total Cr and Cr(VI) through the use of controlled laboratory experiments on freshly collected aquifer cuttings obtained from drilling wells. We will use reactor studies to evaluate oxidation state specific release and dissolution rates from aquifer material, as well as reactors amended with reference material, which will be measured during timed kinetic studies to provide a mechanistic understanding of Cr(VI) cycling. Detailed chemical and oxidation state speciation measurements of both solution-phase and solid phase materials will be done using state-of-the-art low level analyses and established methods for a series physical, inorganic and organic parameters. By integrating the data from the reactor studies and detailed chemical and oxidation measurements, we will develop a mechanistic model of Cr release from the contrasting aquifers. Our findings will help both private well owners, public utilities and agencies better assess human health concerns regarding exposure to Cr(VI) and allow for predictions as to which aquifers are disposed to greater Cr(VI) release and formation under both natural and anthropogenic perturbation.

Location of Research:

Wisconsin, state-wide

Investigator(s):

Patrick Gorski, UW-Madison (Principal Investigator)

Martin Shafer, UW-Madison (Principal Investigator)

Information Transfer Program Introduction

The University of Wisconsin Water Resources Institute (WRI) facilitates research, training and information transfer on state, regional and national water resource problems. It is the focal point for water resources research, education and outreach within the University of Wisconsin System, fostering strong collaborative scientific exploration that links researchers with state water managers and users statewide.

The new knowledge and technology born of WRI-funded work is shared with varied audiences and is within the scope of work of the information transfer program. Depending on the receiving audiences, the non-advocating, science-based information then leads to certain activities and results. For WRI's research audience, it is inspiration for further work, or validation of prior work. For WRI's policy maker/decision maker audience, it leads to science-based policies and decisions. For WRI's student audience, it encourages a career in the water resources field, and fosters the skills needed for success. For WRI's general public audience, it builds science literacy, which in turn, leads to understanding and stewardship of water resources.

The information transfer program adopts both strategic and tactical methods to disseminate WRI results and techniques. Information is pushed out through the program's websites, outreach activities, social media channels, earned media efforts and publications of various types. This ensures the latest water-related research findings and processes reach those who will convert it to further results. Faculty, staff and students; public officials; administrators; and industry representatives rely on WRI as a source of objective, scientifically sound information.

University of Wisconsin Water Resources Institute - 5 Year Information Transfer Program

Basic Information

Title:	University of Wisconsin Water Resources Institute - 5 Year Information Transfer Program
Project Number:	2011WI265B
Start Date:	3/1/2011
End Date:	2/28/2015
Funding Source:	104B
Congressional District:	WI-2
Research Category:	Not Applicable
Focus Category:	Education, Climatological Processes, Groundwater
Descriptors:	
Principal Investigators:	Moira Harrington

Publications

1. White, Elizabeth; Carolyn Rumery Betz; Aaron Conklin; Moira Harrington; Ann Moser. 2011, Volume 1 Aquatic Sciences Chronicle 8 pages
2. White, Elizabeth; Carolyn Rumery Betz; Aaron Conklin; Moira Harrington; Ann Moser. 2011, Volume 2 Aquatic Sciences Chronicle 8 pages
3. White, Elizabeth; Carolyn Rumery Betz; Aaron Conklin; Moira Harrington; Ann Moser. 2011, Volume 3 Aquatic Sciences Chronicle 10 pages
4. White, Elizabeth; Carolyn Rumery Betz; Aaron Conklin; Moira Harrington; John Karl; Ann Moser. 2011, Volume 4 Aquatic Sciences Chronicle 12 pages
5. Karl, John Streams Neutralize Nitrates in Groundwater 2011 5:51-minute video
6. Harrington, Moira; Aaron Conklin. wri.wisc.edu program website
7. Moser, Anne; Sarah Leeman. aqua.wisc.edu/waterlibrary program website
8. Conklin, Aaron; Carolyn Rumery Betz; Moira Harrington. facebook.com/UWiscSeaGrant Facebook page for University of Wisconsin Water Resources Institute and University of Wisconsin Sea Grant Institute
9. Conklin, Aaron; Carolyn Rumery Betz, Moira Harrington. @UWiscSeaGrant Twitter address for both University of Wisconsin Water Resources Institute and University of Wisconsin Sea Grant Institute
10. Rumery Betz, Carolyn; et al. 2011, 35th Annual Meeting Program and Abstracts Wisconsin's Role in Great Lakes Restoration, American Water Resources Association, Wisconsin Section. 76 pages
11. Babiarz, Christopher; James P. Hurley; David P. Krabbenhoft; James G. Wiener July, 19, 2011, Wisconsin Leads the World in Mercury Research opinion-page column, 2 pages
12. Rumery Betz, Carolyn; Kevin Masarik. March 7, 2011 Spring is a Good Time to Test Well Water news release, 2 pages
13. Rumery Betz, Carolyn; Kevin Masarik. March 2, 2011 Celebrate Groundwater Awareness Week by Properly Filling and Sealing Unused Wells news release 2 pages
14. Rumery Betz, Carolyn; Kevin Masarik March 1, 2011 Dispelling Groundwater Myths news release 2 pages

University of Wisconsin Water Resources Institute - 5 Year Information Transfer Program

15. White, Elizabeth; Aaron Conklin; Moira Harrington; Ann Moser; Marie Zhuikov 2012, Volume 2 Aquatic Sciences Chronicle 12 pages
16. White, Elizabeth; Aaron Conklin; Moira Harrington; Ann Moser; Marie Zhuikov 2012, Volume 3 Aquatic Sciences Chronicle 12 pages
17. White, Elizabeth; Aaron Conklin; Moira Harrington; Ann Moser; Marie Zhuikov 2012, Volume 4 Aquatic Sciences Chronicle 12 pages
18. White, Elizabeth; Aaron Conklin; Moira Harrington; John Karl; Ann Moser; Marie Zhuikov 2013, Volume 1 Aquatic Sciences Chronicle 8 pages
19. Karl, John What's a Spring 2012 27-second video
20. Harrington, Moira; Aaron Conklin; Marie Zhuikov wri.wisc.edu program website
21. Moser, Anne; Peter Rudrud aqua.wisc.edu/waterlibrary program website
22. Moser, Anne water.wisc.edu portal website
23. Conklin, Aaron; Marie Zhuikov; Moira Harrington [facebook.com/UWiscSeaGrant](https://www.facebook.com/UWiscSeaGrant) Facebook page for University of Wisconsin Water Resources Institute and University of Wisconsin Sea Grant Institute
24. Conklin, Aaron; Marie Zhuikov; Moira Harrington @UWiscSeaGrant Twitter handle for both University of Wisconsin Water Resources Institute and University of Wisconsin Sea Grant Institute
25. Moser, Anne. @WiscWaterLib Twitter handle for Wisconsin's Water Library
26. Moser, Anne. Facebook page for Wisconsin's Water Library [facebook.com/WiscWaterLib](https://www.facebook.com/WiscWaterLib)
27. White, Elizabeth; et al. 2012, 36th Annual Meeting Program and Abstracts Science-Based Policy for Wisconsin's Water Resources, American Water Resources Association, Wisconsin Section. 93 pages
28. Andren, Anders March 7, 2012, Consider the Tide Under Your Feet, opinion-page column, 2 pages
29. Harrington, Moira April 9, 2012 New Director of Sea Grant Institute and Water Resources Institute Chosen news release, 2 pages
30. Zhuikov, Marie January 2, 2013 Study Shows Mercury Deposited Into Lakes Quickly Finds Its Way Into Fish news release, 2 pages
31. Babiarez, Chris; Marie Zhuikov October 2012 Nitrates in Groundwater fact sheet, 4 pages
32. Babiarez, Chris; Marie Zhuikov October 2012 Arsenic in Groundwater fact sheet 4 pages

Information and Outreach Activities

In this reporting period, the University of Wisconsin Water Resources Institute (WRI) Information Transfer Program produced and/or distributed publications, messages through social media outlets, news releases, a quarterly newsletter, videos, a seven-part audio podcast series and information transfer at public events; maintained websites; co-sponsored and assisted in planning and conducting a major statewide conference on water resources; maintained and expanded a library on water resources that also conducts outreach through lifelong learning presentations and youth activities.

In this reporting period in the area of media relations, the program distributed three news releases and distributed an opinion-page column regarding the importance of groundwater (<http://wri.wisc.edu/pressroom/Details.aspx?PostID=1148>).

A notable achievement in media relations was the distribution of information about WRI-funded research on how quickly “new” mercury is dispersed through the environment. Scientific American published material, along with outlets that appeal to members of the general public. Those outlets included the Huffington Post and the Los Angeles Times both with very large reach, 6 million people daily and 1.6 million people daily, respectively. Wisconsin newspapers and radio stations also distributed the research findings. The research was released in January 2013. The WRI website had a 35 percent increase in visitors over the previous January as people accessed the site for more information on the findings.

Social media offers the means to speak directly, and interactively, with engaged audiences. WRI reached an estimated 1,200 people a week through Facebook and Twitter. If that group of people shared WRI messages with their contacts, there was the potential to reach nearly 345,000 people in a week. WRI also uses the social media tools Flickr, YouTube and Tumblr.

The WRI website, <http://www.wri.wisc.edu>, orients visitors to the Wisconsin program and includes a variety of information for those interested in water-related issues. In this reporting period, the site was redesigned to improve functionality. It also added a home page video player that keeps visitors on the site—rather than sending them off to YouTube—to view videos on topics such as contaminants in groundwater and the role of streams to neutralize nitrates. One of the site’s main audiences is researchers. To that end, the site provides a clear navigational path to the WRI project listing, project reports, a groundwater research database, funding opportunities and conference information sections. The areas are updated on a regular basis to ensure currency of information transfer. The WRI site had 35,819 visitors in this reporting period. That is a 26 percent increase in visitors over the previous reporting period. The topic of funding opportunities drew the most visitors.

Wisconsin Water Resources Institute Publications, Videos and Audio Podcasts

An online publication store, <http://www.aqua.wisc.edu/publicaitons>, serves as a one-stop location to download no-cost WRI material. Other material is available for purchase at a nominal cost. During this reporting period, “Arsenic in Groundwater” and “Nitrate in Groundwater” fact

sheets were updated with the most current information and given new graphics to freshen their appeal.

A WRI publication about rain gardens was the most popular download in the Publications Store. In all, there were 18,329 items downloaded from the store. An additional 41,932 items were requested through the mail (bookmarks, information about aquatic invasive species and other miscellaneous publications). The store generated nearly \$6,000 in sales for the reporting period.

The Aquatic Sciences Chronicle is published quarterly. It highlights water research and the people who conduct water research and information transfer. At <http://www.aqua.wisc.edu/chronicle>, all issues of the publication are archived and searchable. This quarterly publication circulates to an audience of roughly 3,200 people, which includes local and state water management agencies, and water-related non-governmental organizations. Readers are found in Wisconsin and across the country. The Chronicle recently surveyed its readers on a number of topics. Those results provide direction for future content and layout changes to the publication to better serve research and resource manager audiences.

WRI's video catalog includes "What's a Spring," "Streams Neutralize Nitrates in Groundwater," "Testing Well Water for Microorganisms" and "A New Measure of Groundwater Flow." Additionally, WRI began work on a video to explain Wisconsin's Groundwater Monitoring Network, partnering with the state of Wisconsin's Geological and Natural History Survey. WRI also began work on a series of videos highlighting the protocols of water testing in laboratories.

At <http://itunes.apple.com/WebObjects/MZStore.woa/wa/viewPodcast?id=430421609>, visitors can download a WRI-produced seven-part audio podcast series. "Water, Wisconsin and the Mercury Cycle" details mankind's historic uses of mercury, Wisconsin's water resources and mercury in Wisconsin waters. A major part of the series also focuses on WRI-funded research on mercury. At the iTunes university site, WRI has been able to claim an artist's page. Pages such as these are reserved only for those who provide a deep array of content. The special pages allow for a richer display of water-related content. Moreover, they provide a so-called "sticky" experience where users are attracted to the page for a specific need but then stick around for additional, related information.

AWRA 2012 Annual Conference

The Wisconsin Section of the American Water Resources Association conducts an annual meeting. WRI assists with meeting planning and provides material support, as a co-sponsor, for the gathering. In 2012, there was unprecedented interest, with a record 200 attendees, and more abstracts and posters submitted than there had been in the previous 35 years of these meetings. Other conference sponsors were the University of Wisconsin-Stevens Point Center for Watershed Science and Education, Wisconsin Department of Natural Resources, Wisconsin Geological and Natural History Survey and the U.S. Geological Survey's Wisconsin Water Science Center.

Outreach Events

Wisconsin's Water Library held bimonthly sessions with children ages 3 through 6 at Ho Chunk Nation facilities in Wisconsin Dells, Wis. An average of 20 children attended each time. The sessions presented age-appropriate water-sustainability stories and activities. Additionally, the library participated in story hours at the Allied Drive Learning Center in Madison, Wis. Each event included two sessions: one for kindergarten and first-graders (25 students) and one for second- and third-graders (20 students).

Other public outreach events have included water library presentations at a special day called UW-Madison Day in Marinette, and a demonstration of a tabletop groundwater tank model at the Wisconsin State Fair that drew 350 interested people from across the state. It offered the chance to describe how and from where 70 percent of the state's 5.6 million residents get their drinking water. It also offered a chance to educate that remaining proportion of state residents who do not consider groundwater with any frequency since their drinking water comes from the Great Lakes.

Wisconsin's Water Library

Wisconsin's Water Library is a unique resource for researchers, resource managers and all Wisconsin citizens. It contains more than 30,000 volumes of water-related information about the Great Lakes and the waters of Wisconsin. The library includes a curriculum collection, dozens of educational videos, children's collection, and more than 20 journals and 100 newsletters. Each year, about 1,400 publications circulate among interested users.

Wisconsin's Water Library continues to catalog all groundwater research reports from WRI projects into WorldCat and MadCat, two library-indexing tools that provide worldwide access to the science. By having this information permanently indexed, the research results are easily available to other scientists throughout the University of Wisconsin System as well as across the nation and the world.

In addition to archival benefits, the library provides outreach by answering many in-depth reference questions on a wide range of water-related topics. It provides a water research guide (<http://researchguides.library.wisc.edu/waterresearchguide>). It is active on social media and goes out into the community to offer presentations to lifelong learners. It prepares recommended reading lists on topics such as climate change, groundwater, water conservation and water supply.

During the reporting period, in partnership with the Wisconsin Department of Natural Resources and the Wisconsin Wastewater Operator's Association (WWOA), the library continued its outreach to current and future wastewater operators of Wisconsin. The library cataloged the essential technical manuals into the library catalog and provided loans to WWOA members around the state in support of their required state license examinations as well as in support of the educational needs of their daily work.

Additional Websites and Technology

The library maintains several information transfer tools to reach library patrons and the most frequently accessed is the library's website (<http://www.aqua.wisc.edu/waterlibrary>), which had 117,980 visitors during this reporting period.

In addition to its website, Wisconsin's Water Library uses other technology to effect information transfer. Using email, the library sends out a bimonthly "Recent Acquisitions List" to roughly 500 contacts. The message also includes recent updates to the library website and contact information for users to ask any water-related question. The library also supports an email at askwater@aqua.wisc.edu, which is monitored daily.

The library uses social media for real-time relationships with interested patrons. It is active on Twitter, Facebook and maintains a blog.

During this reporting period, WRI staff also was integral to the development and content-population of <http://www.water.wisc.edu>. The site is a portal to the breadth and depth of water-related work on the state's flagship campus, the University of Wisconsin-Madison, and serves as the first stop for anyone interested in water research. Additionally, graduate students can search for departments offering courses and degrees that fit their interests, and staff and faculty can search for colleagues working on topics complementary to their own to facilitate greater interdisciplinary collaboration and exploration. The site launched in late 2012. From that launch until the end of this reporting period, there were about 1,500 visitors.

USGS Summer Intern Program

None.

Student Support					
Category	Section 104 Base Grant	Section 104 NCGP Award	NIWR-USGS Internship	Supplemental Awards	Total
Undergraduate	5	2	0	0	7
Masters	2	3	2	2	9
Ph.D.	3	0	1	1	5
Post-Doc.	0	3	0	1	4
Total	10	8	3	4	25

Notable Awards and Achievements

Professor Zhaohui Li received the “Top cited article of the year” award from the Journal of Colloids and Interfacial Science for the paper: Zhaohui Li, Po-Hsiang Chang, Jiin-Shuh Jean, Wei-Teh Jiang, Chih-Jen Wang (2010) Interaction between tetracycline and smectite in aqueous solution. Journal of Colloid and Interface Science. 341(2) pp. 311-319

Publications from Prior Years

1. 2005WI1540 ("Validation of transport of VOCs from Composite Liners") - Dissertations - Park, M.G. 2010 Volatile organic compound transport in composite liners. PhD Thesis. Department of Civil and Environmental Engineering, University of Wisconsin, Madison, Wisconsin. 156p.
2. 2006WI146G ("Identifying High-Infiltration and Groundwater Recharge Areas") - Articles in Refereed Scientific Journals - Arrington, KE, SJ Ventura, JM Norman. 2013. Predicting Saturated Hydraulic Conductivity for Estimating Maximum Soil Infiltration Rates. *Soil Science of America Journal*. 77(3):748-758. doi: 10.2136/sssaj2012.0288
3. 2010WI287O ("Groundwater Nitrate Processing in Deep Stream Sediments") - Articles in Refereed Scientific Journals - Stelzer, R.S., and L.A. Bartsch. 2012. Nitrate removal in deep sediments of a nitrogen-rich river network: a test of a conceptual model. *Journal of Geophysical Research-Biogeosciences*, 117:G02027 doi:10.1029/2012JG001990
4. 2009WI312O ("DTS as a Hydrostratigraphic Characterization Tool ") - Articles in Refereed Scientific Journals - Leaf, A.T., D.J. Hart and J.M. Bahr, 2012. Active thermal tracer tests for improved hydrostratigraphic characterization, *Ground Water*. 50(5):726-735 doi: 10.1111/j.1745-6584.2012.00913.x
5. 2007WI210O ("Multi-Parameter, Remote Groundwater Monitoring with Referencing Using Crossed Optical Fiber Fluorescent Sensor Arrays.") - Articles in Refereed Scientific Journals - M. Veronica Rigo and Peter Geissinger. 2012. Crossed-Optical Fiber Sensor Arrays for High-Spatial-Resolution Sensing: Application to Dissolved-Oxygen-Concentration Measurements. *Journal of Sensors*. 464092 (10 pp) doi: 10.1155/2012/464092
6. 2007WI200S ("Grant No. 07HQGR0170 ACAP Test Section Exhumation") - Articles in Refereed Scientific Journals - Albright, W., Benson, C., and Apiwantragoon, P. (2012), Field Hydrology of Landfill Final Covers with Composite Barrier Layers, *J. Geotech. and Geoenvironmental Eng.*, in press. doi:10.1061/(ASCE)GT.1943-5606.0000741
7. 2009WI216B ("Combination of Co-Precipitation with Zeolite Filtration to Remove Arsenic from Contaminated Water") - Articles in Refereed Scientific Journals - Du, G., Li, Z., Liao, L., Hanson*, R., Leick*, S. Hoepfner*, N., Jiang, W.-T. (2012) Cr(VI) retention and transport through Fe(III) coated natural zeolite, *J. Hazard. Mater.*, 221-222, 118-123. <http://dx.doi.org/10.1016/j.jhazmat.2012.04.016>
8. 2009WI216B ("Combination of Co-Precipitation with Zeolite Filtration to Remove Arsenic from Contaminated Water") - Articles in Refereed Scientific Journals - Liu, C.-C., Maity, J. P., Jean, J.-S., Reza, A.H.M., Li, Z., Nath, B., Lee, M.-K., Lin, K.-H., Bhattacharya, P. (2012) Geochemical characteristics of the mud volcano fluids in southwestern Taiwan and their possible linkage to elevated arsenic concentration in Chianan plain groundwater, *Environ. Earth Sci.*, 66, 1513-1523. <http://dx.doi.org/10.1007/s12665-011-1391-3>
9. 2009WI216B ("Combination of Co-Precipitation with Zeolite Filtration to Remove Arsenic from Contaminated Water") - Articles in Refereed Scientific Journals - Liu, C.-C., Maity, J. P., Jean J.-S., Li, Z., Kar, S., Sracek, O., Yang, H.-Y., Chen, C.-Y., Reza, A. H. M. S., Bundschuh, J., Lee, C.-Y. (2013) The geochemical characteristics of the mud liquids in the Wushanting and Hsiaokunshui Mud Volcano region in southern Taiwan: Implications of humic substances for binding and mobilization of arsenic, *J. Geochem. Exploration.*, 128, 62-71. <http://dx.doi.org/10.1016/j.gexplo.2013.01.006>